CRITICAL ASSESSMENT OF EXISTING SLOPE STABILITY FORMULAE AND APPLICATION TO SLOPE STABILISATION

by

SEYHAN FIRAT *B.Sc., M.Sc.*

School of the Built Environment
University of Glamorgan

A thesis presented in fulfilment of the requirement for the degree of Doctor of Philosophy of the University of Glamorgan

November 1998

CERTIFICATE OF RESEARCH

This is to certify that, apart from where specific reference to other publications is made, the work presented in this thesis is the result of the investigation undertaken by the candidate.

.....
S. Firat
(Candidate)

.....
(Date)

.....
Dr R. Delpak
(Director of studies)

1st February 1999
(Date)

.....
Dr R.W. Williams
(Supervisor)

.....
(Date)

.....
G.I. Jones
(Supervisor)

.....
(Date)

DECLARATION

This is to certify that neither this thesis, nor any part of it has been presented, in candidature form for any degree at any other academic institution.

.....
(Candidate)

DEDICATION

I wish to dedicate this thesis to the entire house of GENCALLAR whence I trace my roots, and to my immediate family Refika, my wife, and Ismail, my son.

ACKNOWLEDGEMENTS

The author would like to express his sincere gratitude to Dr. R. Delpak, director of studies, and Dr. R. W. Williams, supervisor, for many stimulating discussions and constructive criticism. I would also like to thank the aforementioned for their patience and careful evaluations of the manuscript which were of invaluable assistance in the preparation of this thesis. Appreciation is also expressed to my supervisor Mr. G. I. Jones who critically reviewed the manuscript and gave helpful suggestions.

I am indebted to the Sakarya University (Turkiye) for providing financial support during the course of my study.

Thanks also to the Turkish students I have befriended and my friends in Wales.

Finally, I would like to express my sincere gratitude to my wife Refika, my son Ismail and my parents for without their support this thesis would not have been completed.

ABSTRACT

In this research, extensive use has been made of limit equilibrium methods of analysis for studying the stability of slopes. For the determination of the factor of safety (*FOS*) of slopes, the usual two-step process has been adopted; (a) assuming a slip surface for the soil mass, and (b) using the appropriate limit equilibrium equation(s). Eight well-known limit equilibrium methods have been programmed to calculate different *FOS* values. The comparative performance of the various analyses has been carried out successfully using case studies. The innovative use of Gauss quadrature to calculate the *FOS* values has been shown to reduce the iterative sequences dramatically with no loss of accuracy.

A visco-plastic flow model has been proposed to estimate lateral forces on piles used for slope stabilisation. The present research data occupies an "in-between" position to the previously reported values, with the variation trend being confirmed satisfactorily in all cases.

Slope stabilisation due to the presence of a row of piles has been investigated using two distinct lateral load estimations. These include theories of plastic deformation and the proposed visco-plastic flow which are modelled and implemented in a computer program. Eight well-known methods of slope stability analyses have been adopted and computer coded to re-calculate *FOS* values for a slope reinforced by a row of piles. A Finite Element computer program has been developed to evaluate the displacement, bending moment and shear force along the pile axis. The pile is analysed at two levels above and below the slip failure surface.

LIST OF CONTENTS

LIST OF FIGURES

LIST OF TABLES

LIST OF SYMBOLS

A	Values of coefficient to calculate K_s
A_0, A_1, A_2	Coefficient of the parabolic curve for slip surface representation
a	Pile (cylinder) diameter
b	Width of a slice
c	Cohesion
c_u	Undrained (total stress) cohesion
c'	Drained (effective stress) cohesion
D_1	Centre to centre distance between two piles
D_2	Clear distance between two piles
d	Depth of the sliding soil mass
dv/dy	Velocity gradient (strain rate)
E	Overall force
EI	Flexural rigidity of pile
E_i, E_{i+1}	Normal force on vertical side of a slice
E_s	Modulus of elasticity of soil
F	Factor of safety
F	Force on a pile
F_f	Factor of safety with respect to force calculation
F_m	Factor of safety with respect to moment calculation

F_m	Mobilised lateral force
F_p	Lateral force per unit length
f_r, f_θ	Forces in the r and θ directions
f_0	Correction factor in order to take into account interslice shear forces for Janbu simplified method
h	Height of slice
h_t	Line of thrust
h_w	Depth of the base of a slice below the water table
K	Elastic constant
K_c	Critical horizontal acceleration
K_s	Subgrade Reaction
L	Length of the sliding soil mass
l	Length of base of a slice
M	Number of grid points in the $\xi(r)$ direction
M	Overall moment
N	Number of grid points in the θ direction
N	Total normal force on the base of a slice
N'	Effective normal force on the base of a slice
ng	Number of Gauss points
ns	Number of slices
p	Lateral force on a pile
p	Pressure

p'	Earth pressure due to gravity
Q	Interslice force for the Spencer method
q_a	Allowable bearing capacity
q_u	Unconfined compressive strength
R	Radius of slip circle
Re	Reynolds number
Ro	Distance from a pile (cylinder)
r_u	Coefficient of pore water pressure
S	Shear force on the base of a slice tangential to the slip circle
S	Smoothing parameter
$T_{rr}, T_{\theta\theta}, T_{r\theta}$	Extra stress tensors
TolZ	Tolerance value for iterations
Tol ω	Tolerance value for convergence of vorticity function
Tol ψ	Tolerance value for convergence of stream function
u	Normal pore water pressure on the base of a slice
u	Velocity component in the r direction
V	Flow velocity
v	Pile deflection
v	Velocity component in the θ direction
WI	Gauss weight factor
W_i	Weight of i-th slice
X_i, X_{i+1}	Shear force on vertical side of a slice
XL	Intersection point on the ground surface (left hand side)

XR	Intersection point on the ground surface (right hand side)
x_c	Centre of slip circle along x direction
x_g, y_g	Co-ordinate of centre of gravity of sliding mass with respect to the axis
x_i, y_i	Co-ordinates of mid point of base of i-th slice with respect to the axis
y_c	Centre of slip circle along y direction
z	Depth along a pile
z_i, z_{i+1}	Height of point of application of interslice normal forces on the vertical side of i-th slice
α	Angle of base of a slice
α	Positive yield stress modelling parameter
γ	Unit weight of soil
γ'	Effective unit weight
γ_b	Bulk unit weight of slice
γ_{sat}	Saturated unit weight of soil
γ_{sub}	Submerged unit weight of soil
γ_w	Unit weight of water
$\dot{\varepsilon}_{rr}, \dot{\varepsilon}_{\theta\theta}, \dot{\gamma}_{r\theta}$	Rates of strains in polar co-ordinates
η	Apparent viscosity
η_0	Newtonian flow viscosity
η_p	Bingham plastic viscosity
ρ	Density
σ'	Effective normal stress

$\sigma_{allow.}$	Allowable bending moment
$\sigma_{max.}$	Maximum induced bending stress
σ_{rr}	Normal stress radially (*r* direction)
$\sigma_{\theta\theta}$	Normal stress circumferentially (θ direction)
τ	Shear stress
τ_y	Yield stress
ϕ'	Drained (effective stress) angle of friction
ϕ_u	Undrained (total stress) internal friction angle
θ	Interslice force angle for the Spencer method
θ , r	Polar co-ordinates
∇^2	Laplacian operator
ϑ	Pile rotation
λ	Scaling factor
ϖ	Vorticity function
ξ_0	Effective distance in the vicinity of a pile
ξ	Gauss abscissa
ξ	Scaling factor for *r*
ψ	Stream function

LIST OF ABBREVIATIONS

BEM	Boundary Element Method
BM	Bending Moment
FDM	Finite Difference Method
FEM	Finite Element Method
FOS	Factor of Safety
GQ	Gauss Quadrature
KONS	Product of velocity and plastic viscosity
MOS	Method of Slice
PDE	Partial Differential Equations
RHS	Right Hand Side
SF	Shear Force
SR	Subgrade Reaction
USBR	United States Bureau of Reclamation

CHAPTER 1: INTRODUCTION

1.1 Foreword

The impending threat of a land slip, particularly in South Wales, with a high landslide potential per given area, can become a life threatening hazard as experienced in Aberfan and elsewhere (Bromhead, 1992). Many different analytical techniques exist at present. These techniques can be used by engineers when assessing whether a particular natural or man-made slope is stable.

The most common method of determining the stability of slopes is to use limit equilibrium in order to estimate the factor of safety at the most critical set of conditions. This objective is attained through a two-step procedure (Nash, 1987):

- assuming a potential slip surface, and
- applying the limit equilibrium equations and solving the factor of safety for the soil mass defined by this surface (i.e., the ratio of the stabilising force to the disturbing force or, the stabilising moment to the disturbing moment).

For simple homogeneous soil, experience indicates that the shape of the slip surface can be idealised as a circle (Craig, 1997). Circles are convenient and popular for analyses and often approximate to the observed failure surface. However, non-

homogeneous problems or complicated geological conditions may require consideration of slip surfaces of non-circular shape (Arai and Tagyo, 1985).

Assumptions are needed to implement the limit equilibrium equations, since the slope stability problem is statically indeterminate. There is a wide range of possible static assumptions made in order to enable these methods of analysis to be statically determinate.

1.2 Aims

One purpose of this research is to evaluate an in-house developed suite of computer slope stability programs. The enhanced programs will have the capability of determining factors of safety using a variety of existing formulae applied to specified ground geometries.

The in-house program will be compared with more traditional methods of analysis by testing it on published case studies.

The method of slices is a well understood and widely used procedure for the division of the potential failure mass. To obtain an accurate *FOS*, a high number of slices are required. Obviously this requires an increased calculation time. It is thought that an alternative method of numerical approximation should be studied and comparison should be viewed critically.

The other main feature of the research is to develop a numerical evaluation of remedial measures for slopes. The analysis will be related to classical and innovative rigorous formulations based on mathematical principles where applicable.

With extensive use of piles as landslide countermeasures, the interaction mechanism between the piles and the surrounding soil is still a matter of discussion (Anagtopoulos et al., 1991). There is limited reported data, of which candidate has made maximum use. Since site measurement procedures are known to be costly and time consuming, it is felt that there should also be different credible predictive methods to establish bounded solutions in order that a variety of lateral forces could be examined. In this work attempts will be made to formulate a predictive model in order to estimate mobilisation forces due to landslide initiation.

During the past two decades, pile stabilisation has became one of the most innovative techniques for slope stabilisation (Poulos, 1995). Researchers have developed a limited number of methods of analysis to obtain stabilised factors of safety using piles (e.g., Nakamura, 1984; Lee et al., 1995 and Hassiotis et al., 1997). There is a clear need for researchers to devise a wide range of methods of analysis to obtain stabilised factors of safety (*FOS*) using piles. Therefore, it is thought that various limit equilibrium methods may be used to evaluate the *FOS* with pile stabilisation.

The *FOS* calculations of slopes, for normal (unstabilised) and stabilised (deploying piles) conditions, have been carried out using eight distinct limit equilibrium

formulations. A novel approach has also been introduced using Gauss quadrature for pile stabilisation.

1.3 Synopses of the studies ahead

Chapter 2 reports on some types of mass movements. The techniques of selecting the most critical failure surface, which gives the lowest *FOS*, are examined. Since different failure modes can give different *FOS* for the same slope analysed the importance of mode and mechanism of a slope failure are studied as an important part of slope stability assessment.

Chapter 3 summarises the limit equilibrium methods available, together with the discussion of other existing two-dimensional methods of slope stability analysis. The methods are compared and contrasted in terms of the assumptions made for the evaluation of the corresponding *FOS*. The merits and demerits of each are critically examined.

Chapter 4 details a computer modelling system, named SLIDE, which is used for the application of limit equilibrium methods in two dimensions. Eight limit equilibrium methods, namely Fellenius, Bishop simplified, Janbu simplified, Janbu generalised, Morgenstern and Price, Spencer, Sarma and Fredlund and Krahn (GLE), have been computer coded in-house by the author. A comparative study of the selected eight

limit equilibrium methods, including the results of comparative slope stability analyses for circular and non-circular surfaces, are considered.

Chapter 5 introduces an alternative method of failure mass division i.e., method of slices and Gauss quadrature. This approach is compared to traditional methods using the author's SLIDE program for circular slip surfaces. The critical review highlights the merits of each method.

Chapter 6 considers creeping flow of a visco-plastic fluid past a cylindrical pile or a row of piles. This proposed method is formulated to estimate the lateral load on the pile due to a slow flowing soil mass. A Bingham plastic material approximation is used to model the failure soil mass. The effect of various parameters are evaluated in the proposed visco-plastic flow.

Chapter 7 is planned to provide a comparison of three different formulations for lateral load estimations using the plastic flow theories and the proposed visco-plastic flow.

Chapter 8 summarises the behaviour prediction of laterally loaded piles used in slope stabilisation. A pile is modelled as a beam member supported on an elastic foundation. The Subgrade Reaction approach is used to model the pile/soil interaction. A Finite Element analysis procedure is used to estimate deflections, bending moments

and shear forces, taking into consideration alternative boundary condition representation.

Chapter 9 contains analysis of the mechanical stabilisation of a slope subjected to failure risk. Theories developed in Chapter 6 and those given in the literature are tested. The appraisal hinges on whether there are improvements of the *FOS* values using a row of piles. In this chapter, slope stabilisation is considered as well as pile stability.

Chapter 10 contains the conclusions drawn relating to this study and suggests some recommendations for extension of the work.

Janbu simplified and Morgenstern and Price derivations of slope stability equations are shown in Appendices A and B.

CHAPTER 2: GENERAL METHODS OF PROBLEM DEFINITION AND SOLUTION

2.1 Introduction

In this chapter, various modes of slope failure are reported in a scientific/technical classification. In the latter part of this chapter, the development will hinge on the choice of the mathematical representation in order to that the observed failure curves are formulated with sufficient accuracy.

Movements of soils and rock masses may occur under the influence of body forces, e.g., gravity and seismic acceleration. When the disturbing action exceeds the available shear strength of the soil on a sloping ground, the latter may become unstable. The resulting mass slide can be serious in damaging properties with potential loss of life. In unpopulated areas failure may only have a small effect, simply being part of the natural deterioration of the earth's surface.

The threat of landslides in many countries exists but with varying degrees of risk. Landsliding is an important and costly impending threat where it may be a continual source of concern for responsible authorities and geotechnical engineers.

2.2 Identification of a failure mass transportation system

The identification of a failure mass in an area with a potential of slope instability requires the accumulation of sufficient information from the site conditions to enable risk analysis by the solving of trial problems. It is usually necessary to conduct a preliminary study of the slope. This may be carried out through:

- a physical site visit
- studies of historic and archival records
- aerial photography
- satellite data analyses
- high-precision camera data analysis
- laboratory testing of soil samples
- compilation, analysis and presentation of data (Walker et al., 1987).

A landslide is the downward and outward movement of slope-forming materials composed of soil, natural rock, artificial fill or a combination of these materials. Ground movements have been classified into different groups by many authors. Skempton and Hutchinson (1969) and Kumsar (1993) have given a comprehensive illustration and information of some basic types of mass movement. It is the general consensus that the sliding mass may proceed in three principal categories of displacement defined by slides, falls and flows (Bromhead, 1992 and Abramson et al., 1996).

2.2.1 Slides

The mass of the moving soil remains largely in contact with the hard strata during the movement. Slides may be sub-divided into four subsections as follows:

1 **Rotational slide or slump.** Rotational slides or slumps are generally characterised by concave (mainly circular in slope stability analysis) shear planes (Walker et al., 1987). These commonly occur in fairly homogeneous materials, e.g., in constructed embankments, soil and fill (Kumsar, 1993). They are generally deep in terms of their length, see Fig. 2.1(a)-(b).

2 **Translational slide.** This type of failure occurs where the adjacent stratum is at a relatively shallow depth below the slope surface. Usually the failure surface is observed to be approximately parallel to the slope, see Fig. 2.1(c)-(d). Translational slides may take place in any earth material that has a discontinuity or failure surface (Kumsar, 1993).

3 **Compound slide.** Compound slides result from complex constituent material structure and make up. They generally occur when an adjacent stratum is more deeply situated, Fig. 2.1(e).

4 **Block slide.** Block slides involve the movement of a large block that has moved out and down with varying degrees of backtilting, shown in Fig. 2.1(c).

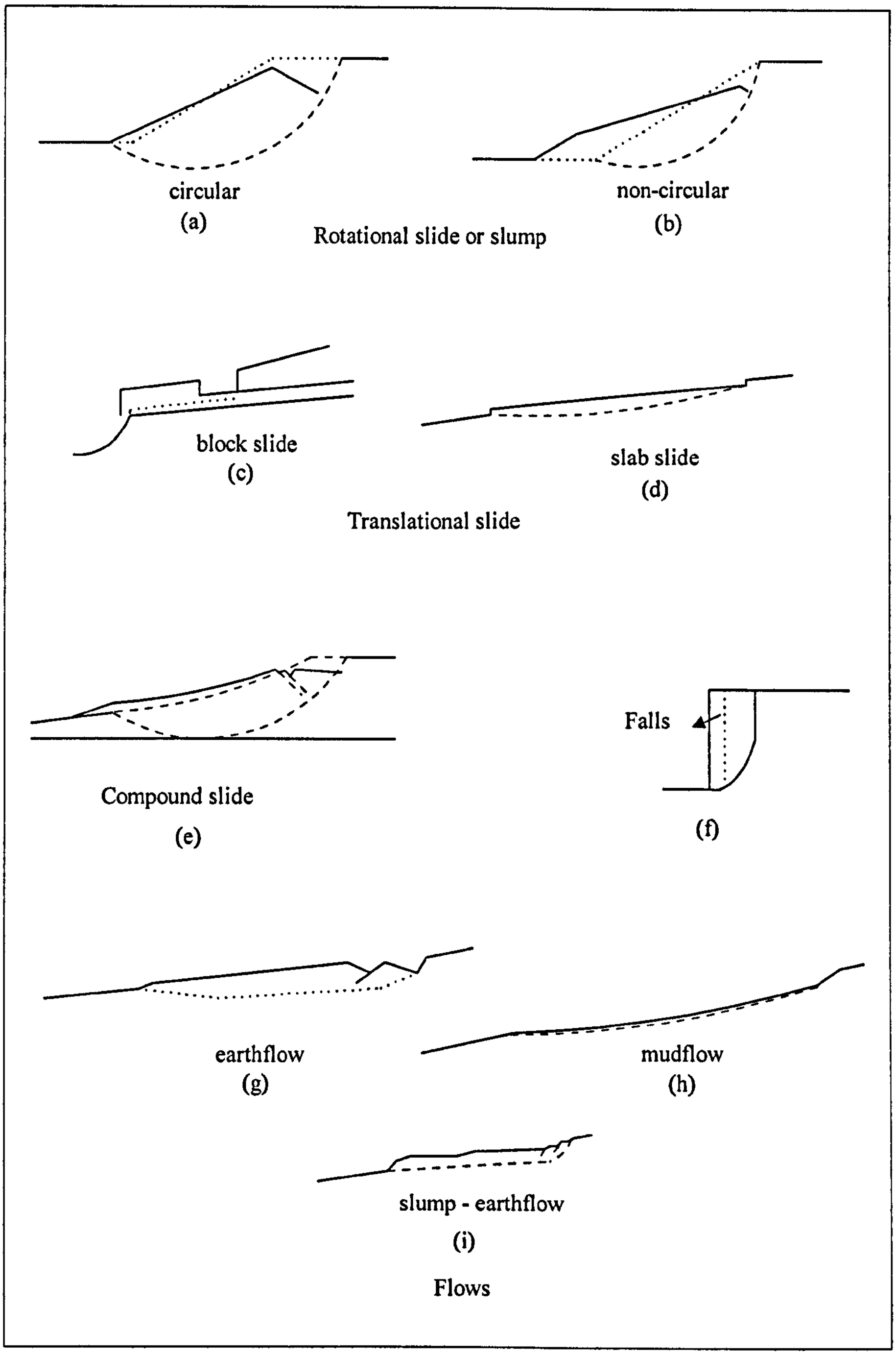

Figure 2.1 Some basic types of mass movement (Skempton and Hutchinson, 1969).

2.2.2 Falls

This type of failure occurs especially when the slope is very steep, see Fig. 2.1(f). Falls involve direct outward and downward movement of detached blocks falling under the influence of gravity (or body forces) and under conditions of low resistance once movement is initiated. Some falls also involve toppling failure. Falls occur commonly along the banks of rivers, accelerated by agitation due to water and may well be initiated by weathering and careless excavation. Kumsar (1993) stated that weathering has been found to be important in several aspects of slope development, not only weakening soil but also rocks.

2.2.3 Flows

Flows involve much greater internal deformation than a slide (Bromhead, 1992). Their geometry takes parallel forms of failure to the firm ground surface, see Fig. 2.1(g)-(h). A moving mass flows in a downward direction as a viscous material (Walker et al., 1987). It is able to travel a considerable distance from its source. Flows have considerable length compared to their depth. When flows consist of slow movement of softened or weathered debris, it is called an earthflow, whereas faster movement of clay debris, softened and lubricated by water, is called a mudflow (Barnes, 1995).

The sliding mass may be triggered by one or more of the three principal types of movement (i.e. sliding, falling and flowing). Larger movements may often change from one to another during the progress of movement, see Fig. 2.1(i) (Bromhead, 1992).

2.3 Analytical or functional representation of the above modes of failures

Failure surfaces are varied in nature, so that mathematical expressions are used only to approximate the shape of failure surfaces. As a result of geometric approximation, it becomes possible to estimate the resisting (stabilising) forces as well as the corresponding failure mass causing the disturbing (destabilising) action. The location and shape of the possible failure surface are unknown factors at the start of the analysis stage. This unknown slip surface is expected to be related to the factor of safety corresponding to a minimum numerical value. In practice, the shape of the unknown slip surface is assumed. The following surfaces are possible:

- **Circular slip surface**

The representation of the failure surface as a single curve greatly simplifies the problem see Fig. 2.5. Curve selection methods will be given in section 2.4.1 in detail. The centre of the slip circle has three location parameters; namely the abscissa x_c , the ordinate y_c and the radius R. The curve can easily be expressed as a mathematical function by using the equation of a circle, namely;

$$(x-a)^2+(y-b)^2=R^2\,, \qquad 2.1$$

where

a and b are the centre of the circle with respect to the x and y axis respectively.

x and y are the translation of the circle along the x and y directions respectively.

R is the radius.

- **Non-circular slip surface**

The position of a non-circular slip surface can be defined by a series of straight lines, see Fig. 2.6. The co-ordinates of the nodal points are denoted by (x_i , y_i). The two extremities of the failure surface intersect the slope geometry. Available possible non-circular slip surface determinations will be given in section 2.4.2 in detail.

- **Parabolic geometry**

The slip surface may be defined as one parabola, a series of parabolic curves or even a sophisticated power series, see Fig. 2.2. The co-ordinates of the nodal points are stored as (x_i , y_i) pairs of co-ordinates. Once again, the defined domain of the curvilinear geometry coincides with the failed slope extremities. The parabola has a familiar form;

$$y=A_0+A_1x+A_2x^2\,, \qquad 2.2$$

where the A_i's are constant.

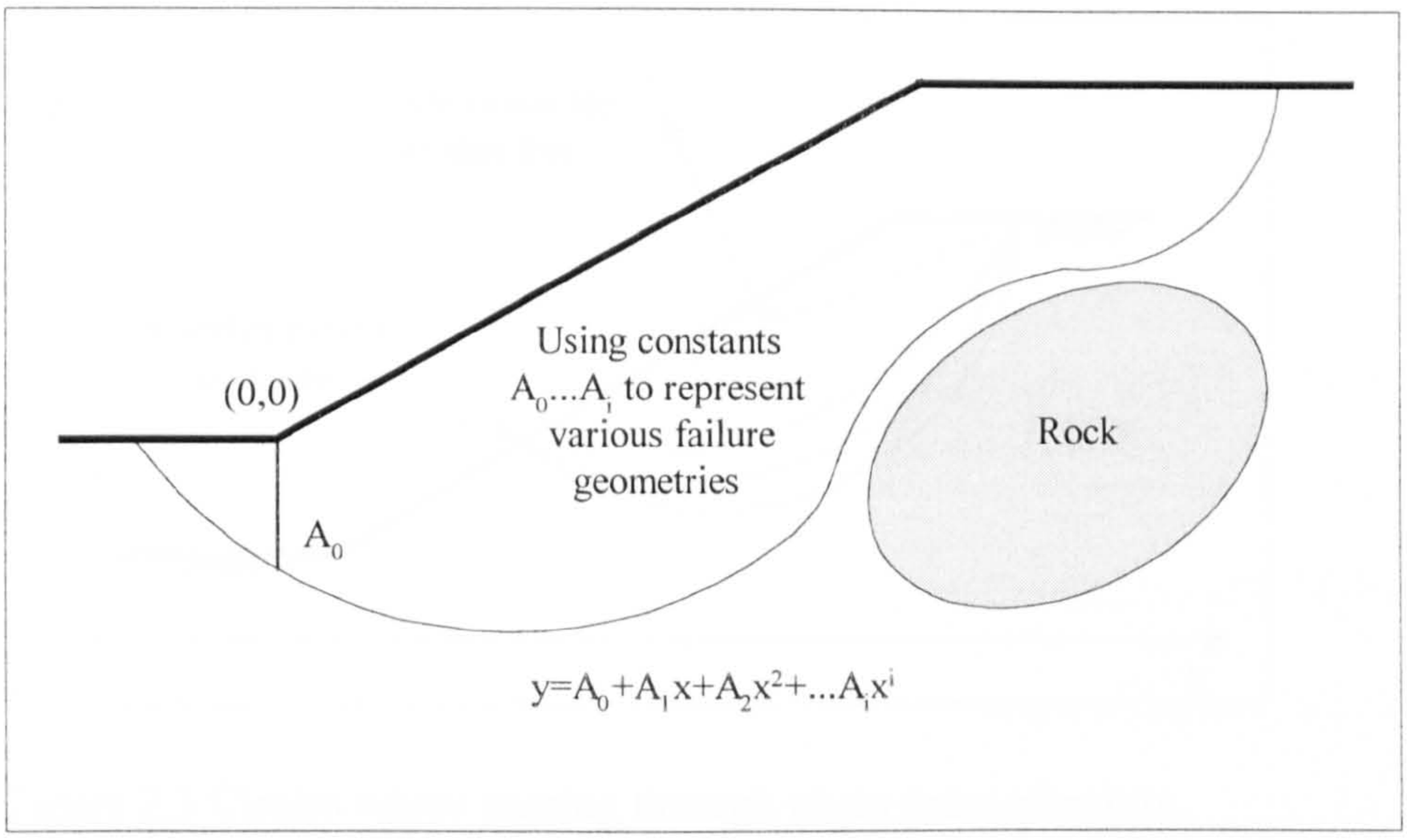

Figure 2.2 Schematic for failure surface representation using power series.

2.4 Possible failure curve selection

2.4.1 Circular slip surface

For all methods of slope stability analysis, it is essential to search for the possible failure surface in order to obtain the one which gives the lowest factor of safety. This long procedure of analysing many trial circles can be carried out quickly and effectively by using a computer.

When the soil mass is cohesive and relatively homogeneous, the slip surface may take a near circular form. The coding of the program can take the following forms,

- using circles which can be generated to pass through a given set of points, see Fig. 2.3,

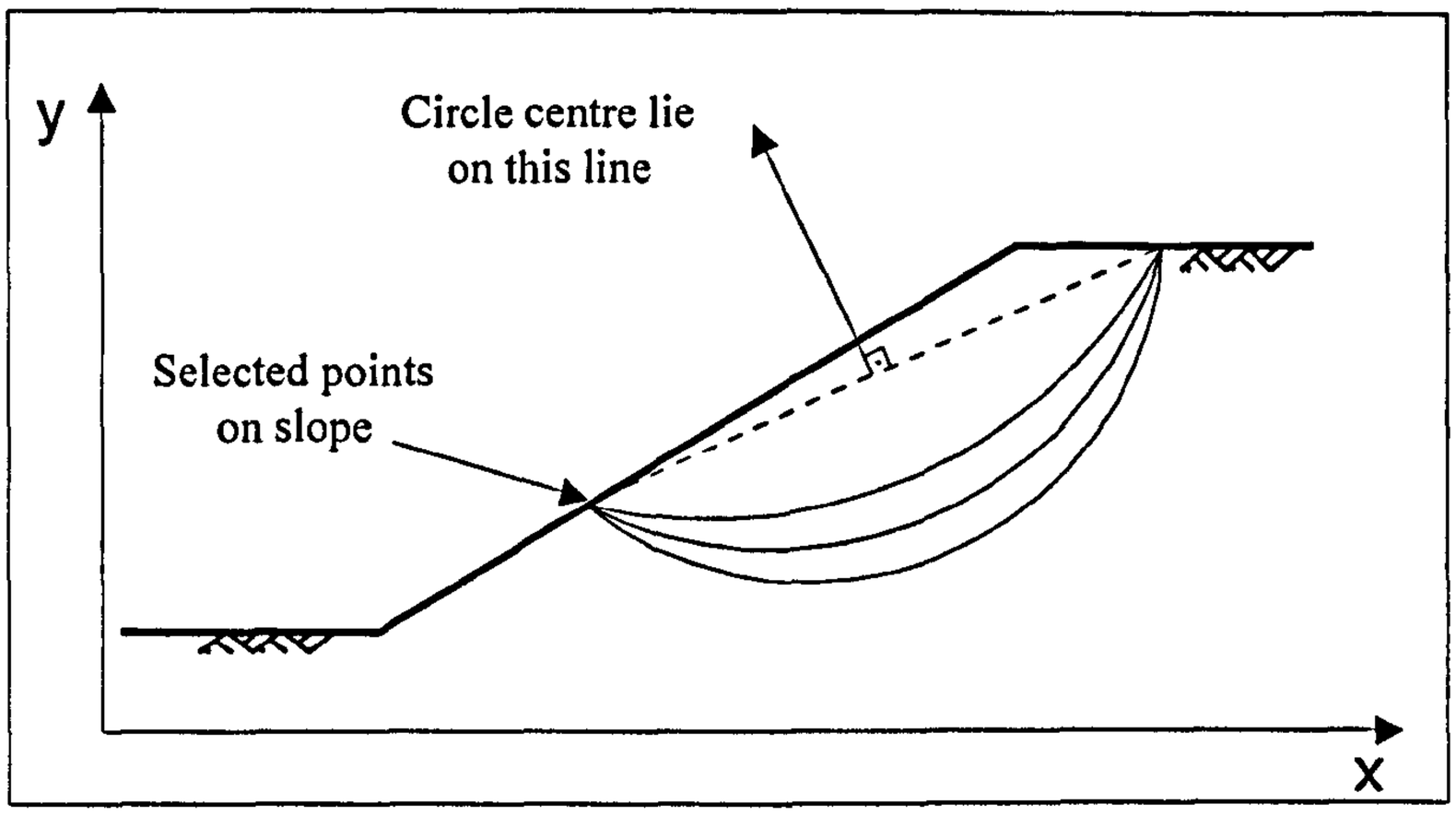

Figure 2.3 Circles where passing through given pairs of points
(Mostyn and Small, 1987).

- generating circles which can be specified to go through particular points, see Fig. 2.4, (i.e., the toe of a slope),

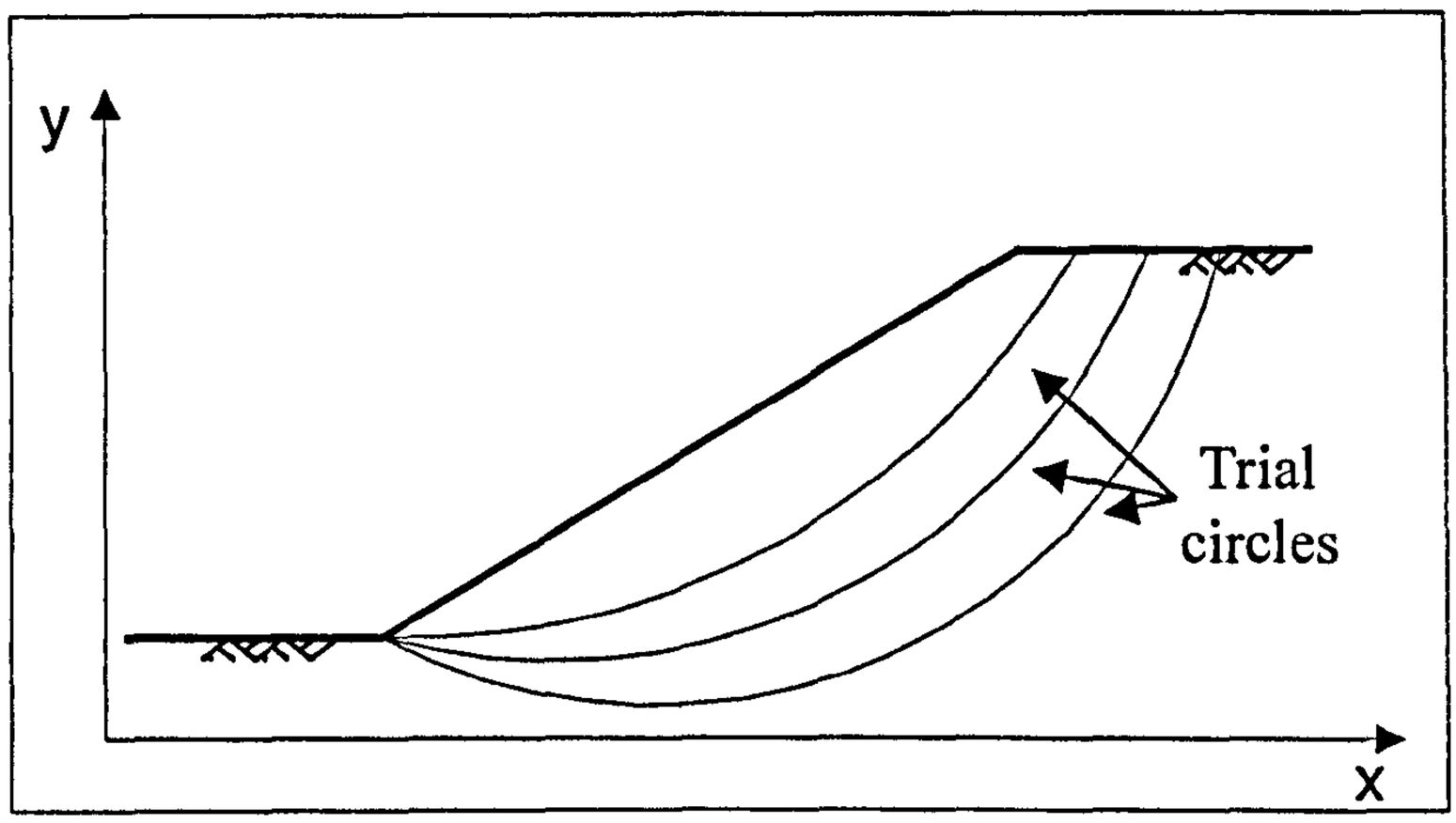

Figure 2.4 Toe circles for circular slip surface.

- forming grid lines. This may be the most accurate and widely used method. In this method, see Fig. 2.5, centres of circles are located at different specified grid intersection lines thus taking different radii for every point on the grid,

- forming an optimisation technique which can be used to reduce the amount of computation. Nguyen (1985) described such a technique by using a method he called simplex reflection. It involves the determination of the set of circle centre co-ordinates (i.e., x_c, y_c, R) to locate the least factor of safety. This is achieved by finding the *FOS* (factor of safety) at the four corners of a tetrahedron specified x_c, y_c, and R (i.e., the co-ordinates of four corners values). The *FOS* at the four corners are then compared to decide in which vectorial direction to carry out the search for a minimum *FOS*, to be consistent with the rest of the points.
- grid lines can be located by extracting normals to the slope surface. This method was actually used for the present research. Once a few values of *FOS* have been calculated, a grid can be established and a search to find the minimum *FOS* can commence. This has been verified to reduce the number of calculations required in any trial-and-error algorithm, since unnecessary search effort is much reduced.

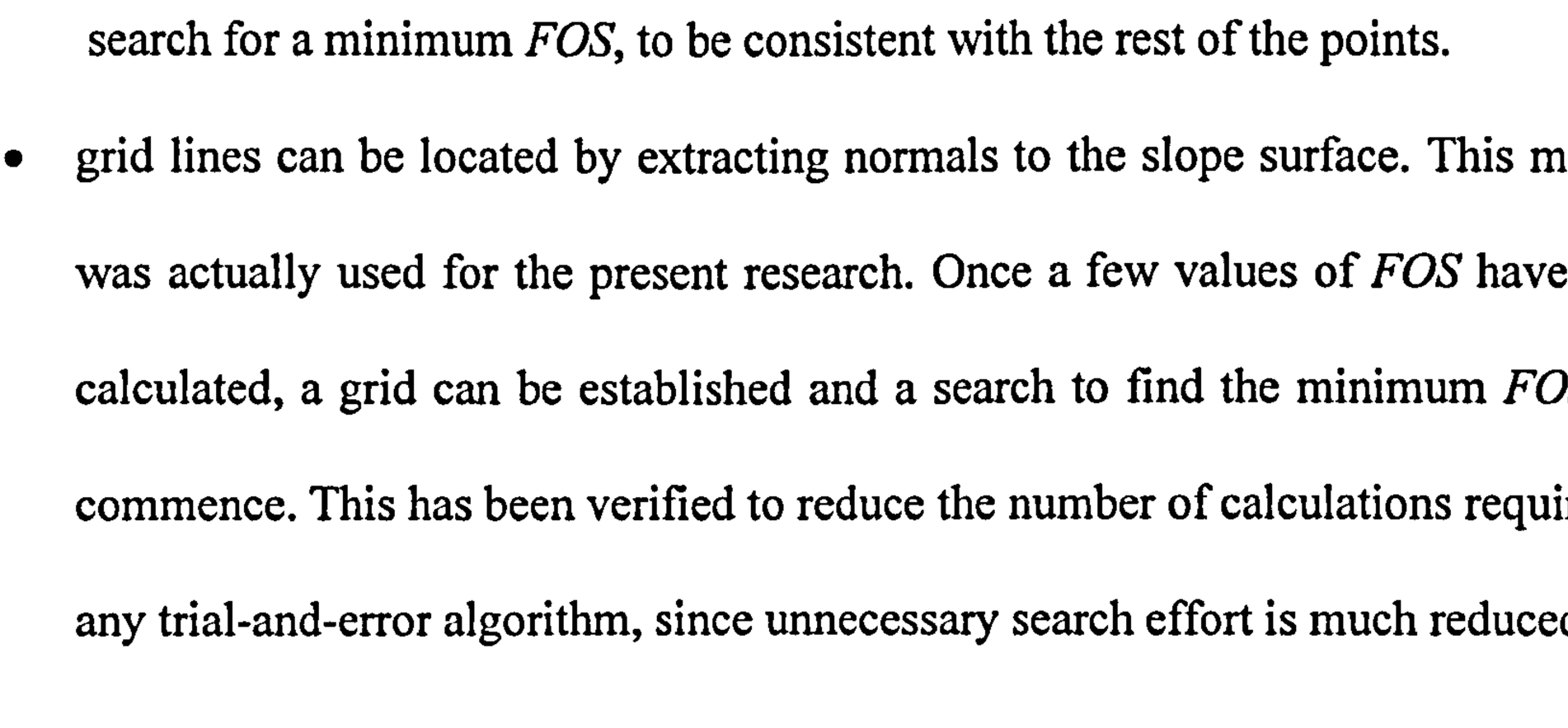

Figure 2.5 Technique for systematic grid search pattern.

The shape of the failure surface may also be assumed as a logarithmic spiral shape. A search for the most critical location of the slip surface may be performed by a grid search technique as given above. In order to locate the most probable slip surface, the centre of the pole of the logarithmic spiral is varied according to a chosen grid pattern. To do this, an initial radius is required and then is varied between R_{max} and R_{min} to obtain the most critical failure surface which gives the least *FOS* (Boutrop and Lovell, 1980).

2.4.2 Non-circular slip surface

When the shear strength is not uniform in the soil mass, the slip surface will depend on the distribution of shear strength. This means the slip surface may no longer be circular. Generally slip surfaces are observed to be non-circular (Arai and Tagyo, 1985). As Morgenstern and Price (1965) stated; the condition of limiting equilibrium together with the method of slices assists a reasonable basis to develop a method with sufficient generality in its applicability. This was first applied by Janbu (1957).

As suggested above, Fig. 2.6 shows that slip surfaces can be specified to go through a particular set of points (DeNatale, 1991). Several automatic search methods have been proposed by many authors. Celestino and Duncan (1981) described an alternating variable method, which can be used to locate a non-circular slip surface. In this method, a number of trial straight lines are used, Fig. 2.7. One point is shifted until its optimum position is located and the same procedure is continued for other points. The

authors reported that it has been found to be effective to shift the end points along the slope surface and to shift interior points vertically and horizontally. Also the authors found an acceptable geometry by defining the slip surface using four to six points.

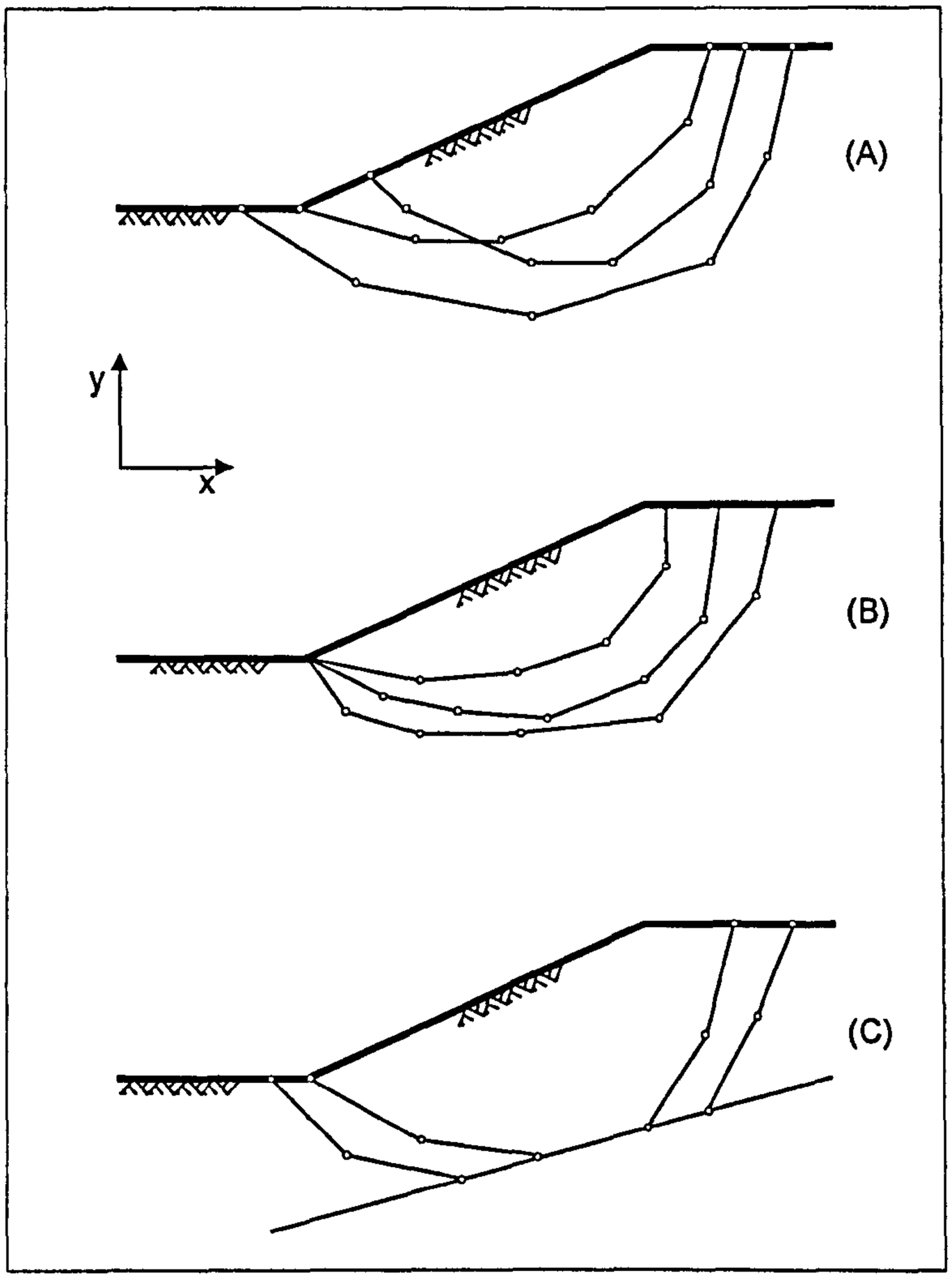

Figure 2.6 Typical non-circular slip surfaces: (A) Unrestricted surfaces; (B) Toe surfaces; (C) Tangent surfaces (DeNatale, 1991).

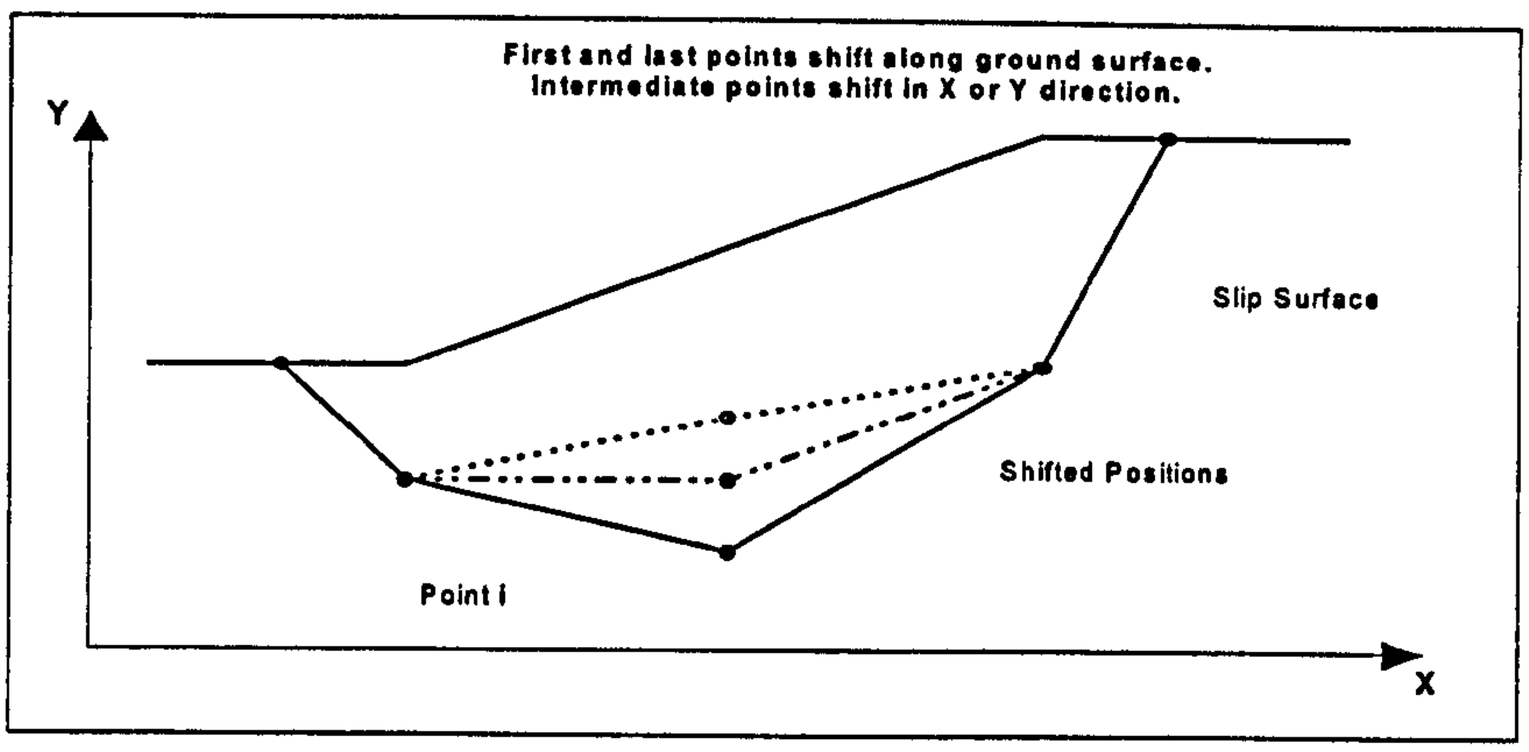

Figure 2.7 Shifting points on the slip surface (Celestino and Duncan, 1981).

Siegel et al (1981) proposed a random surface generator to locate the critical slip surface. The method uses a random number generator, Fig. 2.8, and some restrictions are imposed on the direction of segments of the slip surface to avoid generation of unacceptable failure surfaces. The potential slip surface is approximated as a series of straight line segments with the following restrictions,

- the starting points on the boundary should be within an acceptable range,
- the shape of the slip surface must satisfy a kinematic condition of analysis,
- the slip surface must lie above a firm stratum, and
- the end position of the slip surface must be within a reasonable range on the boundary.

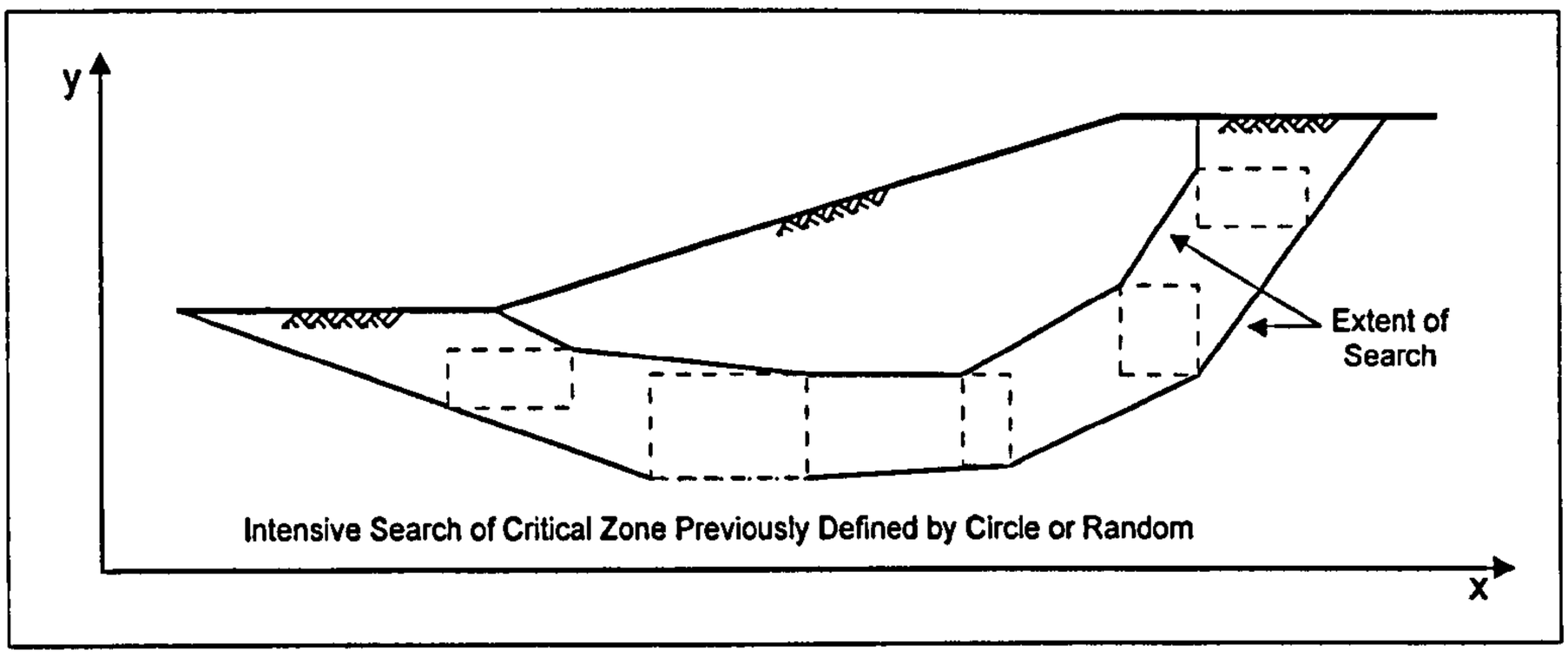

Figure 2.8 Sliding block generator using more than two boxes (Siegel et al., 1981).

With the advent of computers, numerical approaches have become competent in dealing with geotechnical problems that involve heterogeneous and constitutive behaviour in addition to complicated boundary conditions. Since the 1950's, optimisation theory, which seeks the extrema numerically, has been successfully developed and applied in various fields including *FOS* determination in slope stability analysis.

The calculus of variation method can be used to locate the critical slip surface (Castillo and Revilla, 1977; Baker and Garber, 1977, 1978). In these methods, Euler's equations are allowed to directly compute the shape and position of the failure surface with corresponding minimum *FOS* values.

Boutrop and Lovell (1980) presented a strategy that included random generation of slip surfaces and repeated comparisons of up-dated *FOS* figures. Baker (1980) developed dynamic programming which, as he stated, is only applicable to additive

functions. Baker introduced a sophisticated management system to enable a solution of Spencer's (1973) formulation. In each iteration, dynamic programming was involved or solving force and moment equilibrium equations. Coupling the solution of the equilibrium equations with *FOS* minimisation sequences, increased the complexity of the algorithm and complicated its extensions to other slice-based methods as discussed by Li and White (1987).

The earlier mentioned technique of simplex reflection (Nguyen, 1985) can also be applied to non-circular slip surfaces in a similar fashion to that of Celestino and Duncan (1981) in terms of shifting points. Li and White (1987) extended the previously cited method to improve its reliability.

Arai and Tagyo (1985) used a numerical procedure called the conjugate gradient technique to determinate the critical non-circular slip surface. Sridevi and Deep (1991) presented a global optimisation technique to locate general failure surfaces with the minimum *FOS*. In both methods, the initial guess of the slip surface has not been made but the slip surface has been arrived at by giving the lower and upper bounds of co-ordinates in which the non-circular slip surface lies.

Greco (1996) proposed an efficient Monte Carlo method, based on the generation of random numbers (walking type), for locating critical slip surfaces of general shape.

2.4.3 Parabolic slip surface

This proposed method may be implemented by generating one or a series of parabolic curves, see Fig. 2.2. The x co-ordinate values are shifted along the slope surface whereas interior values of y are shifted until the minimum value of *FOS* is found. Restrictions (see non-circular slip surface) may be applied to this proposed method.

2.4.4 Composite slip surface

When geological discontinuity occurs within a soil mass, the slip surface may take circular and non-circular form simultaneously. This is called a composite slip surface (Fredlund et al., 1981). The slip surface, Fig. 2.9, starts and ends with circular parts (AB and CD), and has a central non-circular portion (BC). This intermediate segment is assumed to be as a result of the presence of an impenetrable layer. In this method, it is still possible to use a grid convention and vary the radius to seek a critical slip surface.

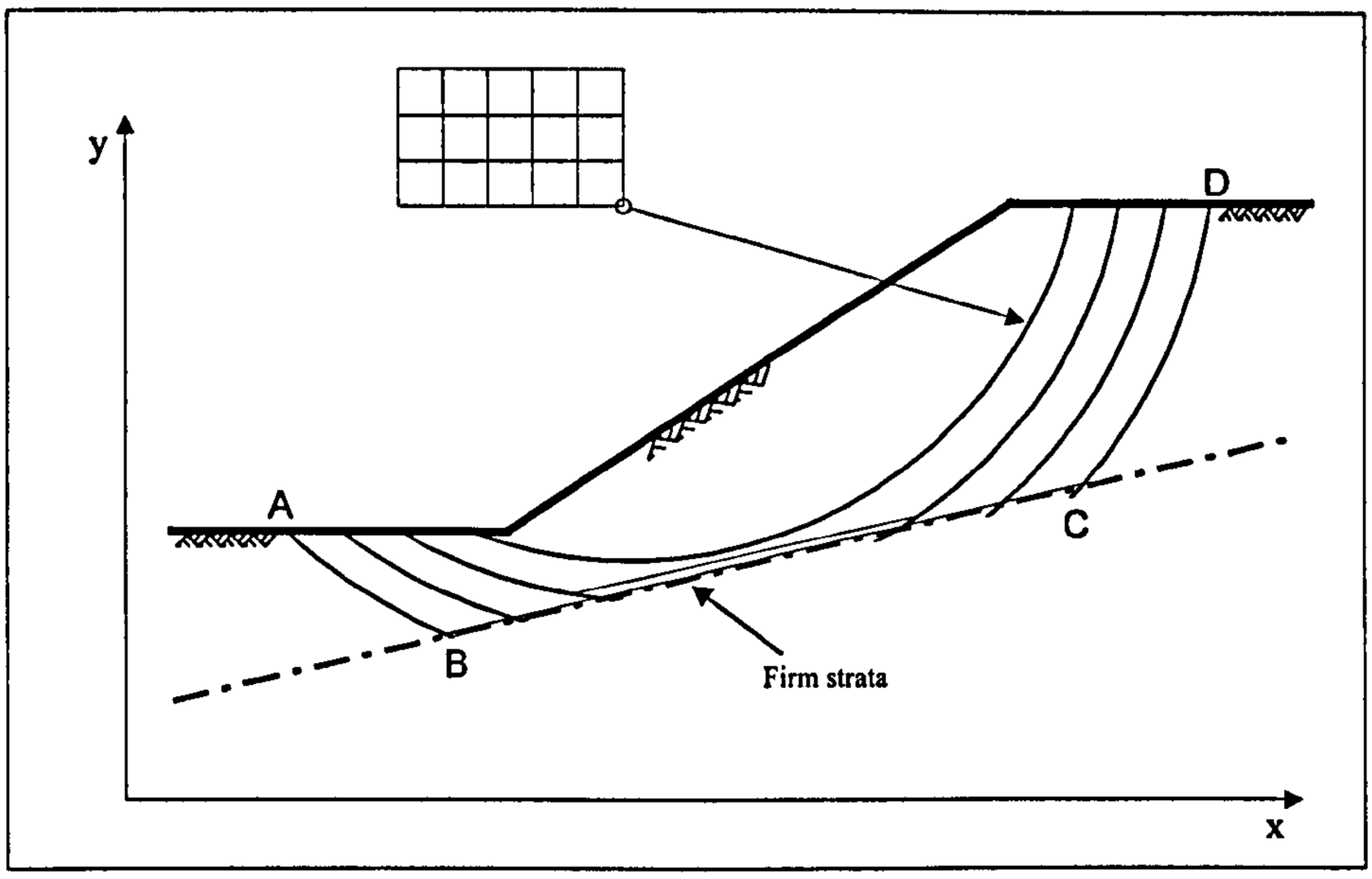

Figure 2.9 Composite slip surface.

2.5 Soil material and mechanical properties

Before the failure slip surface calculations on an assumed slope geometry, both physical and mechanical properties of the soil have to be represented. An adequate ground investigation is an essential part of the process. Relevant information should be obtained to enable an economic and safe design. The investigation should be carried out to an adequate depth and, if appropriate, to the level of the bedrock. Fredlund and Rahardjo (1993) and Craig (1997) reported that the scope of the investigation is:

1. to determine the sequence, thicknesses and horizontal length of the soil stratum;
2. to obtain representative samples of the soil for use in laboratory tests in determining strength parameters (c, ϕ); and

3. to identify the groundwater conditions. The amount of data produced will depend on the number and locations of the boreholes examined.

For uniform soils, it is assumed that the soil properties of c, ϕ and γ remain constant between a given band of co-ordinates. Even within the context of uniformity of soil properties, there could be variation in material strength parameters such as those due to overburden pressure. In the present work, changes due to overburden related calculations could be applied to all aspects of slope stability analysis. Uniform soils in need of overburden action calculations, may be divided into "imaginary" layers of increasing overburden pressure (due to self weight of the soil). In this situation, the soil strength parameters can be viewed as different for different soil layers. Since there is significant change in average values of strength parameters, there would be a new set of co-ordinates for the different layer types. This is expected give more realistic calculation results since overburden pressure has been taken into account.

2.5.1 Multi-layer conditions

After obtaining sufficient information about the site, the soil mass can be divided into different layers in terms of the strength parameters (c, ϕ), pore water pressure (u) and unit weight of soil (γ). It is obvious that different soil classifications give a new set of layers. These layers may be represented by a different band of co-ordinates which involve a sequence of straight lines, see Fig. 2.10.

2.5.2 Failure surface with geometric constraint

An obstruction such as a geological discontinuity or man-made structure (such as a tunnel) may stabilise the moving soil mass, Fig. 2.10. This is because the slip surface cannot penetrate into the discontinuity. There are two possibilities for the sliding surface. The slip surface may pass either above the discontinuity or slide over the discontinuity surface. For the case of non-circular analysis (as mentioned in section 2.2), the slip surface involves a sequence of straight lines whereas for circular analysis the slip surface may involve a circular or composite surface.

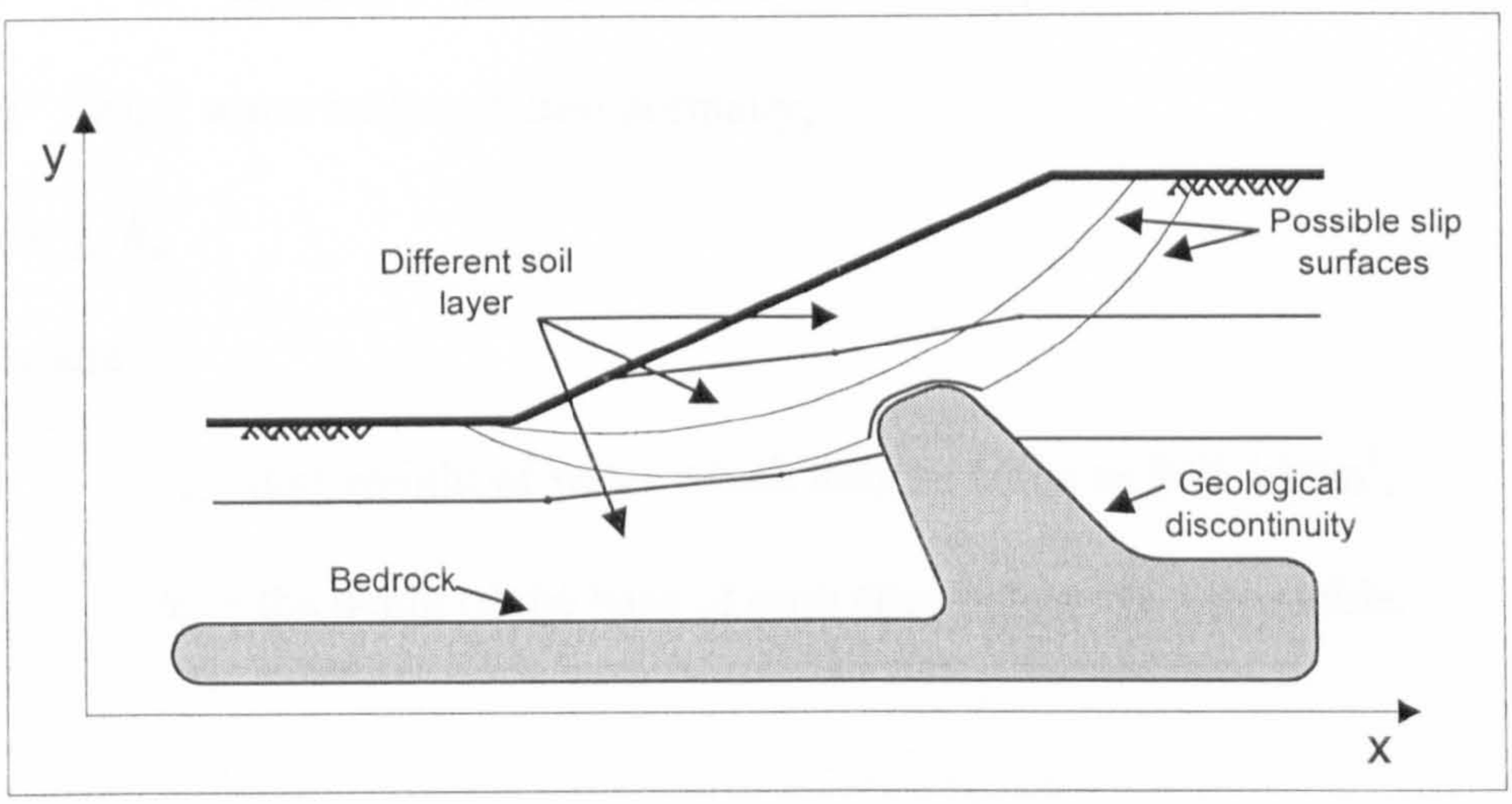

Figure 2.10 Failure surface with geological constraint.

2.5.3 Pore water pressure

Pore water pressures are likely to vary during the design life of earthworks and are relatively less well controlled than other parameters. The magnitude of pore water pressure quantities can be computed using the following alternatives:

- in terms of the pore water pressure coefficient, r_u,

$$r_u = \frac{u}{\gamma h}, \qquad 2.3$$

where

u= pore water pressure

γ= unit weight of soil

h= depth of overburden directly above the point in question, or

- using water table notation normally,

$$u = \gamma_w h_w \qquad 2.4$$

where

γ_w = unit weight of water which may be taken as 9.81 kN/m^3,

h_w = the depth of the base of each slice below the water table.

Using the r_u notation, it should be noted that the water pressure coefficient has been averaged out to represent the state of pressure due to water within the problem domain under analysis. The second notation, Eqn. [2.4], i.e. using the water table values will allow flexibility of input for local conditions.

2.5.4 Submerged slope

In the case of fully or partially submerged slopes, Fig. 2.11, the vertical weight of each slice is computed on the basis of the submerged weight below the line AB, and bulk unit weight above the line AB. If the water table within the slope lies above the line AB, then the remaining pore pressure is obtained from the difference between the piozemetric surface in each slice and the external water level AB (Barnes, 1995).

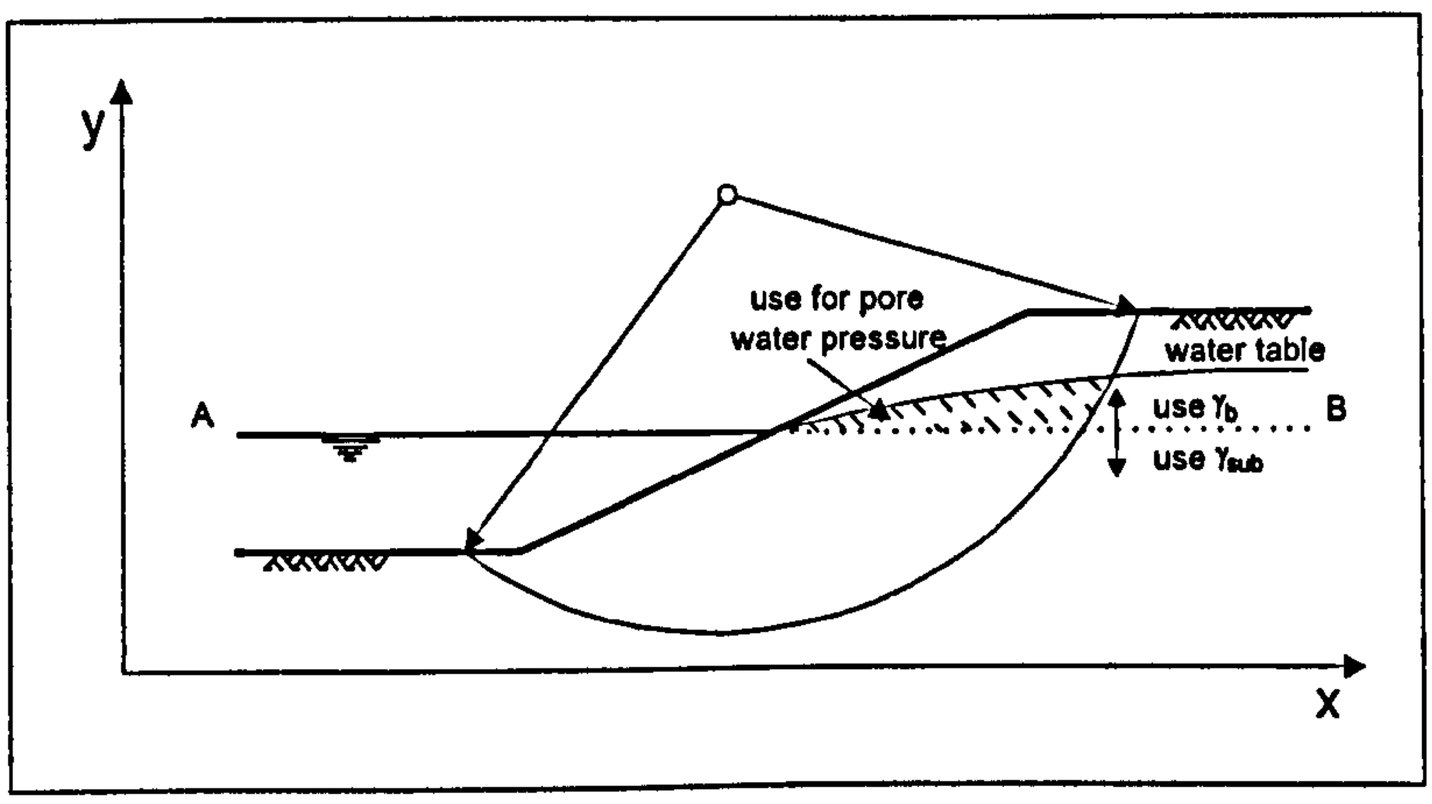

Figure 2.11 Effect of submergence (Barnes, 1995).

2.5.5 Tension crack

In cohesive soils, a tension crack may form near the top of the slope, Fig. 2.12, as the condition of limiting equilibrium develops. No shear strength can be developed in the tension crack, and when it fills with water a horizontal hydrostatic force will increase the disturbing force. This reduces the *FOS* owing to the reduced surface, AB, for the generation of shear resistance (see Fig. 2.12).

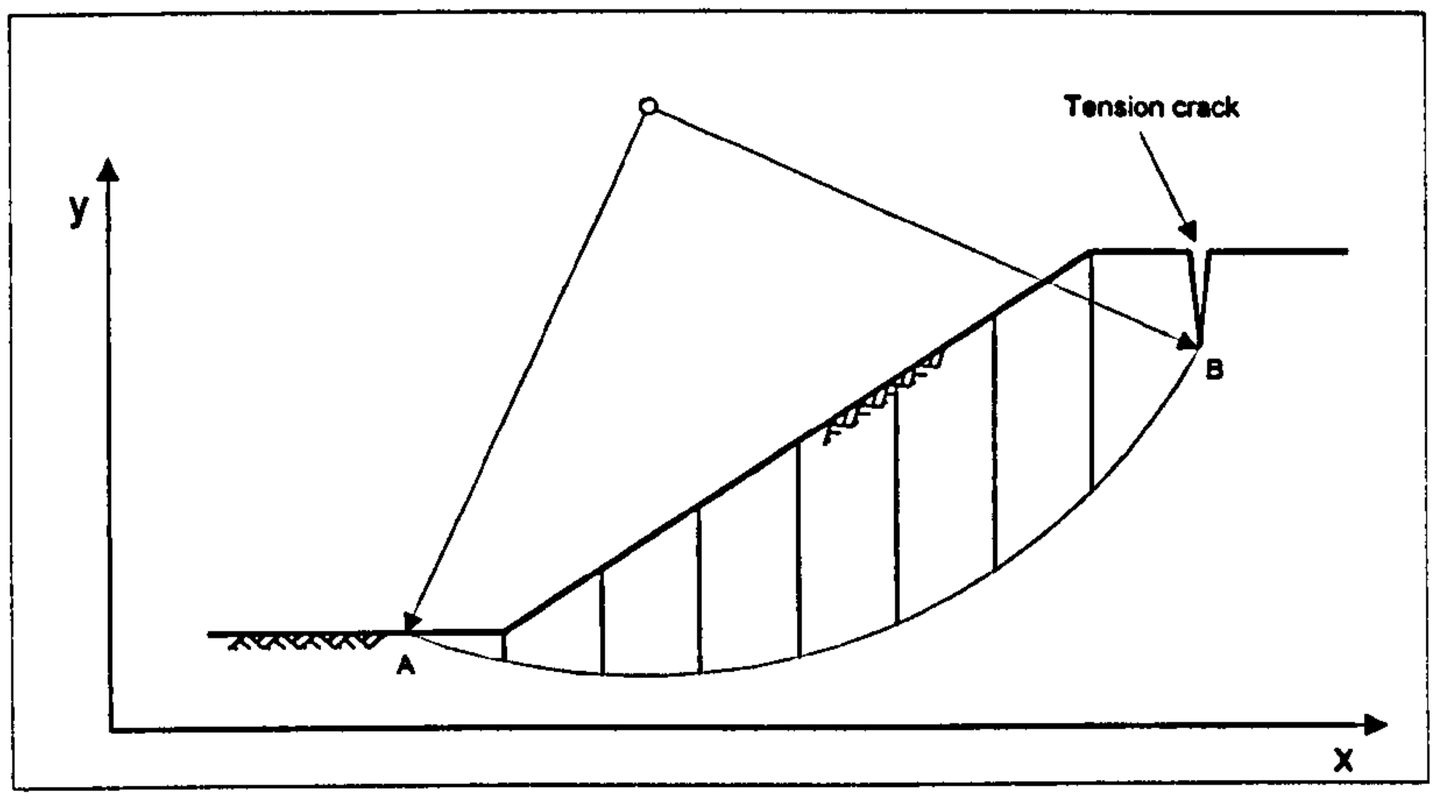

Figure 2.12 Failure surface with tension crack.

2.6 Conclusions

The possible types of slope failures and the selection of the failure surface has been reviewed in this chapter. In practice, circular failure surface determination is much easier then non-circular. However, a failure surface generally takes a non-circular form. The identification of a failure mass in a slope depends on physical and geotechnical properties of discontinuities, ground water conditions and slope geometry. These parameters should be recorded by a geotechnical engineer both in-situ and in the laboratory to define a high risk area, and possible modes of failure which are kinematically acceptable, should be identified.

CHAPTER 3: LIMIT EQUILIBRIUM THEORIES AND METHODS

3.1 Introduction

This chapter is devoted entirely to reporting the salient published methods available for slope stability analysis and for critical appraisal of various features inherent in each formulation.

Slope stability is an important field of geotechnics, which is of particular interest to many soil scientists and technologists responsible for soil management and engineering. The idea is to have a means of predicting the balance of actions which are responsible in disturbing or restoring the equilibrium of a given soil (or rock) produced mass, with a given specific geometry and properties. Significant effort has been made in proposing formulae in an attempt to model and predict a "factor of safety" analytically for man-made and natural slopes.

Limit equilibrium methods are the most widely used in slope stability investigations, although they have a great deal of mathematical calculations needed for the iterations to evaluate a factor of safety (*FOS*). Some of the most important characteristics of these methods are the inclusion of the pore pressure effect and the calculation of the

interslice force in the *FOS* calculations (Kumsar, 1993). Experience shows that these methods can be useful in practise (Nash, 1987).

Slope failures generally occur in three-dimensional form, conventional limit equilibrium methods have been developed mostly in two-dimensional assumptions owing to the considerable mathematical complexities introduced in three dimensions (Kumsar, 1993).

The various methods, to include the formulae and appropriate illustrations, have been compiled and presented in Appendices A and B for succinctness. The focus in this section is to provide a critical assessment of the method rather than justification for original formulation.

3.2 Limit equilibrium methods of analysis

In limit equilibrium methods it is assumed that the slope will slide by a mass of soil sliding on a failure surface. At the moment of failure, the shear strength is fully mobilised all the way along the failure surface, and the overall slope and each part of it are in static equilibrium (Nash, 1987). Graham (1984) stated that the term limit equilibrium is applied to a system of forces, which are just on the point of failing.

The shear strength of the soil is given by the Mohr-Coulomb failure criterion;

$\tau = c_u$ (for total stress analysis), or

$\tau = c' + \sigma' \tan \phi'$ (for effective stress analysis),

where τ is shear strength, c_u is apparent undrained cohesion, c' is effective cohesion, σ' is effective normal stress and ϕ' is effective frictional angle.

3.2.1 Factor of safety

Factor of safety (*FOS*, in the equation form it will be taken as *F*) is the most widely used index of stability. It may be determined as the proportion of the total force available to resist failure to the total force tending to cause failure. This can be shown as;

$$F = \frac{\sum \text{Resisting force}}{\sum \text{Disturbing force}}.$$

When the total resisting force is equal to the total disturbing force, the slope is in equilibrium and $F = 1$. Nevertheless, the slope may fail under the effect of any amount of disturbing actions (loading). Kumsar (1993) reported that the acceptable *FOS* for slope stability may vary from organisation to organisation however many of them utilise values of 1.2-1.3 for short term, less important slopes and 1.4-1.5 for important long term slopes.

In the following part of this chapter, some of the well-known limit equilibrium methods which have been developed in two dimensions will be summarised in detail.

3.2.1.1 Fellenius method

Fellenius (1936) is thought to be amongst the first to propose the simplest of all the methods which makes use of vertical sided slices. The method is easy to understand and to use, but is viewed as rather simplistic these days. It is also known as the 'Swedish', 'Ordinary' or 'USBR' method.

Considering the equilibrium of the *i*-th slice of Fig. 3.1(a), and resolving perpendicular to the slip surface;

$$W_i \cos\alpha_i = N_i + u_i l_i \ , \qquad 3.1$$

$$N'_i = W_i \cos\alpha_i - u_i l_i \ . \qquad 3.2$$

where W is weight of slice, l is length of base of slice and α is angle of base of slice to horizontal.

The normal effective force on the base of each slice can be found by resolution to be $W_i \cos\alpha_i$, the subtraction of the pore water pressure u_i resultant along the slip surface (l_i) $u_i l_i$ gives the normal effective force N'.

The factor of safety is derived from the summation of the moments about a common point i.e. either a fictitious or real centre of rotation for the entire mass.

$$\sum \text{disturbing moments} = \sum RW_i \sin\alpha_i$$

$$= R\sum W_i \sin\alpha_i \quad , \qquad 3.3$$

$$\sum \text{restoring moments} = \frac{R}{F}\sum c'l_i + N'_i \tan\phi' \ ,$$

$$= \frac{R}{F}\sum c'l_i + (W_i \cos\alpha_i - u_i l_i)\tan\phi' \ , \qquad 3.4$$

for equilibrium of the whole sliding mass,

$$R\sum W_i \sin\alpha_i = \frac{R}{F}\sum c'l_i + (W_i \cos\alpha_i - u_i l_i)\tan\phi' \ ,$$

therefore;

$$F = \frac{\sum c'l_i + (W_i \cos\alpha_i - u_i l_i)\tan\phi'}{\sum W_i \sin\alpha_i} \ , \qquad 3.5$$

where R is radius.

A search should be made for the slip surface, which gives the lowest factor of safety.

In this method, it is assumed that the interslice vertical and horizontal forces, see Fig. 3.1(a), X_i and X_{i+1}, E_i and E_{i+1} are equal and opposite for each slice, and so cancel. The above formula can easily be calculated, but it has been found to yield conservative results (lower than actual factors of safety) especially where the slip surface is deep or the pore water pressures are high. This inaccuracy has been

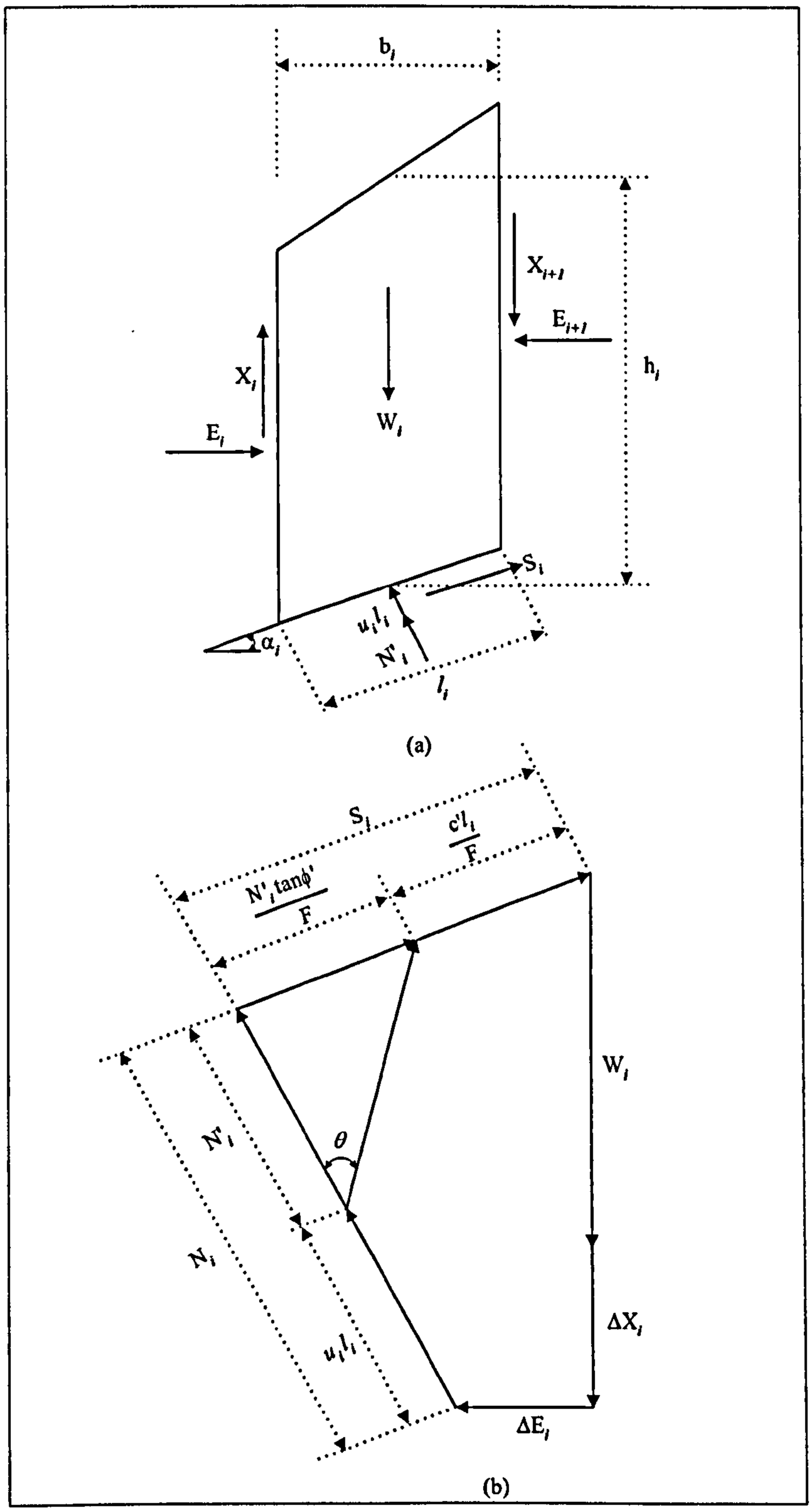

Figure 3.1 Polygon of forces on a slice.

ΔX is the difference between the interslice shear forces ($X_i - X_{i+1}$)

ΔE is the difference between the interslice normal forces ($E_i - E_{i+1}$).

evaluated; for example, according to Whitman and Bailey (1967), Fellenius's method may err by as much as 60% for problems with deep failures and high pore pressure. Generally the Fellenius solution underestimates the factor of safety by between 5-20%. Results are acceptable, but this may lead to uneconomical design (Clayton et al., 1993).

3.2.1.2 Bishop method

Bishop (1955) presented a method in which the interslice vertical and horizontal forces X and E were taken into account in the analysis. Both methods are only applicable to circular slip surfaces where moment balancing of actions are considered, since the circular geometry is ideal for constant lever arm values for tangential forces at the circumference.

For a mathematically correct static solution, equilibrium of forces and moments must exist for each slice as well as the sum of the slices. Bishop's rigorous formulation contains too many unknowns to enable a direct solution to be found. Some assumptions must be made regarding the distribution of some of the unknown quantities, and for this method assumptions are made concerning the X force distribution.

The analysis reduces to balancing vertically the critical forces (from a force polygon) as shown Fig. 3.1(b) and then rearranging the equation. The normal effective force N' is found as;

$$N' = \frac{W_i + (X_i - X_{i+1}) - u_i l_i \cos\alpha_i - \frac{c'}{F} l_i \sin\alpha_i}{\cos\alpha_i + \frac{\sin\alpha_i \tan\phi'}{F}} \quad . \qquad 3.6$$

This normal effective force can replace that assumed in the conventional method in the computation of the maximum available strength on the appropriate segment of the slip surface. The factor of safety is derived from the summation of moments about a common point and on substituting $l_i = b_i \sec\alpha$, it follows as;

$$F = \frac{\sum \{c' b_i + [W_i - u_i b_i + (X_i - X_{i+1})] \tan\phi'\} m\alpha_i}{\sum W_i \sin\alpha_i} \qquad 3.7$$

where b is width of the slice, and

$$m\alpha_i = \frac{\sec\alpha_i}{1 + (\tan\alpha_i \tan\phi' / F)}$$

Values of F, and of X (i.e. ΔX) for every slice that satisfy this equation give a rigorous solution to this problem.

Having to make an assumption about the X forces makes the solution process more complex and so the form of Bishop's equation which is used by many engineers, is the

simplified or modified version, for which it is assumed that the difference in the X forces (i.e. ΔX) for any slice is zero. This type of analysis is sufficiently accurate for most practical purposes and is probably the most widely used method of slope stability analysis. The simplified form is,

$$F = \frac{\sum [c' b_i + (W_i - u_i b_i) \tan \phi'] \frac{\sec \alpha_i}{1 + (\tan \alpha_i \tan \phi' / F)}}{\sum W_i \sin \alpha_i} \quad . \qquad 3.8$$

The pore pressure coefficient, r_u, can be used to represent overall or local pore pressure in a slope. This is given by the ratio of the pore water pressure in Eqn. [2.3] and for convenience is rewritten below as;

$$r_u = \frac{u}{\gamma h} \quad , \qquad 3.9(a)$$

where γ is unit weight of soil, h is height of slice and u is related to local pore pressure in terms of γ_w (unit weight of water) and h_w (height of water table from base of the sliding surface to the water table) given in Eqn. [2.4] as;

$$u = \gamma_w h_w \quad . \qquad 3.9(a)$$

Equation [3.8] can be rewritten as,

$$F = \frac{\sum [c' b_i + W_i (1 - r_u) \tan \phi'] \frac{\sec \alpha_i}{1 + (\tan \alpha_i \tan \phi' / F)}}{\sum W_i \sin \alpha_i} \quad . \qquad 3.10$$

Bishop and Morgenstern (1960) pointed out that the difference between the rigorous and simplified equations is generally less than 1%. Whitman and Bailey (1967) have looked closely at the performance of the Bishop simplified method and have concluded that the error involved in using this type of analysis against the more rigorous formulation is "7% or less, usually only 2% or lower". These authors also point out that the method may be inaccurate in the case where the angle α of the base of the slice was negative (which may happen at the toe of the circle). They suggest that the value of the term $m\alpha$ should be checked and if $m\alpha \leq 0.2$ the results should be regarded as unreliable. Then more slices should be tried to improve accuracy and if this fails another method of analysis should be tried to determine if a feasible solution can be obtained.

Bishop's equation involves a factor of safety on both sides and so an iterative technique must be used in order to obtain a solution. In practice this is often done by computing the *FOS* using the Fellenius method, which is then used as an initial value to estimate the quantity $m\alpha$. Mostyn and Small (1987) pointed out that in most cases, if the Fellenius method is used for estimating the *FOS* initially, only 2 or 3 iterations are necessary to obtain a converged solution accurate to 2 decimal places with the simplified Bishop method.

Fredlund et al. (1992) reported that Bishop simplified method is probably the most widely used of all the methods of analyses in circular failure analysis since it is easy

to apply and gives a *FOS* similar to that of rigorous methods such as those developed by Morgenstern and Price (1965) and Spencer (1967).

3.2.1.3 Janbu Simplified method

Janbu (1954, 1973) proposed the first method for the analysis of non-circular failure surfaces. This method is applicable to both circular and non-circular slip surfaces. The interslice shear forces are assumed to be zero. The Janbu simplified method uses the horizontal force equilibrium equation, rather than the moment equilibrium equation;

$$F = \frac{\sum \left[c' b_i + \left(W_i - u_i b_i \right) \tan \phi' \right] \frac{\sec^2 \alpha_i}{1 + \left(\tan \alpha_i \tan \phi' / F \right)}}{\sum W_i \tan \alpha_i} \quad . \qquad 3.11$$

(See Fig. 3.2 and Appendix A for full derivation the formula.)

There are only two differences between Eqn. [3.11] and Eqn. [3.8], Bishop simplified method. These are:

- Janbu uses $\sec^2 \alpha$ instead of $\sec \alpha$ in the numerator, and
- Janbu uses $\tan \alpha$ instead of $\sin \alpha$ in the denominator.

Once the factor of safety is obtained by iteration, then the empirical correction factor is multiplied by the computed *FOS* in order to account for the effect of the interslice shear forces, so that;

$$FOS = f_o \, F_{calculated} \,, \qquad 3.12$$

where f_o is a correction factor which depends on the slip surface ratio (d/L) and the strength parameters, see Fig. 3.2.

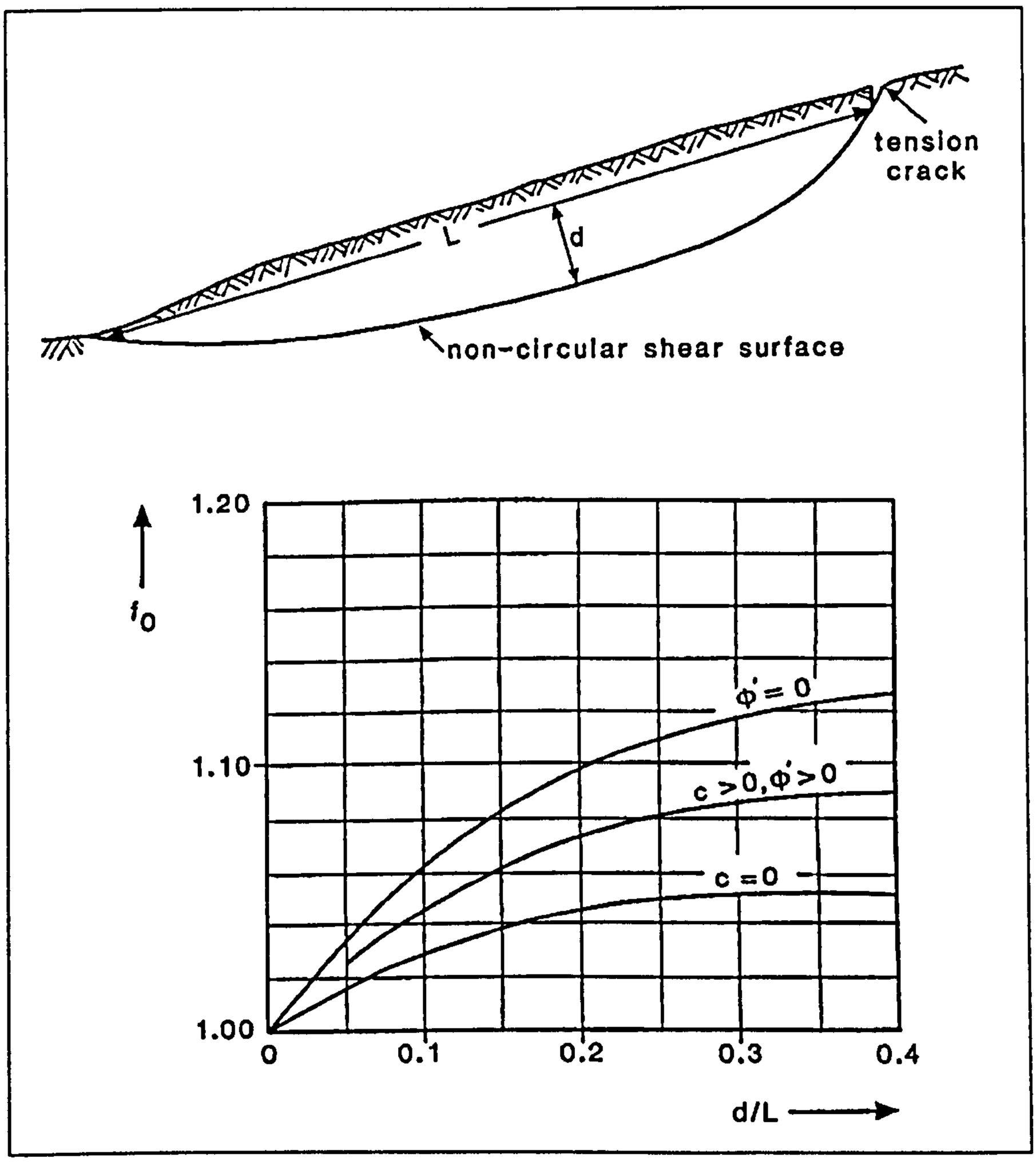

Figure 3.2 Correction factor, f_o, for Janbu simplified method (Clayton et al., 1993).

Fredlund et al. (1981) pointed out that the correction factor generally increases the factor of safety by up to 10%. Bromhead (1992) asserted that the correction factor has a maximum value of 13% for the increase in the factor of safety. Janbu (1973) suggested that the simplified method should only be used when a computer was not available.

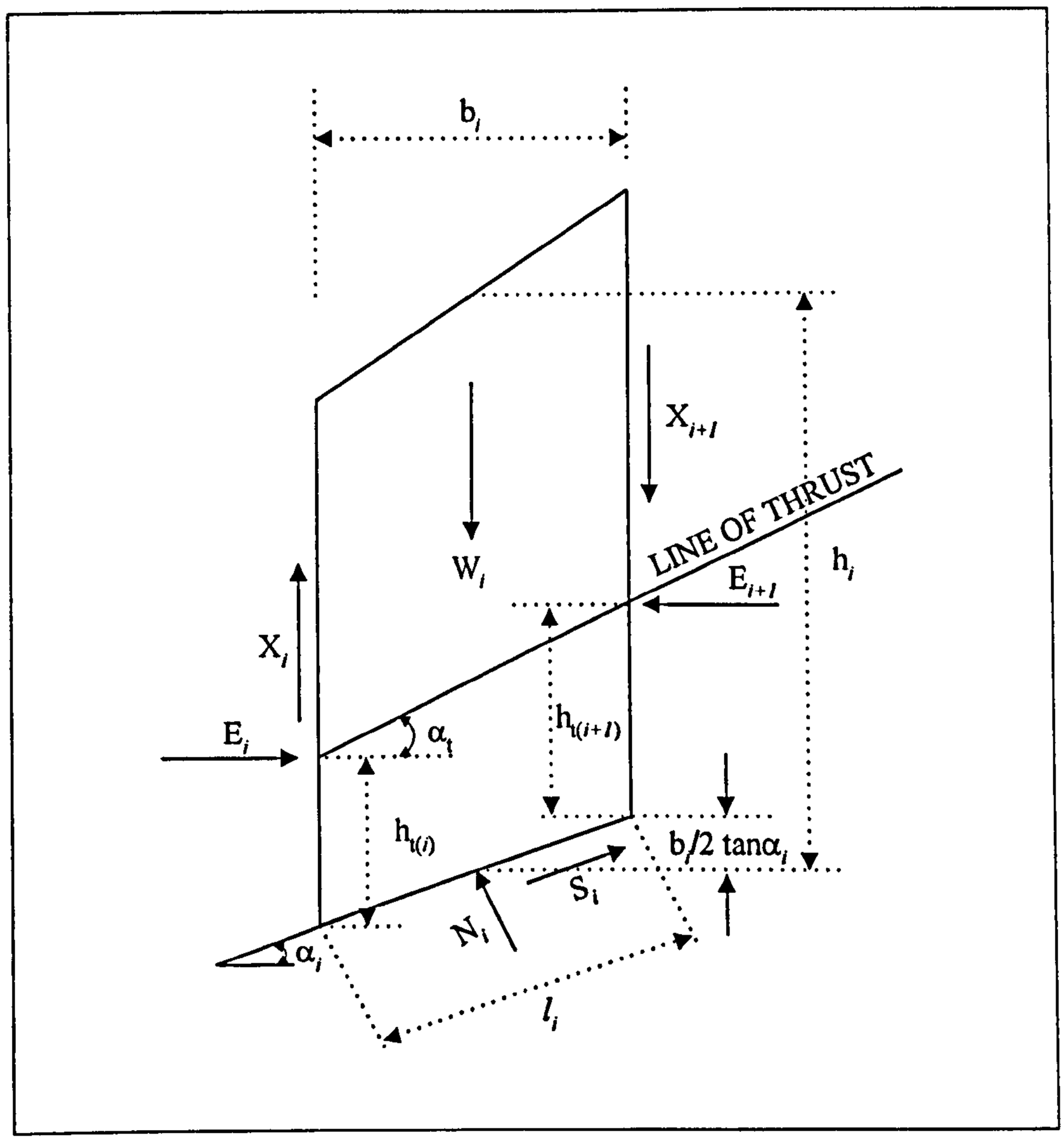

Figure 3.3 Forces acting on each slice for generalised Janbu method (Janbu, 1973).

3.2.1.4 Janbu generalised method

Janbu (1957, 1973) presented a generalised method of analysis which may also be applied to both circular and non-circular slip surfaces. This was the first method of slices in which overall force equilibrium and overall moment equilibrium are satisfied (Nash, 1987). Once again the horizontal force equilibrium is used to compute the *FOS*. Janbu's generalised method differs from the simplified method in that the shear forces are retained during the derivation of the normal force. In this method, Janbu takes the interslice normal forces into account by assuming the existence of a line of thrust (h_t) through the points where interslice forces act, see Fig. 3.3. The line of thrust is assumed to act at one-third the height of each slice.

In order to solve the *FOS* equation, the interslice shear forces must be evaluated. For the first iteration, the shear forces are set to zero. The horizontal interslice normal forces are obtained by combining the summation of both the vertical and horizontal forces on each slice to provide;

$$E_i = (W_i + \Delta X_i)\tan\alpha_i - [c'b_i + (W_i + \Delta X_i - u_i b_i)\tan\phi']\frac{\sec^2\alpha_i}{1+(\tan\phi'\tan\alpha_i/F)}, \qquad 3.13$$

here

$\Delta X_i = X_{i+1} - X_i$.

For subsequent iterations, Janbu takes the summation of the moments at the centre of the base of each slice to calculate the interslice shear forces as;

$$X_i = E_i \tan\alpha_i - \frac{(E_{i+1} - E_i)}{b_i} h_{ti} \quad . \qquad 3.14$$

Equation [3.11] can be rewritten in generalised form to provide;

$$F = \frac{\sum [c' b_i + (W_i + \Delta X_i - u_i b_i)\tan\phi'] \frac{\sec^2 \alpha_i}{1 + (\tan\alpha_i \tan\phi' / F)}}{\sum W_i \tan\alpha_i}. \qquad 3.15$$

The magnitude of the interslice shear forces will lag by one iteration and each iteration gives a new set of shear forces. Sarma (1979) pointed out that the moment equilibrium of the last slice is not satisfied; this influences of the line of thrust but does not affect the factor of safety.

3.2.1.5 Morgenstern and Price method

This is the first method by Morgenstern and Price (1965, 1967) where all boundary and static equilibrium conditions are satisfied. The method can be used to analyse the failure surface in any shape, circular, non-circular or compound. The process basically involves dividing the failure surface into infinitesimal slices. The solution for the factor of safety is derived from the summation of forces tangential and normal to the base of a slice and the summation of moments about the centre of the base of each slice (see Fig. 3.4).

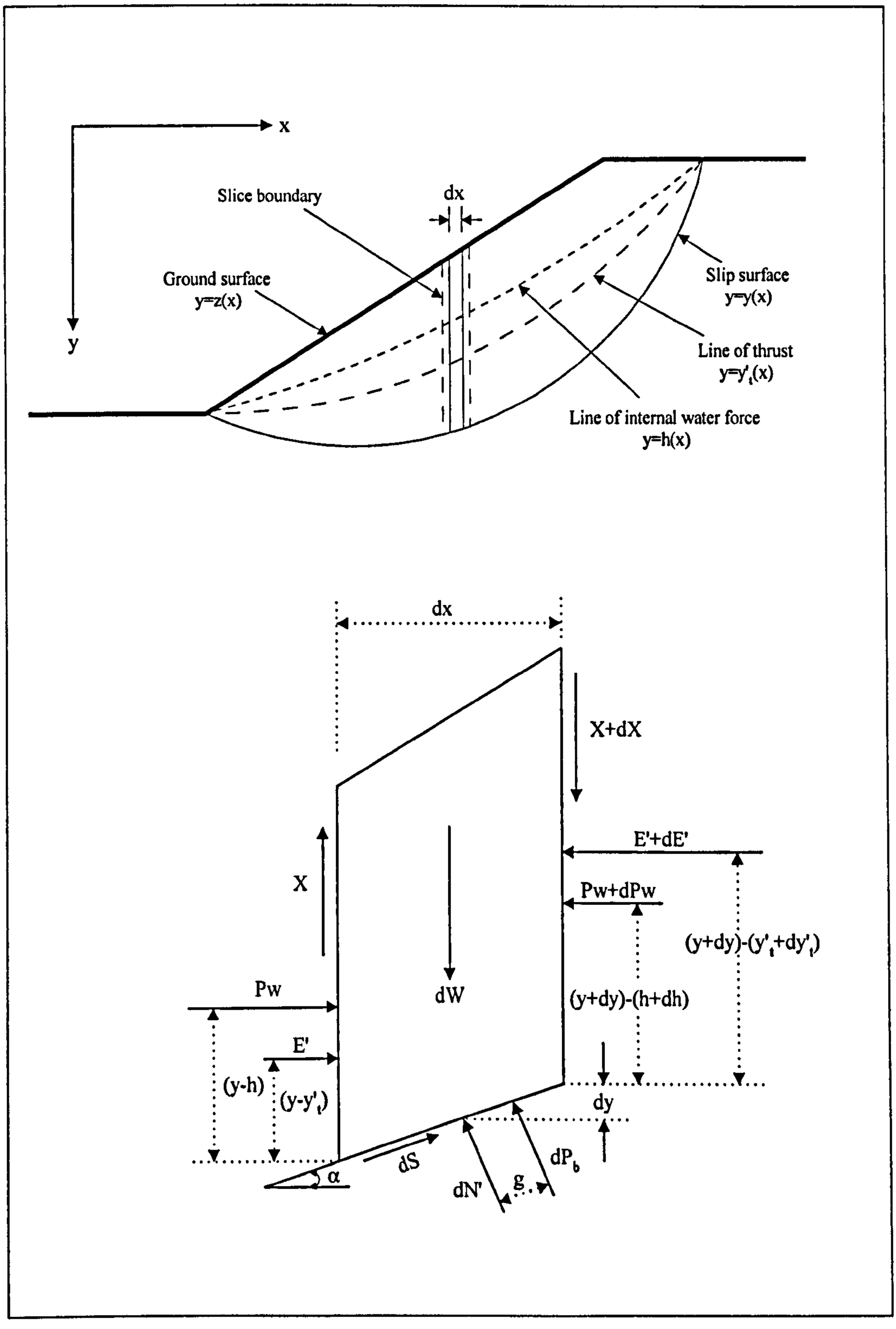

Figure 3.4 Forces acting on a slice for Morgenstern and Price (Craig, 1997).

The main difference between the Janbu generalised method and the Morgenstern and Price method is in the way that interslice forces are defined. For this method, the solution requires an arbitrary mathematical assumption regarding the direction of the resultant of the interslice shear and normal forces given as;

$$X = \lambda f(x) E \ ,$$

here $f(x)$ is a function chosen to represent the pattern of variation of the ratio X/E across the slip surface and λ is a constant scaling factor, see Fig. 3.5.

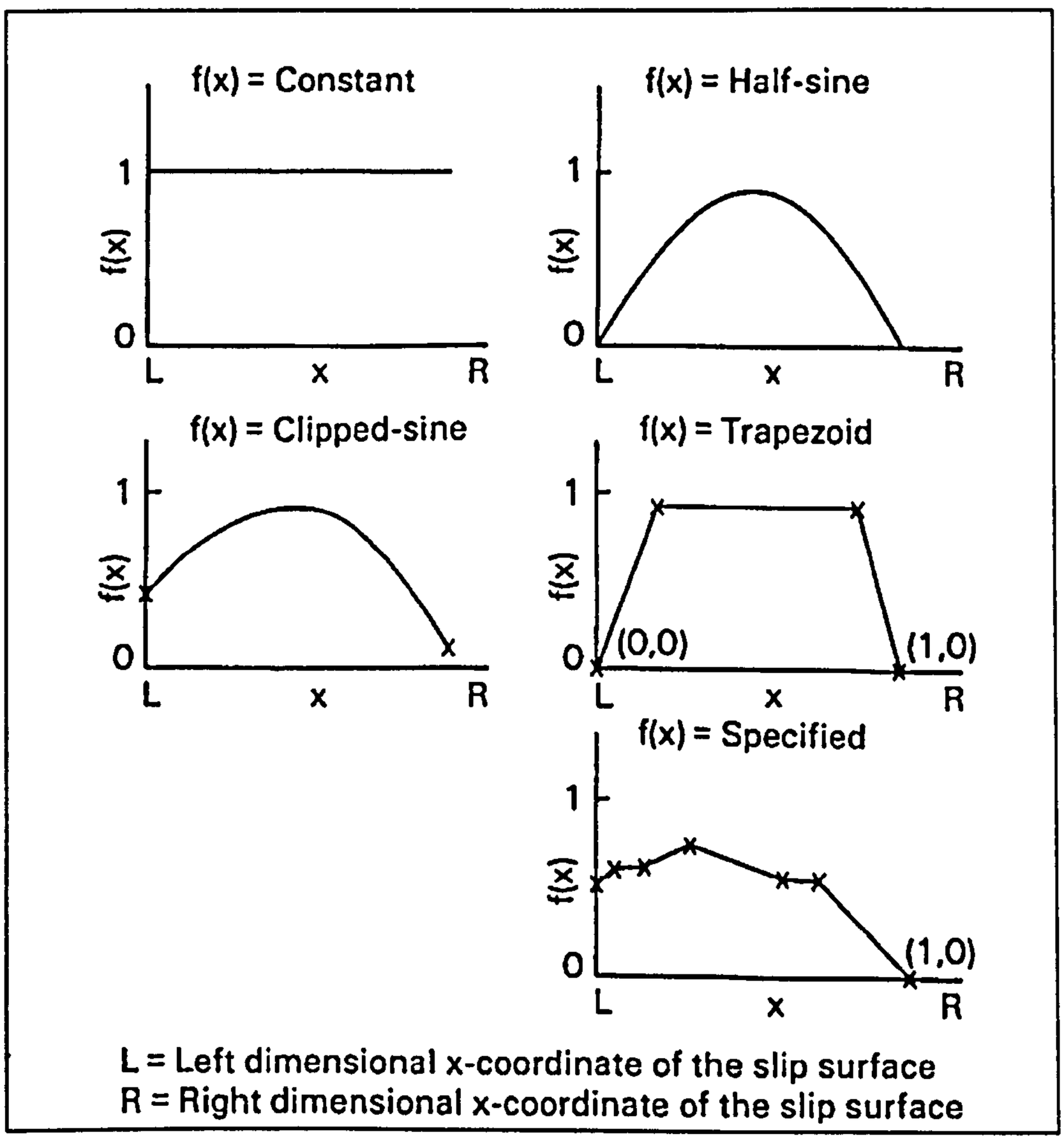

Figure 3.5 Various possible interslice force functions (Fredlund and Rahardjo, 1993).

To obtain a solution the slip surface, with any slope geometry and material properties, is divided into a series of slices of finite width by vertical lines.

The boundary conditions are in terms of the force E and moment M taken as zero when $x = x_0$. Integration is carried out across each slice in turn. The calculation starts with "guessed" values for λ and F. However specification of $E_n = 0$ and $M_n = 0$ at the end of the failure surface, will not be satisfied in general. Then, a systematic iteration technique, based on the Newton-Raphson method (Morgenstern and Price, 1967), is used to modify the values of λ and F until the values of E_n and M_n at the end of the slip surface are both effectively zero. (For the calculation of E_n, M_n and their derivatives see Appendix B).

Bromhead (1992) reported that the *FOS* is not significantly affected by the choice of the function *f(x)* and as a consequence *f(x)*=1 is a common assumption.

The following conditions must result for a solution to be admissible:

- The calculated line of thrust must be reasonable; that is the resultant of the interslice forces on any section should pass within the bounds of the ground surface and the slip surface.
- The failure criteria for the soils must not be violated. Thus the shear strength between the individual slices must not be exceeded.
- The normal stress at the base of each slice should be compressive, Mostyn and Small (1987), Clayton et al. (1993) and Craig (1997).

3.2.1.6 Spencer method

Another way of taking interslice forces into account is the Spencer (1967) method. The method is considered in terms of effective stress and is based on a modification to the Bishop simplified method. Unlike the latter, the Spencer method satisfies both force and moment equilibrium conditions. By resolving forces perpendicular and parallel to slip surface, the resultant of two interslice forces (Q_i) are derived. Moreover, it is assumed that these interslice forces act at the middle of the base of the slice with an angle of θ, see Fig. 3.6.

The resultant of the two interslice forces are obtained by the following equation;

$$Q_i = \frac{\frac{c'b_i}{F}\sec\alpha_i + \frac{\tan\phi'}{F}\left(W_i\sin\alpha_i - u_i b_i \sec\alpha_i\right) - W_i\sin\alpha_i}{\cos\left(\alpha_i - \theta\right)\left[1 + \frac{\tan\left(\alpha_i - \theta\right)\tan\phi'}{F}\right]} \quad . \qquad 3.16$$

The Spencer (1967) method involves two factors of safety equations. The first is based on the summation of forces parallel and normal to the base of the slice, [factor of safety with respect to force calculation (F_f)], whereas the second represents the summation of moments about a central point such as a trial centre of circle giving a factor of safety in terms of moment calculation (F_m).

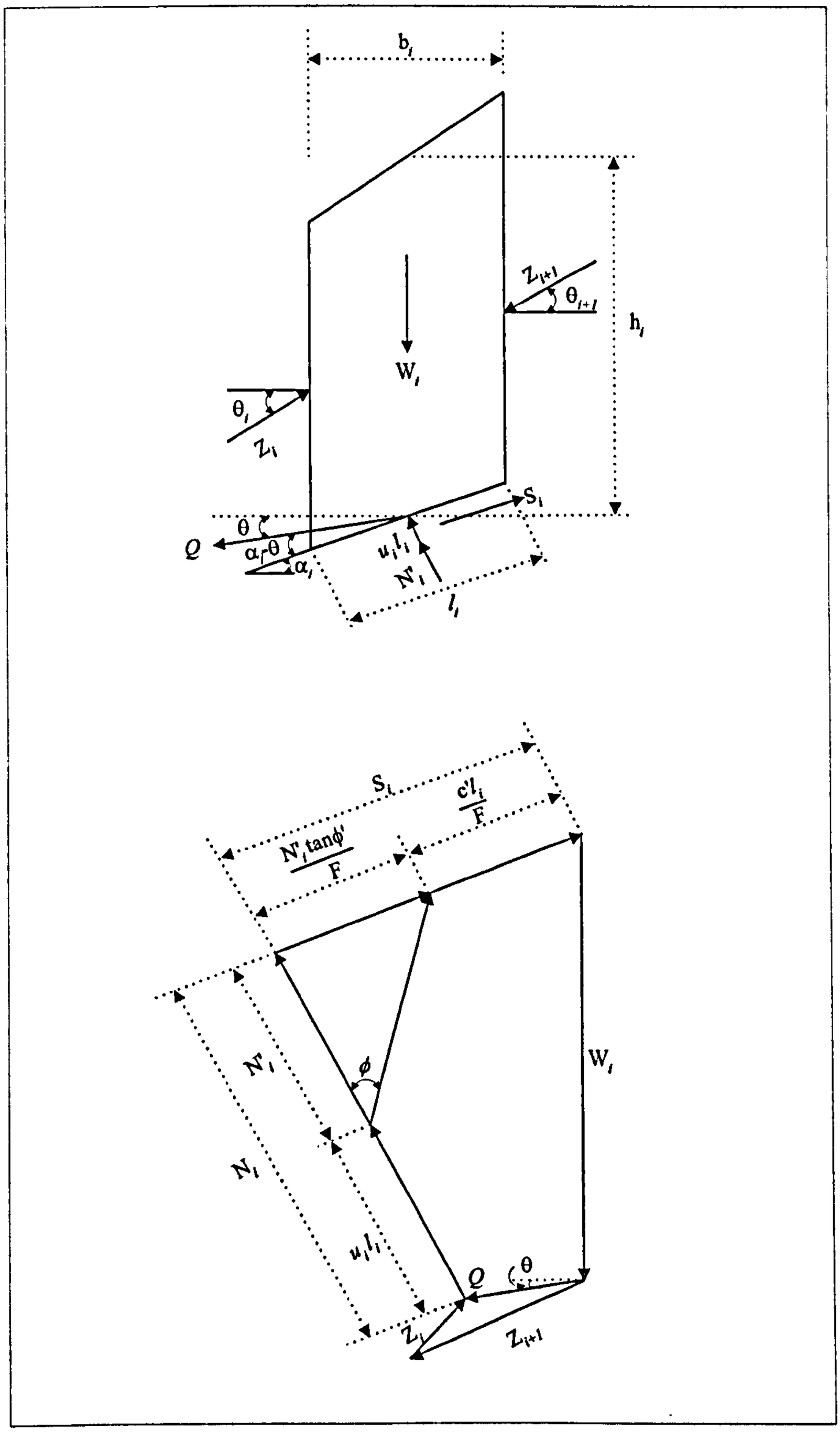

Figure 3.6 Polygon of forces on a slice as result of identifying interslice forces (Spencer, 1967).

For equilibrium, the vectorial sum of the horizontal interslice forces and the sum of their vertical components must be zero. This expression yields for F_f ;

$$\sum(Q_i \cos\theta) = 0 \ , \qquad 3.17$$

$$\sum(Q_i \sin\theta) = 0 \ , \qquad 3.18$$

and also the sum of the moments of the interslice forces about the centre of rotation must be zero. The following can be obtained for F_m ;

$$\sum[Q_i \cos(\alpha - \theta)] = 0 \ . \qquad 3.19$$

The forces can be found by solving Eqns. [3.17] and [3.18], whereas the moments are available from Eqn. [3.19].

To simplify the solution, the interslice forces are assumed to be parallel (i.e. θ is constant). Therefore Eqns. [3.17] and [3.18] become;

$$\sum Q_i = 0 \ . \qquad 3.20$$

Constant values of θ correspond to $f(x)$ = constant in the Morgenstern and Price (1965) method. According to Mostyn and Small (1987) and Chowdhury (1992), this assumption is quite unrealistic because θ varies from slice to slice. Nash (1987) stated

that the Spencer method is in line with Bishop's equation and justifies the widespread application of Bishop's method.

3.2.1.7 Sarma method

Sarma (1973) proposed a totally different approach to the slope stability calculations. The method is applicable to any shape of configured slip surface. It is based on the principle of limit equilibrium and the method of slices. Effective stress analysis is used to determine the problem. His method determines the critical horizontal acceleration (K=K_c) which would just cause failure of the slope.

The sliding mass is divided into a number of slices with vertical boundaries. (In the latest modified version of this method, Sarma (1979) provides for inclined interslice boundaries. This is outside the scope of the present work.) From Fig. 3.7, forces parallel and perpendicular to each slice, relative to the slip surface, are resolved using the Mohr-Coulomb failure criterion. Equations for normal and shear forces at the base of the slice are written to be;

$$N_i = \frac{(W_i - \Delta X_i - c'_i b_i \tan\alpha_i + u_i \tan\phi'_i \sin\alpha_i)\cos\phi'_i}{\cos\alpha_i \cos\phi'_i + \sin\phi'_i \sin\alpha_i} \quad \text{, and} \qquad 3.21$$

$$S_i = \frac{(W_i - \Delta X_i - u_i \cos\alpha_i)\sin\phi'_i - c'_i b_i \cos\phi'_i}{\cos\alpha_i \cos\phi'_i + \sin\phi'_i \sin\alpha_i} \quad . \qquad 3.22$$

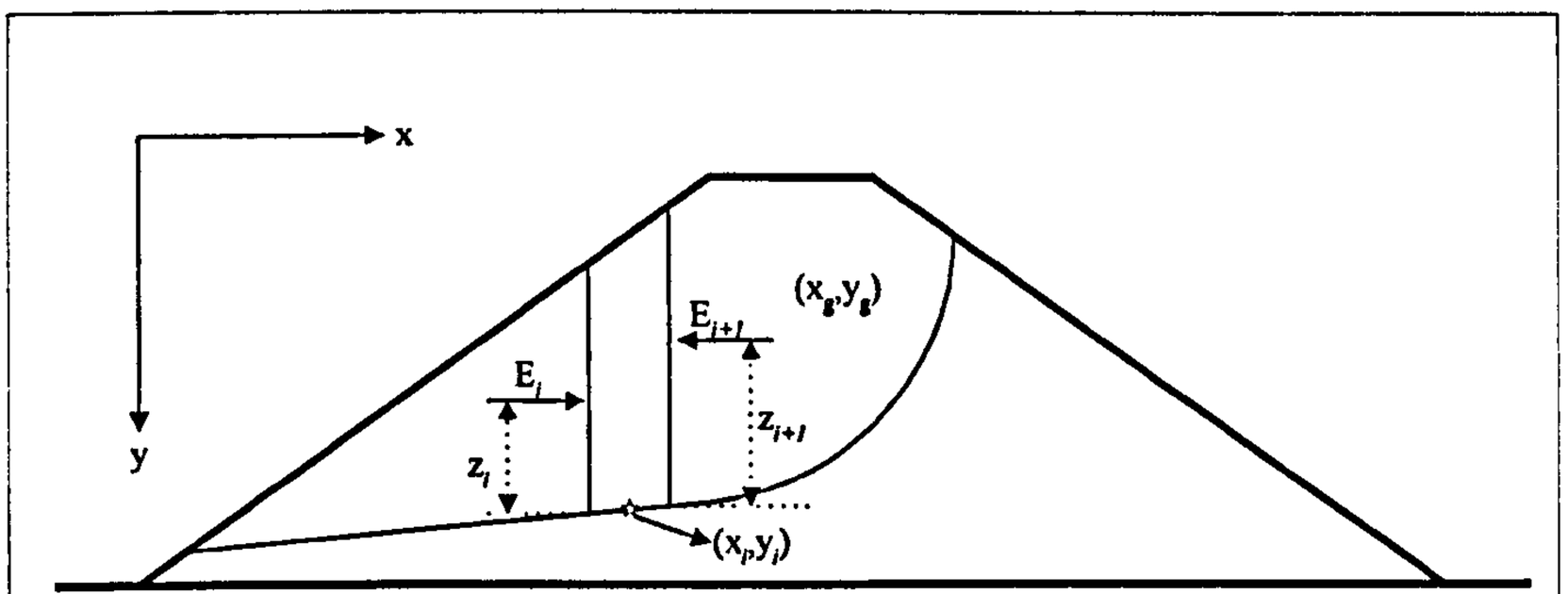

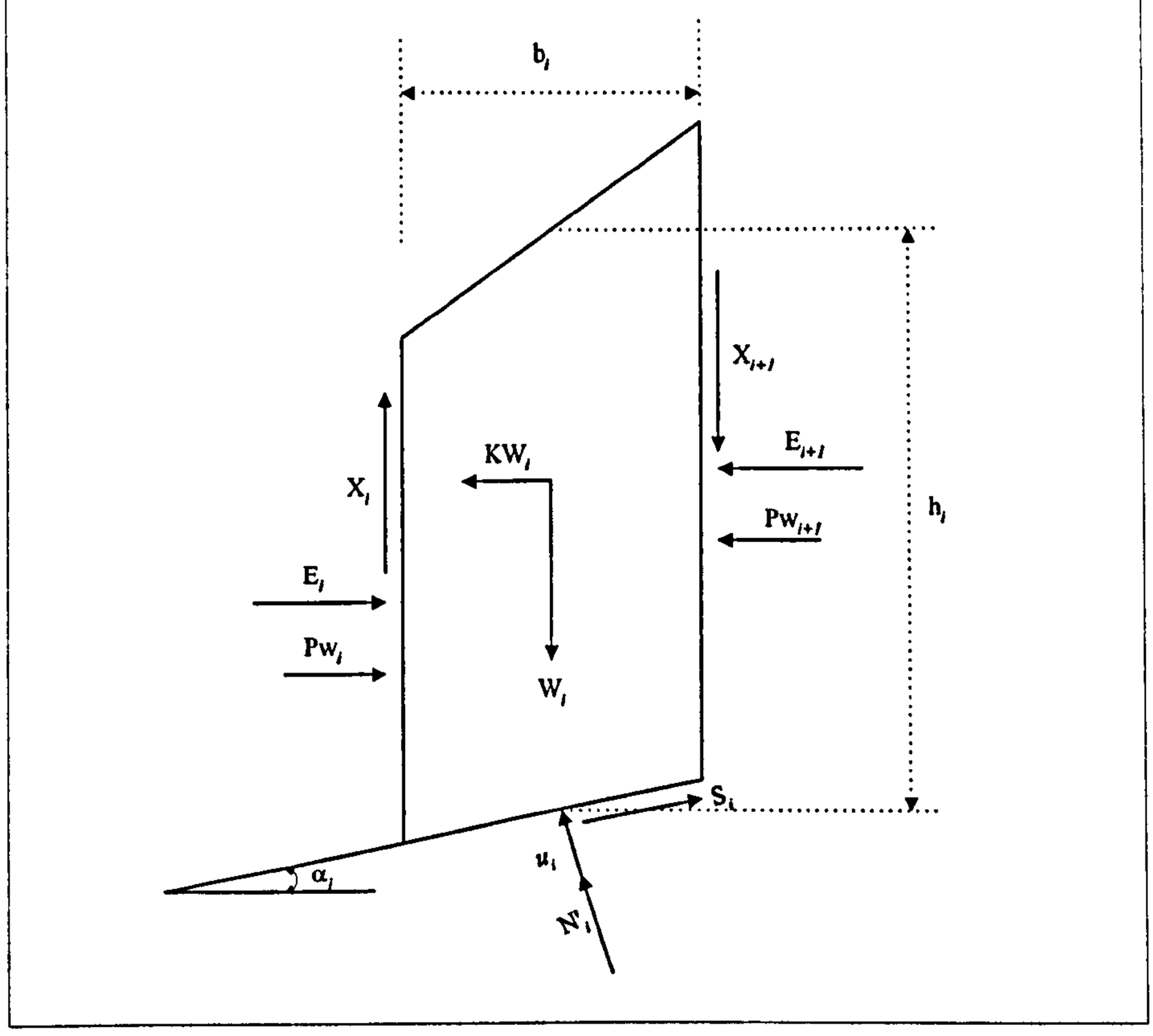

Figure 3.7 Forces acting on a slice for Sarma method (Sarma, 1973).

The maximum horizontal seismic force which can be applied to the slice is obtained from;

$$KW_i = D_i - \Delta E_i - \Delta X_i \tan(\phi'_i - \alpha_i) , \qquad 3.23$$

where $\Delta E_i = E_i - E_{i+1}$ and D_i is given by;

$$D_i = W_i \tan(\phi'_i - \alpha_i) + \frac{c'_i b_i \cos\phi'_i \sec\alpha_i + u_i \sin\phi'_i}{\cos\alpha_i \cos\phi'_i + \sin\phi'_i \sin\alpha_i} \quad , \qquad 3.24$$

see Fig. 3.7.

Equation [3.23] can be summed over all the slices to determine the horizontal seismic force. Upon completion of the process, the sum of $\Sigma\Delta E$ must be zero. This yields the main force equilibrium equation for the sliding mass which results in the following;

$$\sum \Delta X_i \tan(\phi'_i - \alpha_i) + \sum KW_i = \sum D_i \quad . \qquad 3.25$$

In order to obtain complete equilibrium of the sliding mass, the moment equilibrium must also be satisfied. To produce this, moments can be taken at any point. Sarma has chosen the centre of gravity of the sliding mass, with co-ordinates (x_g, y_g), see Fig. 3.7. Noting that the sum of W_i and KW_i vanish and that the interslice body forces do not produce any net moment, the following may be obtained;

$$\sum (S_i \cos\alpha_i - N_i \sin\alpha_i)(y_i - y_g) + \sum (N_i \cos\alpha_i + S_i \sin\alpha_i)(x_i - x_g) = 0 \quad , \qquad 3.26$$

in which x_i and y_i correspond to the midpoint of the base of the slice, see Fig. 3.7.

Equation [3.26] may be rewritten in terms of the Eqn. [3.25] and together with the Mohr-Coulomb expression, the following may be obtained;

$$\sum \Delta X_i \left[(y_i - y_g) \tan(\phi'_i - \alpha_i) + (x_i - x_g) \right] = \sum W_i (x_i - x_g) + \sum D_i (y_i - y_g) \quad . \qquad 3.27$$

To determine the set of X forces, the following is suggested by Sarma;

$$\Delta X_i = \lambda F_i \quad , \qquad 3.28$$

where F_i is assumed to be known, and $\Sigma F_i = 0$. Then Eqns. [3.25] and [3.27] become;

$$\lambda \sum F_i (\phi'_i - \alpha_i) + K \sum W_i = \sum D_i \quad , \text{ and} \qquad 3.29$$

$$\lambda \sum F_i \left[(y_i - y_g) \tan(\phi'_i - \alpha_i) + (x_i - x_g) \right] = \sum W_i (x_i - x_g) + \sum D_i (y_i - y_g) \quad . \qquad 3.30$$

Using Eqns. [3.29] and [3.30] simultaneously, λ and K may be obtained as;

$$\lambda = \frac{\sum W_i (x_i - x_g) + \sum D_i (y_i - y_g)}{\sum F_i \left[(y_i - y_g) \tan(\phi'_i - \alpha_i) + (x_i - x_g) \right]} \quad , \qquad 3.31$$

$$K = \frac{\sum D_i - \lambda \sum F_i \tan(\phi'_i - \alpha_i)}{\sum W_i} \quad . \qquad 3.32$$

Here λF_i gives the change of X forces and K gives the critical acceleration (K_c).

It is now possible to determine the line of thrust (z) where the E forces act, see Fig. 3.7. Taking moments from the centre of the base of the slice, one may obtain;

$$z_{i+1} = \frac{[E_i z_i - 0.5 b_i \tan\alpha_i (E_i + E_{i+1}) - 0.5 b_i (X_i + X_{i+1}) - 0.25 K W_i (h_i + h_{i+1})]}{E_{i+1}} \quad . \qquad 3.33$$

where z_1=0 is known as an initial value.

In order to obtain a conventional *FOS*, an iterative method is suggested. This is achieved by reducing the strength parameters until zero critical acceleration (K_c=0) is obtained. Sarma (1973) says "The value of the factor which gives zero critical acceleration is the factor of safety, which is obtained without the earthquake forces". Sarma (1973) and Moysten and Small (1987) pointed out that this procedure takes only three iterations. However, critical acceleration is obtained without any iteration. Then this K_c value can be used as a measure of factor of safety (Sarma and Bhave, 1974). This gives;

$$F = 1 + 3.33 K_c \; . \qquad 3.34$$

Fredlund (1984) suggested that the critical acceleration can be used as a measure of safety factor for cohesive soils whereas the usual factor of safety can be used for cohesionless soils.

3.2.1.8 Fredlund and Krahn (GLE) method

Fredlund and Krahn (1977) proposed a general theory wherein other methods could be viewed as special cases. This method is also known the General Limit Equilibrium Method (GLE). The elements of statics used in this method to derive the factor of safety are the summation of forces in vertical and horizontal directions and the summation of moments about a centre of circle. Once again the method of slices is used to calculate the *FOS*.

The normal force, *N*, is found by resolving perpendicular to the slip surface as seen from Fig. 3.1(a);

$$N_i = \frac{W_i - (X_{i+1} - X_i) - \dfrac{c' l_i \sin\alpha_i}{F} + \dfrac{u_i l_i \tan\phi' \sin\alpha_i}{F}}{\cos\alpha_i + \dfrac{\sin\alpha_i \tan\phi'}{F}} \quad . \qquad 3.35$$

Two different factors of safety are given similar to the Spencer (1967), one with respect to force equilibrium (F_f) and the other with respect to moment equilibrium (F_m).

The force equilibrium equation is obtained by summing the forces parallel to the slip surface as;

$$F_f = \frac{\sum[c'l_i + (N_i - u_i l_i)\tan\phi']\cos\alpha_i}{\sum N_i \sin\alpha_i} \quad . \qquad 3.36$$

The moment equilibrium equation is derived from the summation of moments about the centre of the circle; the following is found;

$$F_m = \frac{\sum[c'l_i + (N_i - u_i l_i)\tan\phi']R}{\sum W_i x_i} \quad , \qquad 3.37$$

where x_i is horizontal distance between circle centre and centre of the slice.

The interslice normal forces are computed by summing horizontal forces on each slice. This gives;

$$E_{i+1} = E_i + [W_i + (X_{i+1} - X_i)]\tan\alpha_i - S_i/\cos\alpha_i \quad , \qquad 3.38$$

where

$$S_i = [c'b_i \sec\alpha_i + (N_i - u_i b_i \sec\alpha_i)\tan\phi']/F \quad . \qquad 3.39$$

The interslice shear force is found an adopting a similar assumption as Morgenstern and Price (1965), to provide;

$$X = \lambda f(x) E \quad . \qquad 3.40$$

The GLE method can solve the slope instability problem using different methods of analysis which in turn depends on the in formulating the interslice force direction of approach.

3.3 Other methods

The $\phi_u = 0$ or circular arc analysis

The earliest reported procedure for stability analysis, as proposed by Fellenius in 1918, is for circular shear surfaces and today is known as the $\phi_u = 0$ method (Wright 1969). This method is widely used for short-term stability analysis (Kumsar, 1993). In this approach, clay soil is assumed to be purely cohesive and there is no change in water content. Moment equilibrium is used and the slip surface is assumed to be circular. Interslice forces are not considered in the calculation of the *FOS*. A trial-and-error method must be used to obtain the centre of the circle in order to find the least factor of safety.

The friction circle method

Taylor (1937) proposed the friction circle method which considers the stability of the entire sliding mass as a whole and involves taking moments with respect to the centre of a circular failure surface. Through investigating all potential failure surfaces, the critical slip circle and the corresponding least *FOS* is found. Abramson et al. (1996) reported that this method is useful for homogeneous soil and is suitable for total or effective stress types of analysis. Lambe and Whitman (1979) stated that the normal stresses are assumed to be concentrated at a single point on the failure surfaces.

The infinite slope analysis

Several soil mechanics textbooks (e.g., Lambe and Whitman, 1979; Barnes, 1995; Craig, 1997) presented the derivation of the factor of safety for the "infinite" slope

analysis. In this method, the slope is assumed to be uniform and in an infinitely long plane. Movement of a failure mass above a single planer slip surface is parallel to the ground surface. It is assumed that the forces on the sides of vertical slices are equal and opposite in direction. Barnes (1995) reported that this type of analysis is most applicable to;

- granular soils,
- soils with no cohesion ($c = 0$),
- soils with bedding or laminations dipping parallel to the slope,
- soils with weathering profiles producing upper weaker horizons, and
- slopes where there has already been a shallow slab slide such as when shear strength on the slip surface has been reduced to its residual value. Bromhead (1992) pointed out that for the case of a very shallow, translational landslide, the infinite slope expression is as useful as any other method of slope stability analysis.

Lowe and Karafiath (1960) proposed an approach primarily for the analysis of sloping core earth and rock fill dams under the condition of rapid drawdown. In this method, the factor of safety is computed from the force equilibrium equation using the method of slice analysis.

Seed and Sultan (1967) presented a wedge method for analysing sloping core earth dams. This method also uses only the force equilibrium analysis and a trial slip surface is divided into wedge shapes. The analysis can be obtained by trial-and-error

using either graphical or numerical calculations. A value of *FOS* is assumed and a trial force polygon or a numerical calculation is used for each wedge. If the last sliding block is in equilibrium, the assumed value of *FOS* is deemed correct. The method is also useful for rock stability analysis. This procedure was later developed by the Department of Transport (1994) to accommodate reinforced slopes such as reinforced soil and soil nailing.

Wright (1969) and Duncan and Wright (1980) reported a log spiral method that is not a method of slices. By assuming that the slip surface has the shape of a logarithmic spiral, the equilibrium of the mass bounded by the slip surface can be satisfied completely without further assumption. The method involves three equations (i.e., overall moment, horizontal and vertical force equilibrium). The normal stress distribution is not known for the logarithmic spiral shear surface, so that the available shear strength and distribution of shear stresses are indeterminate. The authors also pointed out that this method is not useful for practical purposes because it is too complex.

Castillo and Revilla (1977) presented the mathematical theory of the variational calculus method for cohesive soil. In this method limit equilibrium criteria are similar to those formulated for the Janbu simplified method without the empirical correction factor (f_o) to account for interslice forces.

Baker and Garber (1977) proposed another variational calculus method in which all equilibrium conditions are satisfied. The method is based on the "limit equilibrium" approach where both cohesive and frictional components are taken into account.

Maksimovic (1979) described an analytical method with a curvilinear failure envelope. The assumptions made are similar to those made by Morgenstern and Price (1965) but the solution involves using recurrence formulae.

Chugh (1982) presented a method which includes earthquake forces in factor of safety calculations. This method is similar to Spencer's method in terms of satisfying static equilibrium with regards to interslice force components.

Fredlund (1984) reported that the finite element method theoretically satisfies the necessary requirements for a complete solution of a slope stability computation. However, he stated that there are restrictions that have limited its use in practice.

Mostyn and Small (1987) in their work on methods of stability analysis reported that finite difference methods may also be used for the solution of non-linear problems. In the case of finite difference methods, they pointed out that both finite element and finite difference techniques are being widely used by consulting firms, although both methods are more complex to use in comparison with the conventional limit equilibrium analysis. For the case of experimental verification using centrifuge modelling, they reported that slopes can be analysed by small scale physical

modelling in a centrifuge. Centrifuges are not generally available and are expensive to operate.

Leshchinsky (1990) and Leshchinsky and Huang (1992) presented a generalised variational slope stability analysis which is an extension of the Baker and Garber (1977) method. In their method attempts are made to avoid the customary assumptions leading to static equilibrium equations by using a variational approach. This method is different from Baker and Garber in the way that the slip surface is specified by the user as in more conventional methods (e.g., Janbu, Morgenstern and Price).

3.4 Discussion of analyses

The methods of analysis presented above have a wide range of applications for slope stability analysis, such as circular or noncircular slip surfaces, simple or complicated ground geometry, homogeneous or non-homogeneous soil conditions, different soil strata and water pressure conditions etc.

Limit equilibrium methods are the most popular analytical methods for slope stability analysis in use today. This popularity is due to the simplicity and ease of use of the methods. Of these methods the "slice" technique is used frequently with circular and non-circular failure surfaces. The most popular and widely used eight limit equilibrium methods of analyses (Fellenius, Bishop simplified, Janbu simplified,

Janbu generalised, Morgenstern and Price, Spencer, Sarma and GLE) have been presently chosen for computer codification. The main purpose of selecting these eight methods is to determine a range of values by using classical and modern methods of analysis when determining the factors of safety in slope stability analyses.

Most of the methods mentioned above involve a numerical search to determine the critical slip surface which gives the least factor of safety. Such a search is a long procedure and is time consuming. In addition, problems of nonconvergence may occur especially for rigorous methods. To avoid these problems, Chandra and Jiang (1993) performed the Janbu simplified method to obtain a possible critical slip surface. Then they applied the Spencer method to the obtained critical slip surface.

Although currently available slope stability analyses are well developed and arithmetically correct, a geotechnical engineer should be careful to select suitable failure surfaces to study and to identify appropriate shear strength parameters. As clearly stated by Nash (1987) "...a sophisticated analysis is no substitute for experience and engineering judgement".

The functional representations of equations do not readily lend themselves for accurate scrutiny. These comparisons are best carried out by benchmarking *FOS* values from case studies. These are carried out in Chapter 4.

CHAPTER 4: CURRENT SOLUTION METHODS OF SLOPE STABILITY PROBLEMS AND NUMERICAL BENCHMARKING

4.1 Introduction

This chapter brings together in the form of suite of computer programs. The formulae used by previous researchers (Chapter 3) and the geometric representations given in other published reports as well as the material uniquely featured within this research, see Chapter 2. The entire suite of programs, operates under the general name of SLIDE which is coded in FORTRAN, since the latter is thought to be the most extensively used technical and scientific language. SLIDE, which calculates the factors of safety of arbitrary and complicated slope profiles, is based on the method of slices and was uniquely configured and synthesised by the author.

Again all calculations presented either graphically or in tabular forms, are due to the candidate using his own software. Where comparisons are made with other published data or commercial slope stability programs, clear reference has been made to the authors or the code source.

The listing of the most popular and widely used solution methods for slope stability formulations, has been given later in this chapter (section 4.4.1-4.4.8). Eight of the methods listed have been adopted for the present work, aimed at benchmarking the factors of safety under various conditions. The procedure was applied both for circular and non-circular slip surfaces (where formulation permitted it).

To analyse a failure slip surface, the method of slices is used for all eight coded methods of analysis. The method of slices is explained in Chapter 5.

4.2 Setting up of problem

The information presentation component of the following sections show the methods used to codify the program designed for this project. Some of the techniques are established procedures and some are novel approaches designed for this research. The reason for including the methodology is to inform the reader of how the solution strategy has been set up.

There are some procedures in setting up the parameters which are specified by the user before calculations start and are common to all the analyses available in the program. These are:

- The ground surface is input to the program with respect to an x, y co-ordinate system. This could be a simple or arbitrary slope shape which involves straight line segments.

- Soil properties (c,ϕ and γ) are required for every single soil layer, where c is cohesion, ϕ is frictional angle and γ is unit weight of soil.
- Pore water pressure to be defined by either **(1)** using water table or **(2)** r_u values. Different unit weights of soil may be taken above and below the water table (i.e., γ_b, bulk unit weight of soil, γ_{sat}, saturated unit weight of soil and γ_{sub}, submerged unit weight of soil see Fig. 2.11). The water table is defined by x, y co-ordinates.
- The specification of grid lines geometry as the last input stage.

Circular slip surfaces are analysed by defining a rectangular grid where the corners represent the centres of circles of which the trial slip surfaces are apart, see Fig. 2.5. The grid is specified by giving the co-ordinates of the point labelled;

- by the minimum x and y values, and
- by the maximum x and y values.

The division of the bounded area is then prompted which gives the step size of the increment. The program automatically computes the shortest distance from the grid points to the slope surface and using increments of radius for every grid points, trial circular slip surfaces are found. Then the program takes the critical circular slip surface which gives the least factor of safety *FOS*.

For every trial circular slip surface, there are normally two intersection end points on the slope surface. The soil mass, between two intersection end points, is divided

automatically into a number of specified slices with equal widths. This slice division number is determined by the user, based on engineering judgement.

For the case of a non-circular slip surface, trial slip surfaces are specified by straight lines with respect to an (x, y) co-ordinate system. Division of slices is also specified by the user.

4.3 Description of slice parameters

Common assumptions are made for the description of slice parameters. The slice is always represented by the abscissa of its mid-co-ordinate. Other calculations are carried out at the centre of the base of each slice to compute:

- slice height "h",
- angle of slice base "α" and,
- length of slice base "l".

4.4 Codification of the formulae

Since Chapter 3 and Appendices A and B are dedicated to the survey and derivation of slope stability formulations, no theory will be repeated in this section. Equations will only be quoted if they become relevant to a particular programming difficulty or facility.

All eight methods of analysis involve a numerical search to determine the critical slip surface. This search is a long procedure and is time consuming. Besides, problems of nonconvergence may occur for the rigorous methods used. To avoid these problems, the Bishop simplified method is initially used to find the most critical slip surface according to Bishop simplified method. Then, programs relating to other theories are also run to calculate different factors of safety using the obtained critical slip surface. This is achieved by using different subroutines within the program. After completing the input in section 4.2, the present program computes the factors of safety using one or more different methods of analysis, based on the engineer's specification. The choice for methods of analysis are:

4.4.1 Fellenius method

This simple method is only applicable to the circular slip surfaces. Interslice normal and shear forces are assumed to be equal and opposite such that there is an implied cancellation of matching pairs. Force equilibrium is used by taking forces in the normal direction to the slip surface for each slice. Moment equilibrium is used for the whole failure mass, by taking the moment at the centre of the circle. The factor of safety is found by using Eqn. [3.5]. There is no requirement for iteration in this method.

4.4.2 Bishop simplified method

The only difference between the Fellenius and this method is the $m\alpha$ term (see Eqn. [3.7]). In this method, F appears in both sides of the equation (see Eqn. [3.8]). A trial value of F is used for all slice calculations to initiate the iteration, and leads to convergence to the ultimate *FOS* value. The convergence condition is set on the difference criterion from one iteration to another, say; (a) if $|F_n - F_{n-1}| > 1\text{x}10^{-4} F_{n-1}$ continue, and (b) if $|F_n - F_{n-1}| \leq 1\text{x}10^{-4} F_{n-1}$ end iteration.

4.4.3 Janbu simplified method

This method is applicable to both circular and non-circular slip surfaces. Only the force equilibrium conditions are satisfied in this analysis. Interslice normal and shear forces are neglected and the factor of safety is computed by using Eqn. [3.11]. The iteration procedure is similar to the Bishop Simplified method. There are two variations between Eqns. [3.8] and [3.11]. These are:

1. Janbu uses the 'tangent' parameter ($\tan\alpha$) in the denominator, rather than 'sine' ($\sin\alpha$), and
2. a '$\sec^2\alpha$' term appears in the numerator, instead of the '$\sec\alpha$' (normal).

The correction factor is not used in the present program, see Eqn. [3.12].

4.4.4 Janbu generalised method

The only difference between Janbu Simplified and this method is that interslice normal and shear forces are taken into account, see Eqn. [3.14]. It is assumed that interslice normal forces act at one-third of the height of each slice, Fig. 3.2. First trial *FOS* value is found by using the Janbu simplified method. The program is then coded to calculate interslice shear and normal forces, and a new *FOS* for the generalised form of Eqn. [3.14] is generated. This is achieved by performing only one or two iterations.

4.4.5 Morgenstern and Price method

The method is applicable to both circular and non-circular slip surfaces. Force equilibrium conditions are satisfied by taking directions along normal and parallel directions to the base of each slice. Moment equilibrium conditions are satisfied by taking the moment from the centre of the base of each slice. The calculation starts with guessed initial values of F (factor of safety) and λ (scaling factor). In this program the common $f(x)=1$ assumption is made. This helps to compute the direction of the resultant of the interslice normal and shear forces.

The calculation of moments depends on the range of H_i values (see Eqn. [B.37] in Appendix B). For the case of $-0.4 > H_i > 0.5$, moments and their derivatives are computed from recurrence formulae (see Eqns. [B.44a, b, c] and [B.45a, b, c] in Appendix B). For the case of $-0.4 < H_i < 0.5$, a five point quadrature scheme is used to

evaluate moments and their derivatives (using Eqns. [B.48], [B.49] and [B.50] in Appendix B).

After obtaining force (E), moment (M) and their derivatives, the Newton-Raphson iteration technique is used to re-evaluate F and λ values (see Eqns. [B.25] and [B.26] in Appendix B). This procedure is carried out until the force (E_n) and the moment (M_n), n being the final iterative sequence, are both zero or negligible. At the end of the iteration process the program gives updated values of F and λ.

4.4.6 Spencer method

This method is applicable to both circular and non-circular slip surfaces. In this present program only circular slip surface calculations are coded. The force equation results from summing forces in normal and parallel directions to the base of each slice (see Eqn. [3.20]), whereas the moment equation is taken by summing moments at the centre of the circle (see Eqn. [3.19] and Fig. 3.4).

Several trial values of θ, defined in Fig. 4.1, and two trial F values are chosen. For each θ value, Eqn. [3.15] is solved by using the trial value of F_f (which indicates the force equilibrium) and the corresponding trial F_m value (indicating the moment equilibrium). The process is repeated until Eqns. [3.19] and [3.20] are both satisfied. At the unique occasion when F_f and F_m curves intersect, the common factor of safety (F_i) will satisfy both force and moment equilibrium requirements, which would then correspond to the value of interslice force angle (θ_i); which is shown in Fig. 4.1.

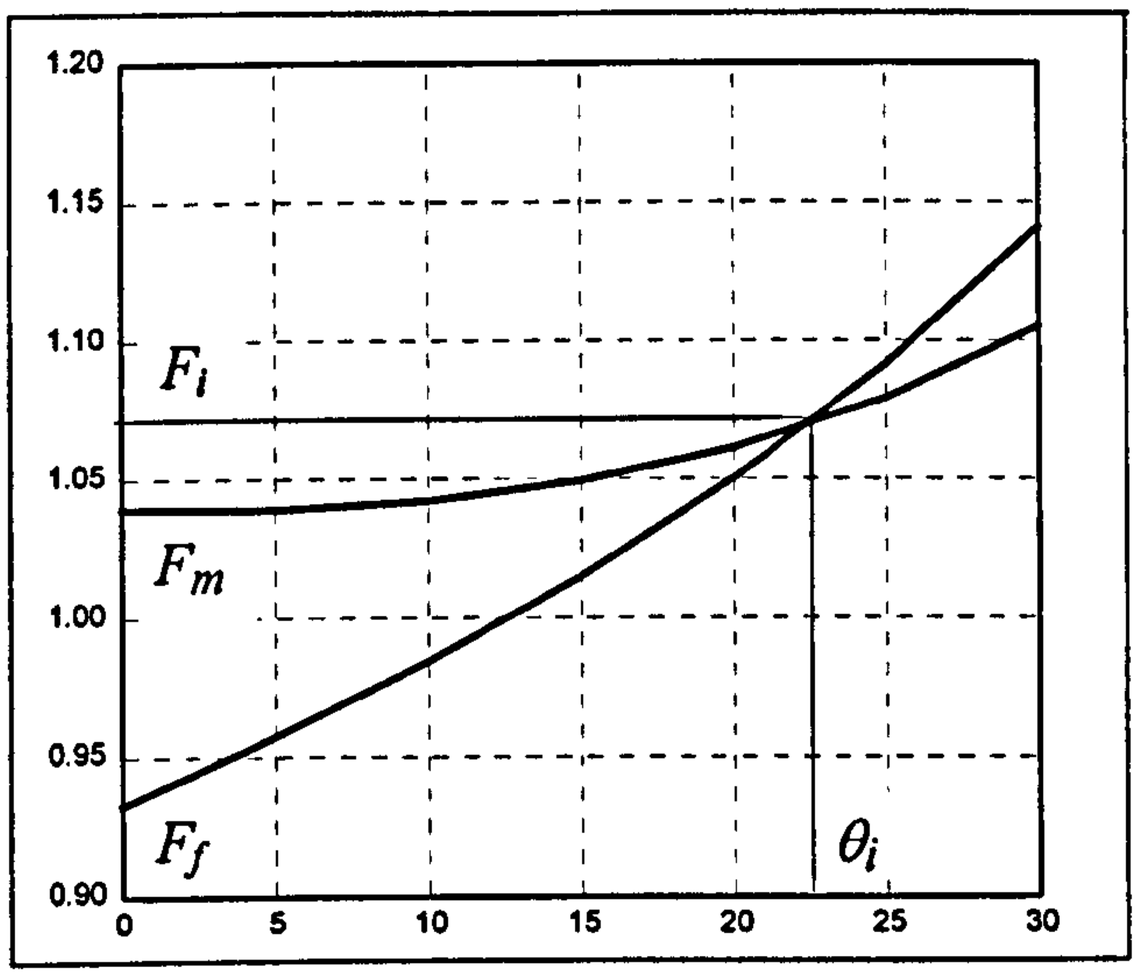

Figure 4.1 Variation of F_m and F_f with interslice force angle θ.

4.4.7 Sarma method

The method is applicable to both circular and non-circular slip surfaces. The force equilibrium equation is taken normal and parallel to the base of each slice, whereas the moment equilibrium condition is satisfied by taking the moment of all the forces from the centre of gravity of the soil mass.

By using Eqns. [3.31] and [3.32], λ and K_c are obtained without any iteration. This K_c value can then be used as a measure of the *FOS* by using Eqn. [3.34]. However the conventional factor of safety is obtained by iteration. This is carried out by reducing the strength parameters. When the value of K_c=0 is obtained, the *FOS* is taken at that particular condition.

4.4.8 Fredlund and Krahn (GLE) method

This method is applicable to both circular and composite slip surfaces. In the present program only circular slip surface calculations are coded. The summation of forces is taken in normal and parallel directions to the base of each slice, and the summation of moments is evaluated about the centre of the circle. The interslice normal forces are computed by summing horizontal forces on each slice, see Eqn. [3.38]. The interslice shear forces are obtained by assuming $f(x)=1$, as assumed for the Morgenstern and Price method, which is a common assumption (see Eqn. [3.40]).

Again, two independent factors of safety are computed; one with respect to the force equilibrium (F_f), Eqn. [3.36], and the other with respect to the moment equilibrium (F_m), Eqn. [3.37]. Iteration procedures and simultaneous determination of moment and force equilibrium factors of safety, are similar to the Spencer method see Fig. 4.1.

4.4.9 Summary of methods used

Each of the methods of analysis given above have some of the characteristics of equilibrium conditions. The methods may satisfy all or some of these conditions (i.e., horizontal force, vertical force and moment). The assumptions involved in these various methods, and the applicability of the shape of the slip surface, are summarised in Table 4.1.

Method of analysis	Equilibrium conditions				Shape of slip surface	Assumptions employed for interslice forces	Determination of *FOS* 1. Explicit 2. Needs iteration
	Overall moment	Slice moment	Vertical force	Horizontal force			
Fellenius	Yes	No	Yes	No	Circular	Ignored	1
Bishop simplified	Yes	No	Yes	No	Circular	Ignored	2
Janbu simplified	No	No	Yes	Yes	Any	Ignored	2
Janbu generalised	Yes	Yes	Yes	Yes	Any	Interslice normal force acts as one third of the slice height	2
Morgenstern and Price	Yes	Yes	Yes	Yes	Any	Arbitrary mathematical function used to describe the direction of the interslice forces	2
Spencer	Yes	Yes	Yes	Yes	Any (*)	Side forces are parallel	2
Sarma	Yes	Yes	Yes	Yes	Any	Calculated	2
Fredlund and Krahn (GLE)	Yes	Yes	Yes	Yes	Any (*)	As Morgenstern and Price	2

Table 4.1 Characteristics of equilibrium methods.

* Only circular slip surface considered in this work.

4.5 Case studies

Case studies are a useful means for detecting some of the many different sources of errors which may exist within in-house developed computer programs. The following sections are due to Wright (1992) who commented on "the importance and effectiveness of benchmarking in order to detect errors, depends on the type of errors involved, the errors being:

- Errors in coding computer software or in the basic algorithms implemented in the computer code. Benchmark problems are essential and effective for detecting errors of this type. This is probably the most common use of benchmark problems.
- Errors due to the method of stability analysis used. Errors likely to be caused by a particular method of slope stability analysis are now well understood. Experience and extensive research have shown that errors due to the mechanics are usually negligible provided that the method of stability analysis satisfies complete static equilibrium (e.g. Morgenstern and Price, Spencer, Sarma, etc.).
- Errors inherent in the theory and algorithms employed for the slope stability analysis. All methods of slope stability can produce erroneous results.
- Errors in entering input data into a computer program.
- Errors in defining the type of problem to be solved. A common error of this type is the use of short-term stability analyses when long-term stability is more critical. Regardless of the correctness of the input values the analysis will not be correct if the wrong problem was solved. Benchmark problems may serve to provide well

illustrated examples of slope stability problems and might indirectly reduce some errors.

- Errors in selecting and defining input values for the problem. This includes use of inaccurate strength values and incorrect slope profile geometry".

Not all the errors described above can be eliminated through benchmarking. However, the process is essential and can be used to eliminate or reduce the occurrence of some of these errors.

4.5.1 Problem 1

Problem 1 is thought to be first reported by Spencer (1967). As seen in Fig. 4.2, the slope is 30.48 m high consisting of soil with properties $c'/\gamma h = 0.02$, an effective angle of internal friction of $\phi' = 40°$ and with pore pressure coefficient r_u=0.5. The slope is inclined at an angle of 26.5° to the ground surface. The reported results have been compared against the output from SLOPE (commercial software program,GEOSOLVE) in addition to the results from the current research in Table 4.2(a). Also the same slope was examined using the water table which is given in Table 4.2(b).

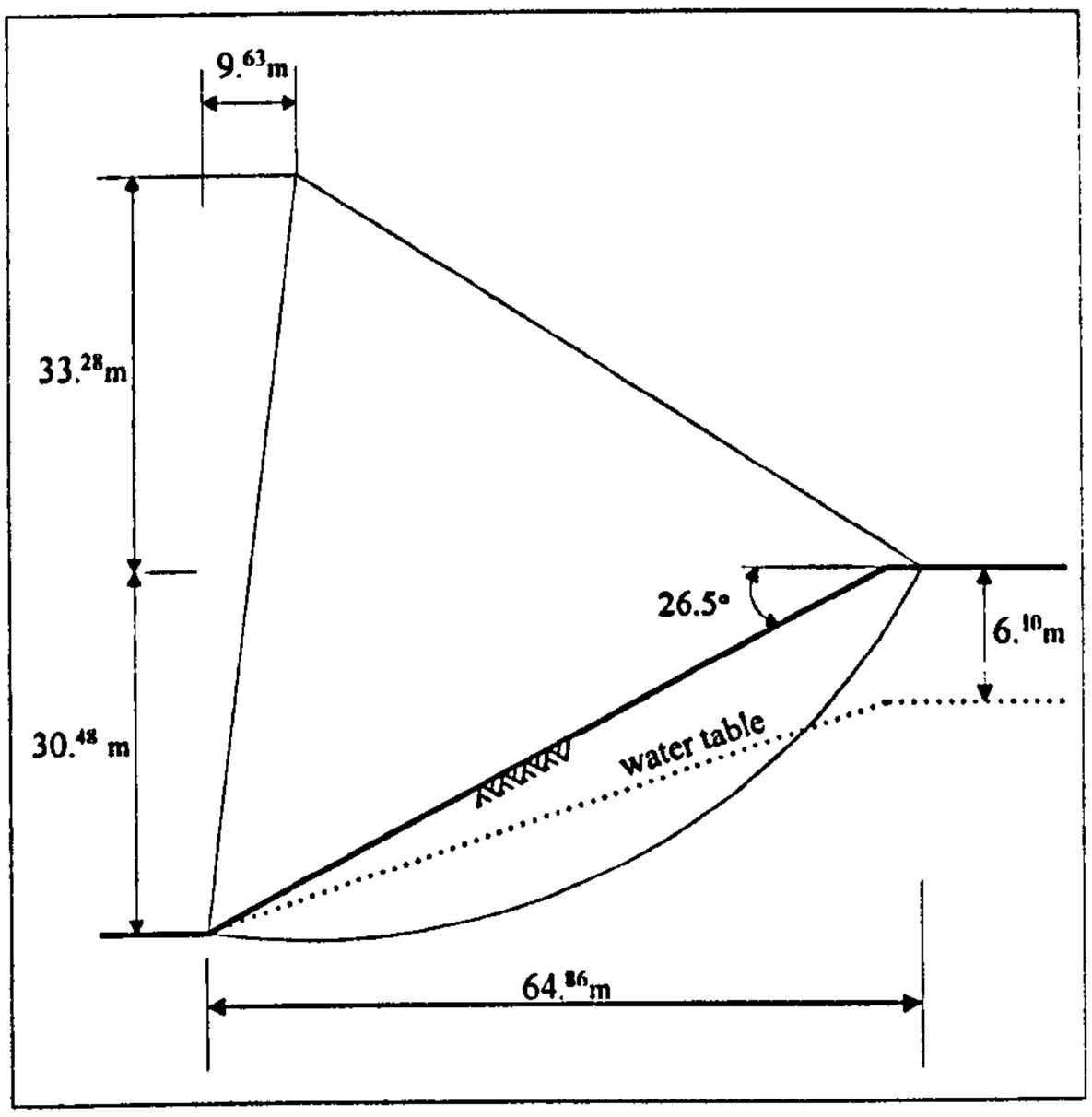

Figure 4.2 Example problem 1 (Spencer, 1967).

Programs	Methods of analysis for *FOS* calculations							
	Fellenius	Bishop Simple.	Janbu Simple.	Janbu General.	Morg. & Price	Spencer	Sarma (K_c=0)	Fredlund & Krahn (GLE)
Spencer	-	1.039	-	-	-	1.070	-	-
SLOPE program	0.849	1.037	0.931	1.070	*	*	*	*
Present research	0.848	1.039	0.932	1.070	1.065	1.070	1.070	1.070

Table 4.2(a) Comparison of *FOS* for problem 1. Key: * - Capability not documented in the "SLOPE" program.

Programs	Methods of analysis for *FOS* calculations							
	Fellenius	Bishop Simple.	Janbu Simple.	Janbu General.	Morg. & Price	Spencer	Sarma (K_c=0)	Fredlund & Krahn (GLE)
SLOPE program	1.628	1.759	1.646	1.763	*	1.760	*	*
Present research	1.625	1.757	1.644	1.765	1.760	1.760	1.762	1.760

Table 4.2(b) Comparison of *FOS* for problem 1 (with water table).

4.5.2 Problem 2

Figure 4.3 depicts the second problem which is reported by Barnes (1995). A 2:1 slope 10 m high, has been constructed on a stiff clay embankment with effective stress parameters c'=5 kN/m^2 and ϕ'=30° and bulk unit weight γ=20 kN/m^3. The pore pressure is generated by the water table that is 5 m blow crest level. Results from the current research and the SLOPE program are shown in Table 4.3(a). The same slope was analysed without a water table but using an r_u=0.3 value in Table 4.3(b).

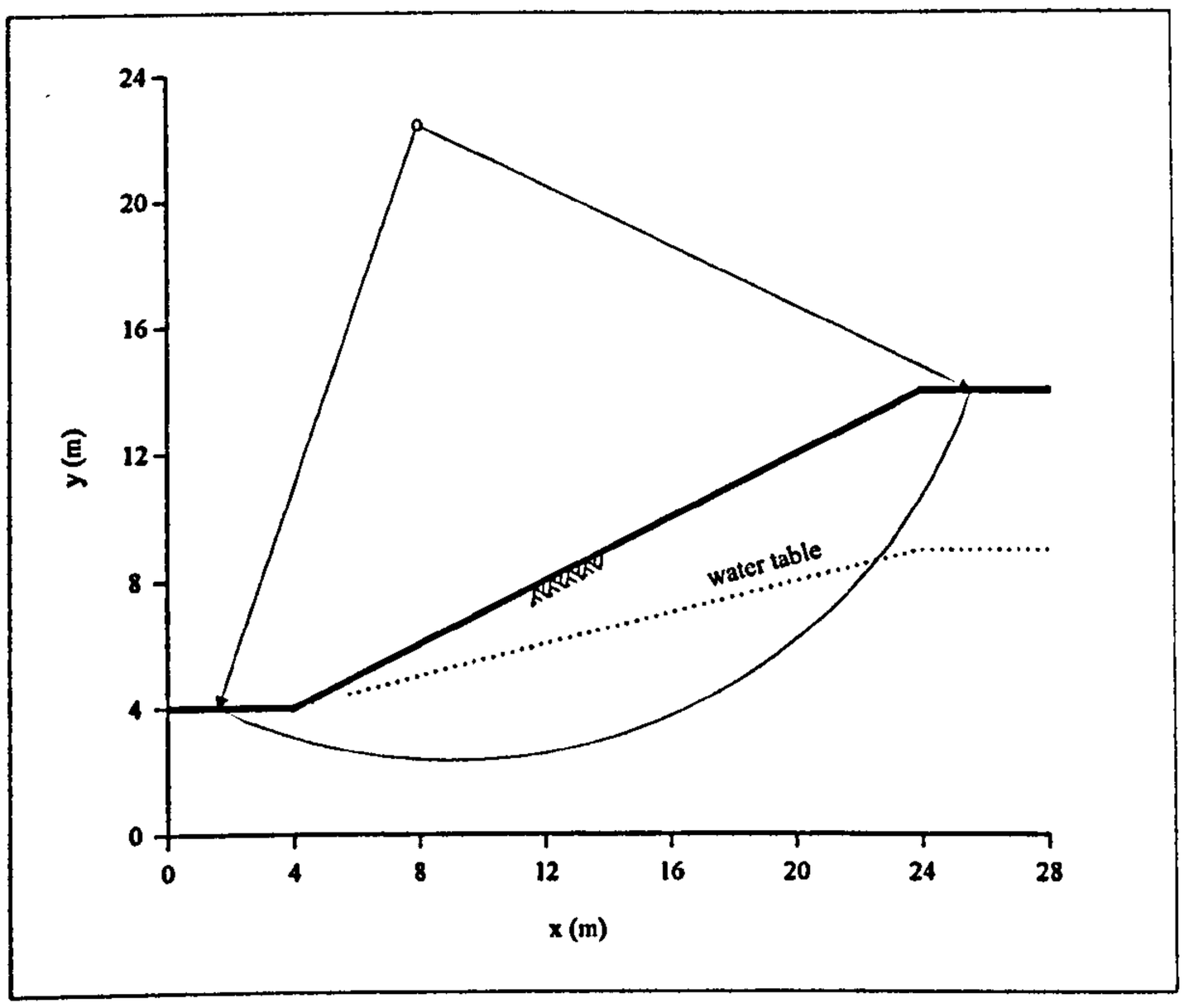

Figure 4.3 Problem 2 (Barnes, 1995).

Programs	Methods of analysis for *FOS* calculations							
	Fellenius	Bishop Simple.	Janbu Simple.	Janbu General.	Morg. & Price	Spencer	Sarma (K_c=0)	Fredlund & Krahn (GLE)
Barnes	-	1.394	-	-	-	-	-	-
SLOPE program	1.260	1.399	1.278	1.401	*	1.401	*	*
Present research	1.260	1.398	1.276	1.401	1.402	1.401	1.401	1.401

Table 4.3(a) Comparison of *FOS* for problem 2.

Programs	Methods of analysis for *FOS* calculations							
	Fellenius	Bishop Simp.	Janbu Simp.	Janbu Generl.	Morg. & Price	Spencer	Sarma (K_c=0)	Fredlund & Krahn (GLE)
SLOPE program	1.049	1.225	1.087	1.232	*	1.232	*	*
Present research	1.048	1.224	1.086	1.234	1.234	1.233	1.236	1.233

Table 4.3(b) Comparison of *FOS* for problem 2 (without water table but using r_u=0.3).

4.6 Inclusion of additional modelling facilities

The slope stability program developed during the current study can also solve the problem with a simple or arbitrary ground surface, circular and non-circular failure surfaces with any specified number of layers and with or without a water table (or with pore water pressure coefficient, r_u, values).

4.6.1 Problem 3

Problem 3, shown in Fig. 4.4, was chosen to illustrate the current program capabilities with regards to implementation of additional parameters in a real engineering environment e.g. multi-layer situation, slopes with "broken" geometries and the inclusion of a water table. The problem was first reported by Whitman and Bailey (1967). The slope profile consists of three layered deposits with no pore water pressure. Reference results and the data from the current research are given in Table 4.4(a). Also the same problem was analysed by using a water table. The results are given in Table 4.4(b). It is suspected that the large differences between reported and present research *FOS* values are due to the surfaces not being exactly the same as also pointed out by Sarma (1973).

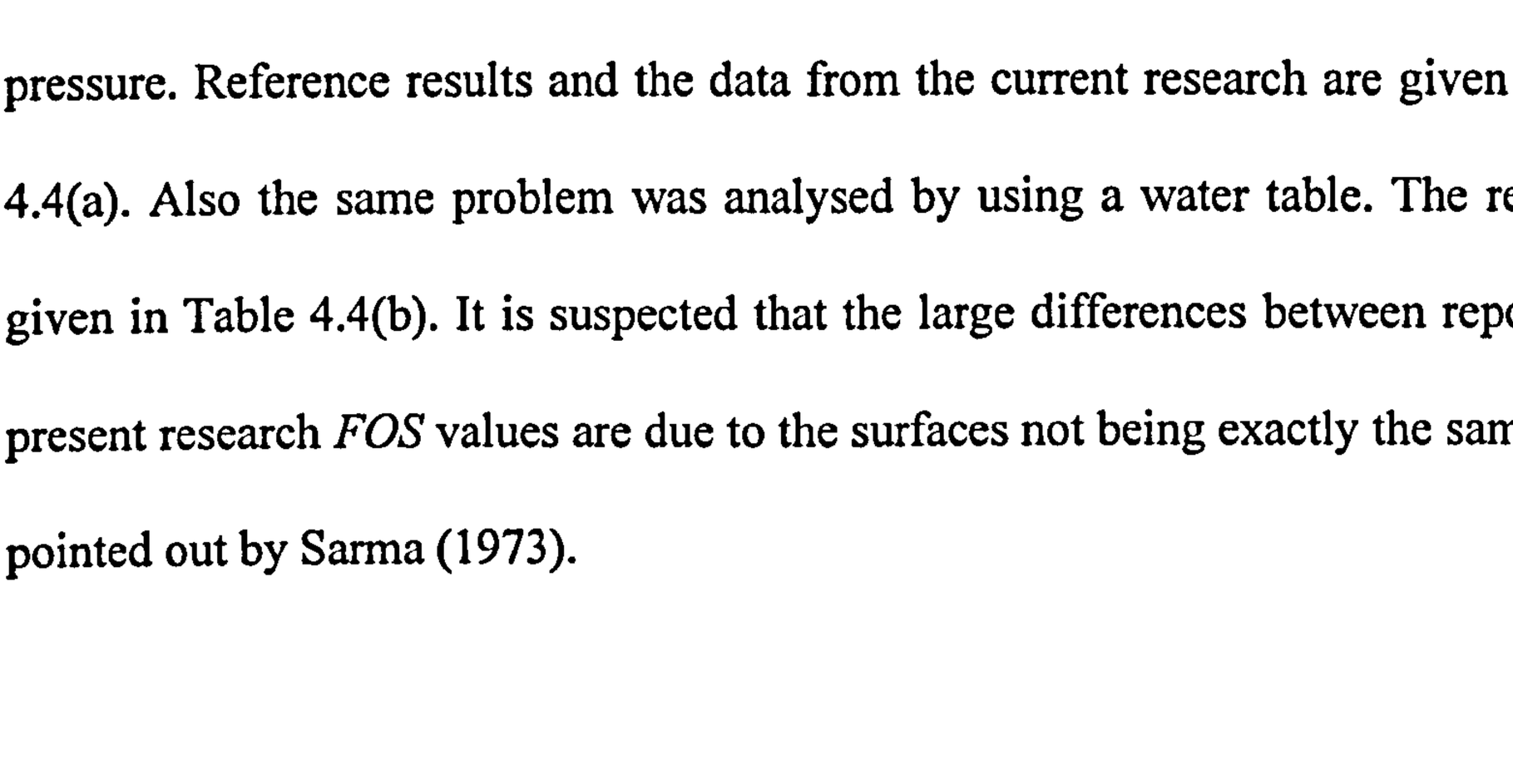

Figure 4.4 Example problem 3 (Whitman and Bailey, 1967).

Programs	Methods of analysis for *FOS* calculations							
	Fellenius	Bishop simple.	Janbu simple.	Janbu General.	Morg. & Price	Spencer	Sarma (K_c=0)	Fredlund & Krahn (GLE)
Whitman & Bailey	1.090	1.330	-	-	1.260	-	-	-
Sarma (1973)	-	-	-	-	1.550	-	1.540	-
SLOPE program	1.143	1.362	1.197	1.336	*	1.358	*	*
Present research	1.141	1.360	1.194	1.363	1.366	1.340	1.367	1.340

Table 4.4(a) Comparison of *FOS* for Problem 3.

Programs	Methods of analysis for *FOS* calculations							
	Fellenius	Bishop simple.	Janbu simple.	Janbu general.	Morg. & Price	Spencer	Sarma (K_c=0)	Fredlund & Krahn (GLE)
SLOPE program	0.917	1.173	1.026	1.153	*	1.161	*	*
Present research	0.923	1.173	1.024	1.158	1.177	1.163	1.186	1.163

Table 4.4(b) Comparison of *FOS* for Problem 3 (with water table).

4.6.2 Problem 4

Problem 4 is adopted from Fredlund and Krahn (1977) and converted to the SI (Le Systeme International d'Units) (see Fig. 4.5). Various combinations of geometry, soil and groundwater conditions were considered. Comparisons of three different program results and number of methods are shown in Tables 4.5(a) and 4.5(b). Table 4.5(a)

represents circular slip surface and Table 4.5(b) represents non-circular failure surface.

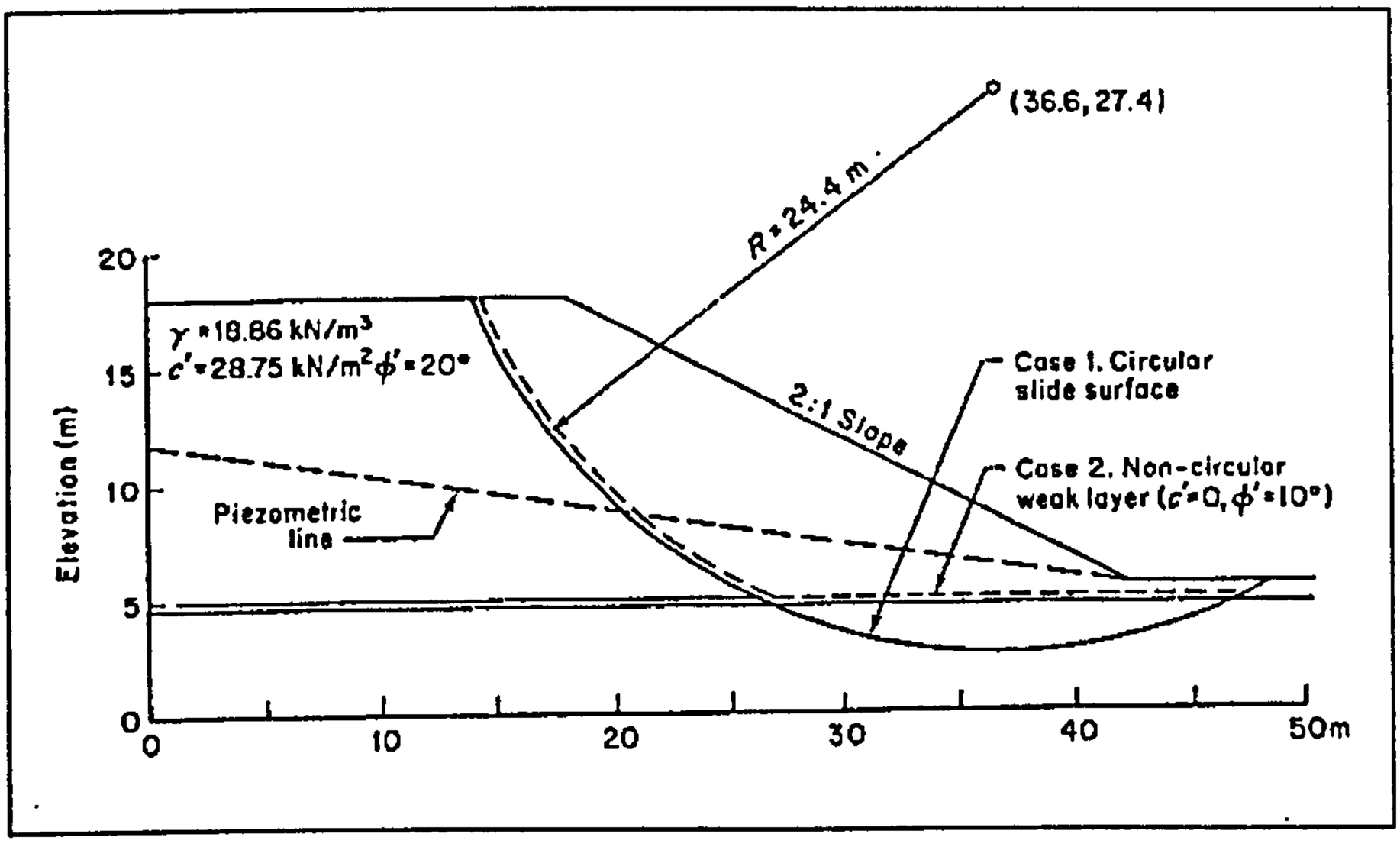

Figure 4.5 Example problem using circular and non-circular failure surfaces (Nash, 1987).

Table 4.5(a) Comparison of *FOS* calculations for problem 4 (circular failure surface).

Case no	Example problem	Programs	Methods of analysis for *FOS* calculations							
			Fellenius	Bishop simple.	Janbu simple	Janbu general.	Morg. & Price	Spencer	Sarma	Fredlund & Krahn (GLE)
1	Simple 2:1 slope, 12 m high, $\phi' = 20°$, $c' = 29$ kN/m^2	Fredlund & Krahn	1.928	2.080	2.041	2.008	2.076	2.073	-	-
		SLOPE program	1.930	2.078	1.878	2.074	*	2.074	*	*
		Present research	1.927	2.075	1.876	2.067	2.073	2.071	2.080	2.071
3	As in 1 except with $r_u = 0.25$	Fredlund & Krahn	1.607	1.766	1.735	1.708	1.765	1.761	-	-
		SLOPE program	1.608	1.762	1.589	1.760	*	1.760	*	*
		Present research	1.606	1.759	1.588	1.748	1.760	1.757	1.780	1.757
5	As in 1 except with a piezometric line	Fredlund & Krahn	1.693	1.834	1.827	1.776	1.833	1.830	-	-
		SLOPE program	1.643	1.841	1.670	1.841	*	1.841	*	*
		Present research	1.697	1.836	1.675	1.833	1.869	1.839	1.878	1.839

Case No	Example problem	Programs	Methods of analysis for *FOS* calculations			
			Janbu simple.	Janbu general.	Morg. & Price	Sarma
2	Same as 1 with a thin, weak layer with $\phi' = 20°$, $c' = 29$ kN/m^2	Fredlund and Krahn	1.448	1.432	1.378	-
		SLOPE program	1.301	1.340	*	*
		Present research	1.325	1.428	1.355	1.348
4	Same as 1 except with $r_u = 0.25$	Fredlund and Krahn	1.191	1.162	1.124	-
		SLOPE program	1.057	1.086	*	*
		Present research	1.080	1.143	1.123	1.095
6	Same as 1 except with a piezometric line	Fredlund and Krahn	1.333	1.298	1.250	-
		SLOPE program	1.300	1.339	*	*
		Present research	1.260	1.323	1.240	1.255

Table 4.5(b) Comparison of *FOS* calculations for problem 4
(non-circular failure surface).

4.6.3 Problem 5

This example is drawn from the slope analysis of Birch Dam in Oklahoma, as described by Celestino and Duncan (1981). The geometrical configuration has been scaled by Nguyen (1984), see Fig. 4.6, from the above author's paper. Only circular failure surface was analysed for various soil properties and results are given in Table 4.6.

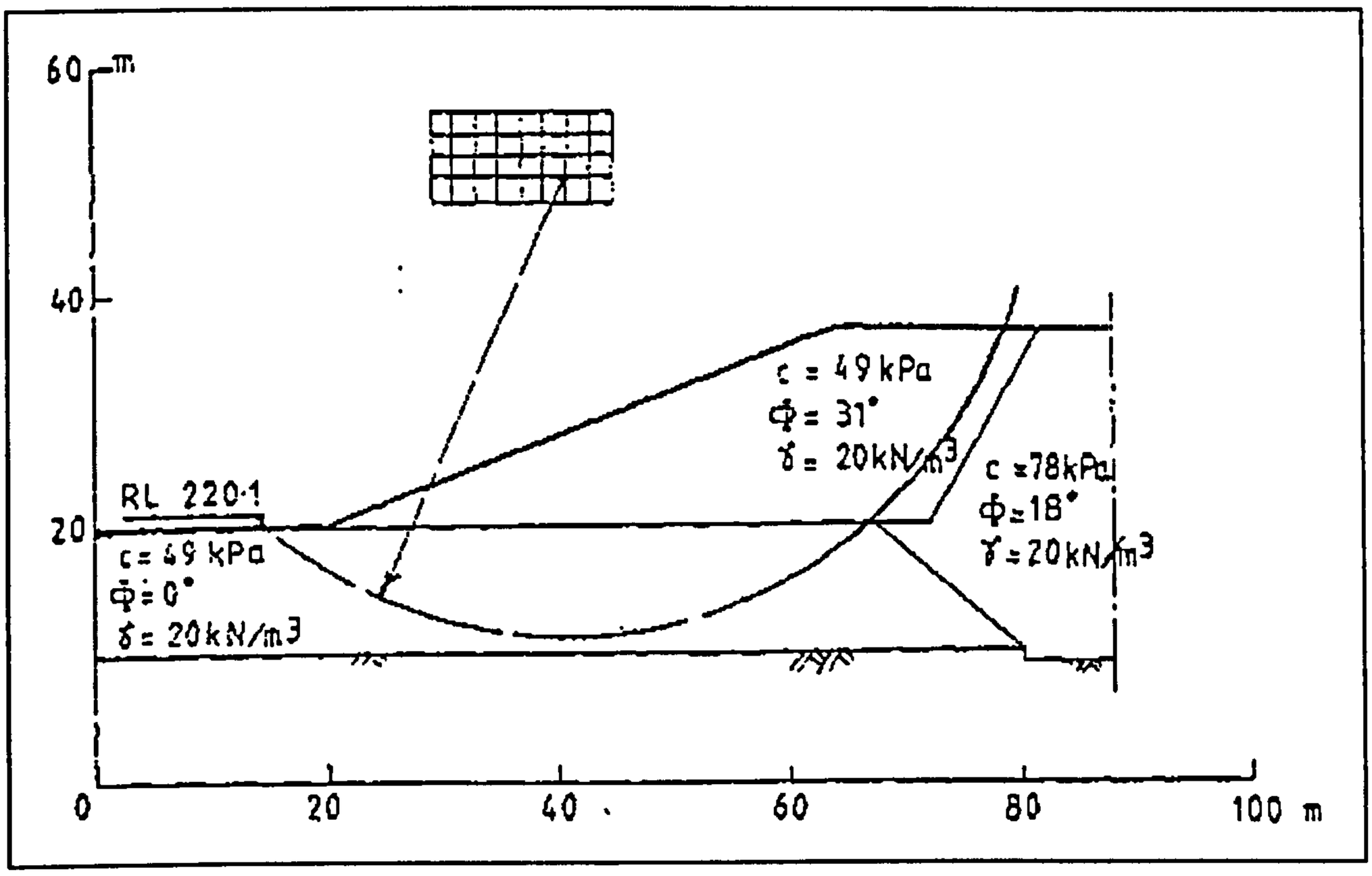

Figure 4.6 Re-analysing stability of Birch Dam (Nguyen, 1984).

Programs	Methods of analysis for *FOS* calculations							
	Fellenius	Bishop simple.	Janbu simple.	Janbu general.	Morg. & Price	Spencer	Sarma	Fredlund & Krahn (GLE)
Nguyen	-	1.170	-	-	-	-	-	-
SLOPE program	1.019	1.036	1.035	1.072	*	1.036	*	*
Present research	1.016	1.170	1.061	1.140	1.190	1.190	1.172	1.190

Table 4.6 Comparison of *FOS* calculations for problem 5.

4.6.4 Problem 6

This problem and solution is reported by Nguyen (1984) to analyse arbitrary ground surfaces with three different soil layers. There are specific soil mechanics properties and pore pressure coefficients allocated to each layer. Three different program results of *FOS* are given in Table 4.7.

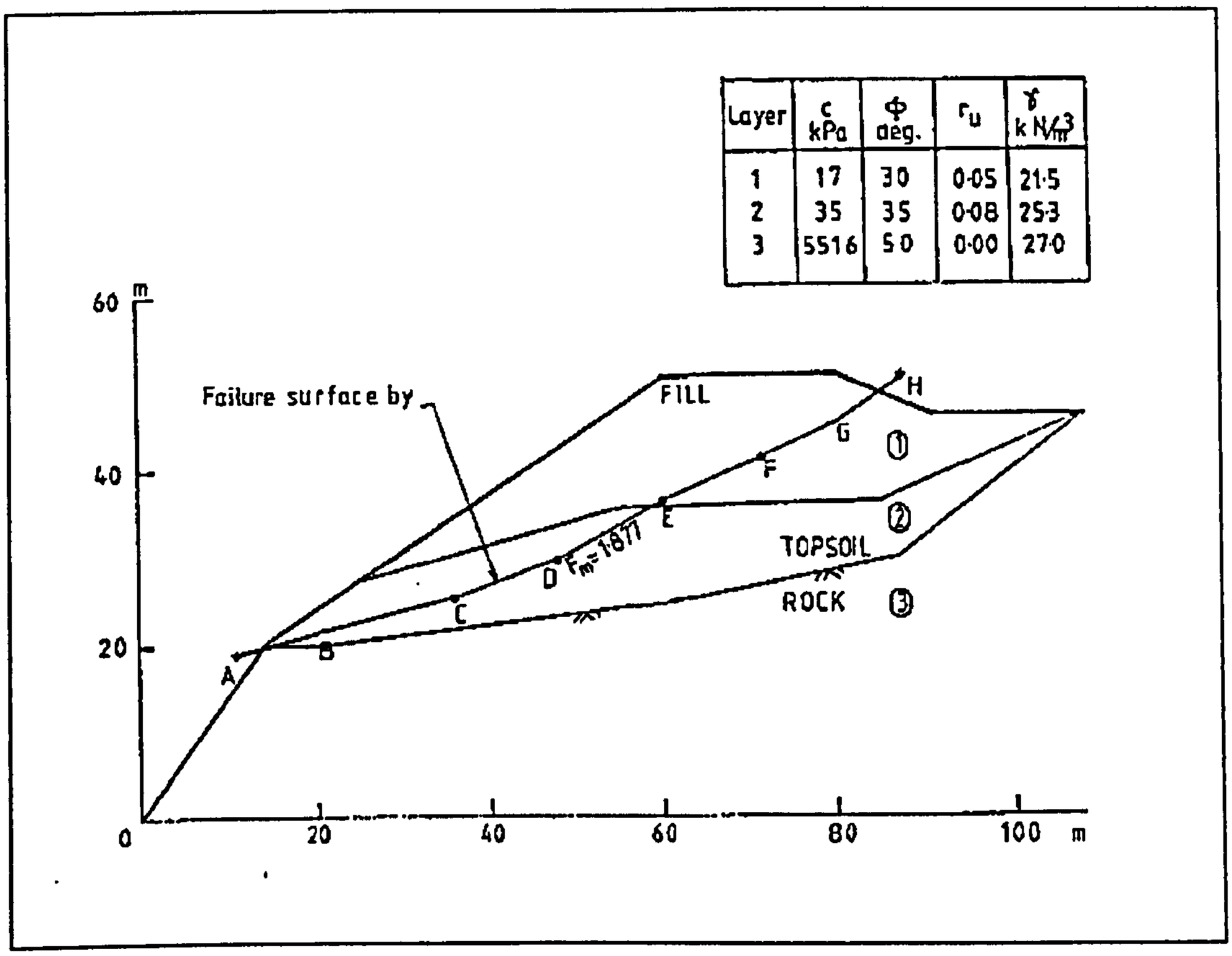

Figure 4.7 Analysis of non-circular slip surface (Nguyen, 1984).

Programs	Methods of analysis for *FOS* calculations			
	Janbu simple	Janbu general.	Morg. & Price	Sarma
Nguyen	-	-	1.877	-
SLOPE program	1.810	1.855	*	*
Present research	1.822	1.880	1.882	1.871

Table 4.7 Comparison of *FOS* calculations for problem 6.

4.7 Critical review of the existing methods

It has been shown in the foregoing examples and numerous tests performed in this study, that the author's codification of 8 different methods of analysis provide reliable factor of safety calculations for circular and non-circular failure surfaces.

As can be seen from the above tables, comparative analysis have shown that all the methods which satisfy all the conditions of equilibrium (Janbu generalised, Morgenstern and Price, Spencer, Sarma, GLE), result in almost the same value of safety factor. The Bishop simplified method, which does not satisfy all the conditions of equilibrium, has also been found to be as accurate as the methods that satisfy all the conditions of equilibrium criteria. Fellenius and Janbu's simplified (without the correction factor, see Eqn. [3.12]) methods give the lowest factors of safety.

The Fellenius method does not require iteration but the remaining seven approaches require a number of built-in iteration sequences.

The values of the factors of safety calculated by the procedure of slices are influenced to some degree by the number of slices used in the analysis. In general, the accuracy of the factor of safety increases with the number of slices used. Ting (1983) reported that the error associated with the Bishop Simplified method becomes small as the number of slice increases. Spencer (1967) standardised the number of slices at 32. Current research has found that all methods of analysis mentioned above give accurate factors of safety by using 30 slices except the Morgenstern and Price method for which more than 30 slices are required in order to achieve accurate factor of safety values.

CHAPTER 5: AN ALTERNATIVE NUMERICAL ALGORITHM TO REPLACE METHOD OF SLICE

5.1 Introduction

Numerical integration (quadrature) has been investigated as an alternative to the method of slices, which itself is an approximate integration sequence. The application and formulation is covered in many textbooks covering numerical analysis and theoretical mechanics. The parameters used in this thesis have been taken from Zienkiewicz (1977), although many presentations are available as a matter of personal preference.

The above method of integration will be explained in the following sections.

5.2 Numerical integration (quadrature) for mass divisions

5.2.1 The method of slices

The method of slices usually uses effective stress analysis (i.e. long-term stability) but it could also be used for short-term stability analysis (i.e. total stress analysis; Clayton et al., 1993 and Barnes, 1995). In this method, a possible failure slip surface is divided by vertical or inclined planes (Sarma, 1979 and Kumsar, 1993) into a series of slices

(see Fig. 3.1). The present research only considers vertical sided slices. The width between slices, b, can be equal or unequal and of necessity each slice has a variable height, h, measured along the centre line. Using a sufficiently large number of slices the base and top of each slice can be approximated to be a straight line. The base is inclined at an angle, α, to the horizontal and has a length l, where $l = b\sec\alpha$.

The potential slip surface is divided into slices only for ease of analysis. The factor of safety is taken to be the same for each slice. This implies that interslice normal and shear forces must act between each slice.

The forces acting on a slice are:

- The total weight of the slice, $W = \gamma bh$ where γ is unit weight of the soil.
- The total normal force on the base, N which has two different force components, the effective normal force $N' = W\cos\alpha$ and the water thrust $U = ul$ where u is the pore water pressure acting at the centre of the base of the slice i.e., $N' = W\cos\alpha - ul$.
- The shear force, which resists the slide force, on the base of the slice, S.
- The total horizontal interslice normal force on the vertical slice sides, E.
- The total vertical interslice shear force on vertical slice sides, X.

5.2.2 The method of quadrature

One of the most accurate numerical methods in ordinary use for integrating polynomials is the Gauss quadrature formula (Akin, 1986). The great mathematician

Karl Friederich Gauss (1777-1855) discovered that by a special placement of the nodes, the accuracy of the numerical integration process could be greatly increased (Cheney and Kincaid, 1985). Consider the definite integral;

$$I = \int_{-1}^{+1} f(\xi) d\xi, \qquad 5.1$$

to be evaluated numerically from a given number of Gauss points, *ng*. Gauss considered the problem of determining which values of ξ should be chosen in order to get the greatest possible accuracy. In other words, how should one subdivided the interval (-1, +1) so as to get the best possible results? Gauss found that the "*ng*" points in the interval should not be equally spaced but should be symmetrically placed with respect to the mid-point of the interval.

5.3 Algorithm leading to numerical integration for slope stability analysis

The forces acting on a single Gauss slice are identical with the forces considered with the method of slices. Only a circular failure surface is considered at this stage.

For simplicity we consider the conventional Fellenius equilibrium equation. Equation [3.5], given in Chapter 3 can also be used for Gauss quadrature. For convenience the equation is re-written here.

$$F = \frac{\sum c' l_i + (W_i \cos\alpha_i - u_i l_i)\tan\phi'}{\sum W_i \sin\alpha_i} \quad . \qquad 5.2$$

By substituting $l = b\sec\alpha$, the following is obtained;

$$F = \frac{\sum c' b_i \sec\alpha_i + (W_i \cos\alpha_i - u_i b_i \sec\alpha_i)\tan\phi'}{\sum W_i \sin\alpha_i} \quad . \qquad 5.3$$

The upper part of the above equation is also known as restoring force, R, and is rewritten as;

$$R = \sum_{i=1}^{ns} c' b_i \sec\alpha_i + (W_i \cos\alpha_i - u_i b_i \sec\alpha_i)\tan\phi' \ , \qquad 5.4$$

where *ns* is number of slices used.

Bearing in mind that b_i, the slice width, represents a finite increment along the horizontal axis, namely Δx_i so that the weight per slice is;

$W_i = h_i \gamma b_i = h_i \gamma \Delta x_i$, hence

$$R = \sum_{i=1}^{ns} [c'\sec\alpha_i + (h_i \gamma \cos\alpha_i - u_i \sec\alpha_i)\tan\phi']\Delta x_i \quad . \qquad 5.5$$

In reality the total restoring force is;

$$R = \int_{XL}^{XR} \left[c' \sec\alpha_x + \left(h_x \gamma \cos\alpha_x - u_x \sec\alpha_x \right) \tan\phi' \right] dx \quad . \qquad 5.6$$

where XL and XR are intersection points on the ground surface, see Fig. 5.1, and α_x, h_x, u_x are function of x.

The same equation could be expressed parametrically as;

$$R = I_1 = \int_{\xi=-1}^{+1} \left\{ c'(\xi)\sec\alpha(\xi) + \left[h(\xi)\gamma(\xi)\cos\alpha(\xi) - u(\xi)\sec\alpha(\xi) \right] \tan\phi'(\xi) \right\} d\xi \, . \qquad 5.7$$

where -1 and $+1$ are boundary conditions, ξ is Gauss abscissa and

$$-1 \le \xi = \frac{2X - (XR + XL)}{XR - XL} \le +1 \text{ see Fig. 5.1.}$$

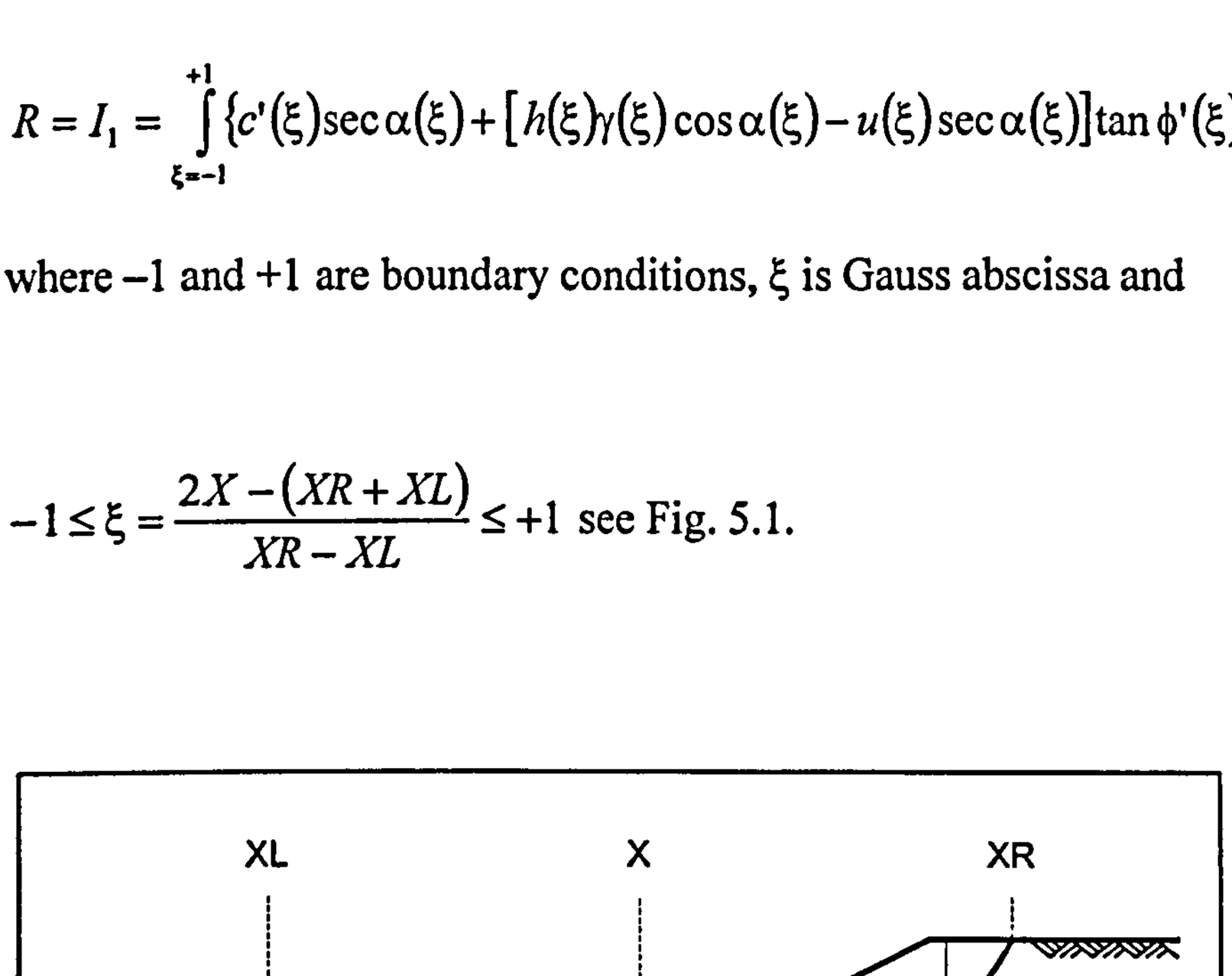

Figure 5.1 Application of Gauss quadrature to slope stability with $ng = 5$.

Using Gauss quadrature notation Eqn. [5.7] may be written as;

$$R = I_1 = \sum_{i=1}^{ng} \{c'(\xi)\sec\alpha(\xi) + [h(\xi)\gamma(\xi)\cos\alpha(\xi) - u(\xi)\sec\alpha(\xi)]\tan\phi'(\xi)\}. \qquad 5.8$$

where *ng* is the number of Gauss points.

Multiplying the above equation by the Gauss weight factor, WI, finally the total restoring forces are obtained as;

$$R = \sum_{i=1}^{ng} I_{1i}\, LE\ . \qquad 5.9$$

where $LE = WI_i\left(\frac{XR - XL}{2}\right)$.

An identical method is used to obtain the disturbing forces, *D*, as follows. The denominator of Eqn. [5.3];

$D = \sum_{i=1}^{ns} W_i \sin\alpha_i = \sum_{i=1}^{ns} h_i\gamma \sin\alpha_i \Delta x_i = \int_{XL}^{XR} h_x\gamma \sin\alpha_x\, dx$ and using Gauss notation, it gives;

$$D = I_2 = \sum_{i=1}^{ng} h(\xi)\gamma(\xi)\sin\alpha(\xi)\ . \qquad 5.10$$

Once again multiplying by the Gauss weight factor, the total disturbing force becomes;

$$D = \sum_{i=1}^{ng} I_{2i}\, LE. \qquad 5.11$$

The above Eqns. [5.8] and [5.11] are put together to obtain a factor of safety as follows;

$$FOS \cong \frac{R}{D} = \frac{\sum_{i=1}^{ng} \{c'(\xi)\sec\alpha(\xi) + [h(\xi)\gamma(\xi)\cos\alpha(\xi) - u(\xi)\sec\alpha(\xi)]\tan\phi'(\xi)\} LE}{\sum_{i=1}^{ng} [h(\xi)\gamma(\xi)\sin\alpha(\xi)] LE}$$

or in short form;

$$FOS \cong \frac{R}{D} = \frac{\sum_{i=1}^{ng} I_{1i}\, WI_i\left(\frac{XR - XL}{2}\right)}{\sum_{i=1}^{ng} I_{2i}\, WI_i\left(\frac{XR - XL}{2}\right)}\ . \qquad 5.12$$

The above form has similarities with conventional "slice" method representation but the number of calculation stations required are expected to be far fewer than in the slice method. As stated by Cheney and Kincaid (1985), the Gaussian quadrature formulae give higher accuracy with fewer function evaluations. A comparison for accuracy and convergence is made in the next section. The suggestion for use of the Gaussian integration is by Delpak (1996) but the full implementation is by the author.

5.4 Case studies

Some of the case studies, shown in Chapter 4, were re-analysed to study the influence that the Gaussian quadrature might have as an alternative way of analysing a potential failure mass. Re-analysed problems are not shown here to avoid repetition. Only the problem numbers are taken, as used in Chapter 4.

The following *FOS* values were calculated using the author's own program. The sign (*) shows that convergence is achieved between the method of slices and the Gauss quadrature for *FOS* calculations. Results for problems 1, 3, 4, 5 are represented in Tables 5.1 to 5.4. *ns* represents number of slices and *ng* represents the number of Gauss points used.

Problem 1

Fellenius	*ns*	**10**	**20**	**30**	**40**	**60**	**100**	**150**	**200**
	FOS	0.835	0.846	0.848	0.848	0.848	0.849 *	0.849	0.849
	ng	**3**	**5**	**6**	**9**	**12**	**16**	**20**	**24**
	FOS	0.816	0.844	0.849 *	0.849	0.849	0.850	0.850	0.850

Bishop simpli.	*ns*	**10**	**20**	**30**	**40**	**60**	**100**	**150**	**200**
	FOS	1.032	1.038	1.039 *	1.039	1.039	1.039	1.039	1.039
	ng	**3**	**5**	**6**	**9**	**12**	**16**	**20**	**24**
	FOS	1.024	1.035	1.036	1.037	1.039 *	1.040	1.040	1.040

Janbu simpli.	*ns*	10	20	30	40	60	100	150	200
	FOS	0.921	0.931	0.932	0.932	0.933 *	0.933	0.933	0.933
	ng	3	5	6	9	12	16	20	24
	FOS	0.909	0.933 *	0.937	0.939	0.939	0.939	0.940	0.940

Janbu general.	*ns*	10	20	30	40	60	100	150	200
	FOS	1.048	1.060	1.062 *	1.062	1.063	1.063	1.063	1.063
	ng	3	5	6	9	12	16	20	24
	FOS	0.982	1.040	1.061 *	1.069	1.070	1.070	1.070	1.070

Spencer	*ns*	10	20	30	40	60	100	150	200
	FOS	1.065	1.069	1.069	1.069	1.069	1.070 *	1.070	1.070
	ng	3	5	6	9	12	16	20	24
	FOS	1.059	1.067	1.070 *	1.070	1.070	1.070	1.070	1.070

Sarma	*ns*	10	20	30	40	60	100	150	200
	FOS	1.066	1.068	1.070 *	1.070	1.070	1.080	1.082	1.082
	ng	3	5	6	9	12	16	20	24
	FOS	1.060	1.064	1.069	1.070 *	1.070	1.080	1.080	1.080

Fredlund & Krahn (GLE)	*ns*	10	20	30	40	60	100	150	200
	FOS	1.065	1.069	1.069	1.069	1.069	1.070 *	1.070	1.070
	ng	3	5	6	9	12	16	20	24
	FOS	1.059	1.067	1.070	1.070 *	1.070	1.070	1.070	1.070

Table 5.1 Comparison of two different mass divisions for problem 1.

Problem 3

Fellenius	ns	10	20	30	40	60	100	150	200
	FOS	1.109	1.141	1.152	1.153	1.154 *	1.155	1.156	1.156
	ng	3	5	6	9	12	16	20	24
	FOS	1.094	1.137	1.154 *	1.159	1.165	1.170	1.180	1.180

Bishop simpli.	ns	10	20	30	40	60	100	150	200
	FOS	1.341	1.365	1.379	1.381 *	1.383	1.384	1.384	1.384
	ng	3	5	6	9	12	16	20	24
	FOS	1.353	1.365	1.371	1.382 *	1.390	1.396	1.400	1.400

Janbu simpli.	ns	10	20	30	40	60	100	150	200
	FOS	1.163	1.194	1.205	1.206	1.207 *	1.208	1.208	1.210
	ng	3	5	6	9	12	16	20	24
	FOS	1.152	1.184	1.201	1.207 *	1.214	1.217	1.220	1.223

Janbu general.	ns	10	20	30	40	60	100	150	200
	FOS	1.332	1.371 *	1.384	1.385	1.387	1.388	1.388	1.388
	ng	3	5	6	9	12	16	20	24
	FOS	1.200	1.273	1.360	1.371 *	1.380	1.390	1.404	1.405

Spencer	*ns*	10	20	30	40	60	100	150	200
	FOS	1.340	1.366	1.381 *	1.381	1.381	1.384	1.384	1.386
	ng	3	5	6	9	12	16	20	24
	FOS	1.314	1.340	1.355	1.360	1.365	1.380 *	1.390	1.390

Sarma	*ns*	10	20	30	40	60	100	150	200
	FOS	1.355	1.370 *	1.372	1.381	1.382	1.384	1.385	1.385
	ng	3	5	6	9	12	16	20	24
	FOS	1.359	1.365	1.370 *	1.380	1.385	1.390	1.397	1.397

Fredlund & Krahn (GLE)	*ns*	10	20	30	40	60	100	150	200
	FOS	1.340	1.366	1.381 *	1.381	1.381	1.384	1.384	1.386
	ng	3	5	6	9	12	16	20	24
	FOS	1.314	1.340	1.355	1.360	1.365	1.380 *	1.390	1.390

Table 5.2 Comparison of two different mass divisions for problem 3.

Problem 4 (Case number 5)

Fellenius	*ns*	10	20	30	40	60	100	150	200
	FOS	1.679	1.697	1.704	1.705	1.706 *	1.706	1.706	1.706
	ng	3	5	6	9	12	16	20	24
	FOS	1.646	1.665	1.699	1.706 *	1.709	1.709	1.709	1.710

Bishop simpli.	*ns*	10	20	30	40	60	100	150	200
	FOS	1.822	1.836	1.841 *	1.842	1.842	1.842	1.842	1.843
	ng	3	5	6	9	12	16	20	24
	FOS	1.755	1.826	1.829	1.841 *	1.843	1.843	1.845	1.845

Janbu simpli	*ns*	10	20	30	40	60	100	150	200
	FOS	1.647	1.675	1.684	1.686	1.687	1.689 *	1.689	1.689
	ng	3	5	6	9	12	16	20	24
	FOS	1.539	1.553	1.675	1.680	1.689 *	1.689	1.689	1.691

Janbu general.	*ns*	10	20	30	40	60	100	150	200
	FOS	1.807	1.825 *	1.831	1.831	1.832	1.832	1.832	1.833
	ng	3	5	6	9	12	16	20	24
	FOS	1.634	1.715	1.765	1.803	1.823 *	1.829	1.840	1.842

Spencer	*ns*	10	20	30	40	60	100	150	200
	FOS	1.818	1.833	1.839 *	1.839	1.839	1.840	1.840	1.840
	ng	3	5	6	9	12	16	20	24
	FOS	1.750	1.824	1.829	1.839 *	1.840	1.840	1.840	1.840

Sarma	*ns*	10	20	30	40	60	100	150	200
	FOS	1.860	1.863 *	1.875	1.878	1.878	1.878	1.878	1.878
	ng	3	5	6	9	12	16	20	24
	FOS	1.760	1.795	1.845	1.850	1.862 *	1.882	1.890	1.891

Fredlund & Krahn (GLE)	*ns*	10	20	30	40	60	100	150	200
	FOS	1.818	1.833	1.839 *	1.839	1.839	1.839	1.839	1.839
	ng	3	5	6	9	12	16	20	24
	FOS	1.750	1.824	1.829	1.839 *	1.840	1.840	1.840	1.840

Table 5.3 Comparison of two different mass divisions for problem 4 (Case no. 5).

Problem 5

Fellenius	*ns*	10	20	30	40	60	100	150	200
	FOS	1.005	1.011	1,016 *	1.170	1.180	1.181	1.182	1.182
	ng	3	5	6	9	12	16	20	24
	FOS	-	0.945	0.980	1.022 *	1.133	1.154	1.163	1.173

Bishop simpli.	*ns*	10	20	30	40	60	100	150	200
	FOS	1.109	1.158	1.170 *	1.180	1.190	1.190	1.190	1.195
	ng	3	5	6	9	12	16	20	24
	FOS	-	1.040	1.050	1.056	1.118	1.124	1.169 *	1.171

Janbu simpli.	*ns*	10	20	30	40	60	100	150	200
	FOS	1.003	1.061 *	1.118	1.132	1.132	1.150	1.150	1.152
	ng	3	5	6	9	12	16	20	24
	FOS	-	0.987	1.042	1.058 *	1.079	1.086	1.097	1.144

Janbu general.	*ns*	10	20	30	40	60	100	150	200
	FOS	1.101	1.120	1.140 *	1.160	1.170	1.190	1.205	1.232
	ng	3	5	6	9	12	16	20	24
	FOS	-	1.028	1.049	1.142 *	1.165	1.185	1.195	1.210

Spencer	*ns*	10	20	30	40	60	100	150	200
	FOS	1.111	1.161 *	1.180	1.180	1.190	1.190	1.200	1.200
	ng	3	5	6	9	12	16	20	24
	FOS	-	1.013	1.025	1.083	1.158 *	1.175	1.186	1.211

Sarma	*ns*	10	20	30	40	60	100	150	200
	FOS	1.001	1.100	1.150	1.172 *	1.180	1.190	1.190	1.209
	ng	3	5	6	9	12	16	20	24
	FOS	-	1.034	1.077	1.148	1.161	1.175 *	1.195	1.198

Fredlund & Krahn (GLE)	*ns*	10	20	30	40	60	100	150	200
	FOS	1.111	1.161 *	1.180	1.180	1.190	1.190	1.200	1.200
	ng	3	5	6	9	12	16	20	24
	FOS	-	1.013	1.025	1.083	1.158 *	1.175	1.186	1.211

Table 5.4 Comparison of two different mass divisions for problem 5.

5.5 Conclusions

The method of slices is well understood and may be the most widely used method for slope stability calculations. Since it is approximate, an adequate number of slices should be used to obtain the closest factor of safety to the real value.

Ting (1983) reported that a high number of slices should be used to reduce the error which comes from the nature of assumption used for the method of slices. Spencer (1967) suggested to use 32 slices generally.

As can be seen the above Tables 5.1-4, nine Gauss points generally gives sufficient accuracy for the calculation of the *FOS*. The candidate suggests that fewer than five Gauss points should not be used. The use of Gaussian integration reduces enormously the calculation time. The case studies show that the Gauss quadrature may be used as an alternative way of *FOS* calculations.

There is no upper limit for the use of Gauss integration points for *FOS* calculations. The author has used up to 24 Gauss points, although nine points were likely to be enough for satisfactory convergence.

CHAPTER 6: LATERAL LOAD ESTIMATION FROM VISCO-PLASTIC FLOW AROUND CYLINDRICAL PILES

6.1 Introduction

In this chapter we will consider the slow, creeping flow of a visco-plastic fluid past a pile and a series of piles. The work presented here is carried out only theoretically. The difference representation of the governing equations is by Williams (1998). However, coding of the program, study of the parametric influences and compilation of the results are the sole effort of the author.

It was thought that in the event of slope failure, the homogenised behaviour of the moving mass could be modelled as a fluid with appropriate inertial and mechanical properties. Part of the present review of the literature is to identify the contribution of other researchers to soil flow and possible application to slope stability studies.

An application of the theory is envisaged as;

- Using mechanical means for slope stabilisation (e.g., piles, soil nailing etc.), and
- Estimating the hydrostatic and frictional forces generated, as the flowing soil interacts with the artificially fixed structure.

6.2 Background theories

Ito and Matsui (1975, 1978) proposed a method, called the theory of plastic flow, which calculates the lateral force on the pile in which the soil is considered as a visco-plastic solid. Details are given in Chapter 7.

A theory is presented by Winter et al. (1983) based on the viscous properties of cohesive soil and a solution for the lateral pressure on the piles in a viscous soil. The viscosity parameters of the cohesive soil may be obtained from water saturated and consolidated samples in undrained triaxial tests subjected to a sudden increase in the rate of strain.

Hutter and Rajagopal (1994) have given a comprehensive review on flows of granular materials without any hint of potential use in slope stability problems.

Cleary and Campbell (1993) described the use of discrete particle computer simulation to test whether the apparent low friction exhibited by long runout landslides could be explained in terms of simple granular mechanics.

Johnson and Rodine (1987) modelled debris flow for sediment-water mixtures using rheological (or constitutive) equations for open channels. The models examined are the Coulomb-viscous model and Bingham models. Using these models, he analysed debris flow in different types of channels.

Craig (1981) has shown that the rheological behaviour of clay rich mudslide material approximates to that of a Bingham model. Craig applied the earlier (1970) mathematical solution of Johnson's Bingham model to the properties of mudslides moving in a plug-flow mode through elliptic and circular channels (see Table 6.1). It was further demonstrated that the observed behaviour of slides in Antrim, Ireland, generally agreed with behaviour predicted by the Bingham model. This is also discussed by Brunsden (1987). The appropriateness of the Bingham model occurred even at small velocities, high and variable strengths, variable water contents and at high estimated viscosities of unsaturated mudslides largely above the water table. This development (Craig, 1981) suggests that the Johnson model may have wide application to studies of mass movement, types of which vary from slide formation to mudflows. This approach goes some-way to provide a practical link between the static and dynamic approaches to mudslide slope instability.

Measured velocity V (10^{-7}m/s)	Average measured strength τ_y (kN/m^2)	Theoretical strength τ_y (kN/m^2)		Bingham viscosity η_p (Ns/m^2)	
		Circular	Ellipse	Circular	Ellipse
8	71	112	90	120	140
11	78	123	112	100	60
26	58	68	68	70	50
77	65	-	85	-	20
100	69	-	84	-	17

Table 6.1 Measured and theoretical properties of mudslides in Antrim (Craig, 1981).

Xiaobi and Lansheng (1991) suggested a method, which may be used to calculate the maximum velocity of a landslide. Their calculations are based on three motion features;

- height drop of rear edge,
- equivalent slope gradient of the rupture surface, and
- friction angle.

The velocity of movement was classified into four grades (see Table 6.2).

Grade	Order	Maximum velocity
High speed	Critical value for debris flow	15-20 m/s
	Super-high speed	>10 m/s
	High speed	>5 m/s
Rapid	Very rapid	>1 m/s
	Rapid	>0.01 m/s
	Sub-rapid	>0.001 m/s
Moderate	Moderate	>0.001 m/m
	Sub-moderate	>0.001 m/h
Slow	Slow	>0.001 m/d
	Very slow	>0.016 m/a
	Extremely slow	<0.016 m/a

Table 6.2 Classification of the movement velocity (Xiaobi and Lansheng, 1991).

A series of open channel experiments was carried out to obtain the flow equations for a debris flow generated by a fluid, the viscosity of which is far larger than that of plain water. Increased levels of viscosity in the experimental fluid was attained by mixing highly absorbent resin powder with water. This powder can absorb water as much as a thousand times in weight and the viscosity of the fluid depends on the

amount of this powder present (Takahashi, 1991). He also discussed the nature of debris flows based on previous field observations.

Debris flows are seen to exhibit behaviour similar to that of Bingham materials. Observations of debris flows moving in a wide, open channel show that the upper part of the flow is rigid (plug flow) and the bottom part is sheared (Taylor and Wilson, 1997).

6.3 Liquid models

During a deformation process the strain may or may not return to zero if the stress is removed after deformation has occurred. If the strain does not finally return to zero, we may say that flow has occurred. If flow occurs, even for an extremely small shear stress, the material can be called a liquid, otherwise it is a solid. It is necessary to specify a extremely small stress because many solids, for example clay, flow under the action of finite stress. No recovery occurs with some materials, which are said to be inelastic (Whorlow, 1980).

The formal distinction between liquids and solids which is given above, is of little practical value. It is more important to know whether or not flow occurs under the action of the stress likely to be present in a particular situation. Consequently no attempted is made to classify models into solid-like and liquid-like types but what is considered are models in order of increasing complexity, as judged by the number of parameters needed to specify the behaviour of the model.

6.3.1 The Newtonian fluid

Fluids for which the shear stress (τ) varies linearly with the velocity gradient (or shear rate) (*dv/dy*) are named Newtonian fluids. There is a linear relationship between τ and *dv/dy* for a given fluid, at a constant temperature, in a steady simple shear situation represented by Fig. 6.1 (Munson et al., 1994). The velocity profile in this case has a constant gradient called the shear rate and the constant of proportionality between τ and *dv/dy* is called the apparent viscosity (η) which is a measure of the 'thickness' or consistency of the liquids. The straight lines of Fig. 6.2 represent two fluids. One has a high viscosity (η_1) and the other a low viscosity (η_2), as indicated by the relative magnitude of the slopes of the two straight lines (Esposito, 1998).

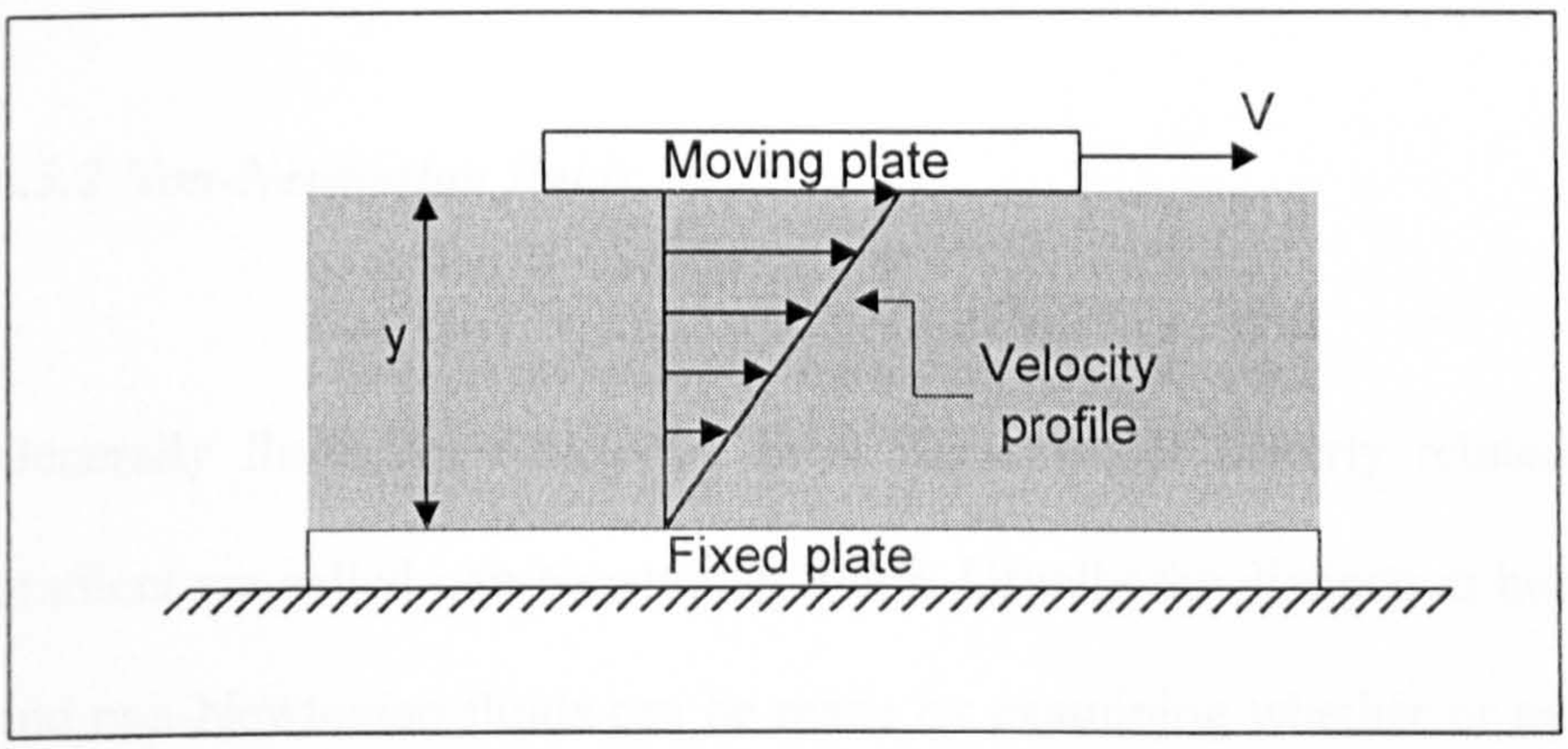

Figure 6.1 Steady simple shear (Esposito, 1998).

The viscosity (η) does not change with changes in velocity gradient (*dv/dy*) for Newtonian fluids; the viscosity varies only with changes in temperature. Most fluids,

including air, methane, carbon dioxide, ethyl alcohol, gasoline, oil, and water, can behave as Newtonian fluids (Esposito, 1998).

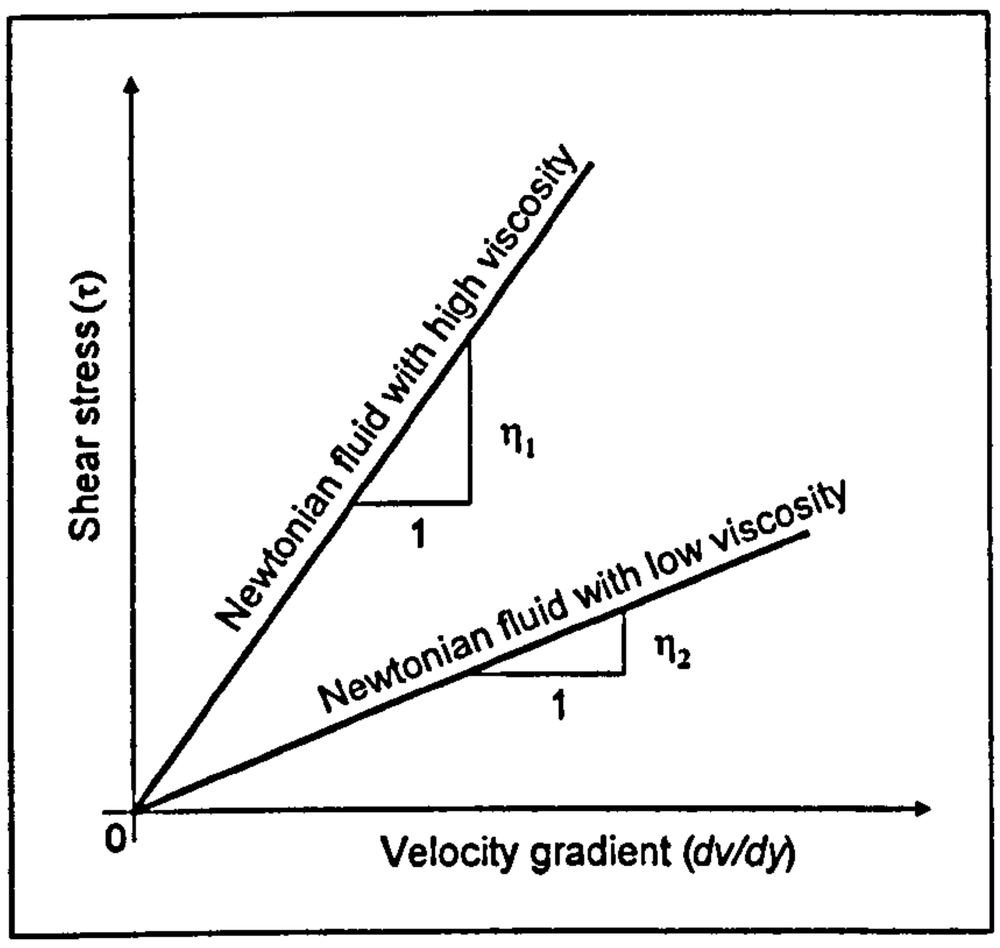

Figure 6.2 Linear relationship of shear stress versus velocity gradient for Newtonian fluids (Esposito, 1998).

6.3.2 Non-Newtonian fluids

Generally fluids for which the shear stress is not linearly related to the velocity gradient are called non-Newtonian fluids. Usually the distinction between Newtonian and non-Newtonian fluids can be made by examining whether or not the ratio of the shear stress to the velocity gradient (viscosity) varies from point to point, see Fig. 6.3. Although there are a variety of non-Newtonian fluid types, the simplest and most common variety are shown in Fig. 6.3 (Munson et al., 1994). Most textbooks on fluid mechanics cover the subject adequately. The presentation here is for completeness of the subject covered.

- For the type of shear thinning fluids, the viscosity decreases with increasing velocity gradient. Thus a shear thinning fluid becomes less viscous as the velocity gradient increases.
- For the type of shear thickening fluids the viscosity increases as the velocity gradient increases. Thus shear thickening fluids become more viscous with an increase in the velocity gradient. A common example of this type of fluid is water-sand mixture (quicksand) (Munson et al., 1994).

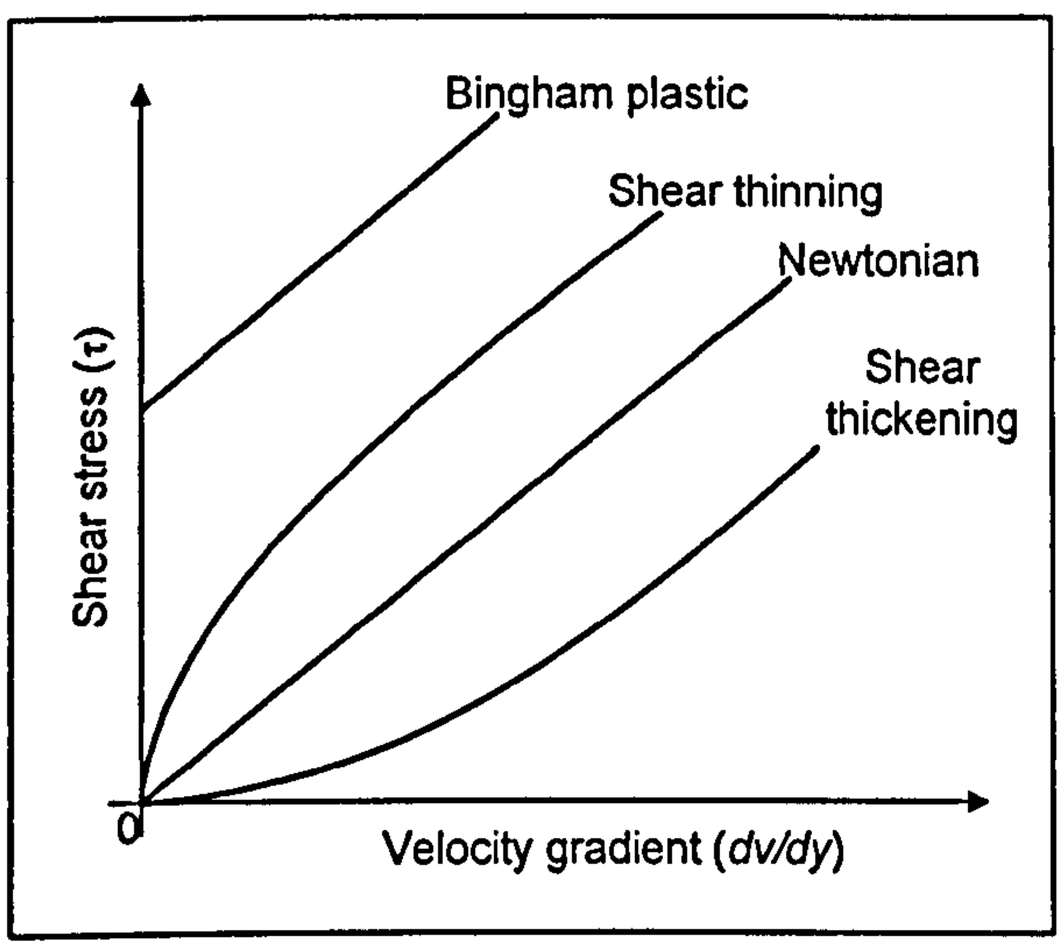

Figure 6.3 Shear stress versus velocity gradient curves for Newtonian fluids, non-Newtonian fluids and a Bingham plastic material (Esposito, 1998).

For non-Newtonian fluids the apparent viscosity, at a particular velocity gradient, is defined as the ratio of shear stress to velocity gradient.

6.3.3 Bingham plastic model

The Bingham plastic model, see Fig. 6.3, is neither completely a solid nor a fluid. Such a material can withstand a finite shear stress without motion (therefore it is not in the fluid phase), but once the yield stress is exceeded it flows like fluid (hence it is not a solid). The behaviour of many common materials, for example clay slurries, plastic emulsions, tooth paste and asphalt may be represented adequately by the Bingham plastic model (Whorlow, 1980).

A Bingham plastic material is not a Newtonian fluid because it requires a finite amount of shear stress to begin flowing (Esposito, 1998). As can be seen from Fig. 6.3, a Newtonian fluid (as well as shear thinning and shear thickening non-Newtonian fluids) begins to flow with even infinitesimal shear stress. Also the apparent viscosity for a Bingham fluid is not constant. The fluid models of interest for this work have the constitutive properties discussed as follows.

6.3.3.1 Bingham plastic model approximations

Viscosity is a measure of the internal friction of a fluid, or its resistance to flow and movement. The actual value of the viscosity depends on the particular fluid, and the viscosity is also highly dependent on temperature. Viscosity is the most important single property that affects the behaviour of a fluid. The more viscous the fluid, the thicker it is and the slower it deforms under stress (Hamill, 1995).

For fluids, the apparent viscosity, which is defined in section 6.3.1 and 6.3.2, is given here by the equation form;

$$\eta = \frac{\text{Shear stress}}{\text{Velocity gradient}} = \frac{\tau}{\left(dv/dy\right)} \quad \text{(Pa s).} \qquad 6.1$$

For ease of representation the notation $q = dv/dy$ for the velocity gradient or shear rate will be used. The equation for a Bingham plastic in this notation is;

$$\tau = \tau_y + \eta_p q \,,$$

$$\eta = \frac{\tau_y}{q} + \eta_p \,, \qquad 6.2$$

provided $\tau > \tau_y$. Here τ_y is the yield stress and η_p the Bingham plastic viscosity, which are the constants that define the model.

As can be seen from the viscous definition of the Bingham model, the viscosity becomes singular as the shear rate vanishes, which leads to difficulties in computer simulations.

6.3.3.1.1 Biviscosity Bingham model

The biviscosity model is a recent popular development used by Whipple (1997) to approximate the Bingham plastic model and to attempt to overcome the

computational singularity difficulty. In a different notation to that adopted by Whipple the following equivalent representation is formulated;

$$\tau = \eta_p(1+\alpha)q \quad \text{for} \quad q \le \frac{\tau_y}{\alpha\eta_p} \tag{6.3}$$

$$\tau = \tau_y + \eta_p q \quad \text{for} \quad q \ge \frac{\tau_y}{\alpha\eta_p}. \tag{6.4}$$

The above are shown graphically in Fig 6.4.

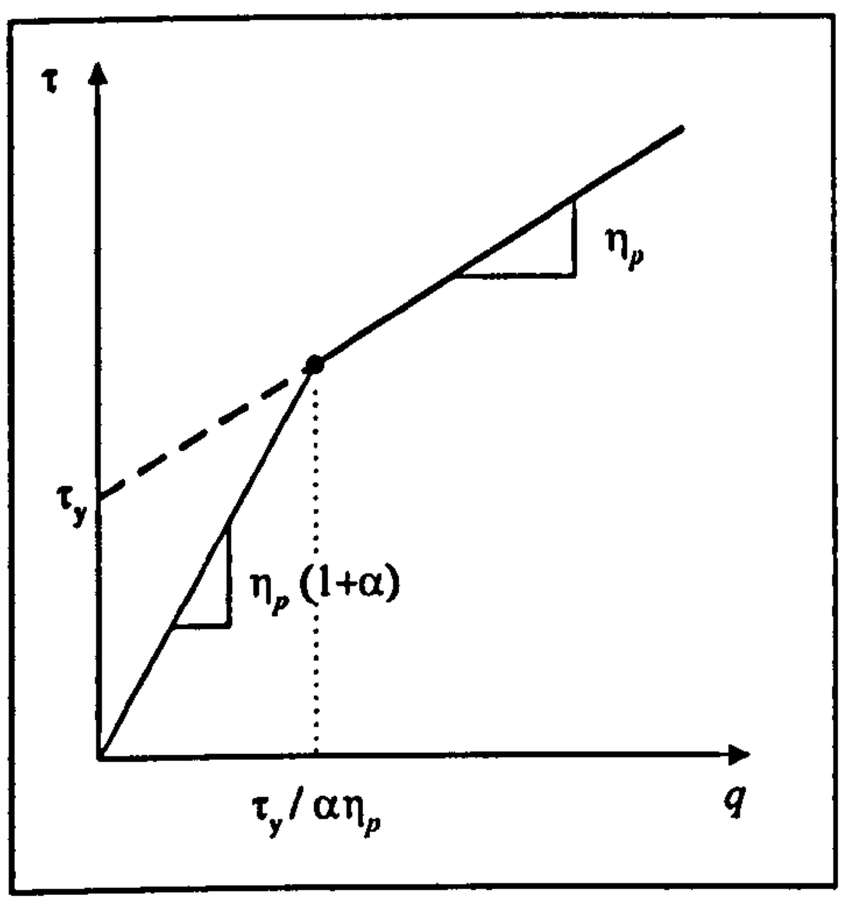

Figure 6.4 Schematic illustration of the biviscosity model.

The approximation is basically a Newtonian fluid for low shear rates, and a Bingham model at high shear rates. As the positive parameter α increases, the biviscosity model approaches the Bingham model more closely.

Although the model provides a continuous relationship between shear stress and shear rate, there is a lack of smoothness at the join point between the two elements of the model.

6.3.3.1.2 Smooth viscosity Bingham model

Another approximation for the Bingham model is;

$$\tau = \frac{\tau_y \left(1+\frac{1}{\alpha}\right)+\eta_p q}{1+\frac{\tau_y}{\alpha \eta_p q}}, \qquad 6.5$$

which again better approximates the true Bingham model as α, the positive yield stress modelling parameter, increases, but has a smooth profile, see Fig 6.5.

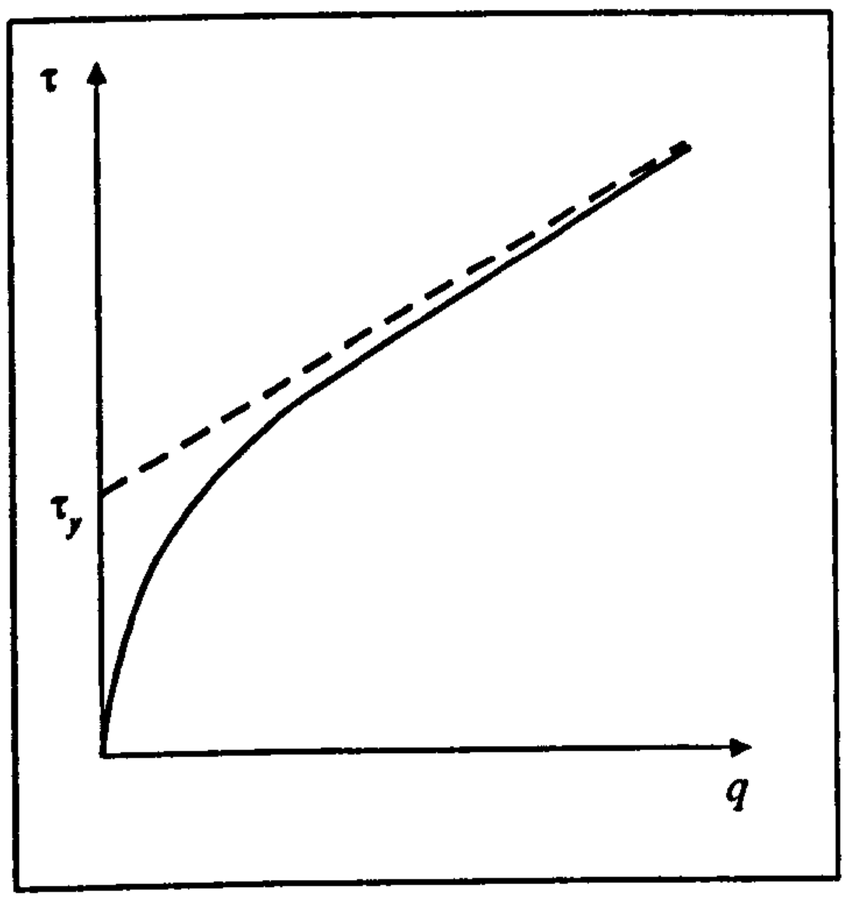

Figure 6.5 Schematic illustration of the smooth viscosity model.

At high shear rates;

$$\tau \approx \tau_y + \eta_p q$$

and at low shear rates;

$$\tau \approx \eta_p (1+\alpha) q .$$

6.4 Flow past a cylinder (pile)

The analysis presented here follows closely the work of Townsend (1980, 1984) for two dimensional fluid flow past a cylinder (pile) that is stationary.

6.4.1 Modelling

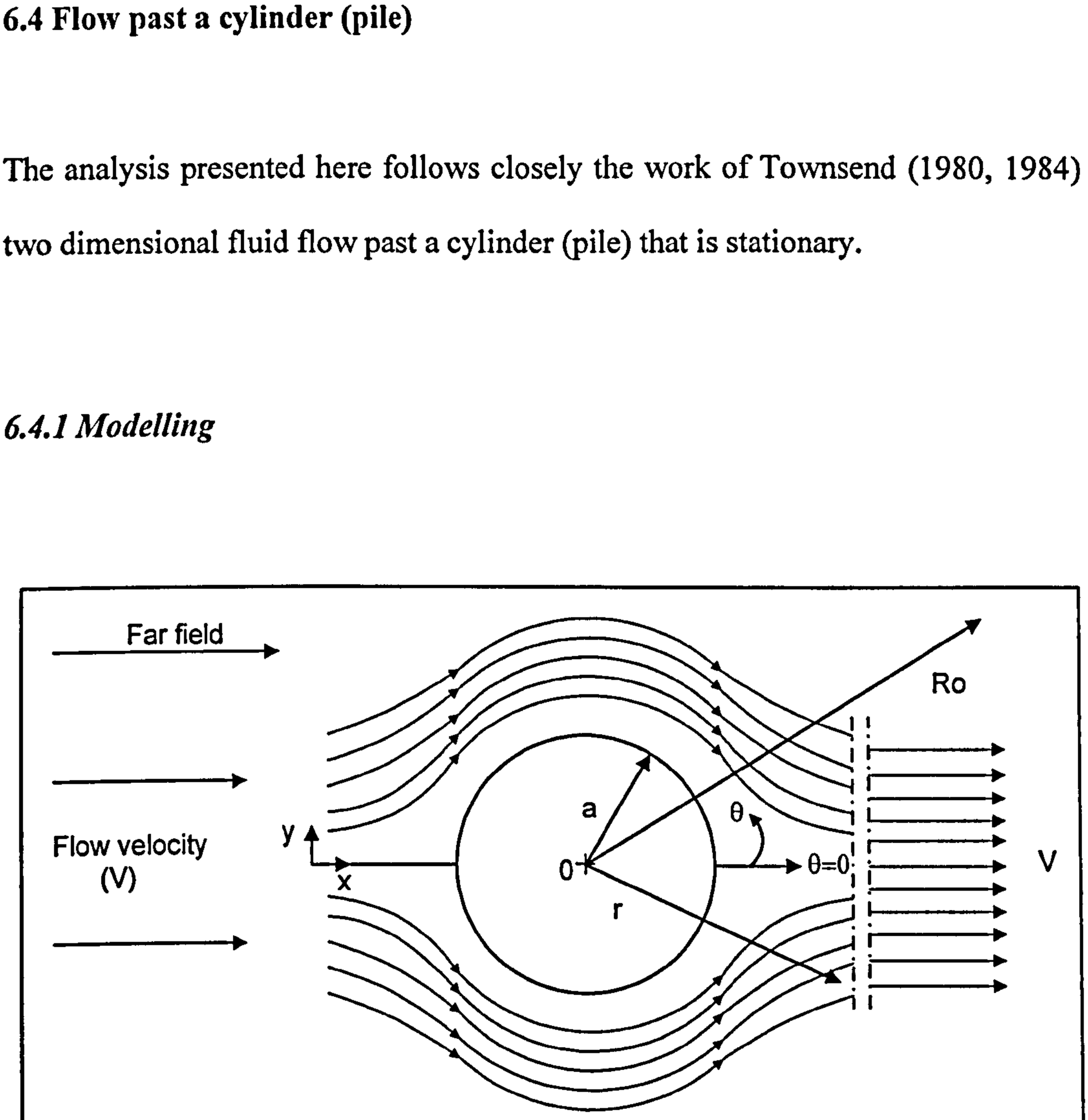

Figure 6.6 Flow past a cylinder.

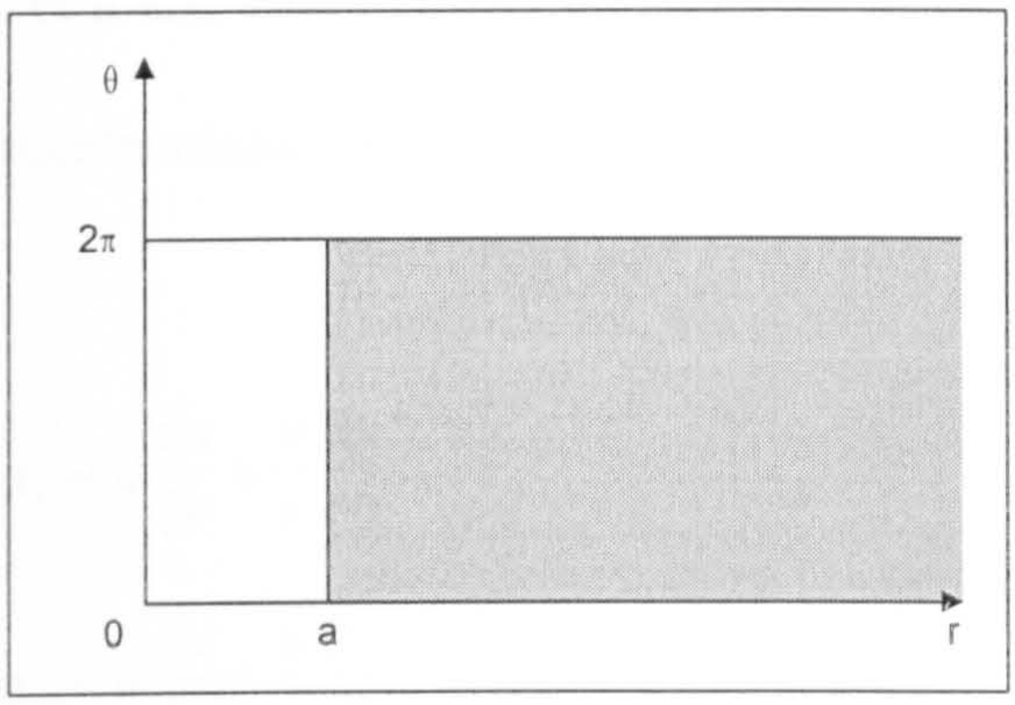

Figure 6.7 Polar co-ordinate system of the shaded flow domain.

The analysis here is based on polar r and θ co-ordinates, Fig. 6.7, with origin 0 at the centre of the cylinder. The fluid domain is $a \leq r \leq$ Ro, where a is the cylinder radius and Ro is a sufficiently large distance from the cylinder. In Fig. 6.6 the cylinder is seen in section and is assumed to be of infinite length with the far field flow of speed V in the x ($\theta = 0$) direction.

A steady symmetrical flow is assumed, so that flow in $\pi < \theta < 2\pi$ below the cylinder (pile) is a mirror image of that in $0 < \theta < \pi$ above the cylinder.

The equations for fluid motion come from Newton's second law of motion;

$$F = m a , \qquad 6.6$$

where F = force (N)

m = mass (kg)

a = acceleration (m/s^2).

Let u and v be velocity components in the r and θ directions respectively so that the accelerations, in the r and θ directions are given by;

$$a_r = u\frac{\partial u}{\partial r} + \frac{v}{r}\frac{\partial u}{\partial \theta} - \frac{v^2}{r}, \tag{6.7}$$

$$a_\theta = u\frac{\partial u}{\partial r} + \frac{v}{r}\frac{\partial v}{\partial \theta} + \frac{uv}{r}. \tag{6.8}$$

Since the flow is steady there is no time dependence so that $\frac{\partial u}{\partial t}$ and $\frac{\partial v}{\partial t}$ do not appear.

If σ_{rr} is the normal stress radially, $\sigma_{\theta\theta}$ the normal stress circumferentially (hoop) and $\tau_{r\theta}$ the shear stress, the forces per unit volume in the r and θ directions are f_r and f_θ where;

$$f_r = \frac{\partial}{\partial r}\sigma_{rr} + \frac{1}{r}\frac{\partial}{\partial \theta}\tau_{r\theta} + \frac{1}{r}(\sigma_{rr} - \sigma_{\theta\theta}), \tag{6.9}$$

$$f_\theta = \frac{\partial}{\partial r}\tau_{r\theta} + \frac{2}{r}\tau_{r\theta} + \frac{1}{r}\frac{\partial}{\partial \theta}\sigma_{\theta\theta}\ . \tag{6.10}$$

Using Newtonian laws, the following may be obtained where mass (per unit volume) is represented by fluid density ρ:

r direction;

$$\rho a_r = f_r \Rightarrow \rho\left[u\frac{\partial u}{\partial r} + \frac{v}{r}\frac{\partial u}{\partial \theta} - \frac{v^2}{r}\right] = \frac{\partial}{\partial r}\sigma_{rr} + \frac{1}{r}\frac{\partial \tau_{r\theta}}{\partial \theta} + \frac{1}{r}(\sigma_{rr} - \sigma_{\theta\theta}). \tag{6.11}$$

θ direction;

$$\rho a_\theta = f_\theta \Rightarrow \rho\left[u\frac{\partial v}{\partial r}+\frac{v}{r}\frac{\partial v}{\partial \theta}+\frac{uv}{r}\right]=\frac{\partial}{\partial r}\tau_{r\theta}+\frac{2}{r}\tau_{r\theta}+\frac{1}{r}\frac{\partial}{\partial \theta}\sigma_{\theta\theta}. \qquad 6.12$$

The fluid is taken to be incompressible, which is manifest through the continuity equation;

$$\frac{\partial u}{\partial r}+\frac{u}{r}+\frac{1}{r}\frac{\partial v}{\partial \theta}=0\ . \qquad 6.13$$

As far as the stresses are concerned we can separate the hydrostatic pressure p from the fluid frictional and other stresses by writing;

$$\sigma_{rr}=-p+T_{rr}\ . \qquad 6.14$$

$$\sigma_{\theta\theta}=-p+T_{\theta\theta}\ . \qquad 6.15$$

$$\tau_{r\theta}=T_{r\theta}\ . \qquad 6.16$$

where the T_{ij} terms are called extra stress components. Equations [6.11] and [6.12] then become;

$$\rho\left[u\frac{\partial u}{\partial r}+\frac{v}{r}\frac{\partial u}{\partial \theta}-\frac{v^2}{r}\right]=-\frac{\partial p}{\partial r}+\frac{\partial T_{rr}}{\partial r}+\frac{1}{r}\frac{\partial T_{r\theta}}{\partial \theta}+\frac{1}{r}\left(T_{rr}-T_{\theta\theta}\right), \qquad 6.17$$

$$\rho\left[u\frac{\partial u}{\partial r}+\frac{v}{r}\frac{\partial u}{\partial \theta}+\frac{uv}{r}\right]=-\frac{1}{r}\frac{\partial p}{\partial \theta}+\frac{\partial}{\partial r}T_{r\theta}+\frac{2}{r}T_{r\theta}+\frac{1}{r}\frac{\partial}{\partial \theta}T_{\theta\theta}. \qquad 6.18$$

The extra stresses are explicitly related to the rates of strain $\dot{\varepsilon}_{rr}$, $\dot{\gamma}_{r\theta}$ and $\dot{\varepsilon}_{\theta\theta}$ within the fluid. The relationship includes the fluid viscosity η which is a function of the strain rates. We have;

$$\dot{\varepsilon}_{rr} = \frac{\partial u}{\partial r}\,, \tag{6.19}$$

$$\dot{\gamma}_{r\theta} = \frac{1}{2}\left[r\frac{\partial}{\partial r}\left(\frac{v}{r}\right)+\frac{1}{r}\frac{\partial u}{\partial \theta}\right]\,, \tag{6.20}$$

$$\dot{\varepsilon}_{\theta\theta} = \frac{1}{r}\frac{\partial v}{\partial \theta}+\frac{u}{r} = -\frac{\partial u}{\partial r} \text{ (through Eqn. [6.13])}\,, \tag{6.21}$$

and viscosity $\eta = \eta(q)$ where q is the general rate of strain given by;

$$q^2 = 4\left(\frac{\partial u}{\partial r}\right)^2 + \left[r\frac{\partial}{\partial r}\left(\frac{v}{r}\right)+\frac{1}{r}\frac{\partial u}{\partial \theta}\right]^2. \tag{6.22}$$

Combining the above, one may have the general expression of the purely viscous fluid model;

$$T_{rr} = 2\eta(q)\dot{\varepsilon}_{rr}\,, \tag{6.23}$$

$$T_{r\theta} = 2\eta(q)\dot{\gamma}_{r\theta}\,, \tag{6.24}$$

$$T_{\theta\theta} = 2\eta(q)\dot{\varepsilon}_{\theta\theta}\,. \tag{6.25}$$

The form of the viscosity function depends on the model used for the fluid, e.g. a Newtonian or a Bingham model type.

To reduce the number of variables which need to be solved it is possible to introduce the stream function ψ, which automatically satisfies Eqn. [6.13] when writing;

$$u = \frac{1}{r}\frac{\partial \psi}{\partial \theta}, \qquad 6.26$$

$$v = -\frac{\partial \psi}{\partial r}. \qquad 6.27$$

Also vorticity ω may be introduced by;

$$\omega = \nabla^2 \psi = \frac{1}{r}\frac{\partial}{\partial r}\left(r\frac{\partial \psi}{\partial r}\right) + \frac{1}{r^2}\frac{\partial^2 \psi}{\partial \theta} . \qquad 6.28$$

Thus, a stream function/vorticity approach is adopted to solve the flow equations.

Elimination of the pressure between Eqns. [6.17] and [6.18] through $\frac{1}{r}\left[\frac{\partial}{\partial \theta}[6.17] - r\frac{\partial}{\partial r}[6.18]\right]$ leads to an equation for vorticity;

$$\frac{1}{r}\left[\frac{\partial \psi}{\partial \theta}\frac{\partial \omega}{\partial r} - \frac{\partial \psi}{\partial r}\frac{\partial \omega}{\partial \theta}\right] = \frac{1}{r}\frac{\partial}{\partial \theta}\left[\frac{\partial}{\partial r}T_{rr} + \frac{1}{r}\frac{\partial}{\partial \theta}T_{r\theta} + \frac{T_{rr} - T_{\theta\theta}}{r}\right] - \frac{1}{r}\frac{\partial}{\partial r}\left[r\frac{\partial T_{r\theta}}{\partial r} + \frac{2T_{r\theta}}{r} + \frac{1}{r}\frac{\partial T_{\theta\theta}}{\partial \theta}\right]. \qquad 6.29$$

If the problem is formulated in a non-dimensional manner, many similar situations can be solved through a single set of equations. Let η be a typical viscosity value (η_0 for Newtonian liquid or η_p for a Bingham fluid) and write non-dimensional values with * superscripts.

$$\eta^* = \frac{\eta}{\eta_0} \ , \quad r^* = \frac{r}{a} \ , \quad u^* = \frac{u}{V} \ , \quad v^* = \frac{v}{V} \ , \quad p^* = \frac{p}{aV^2} \ , \quad \psi^* = \frac{\psi}{aV} \ ,$$

$$\omega^* = \frac{\omega a}{V} \ , \quad \dot{\gamma}^*_{ij} = \dot{\gamma}_{ij}\frac{a}{V}, \quad T^*_{ij} = T_{ij}\frac{a}{\eta_0 V} \ , \quad q^* = q\frac{a}{V}$$

Changing variables and dropping for convenience the *'s the following equations result for Eqns. [6.28] and [6.29];

$$\omega = \frac{1}{r}\frac{\partial}{\partial r}\left(r\frac{\partial \psi}{\partial r}\right) + \frac{1}{r^2}\frac{\partial^2 \psi}{\partial \theta^2} \ , \tag{6.30}$$

$$\frac{1}{r}\left[\frac{\partial \psi}{\partial \theta}\frac{\partial \omega}{\partial r} - \frac{\partial \psi}{\partial r}\frac{\partial \omega}{\partial \theta}\right] = \frac{1}{\mathrm{Re}}\frac{1}{r}\left\{\frac{\partial}{\partial \theta}\left[\frac{\partial}{\partial r}T_{rr} + \frac{1}{r}\frac{\partial T_{r\theta}}{\partial \theta} + \frac{T_{rr} - T_{\theta\theta}}{r}\right] - \frac{\partial}{\partial r}\left[r\left(\frac{\partial}{\partial r}T_{r\theta} + \frac{2}{r}T_{r\theta} + \frac{1}{r}\frac{\partial}{\partial \theta}T_{\theta\theta}\right)\right]\right\} . \tag{6.31}$$

where $\mathrm{Re} = \rho a V/\eta_0$ is the Reynolds number which is the ratio of the inertia to viscous terms. Also a general strain rate q may be defined through;

$$q^2 = 4\left[\frac{\partial}{\partial r}\left(\frac{1}{r}\frac{\partial \psi}{\partial \theta}\right)\right]^2 + \left[-r\frac{\partial}{\partial r}\left(\frac{1}{r}\frac{\partial \psi}{\partial r}\right) + \frac{1}{r^2}\frac{\partial^2 \psi}{\partial \theta^2}\right]^2 . \tag{6.32}$$

In order to consider the 'infinite' nature of the fluid continuum, the r variable is scaled as $\xi = \ln(r)$ or $r = e^{\xi}$. This allows greater attention to be given to the region closest to the cylinder (Townsend, 1980). Then for Eqns. [6.30], [6.31] and [6.32];

$$\frac{\partial^2\psi}{\partial\xi^2}+\frac{\partial^2\psi}{\partial\theta^2}=e^{2\xi}\omega\ , \tag{6.33}$$

and

$$\frac{\partial\psi}{\partial\theta}\frac{\partial\omega}{\partial\xi}-\frac{\partial\psi}{\partial\xi}\frac{\partial\omega}{\partial\theta}$$
$$=\frac{1}{\mathrm{Re}}\left[\frac{\partial}{\partial\theta}\left(\frac{\partial T_{rr}}{\partial\xi}+\frac{\partial T_{r\theta}}{\partial\theta}+T_{rr}-T_{\theta\theta}\right)-\frac{\partial}{\partial\xi}\left(\frac{\partial T_{r\theta}}{\partial\xi}+2T_{r\theta}+\frac{\partial}{\partial\theta}T_{\theta\theta}\right)\right]. \tag{6.34}$$

$$q^2=e^{-4\xi}\left[4\left(\frac{\partial^2\psi}{\partial\xi\partial\theta}-\frac{\partial\psi}{\partial\theta}\right)^2+\left(\frac{\partial^2\psi}{\partial\theta^2}+2\frac{\partial\psi}{\partial\xi}-\frac{\partial^2\psi}{\partial\xi^2}\right)^2\right]. \tag{6.35}$$

Also the stresses can be written as;

$$T_{rr}=2\eta e^{-2\xi}\left[\frac{\partial^2\psi}{\partial\xi\partial\theta}-\frac{\partial\psi}{\partial\theta}\right], \tag{6.36}$$

$$T_{r\theta}=\eta e^{-2\xi}\left[\frac{\partial^2\psi}{\partial\theta^2}-\frac{\partial^2\psi}{\partial\xi^2}+2\frac{\partial\psi}{\partial\xi}\right], \tag{6.37}$$

$$T_{\theta\theta}=-T_{rr}\ . \tag{6.38}$$

These can be substituted into Eqn. [6.34] from which ω can in principle be determined. Use has been made here of;

$$u=e^{-\xi}\frac{\partial\psi}{\partial\theta}\ , \tag{6.39}$$

$$v=-e^{-\xi}\frac{\partial\psi}{\partial\xi}\ , \tag{6.40}$$

and the strain rates $\dot{\gamma}_{ij}$ are given by;

$$\dot{\varepsilon}_{rr} = e^{-2\xi}\left[\frac{\partial^2\psi}{\partial\xi\partial\theta} - \frac{\partial\psi}{\partial\theta}\right], \qquad 6.41$$

$$\dot{\gamma}_{r\theta} = \frac{1}{2}e^{-2\xi}\left[\frac{\partial^2\psi}{\partial\theta^2} - \frac{\partial^2\psi}{\partial\xi^2} + 2\frac{\partial\psi}{\partial\xi}\right], \qquad 6.42$$

$$\dot{\varepsilon}_{\theta\theta} = -\dot{\varepsilon}_{rr} \ . \qquad 6.43$$

After some algebra Eqn. [6.34] may be rewritten as;

$$\eta\left(\frac{\partial^2\omega}{\partial\xi^2} + \frac{\partial^2\omega}{\partial\theta^2}\right) + 2\left[\frac{\partial\eta}{\partial\xi}\frac{\partial\omega}{\partial\xi} + \frac{\partial\eta}{\partial\theta}\frac{\partial\omega}{\partial\theta}\right] + 4\left(\frac{\partial\eta}{\partial\xi}\dot{\gamma}_{r\theta} - \frac{\partial\eta}{\partial\theta}\dot{\varepsilon}_{rr}\right) + 4\frac{\partial^2\eta}{\partial\xi\partial\theta}\dot{\varepsilon}_{rr}$$

$$+ 2\dot{\gamma}_{r\theta}\left(\frac{\partial^2\eta}{\partial\theta^2} - \frac{\partial^2\eta}{\partial\xi^2}\right) = \mathrm{Re}\left[\frac{\partial\psi}{\partial\theta}\frac{\partial\omega}{\partial\xi} - \frac{\partial\psi}{\partial\xi}\frac{\partial\omega}{\partial\theta}\right] \qquad 6.44$$

When $\eta \equiv 1$ the corresponding Newtonian equation is given by;

$$\frac{\partial^2\omega}{\partial\xi^2} + \frac{\partial^2\omega}{\partial\theta^2} = \mathrm{Re}\left[\frac{\partial\psi}{\partial\theta}\frac{\partial\omega}{\partial\xi} - \frac{\partial\psi}{\partial\xi}\frac{\partial\omega}{\partial\theta}\right], \qquad 6.45$$

which agrees with Townsend, (1984) where $T_{ij} = 0$ in his Eqn. [3.2].

A more convenient mathematical form for Eqn. [6.44] that eases the solution process is;

$$\frac{\partial}{\partial\xi}\left(\eta^2\frac{\partial\omega}{\partial\xi}\right)+\frac{\partial}{\partial\theta}\left(\eta^2\frac{\partial\omega}{\partial\theta}\right)+\mathrm{Re}\,\eta\left(\frac{\partial\psi}{\partial\xi}\frac{\partial\omega}{\partial\theta}-\frac{\partial\psi}{\partial\xi}\frac{\partial\omega}{\partial\xi}\right)$$
$$=2\left[T_{rr}\frac{\partial\eta}{\partial\theta}-T_{r\theta}\frac{\partial\eta}{\partial\xi}\right]+T_{r\theta}\left(\frac{\partial^2\eta}{\partial\xi^2}-\frac{\partial^2\eta}{\partial\theta^2}\right)-2T_{rr}\frac{\partial^2\eta}{\partial\xi\partial\theta}\quad . \tag{6.46}$$

Equation [6.35] may be rewritten by using Eqns. [6.41] and [6.42] as;

$$q=2\sqrt{\dot{\varepsilon}_{rr}{}^2+\dot{\gamma}_{r\theta}{}^2}\quad . \tag{6.47}$$

6.4.2 Boundary conditions

The flow domain consists of $a<r<\mathrm{Ro}$ dimensionally or $0<\xi<\xi_o=\ln(\mathrm{Ro}/a)$ non-dimensionally; and $0<\theta<\pi$. On the boundaries of this domain, the following boundary conditions are valid for the ψ and ω differential equations, that are treated as a pair of non-linear coupled partial differential equations (PDE).

- For $\theta=0$ and $\theta=\pi$,see Fig. 6.8.

  Symmetry implies $v=\dfrac{\partial u}{\partial\theta}=0$ which leads to

  $\psi=\dfrac{\partial\psi}{\partial\xi}=\dfrac{\partial^2\psi}{\partial\xi^2}=0$ and $\dfrac{\partial^2\psi}{\partial\theta^2}=0$. It follows that $\omega=\dot{\gamma}_{r\theta}=0$.

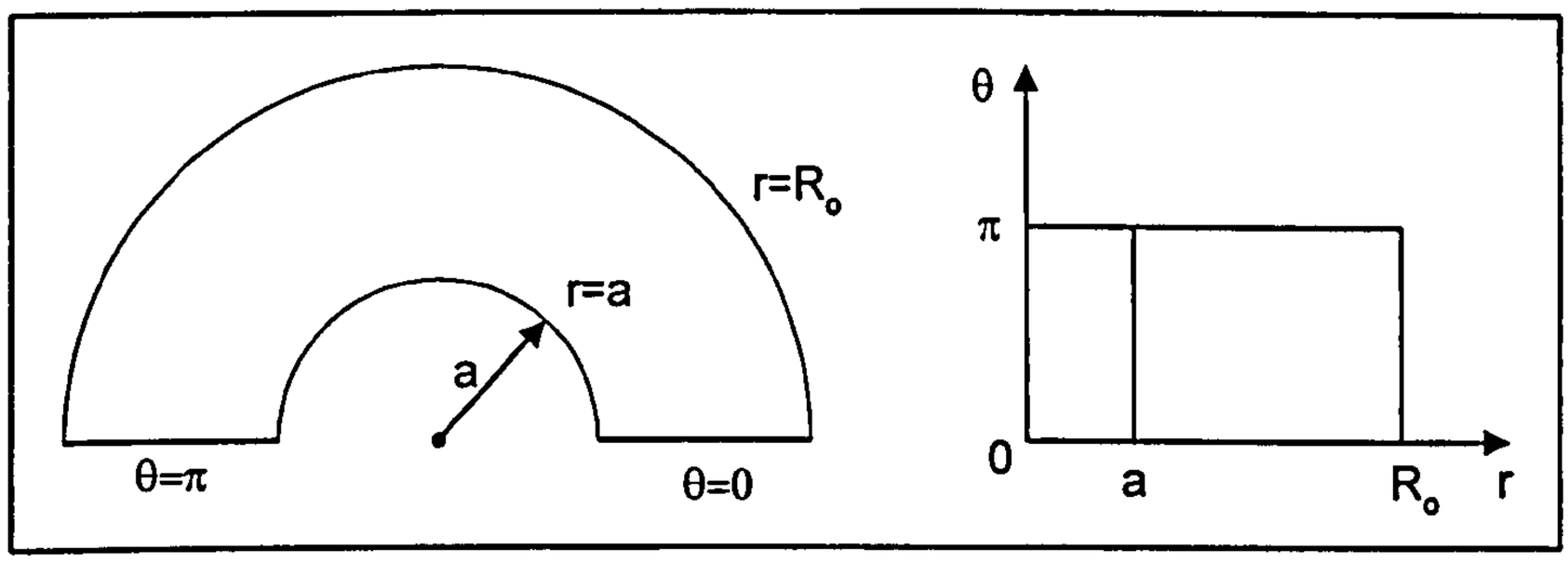

Figure 6.8 Flow domain in polar co-ordinates (dimensional parameters in force).

- For the cylinder boundary $\xi = 0$, Fig. 6.9.

  The no slip conditions is adopted $u = v = 0$ leading to

$$\frac{\partial \psi}{\partial \theta} = \frac{\partial \psi}{\partial \xi} = \frac{\partial^2 \psi}{\partial \xi \, \partial \theta} = \frac{\partial^2 \psi}{\partial \theta^2} = 0,$$

then

$$\omega = \frac{\partial^2 \psi}{\partial \xi^2}, \quad \psi = 0, \quad \dot{\gamma}_{r\theta} = -\frac{\omega}{2}, \quad \dot{\varepsilon}_{rr} = 0 \text{ and} \quad q = |\omega|.$$

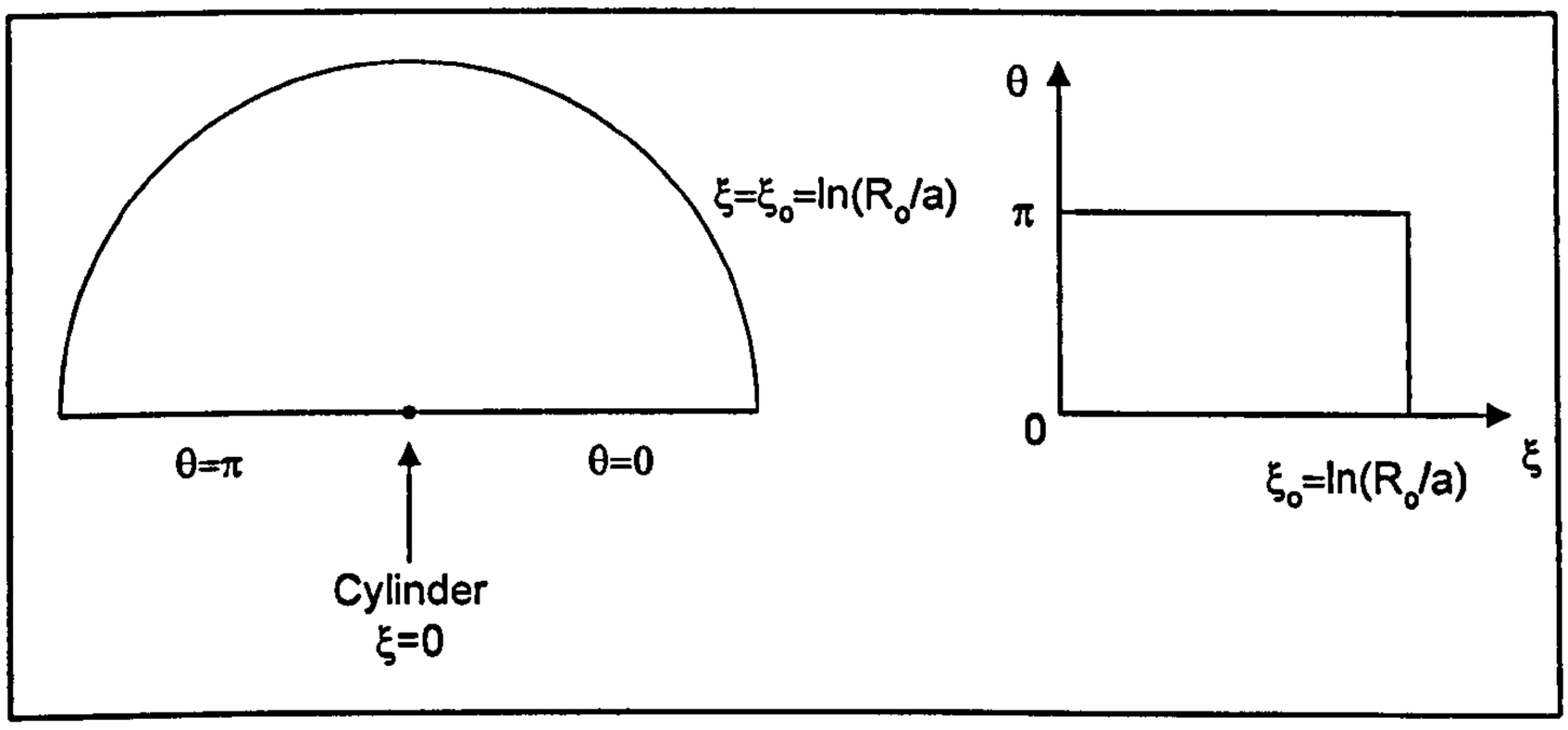

Figure 6.9 Fluid domain in ξ and θ co-ordinates.

- Values at 'infinity' where $\xi = \xi_0$, see Fig. 6.9.

A steady far field flow is assumed where $u = 1$ and $v = 0$. This leads to

$$\psi = \frac{\partial \psi}{\partial \xi} = e^{\xi} \sin\theta \ ,$$

and $\omega = q = 0$.

6.5 Calculation of the force on the cylinder

The fluid force F on the cylinder per unit length may be written in non-dimensional form as;

$$F = \int_0^{2\pi} \sigma_{nx} \, d\theta \ , \qquad 6.48$$

where σ_{nx} is the normal component of stress acting on the cylinder in the x direction $(\theta = 0)$.

σ_{nx} may be expressed as follows;

$$\sigma_{nx} = -p\cos\theta + \left(T_{rr}\cos\theta - T_{r\theta}\sin\theta\right)/\mathrm{Re} \, , \qquad 6.49$$

and for the cylinder boundary $T_{rr} = 0$ and $T_{r\theta} = -\eta\omega$.

The pressure p on the cylinder can be determined from the non-dimensional form of Eqn. [6.18] namely;

$$\frac{\partial p}{\partial \theta} = \frac{1}{\mathrm{Re}}\left[\frac{\partial}{\partial \xi} T_{r\theta} + 2T_{r\theta}\right]. \qquad 6.50$$

This simplifies to provide;

$$\frac{\partial p}{\partial \theta} = -\frac{1}{\mathrm{Re}}\frac{\partial}{\partial \xi}(\eta\omega)\,, \qquad 6.51$$

which upon integration becomes;

$$p = p_0 - \frac{1}{\mathrm{Re}}\int_0^{\theta}\frac{\partial}{\partial \xi}(\eta\omega)(t)\,dt\,, \qquad 6.52$$

where p_0 is the value of p at $\theta = 0$.

Incorporation of Eqn. [6.52] into the expression for force provides;

$$F = -p_0\int_0^{2\pi}\cos\theta\,d\theta + \frac{1}{\mathrm{Re}}\int_0^{2\pi}\cos\theta\int_0^{\theta}\frac{\partial}{\partial \xi}(\eta\omega)(t)\,dt\,d\theta + \frac{1}{\mathrm{Re}}\int_0^{2\pi}\eta\omega\sin\theta\,d\theta. \qquad 6.53$$

Through integration by parts, the second term of the above equation may be simplified to yield the overall expression for force given by;

$$F = \frac{1}{\mathrm{Re}}\int_0^{2\pi}\left(\eta\omega - \frac{\partial}{\partial \xi}(\eta\omega)\right)\sin\theta\,d\theta. \qquad 6.54$$

Using symmetry at $\theta = \pi$ the force is finally obtained as;

$$F = \frac{2}{\mathrm{Re}}\int_0^{\pi}\left(\eta\omega - \frac{\partial}{\partial \xi}(\eta\omega)\right)\sin\theta\,d\theta. \qquad 6.55$$

6.5.1 Numerical modelling

The flow domain is given by $0 \le \xi \le \xi_0$ and $0 \le \theta \le \pi$ incorporating symmetry at $\theta = \pi$, Fig. 6.10. It is required to solve the following coupled non-linear pair of PDEs for the stream function ψ, Eqn. [6.33], and vorticity ω, Eqn. [6.46]. For convenience they are rewritten here;

$$\frac{\partial^2 \psi}{\partial \xi^2} + \frac{\partial^2 \psi}{\partial \theta^2} = e^{2\xi}\omega \,, \qquad 6.33$$

$$\begin{aligned} &\frac{\partial}{\partial \xi}\left(\eta^2 \frac{\partial \omega}{\partial \xi}\right) + \frac{\partial}{\partial \theta}\left(\eta^2 \frac{\partial \omega}{\partial \theta}\right) + \mathrm{Re}\,\eta\left(\frac{\partial \psi}{\partial \xi}\frac{\partial \omega}{\partial \theta} - \frac{\partial \psi}{\partial \xi}\frac{\partial \omega}{\partial \xi}\right) \\ &= 2\left[T_{rr}\frac{\partial \eta}{\partial \theta} - T_{r\theta}\frac{\partial \eta}{\partial \xi}\right] + T_{r\theta}\left(\frac{\partial^2 \eta}{\partial \xi^2} - \frac{\partial^2 \eta}{\partial \theta^2}\right) - 2T_{rr}\frac{\partial^2 \eta}{\partial \xi \partial \theta} \end{aligned} \,, \qquad 6.46$$

given the main boundary conditions;

$\psi, \omega = 0$ on $\theta = 0, \pi$

$\psi = e^{\xi}\sin\theta$, $\omega = 0$ on $\xi = \xi_0$ and

$\psi = 0$ on $\xi = 0$.

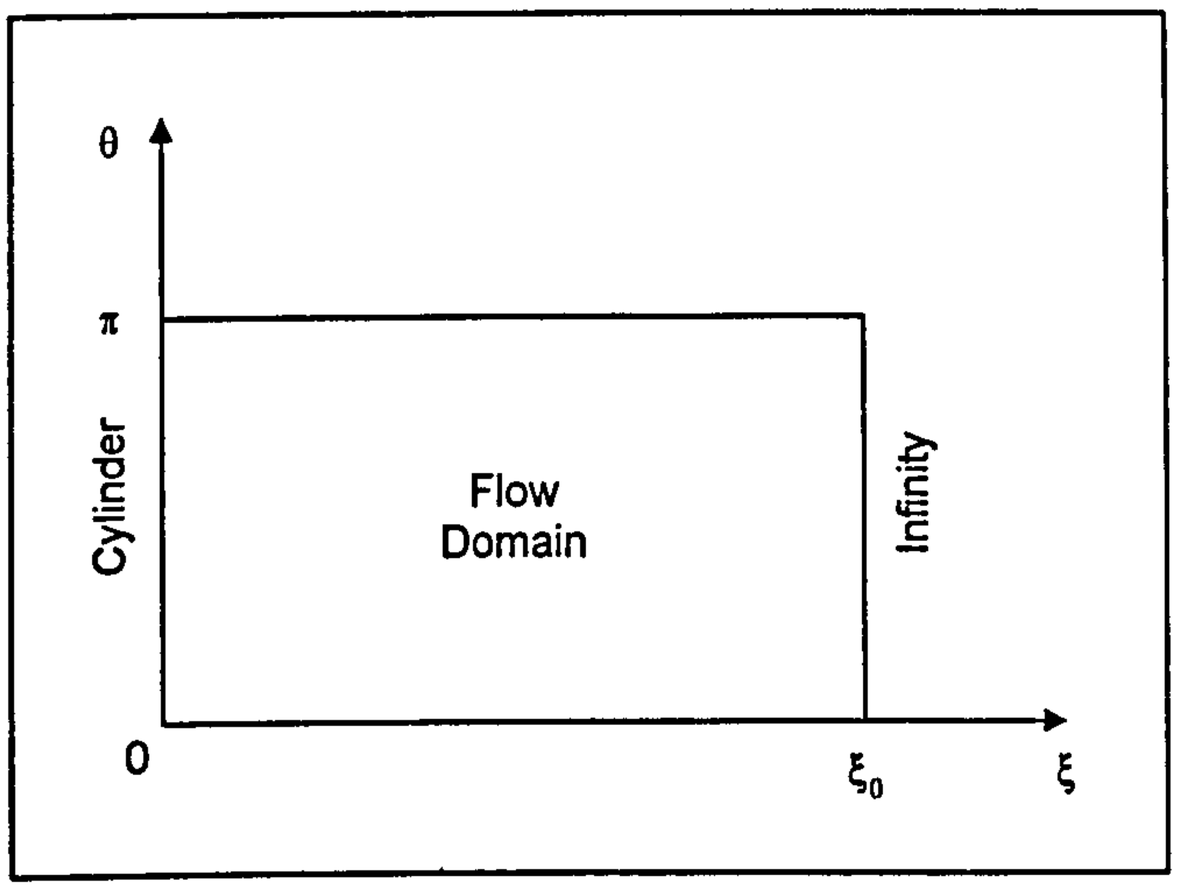

Figure 6.10 Boundary for the flow domain.

The value of ω on the cylinder needs to be prescribed as does the viscous relationship $\eta(q)$ dependent on the deformation rate q.

Because the flow domain is rectangular in nature, it is convenient to use a finite difference scheme to solve the coupled equations numerically, see Fig. 6.11.

In the ξ and θ directions, a mesh is imposed (Fig. 6.11) on the flow domain where the interval between grid lines in the ξ direction is $d\xi = \frac{\xi_0}{M}$ and in the θ directions $d\theta = \frac{\pi}{N}$, for positive integers M and N.

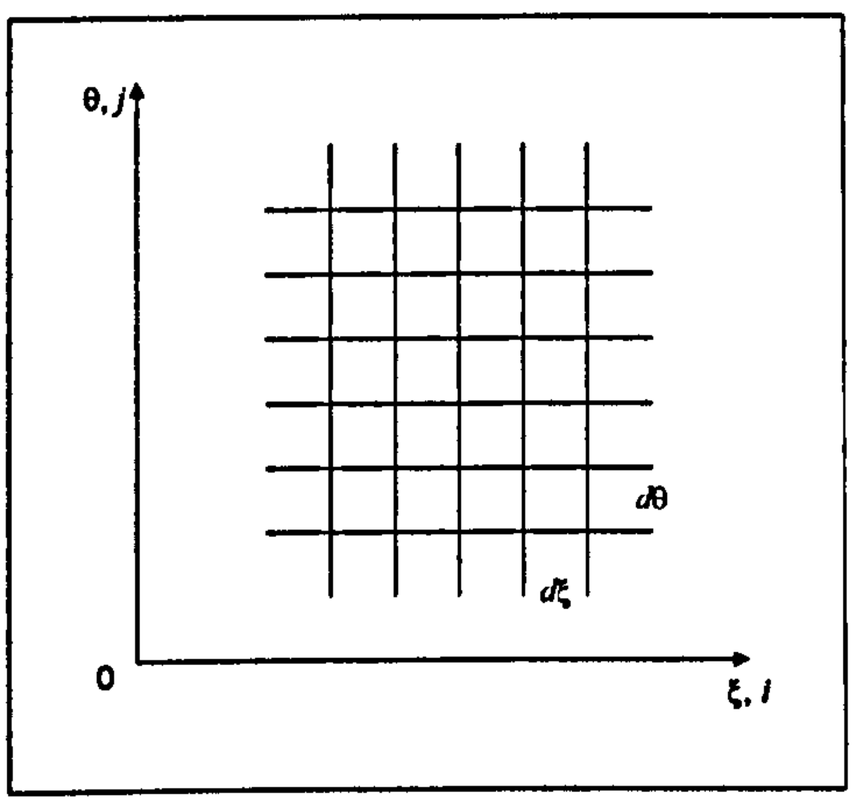

Figure 6.11 Finite difference mesh structure.

Each grid point can then be referenced as $(id\xi, jd\theta)$ where $0 \le i \le \mathrm{M}$ and $0 \le j \le \mathrm{N}$. Due to the scaling $r = ae^{\xi}$ and the r grid lines are compressed near the cylinder allowing greater attention to be paid thereby, see Fig. 6.12.

It is possible to approximate the derivatives of a quantity Z in terms of differences as follows;

$$\left(\frac{\partial Z}{\partial \xi}\right)_{ij} = \frac{Z_{i+1j} - Z_{i-1j}}{2d\xi} \quad , \quad \left(\frac{\partial Z}{\partial \theta}\right)_{ij} = \frac{Z_{ij+1} - Z_{ij-1}}{2d\theta}$$

$$\left(\frac{\partial^2 Z}{\partial \xi^2}\right)_{ij} = \frac{Z_{i+1j} - 2Z_{ij} + Z_{i-1j}}{d\xi^2} \quad , \quad \left(\frac{\partial^2 Z}{\partial \theta^2}\right)_{ij} = \frac{Z_{ij+1} - 2Z_{ij} + Z_{ij-1}}{d\theta^2}$$

$$\left(\frac{\partial^2 Z}{\partial \xi \partial \theta}\right)_{ij} = \frac{Z_{i+1j+1} + Z_{i-1j-1} - Z_{i+1j-1} - Z_{i-1j+1}}{4d\xi d\theta} \quad ,$$

where the value of Z at $(id\xi, jd\theta)$ is Z_{ij} and the principal part of the error in the approximation is second order i.e. $\propto d\xi^2$, $d\theta^2$, $d\xi d\theta$.

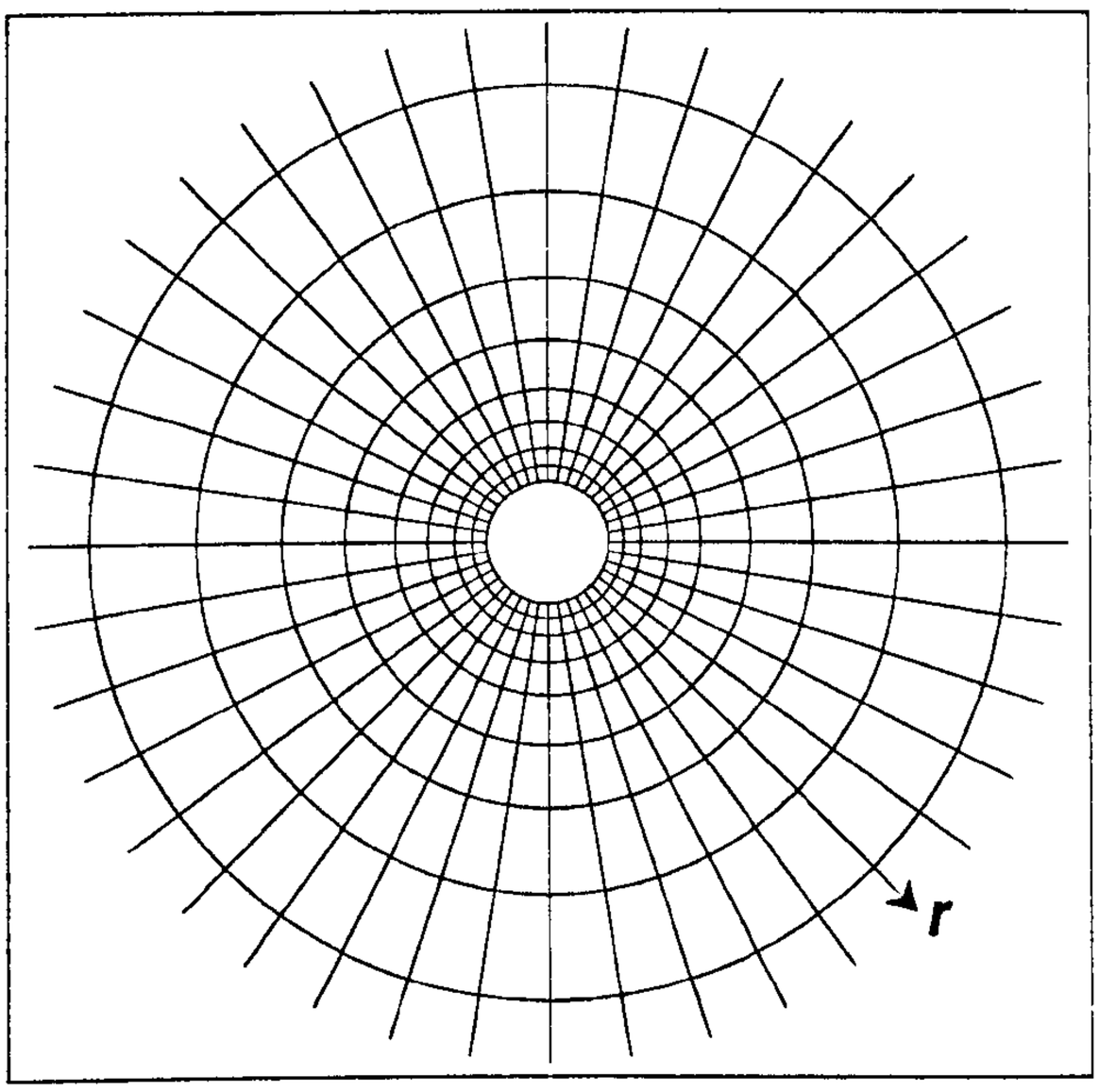

Figure 6.12 Part of the finite difference grid in r, θ co-ordinates showing scaling in the r direction (Townsend, 1980).

There are special formulae for $\frac{\partial^2 Z}{\partial \xi \partial \theta}$ which are used to avoid possible problems at the corners of the flow domain (Crochet et al., 1984). Use is made of the Woods formulation which couples ψ and ω to set the missing ω boundary value on $\xi = 0$ as;

$$\omega_{0j} = \left(\frac{\partial^2 \psi}{\partial \xi^2}\right)_{0j} = \frac{6\psi_{1j} - d\xi^2 \omega_{1j}}{2d\xi^2 \ (1 + d\xi)}\ , \qquad 6.56$$

following Crochet et al. (1984), this is again regarded as being second order.

In order to solve for the discrete ψ_{ij} and ω_{ij} grid values the following procedure is adopted:

1. Rewriting in finite difference approximated form the PDE for ψ and ω as;

$$\psi_{ij} = \left[\psi_{i+1j} + \psi_{i-1j} + h^2\left(\psi_{ij+1} + \psi_{ij-1}\right) - d\xi^2 e^{2id\xi}\omega_{ij}\right] \Big/ \left[2\left(1+h^2\right)\right], \qquad 6.57$$

and

$$\omega_{ij} = \left(A_{ij}\omega_{i+1j} + B_{ij}\omega_{i-1j} + C_{ij}\omega_{ij+1} + D_{ij}\omega_{ij-1} - F_{ij}\right) \Big/ \left(A_{ij} + B_{ij} + C_{ij} + D_{ij}\right), \qquad 6.58$$

where $h = d\xi / d\theta$ and

$$A_{ij} = \eta_{i+1j}^2 + \eta_{ij}^2 - \frac{1}{2}\ \mathrm{Re}\,\eta_{ij}\, h\left(\psi_{ij+1} - \psi_{ij-1}\right), \qquad 6.59$$

$$B_{ij} = \eta_{ij}^2 + \eta_{i-1j}^2 + \frac{1}{2}\mathrm{Re}\,\eta_{ij}\, h\left(\ \psi_{ij+1} - \psi_{ij-1}\right), \qquad 6.60$$

$$C_{ij} = h^2\left(\eta_{ij+1}^2 + \eta_{ij}^2\right) + \frac{1}{2}\mathrm{Re}\,\eta_{ij}\, h\left(\psi_{i+1j} - \psi_{i-1j}\right), \qquad 6.61$$

$$D_{ij} = h^2\left(\eta_{ij}^2 + \eta_{ij-1}^2\right) - \frac{1}{2}\mathrm{Re}\,\eta_{ij}\, h\left(\psi_{i+1j} - \psi_{i-1j}\right). \qquad 6.62$$

Further terms used are;

$$\begin{aligned} F_{ij} = {} & 2d\xi\left[hT_{rrij}\left(\eta_{ij+1} - \eta_{ij-1}\right) - T_{r\theta ij}\left(\eta_{i+1j} - \eta_{i-1j}\right)\right] \\ & + 2T_{r\theta ij}\left[\eta_{i+1j} - 2\eta_{ij} + \eta_{i-1j} - h^2\left(\eta_{ij+1} - 2\eta_{ij} + \eta_{ij-1}\right)\right], \\ & - T_{rrij}\, h\left(\eta_{i+1j+1} + \eta_{i-1j-1} - \eta_{i+1j-1} - \eta_{i-1j+1}\right) \end{aligned} \qquad 6.63$$

$$\dot{\varepsilon}_{rrij} = \frac{e^{-2id\xi}}{4d\xi d\theta}\left[\psi_{i+1j+1} + \psi_{i-1j-1} - \psi_{i-1j+1} - \psi_{i+1j-1} - 2d\xi\left(\psi_{ij+1} - \psi_{ij-1}\right)\right], \qquad 6.64$$

$$\dot{\gamma}_{r\theta ij} = \frac{e^{-2id\xi}}{2d\xi^2}\left[h^2\left(\psi_{ij+1} + \psi_{ij-1}\right) - \left(1 - d\xi\right)\psi_{i+1j} - \left(1 + d\xi\right)\psi_{i-1j} + 2\psi_{ij}\left(1 - h^2\right)\right], \qquad 6.65$$

$$T_{rrij} = 2\eta_{ij}\dot{\varepsilon}_{rrij}, \qquad 6.66$$

$$T_{r\theta ij} = 2\eta_{ij}\,\dot{\gamma}_{r\theta ij}\ , \qquad 6.67$$

and

$$\eta_{ij} = \eta\left(q_{ij}\right), \qquad 6.68$$

where q_{ij} is given in Eqn. [6.47];

$$q_{ij} = 2\sqrt{\dot{\varepsilon}^2_{rrij} + \dot{\gamma}^2_{r\theta ij}}\ . \qquad 6.47$$

There are special provisions for the use of the latter formulae at the boundaries of the flow domain and at the domain corners.

2. Since the equations are non-linear an iterative approach will be adopted that requires initial guess starting values for ψ_{ij} and ω_{ij}.

Although it is usual to adopt zero starting values, the solution for the case of a Newtonian zero Re flow situation leads to a simple solution that is adopted for the general case, and leads to significant reduction in program execution times.

$$\psi = \left[A\left(e^{3\xi} - 4\xi e^{\xi} - e^{-\xi}\right) + B\left((1-2\xi)e^{\xi} - e^{-\xi}\right)\right]\sin\theta\ , \qquad 6.69$$

$$\omega = 4\left[2A\left(e^{\xi} - e^{-\xi}\right) - Be^{-\xi}\right]\sin\theta\left(1 - \frac{\xi}{\xi_0}\right)\ , \qquad 6.70$$

where $\omega = 0$ at $\xi = \xi_0$ has been enforced; here

$$A = 1/2\left[(1-\xi_0)X_0^2 - (1+\xi_0)\right]$$

$$B = \left(X_0^2 - 1\right)A \quad , \quad X_0 = e^{\xi_0} .$$

Also the viscosity values η_{ij} are set to a constant value appropriate to the viscous model used.

3. Since an iterative approach needs to be adopted, the following sequantial steps were used along the lines suggested by Townsend (1980):

a) Set ψ_{ij}^0 and ω_{ij}^0 as the initial guess values for ψ_{ij} and ω_{ij}.

b) Then calculate interior ψ_{ij}^1 using Eqn. [6.57], where the **RHS** values are the updated currently available ψ and ω values, in a single sweep of a Gauss-Seidel procedure.

c) Subsequently ω_{0j}^1 values are calculated using Eqn. [6.56], and then ω_{ij}^1 interior values using Eqn. [6.58], in a single sweep of a Gauss-Seidel procedure as for ψ.

d) Then calculate updated η_{ij} values for the whole flow domain.

e) Test for convergence between iterations *k* and *k+1* for a quantity Z_{ij} as;

$$\left|Z_{ij}^{k+1} - Z_{ij}^{k}\right| / \left(1 + \left|Z_{ij}^{k}\right|\right) < \mathrm{Tol}Z , \qquad 6.71$$

for all *i* and *j* with Tolψ and Tolω both set as appropriate small values. This convergence test gives a combination both absolute and relative comparisons of successive iteration values.

f) Finally a smoothing strategy was adopted by setting;

$$\overline{Z}_{ij}^{k+1} = \mathrm{S}\, Z_{ij}^{k} + (1\text{-}\mathrm{S})\, Z_{ij}^{k+1} , \qquad 6.72$$

where S is a smoothing parameter ($0 < S < 1$) and use the $\overline{Z}_{ij}^{k+1}$ values in subsequent calculations. This helps convergence in difficult cases.

The iteration procedure and flow chart of the program are given Figs. 6.13 and 6.14.

Iteration No: 1	Iteration step
$\psi_{ij}^{0}, \omega_{ij}^{0}$ guess	
ψ_{ij}^{1} interior	1.1
ω_{0j}^{1} cylinder	1.2
ω_{ij}^{1} interior	1.3
η_{ij} flow domain	1.4
Test for convergence and smooth	

Iteration No: 2	Iteration step
$\psi_{ij}^{1}, \omega_{ij}^{1}$	
ψ_{ij}^{2} interior	2.1
ω_{0j}^{2} cylinder	2.2
ω_{ij}^{2} interior	2.3
η_{ij} flow domain	2.4
Test for convergence and smooth	

Iteration No: n	Iteration step
$\psi_{ij}^{n}, \omega_{ij}^{n}$	
ψ_{ij}^{n+1} interior	n.1
ω_{0j}^{n+1} cylinder	n.2
ω_{ij}^{n+1} interior	n.3
η_{ij} flow domain	n.4
Test for convergence and smooth	

Figure 6.13 Iteration process.

The visco-plastic flow program is written in the FORTRAN programming language. The partial differential Finite Difference (FD) flow equations were solved using University of Glamorgan's Alpha network and Research Sun station systems.

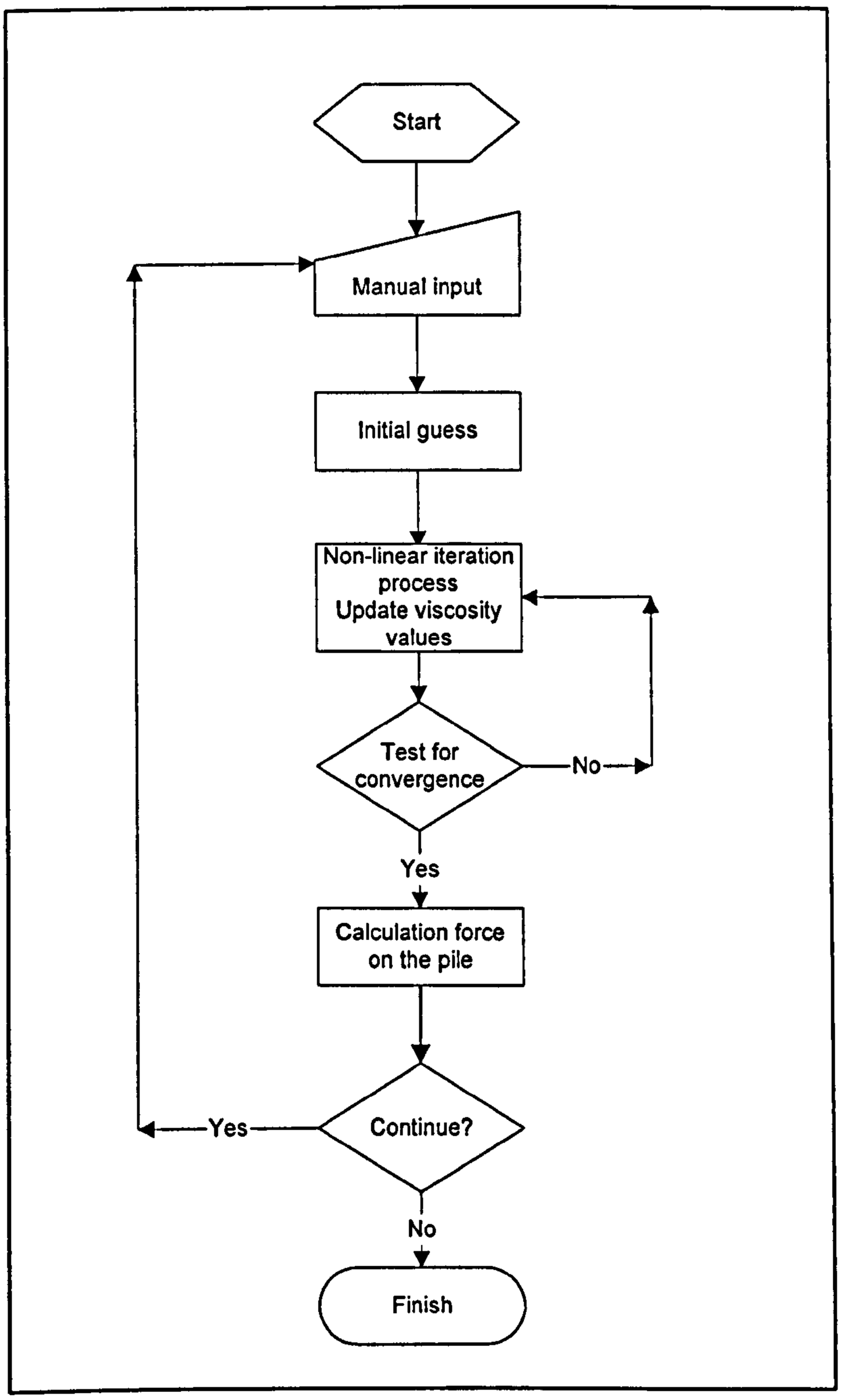

Figure 6.14 Flowchart of the program.

Once satisfactory convergence has been achieved the dimensionless force per unit length on the cylinder may be calculated using a numerical procedure. Since the

methods adopted thus far have been second order, the Trapezium second order integration rule (Burden and Faires, 1989) was used for Eqn. [6.55] to yield;

$$F = 2d\theta \left| \sum_{j=1}^{N-1} \left\{ \eta_{0j}\omega_{0j} - \left[\frac{\partial}{\partial \xi}(\eta\xi) \right]_{0j} \right\} \sin(jd\theta) \right| , \qquad 6.72$$

where the derivative term was calculated using the second order forward difference approximation for a quantity Z as;

$$\left(\frac{\partial Z}{\partial \xi} \right)_{0j} = \frac{4Z_{1j} - Z_{2j} - 3Z_{0j}}{2d\xi} . \qquad 6.73$$

Noting that at $\theta = 0, \pi$; ω and $\frac{\partial \omega}{\partial \xi}$ are both zero, simplifies the calculation of F above. Also the first order forward difference approximation $\left(\frac{\partial Z}{\partial \xi} \right)_{0j} = \frac{Z_{1j} - Z_{0j}}{d\xi}$ was used in a second F calculation as a useful check for appropriateness of results.

6.5.2 Testing of results

Calculations were performed with a variety of grid sizes and convergence tolerances for a Newtonian fluid, for which the Oseen analytical (Batchelor, 1974) value for force is available in dimensionless form as;

$$Fd = \frac{4\pi}{\log(3.7/\mathrm{Re})} , \qquad 6.74$$

in the case of Re<0.5.

Using the Oseen formula and Tritton experimental results, see Fig. 6.15 where R = 2Re and $C_D = F/\mathrm{Re}$, satisfactory comparisons were obtained from about Re = 0.1 to 10 for tolerances of 10^{-3} or less, S of 0.5, and grid lines of 100 or above in both ξ and θ variables, and such values were generally used to good effect in subsequent programming. Inspection at various grid sample points of the dependent variables ω, ψ and also F values exhibited convergence as the grid mesh decreases. Following Townsend (1980, 1984) a value of ξ_0 of 3 was used here. It is noted that Townsend (1980) was interested in results for Re of more than 5, much greater than our proposed values, see Fig. 6.16, based on Ito and Matsui (1975), Table 6.1 and Table 6.2 data.

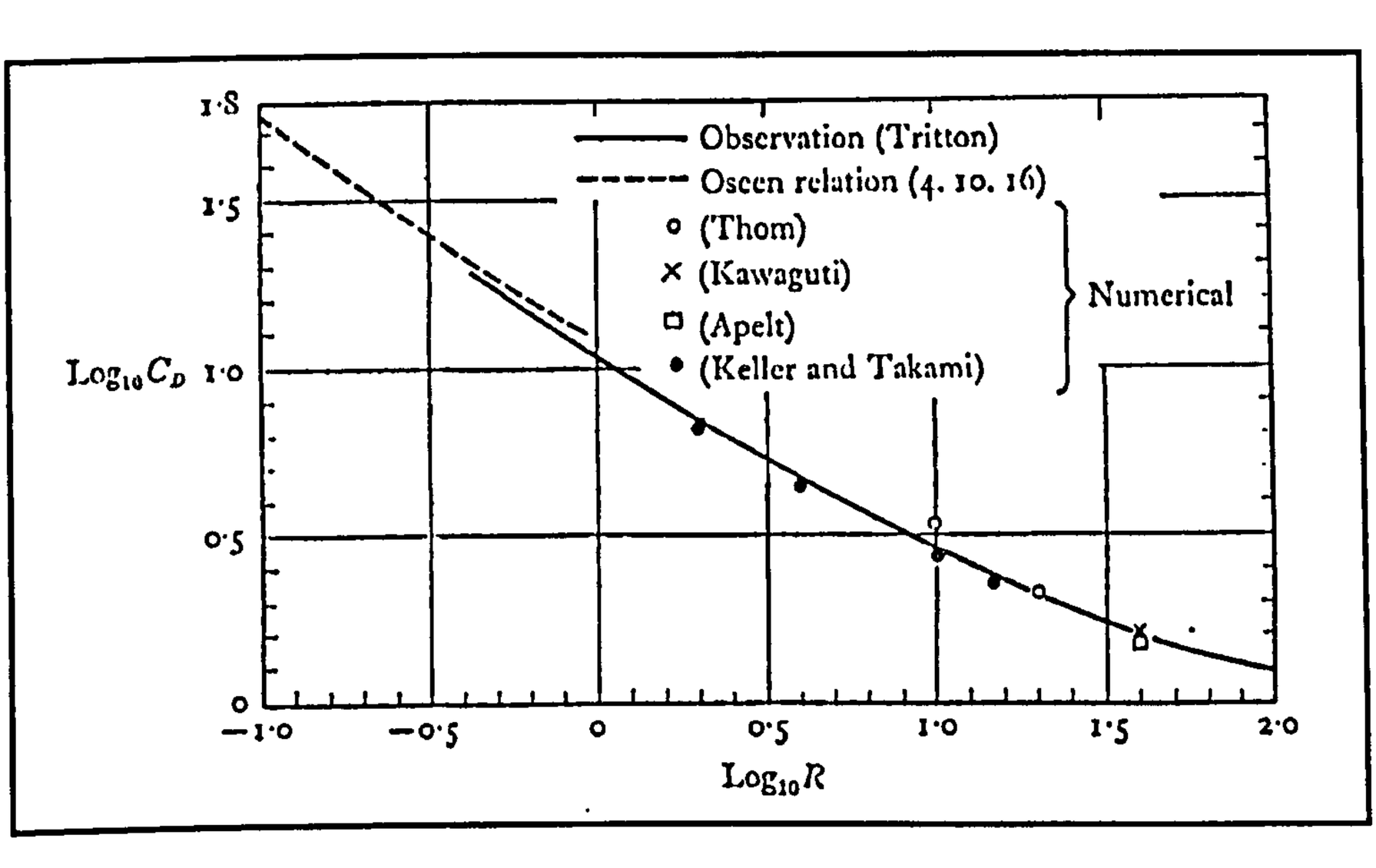

Figure 6.15 Drag force exerted on a circular cylinder of radius a (Batchelor, 1974).

According to Batchelor (1974), section 4.10, the viscous force contribution and inertial force contribution for a drag force become comparable at physical distances of

the order of $\frac{a}{\mathrm{Re}}$. Hence, as Re decreases towards zero the distance from the cylinder which requires consideration for viscous drag contribution increases. Thus a 'calibration' process was necessary to determine the appropriate ξ_0 value for each Re to match the true Oseen value. This resulted in the following linear regression graph (see Fig. 6.16) using;

$$\xi_0 = A + B\,(-\log_{10} \mathrm{Re})\,, \qquad 6.75$$

where $A = 2.6944$, $B = 0.9965$ and coefficient of correlation $r = 0.9999$. The results are consistent with the theory in Batchelor, since B is approximately unity.

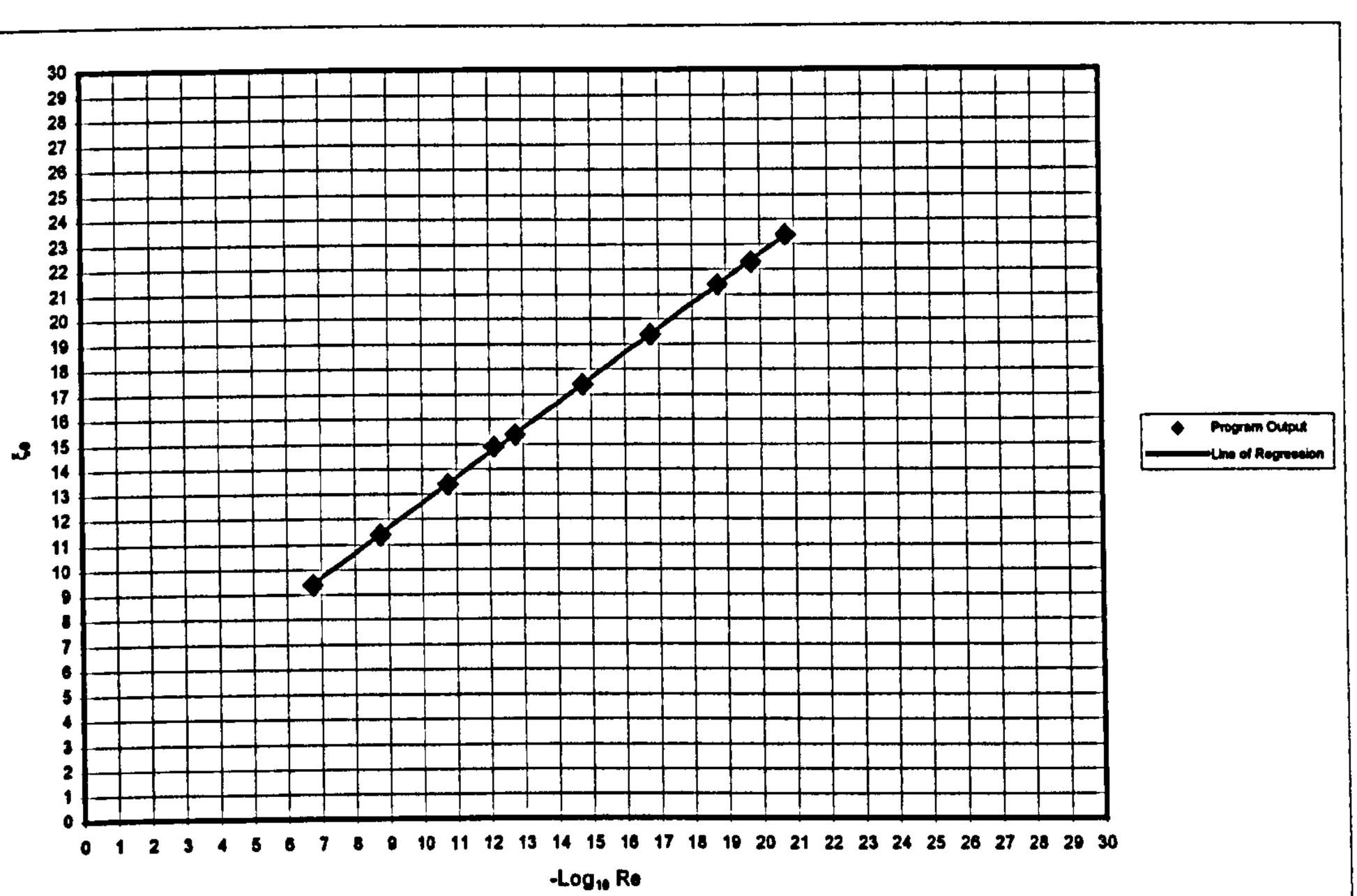

Figure 6.16 Newtonian calibration process.

By observing the above data through increasing α, an adequate value of 20 was found for acceptable results in order to make best use of the smooth model of the Bingham viscosity in all applications.

In this program, only the smooth viscosity model is used and this is to overcome a convergence difficulty. During the iteration process, the biviscosity model often exhibited spurious oscillations and this gives either unacceptable overestimated or underestimated values for the force estimation on the pile. The lack of convergence is attributed to the lack of smoothness in the biviscosity model profile.

For the estimation of the force on the pile, the following Fig. 6.17 is given for a single pile case where KONS = $V\eta_p$ which is a product of plastic viscosity and flow velocity. The ratio $D_2/D_1 = 1$ presents a single pile case owing to a considerable gap specified between two piles, see Fig. 6.18.

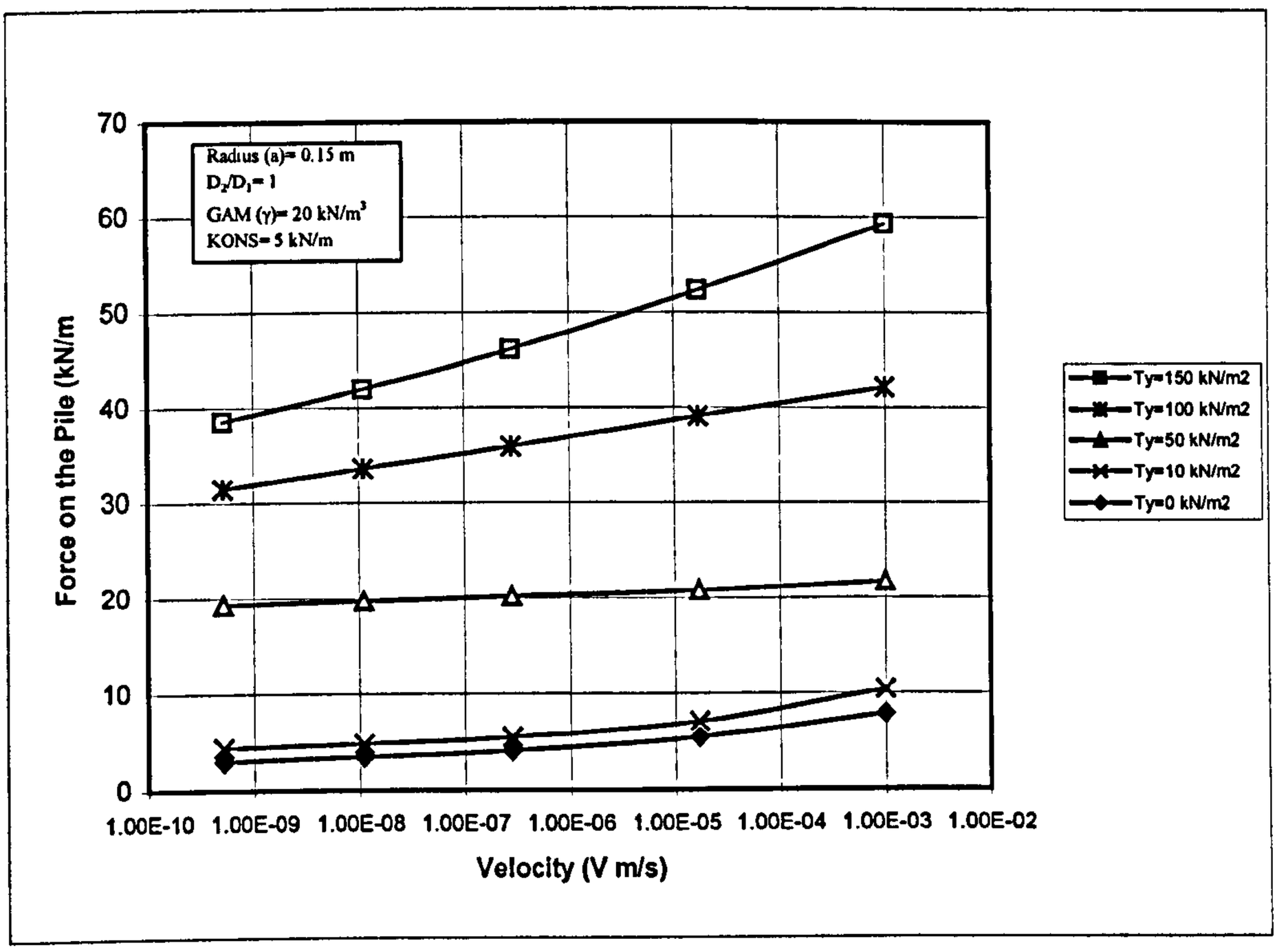

Figure 6.17 Estimation of forces on a single pile due to yield stress τ_y (Ty).

As can be seen from Fig. 6.17 the force on the pile increases as the yield stress τ_y increases, as expected.

6.6 Flow through a row of piles

The theoretical analysis of the lateral force exerted on a single pile due to visco-plastic flow (Bingham type of material) of the surrounding soil has been given in sections 6.4 and 6.5. When analysing an equally spaced row of piles (set out in a continues line), it is sufficient to deal with the behaviour of soil between any two neighbouring piles as shown in Fig. 6.18, where a is the pile radius, D_1 is centre to

centre distance of piles and D_2 is interval between the two piles. The lateral pressure on the piles varies from zero when there is no soil movement, to an ultimate value in the case of a large soil movement (Matsui et al., 1982). It is considered that piles have a preventive effect against slope failure or lateral flow.

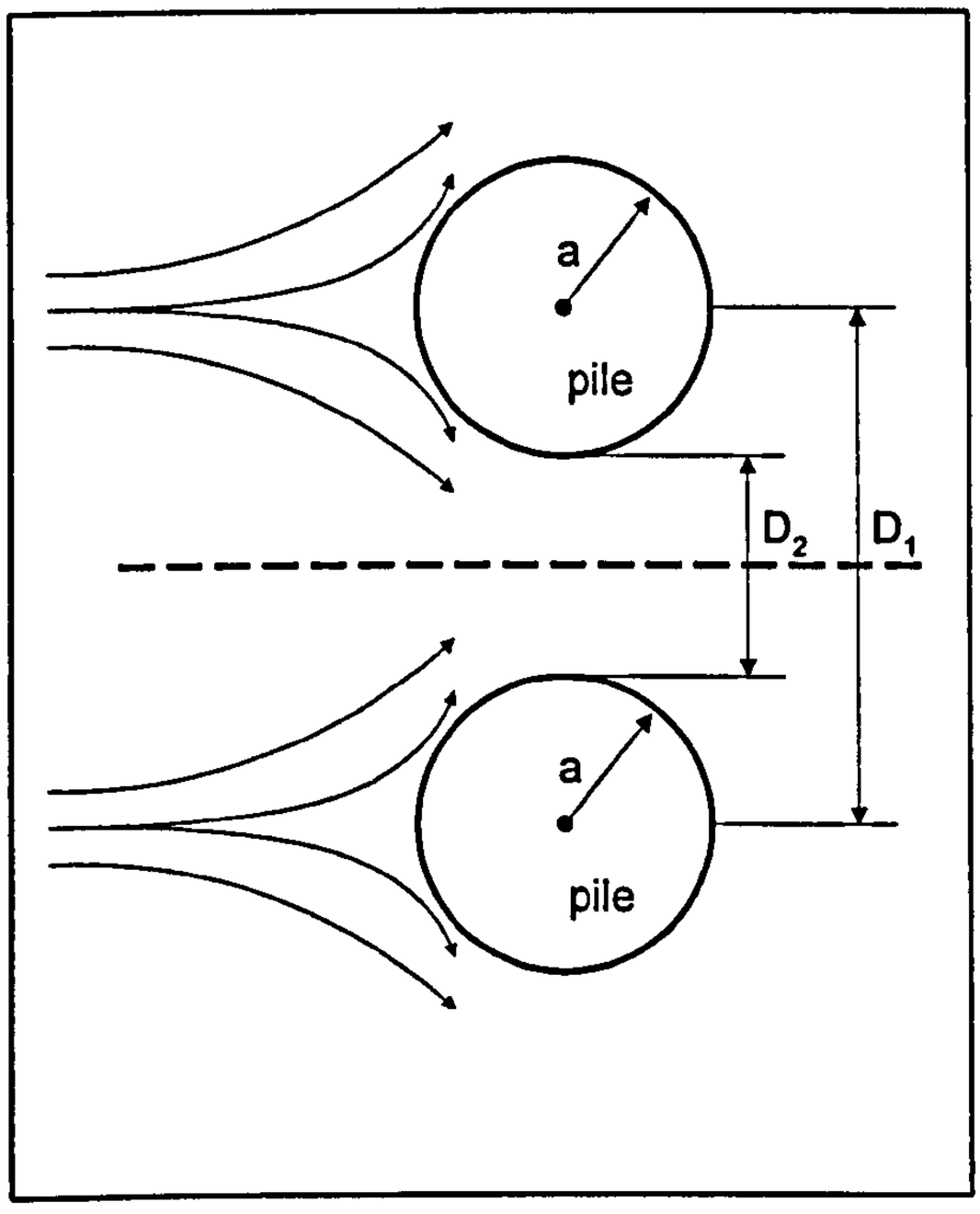

Figure 6.18 Plan view of piles in a row.

6.6.1 Modelling

For this analysis, the assumption of having an infinite continuum between the cylindrical piles is violated due to the presence of other piles. It is assumed that the symmetry lines AB and CD, Fig. 6.19, contain the flow so that a significant configuration of symmetry exists between the piles and therefore only a θ flow region between 0 and π need to be considered, see Fig. 6.19 and Fig. 6.20. However, for ξ it

is required to redefine this range as between 0 and $\xi_1(\theta)$ where $\xi_1(\theta) = \min\left[\log\left(\frac{b}{a\sin\theta}\right), \xi_0\right]$ to accommodate the symmetry lines between the piles.

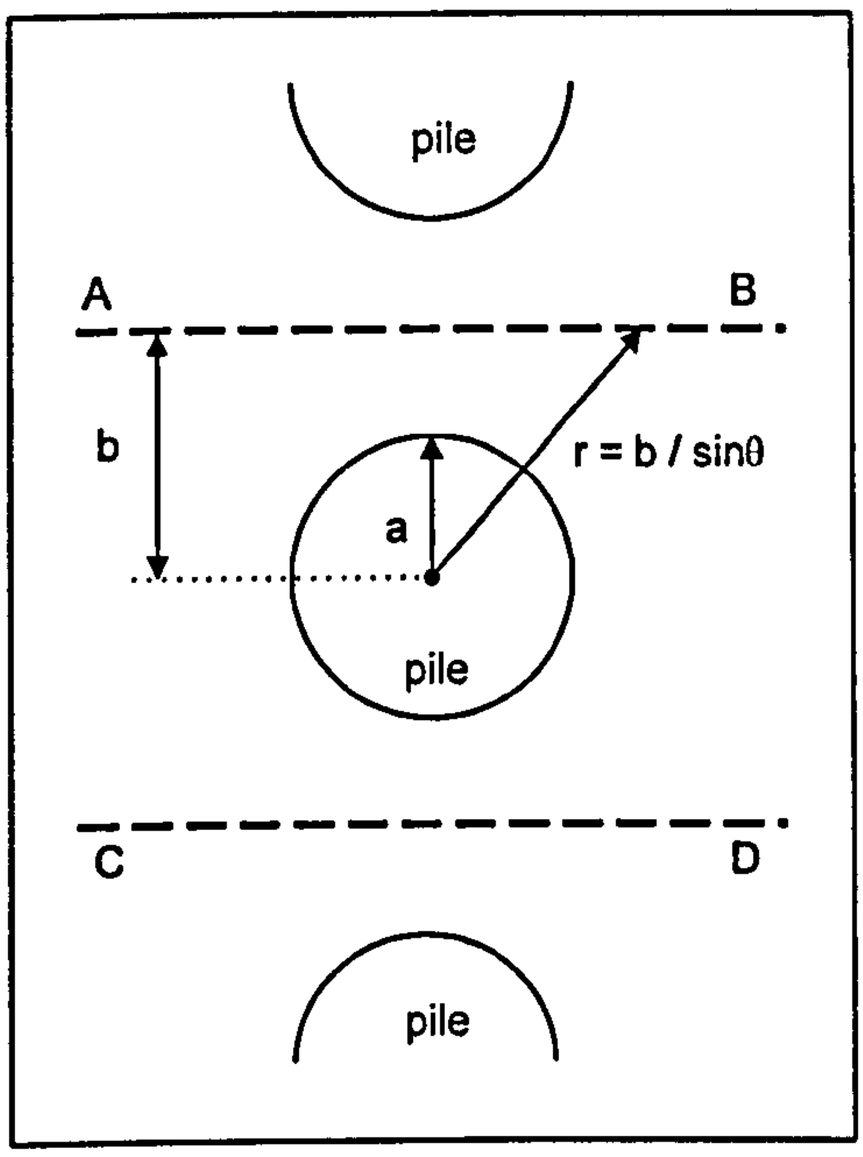

Figure 6.19 Modified approach for a row of piles.

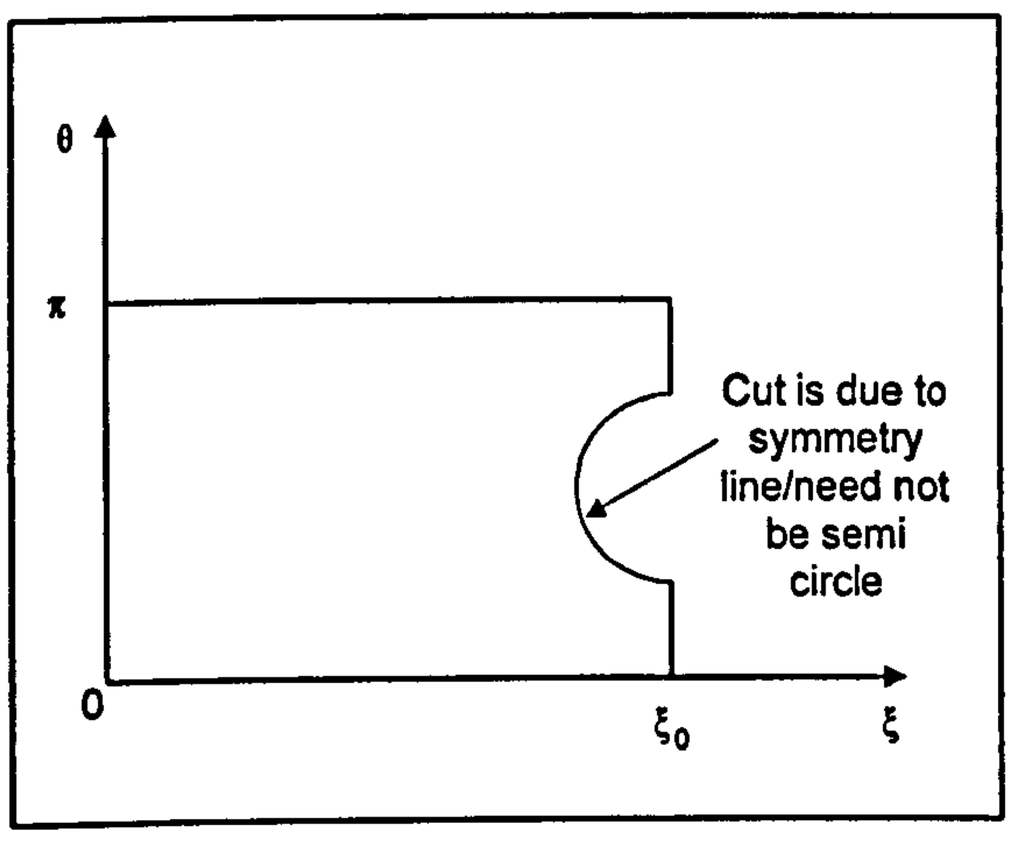

Figure 6.20 Boundary for flow through row of piles, reduced geometry owing to symmetry.

There are two approaches which may be adopted to accommodate the ξ_1 boundary since the FD grid points are not necessarily intersected by the above ξ_1 curve.

- The first approach is to modify the differencing method used to take acount of the boundary curve, passing in-between grid lines. However this generally leads to a first order approximation and lowers the overall accuracy of the method (Morton and Mayers, 1994).
- A second approach is to approximate the boundary itself, so that the regular grid points closest to the boundary can be used as approximations to the boundary itself. Here the advantage lies in retaining second order accuracy terms and is thus adopted for this work.
- On the conditions ξ_1 symmetry boundary the condition $\psi = 0$ and $\omega = 0$ are used.

In the solution procedure, the initial "guess" value was then modified through replacing ξ_0 by $\xi_1(j\,d\theta)$ in Eqns. [6.69] and [6.70] and various changes were made to the loop structures of the program.

6.6.2 Results

The theoretical equations for the lateral force acting on a stabilising pile due to a moving soil mass, includes many parameters to be evaluated in the theory of visco-plastic flow past a row of piles as described above. It may be necessary that the

significance of various parameters in flow/force equations are clarified by examining the effect of each variable. The variable parameters used are:

a) the unit weight of soil γ ($\gamma = \rho g$, ρ is density and g being the gravitational constant, 9.81 m/s^2),

b) the centre to centre distance between piles D_1,

c) the clear interspace between piles D_2,

d) the yield stress τ_y (= c where c is cohesion),

e) Bingham plastic viscosity η_p and,

f) the flow velocity V of the (modelled) soil layer.

These parameters have a significant effect on the calculation of the lateral force on a pile as the present parametric study has shown. A further adjustment was made in parameters (a) to (f), where the product of (V η_p) = KONS was inputted into the program as a constant. This was purposed for benchmarking, since Ito and Matsui (1975) had reported the product as a salient parameter. In order to examine the effects of D_1 and D_2, the ratio D_2/D_1 and the diameter of pile (D_1-D_2) were also chosen as parameters comparable to the work of above authors. Appropriate parameters, for a row of piles, are tolerances of 10^{-3} or below, S of 0.5, α of 20 and grids of 100 or above in both ξ and θ variables, see Fig. 6.21, as used for a single pile. Again various grid sample points for various combination of the dependent variables ω, ψ and also F values exhibited convergence as the grid mesh decreased. The previously "calibrated" ξ_0 values, in section 6.5.2 and Fig. 6.16, and the smooth viscosity model were used for the case of a single row of piles.

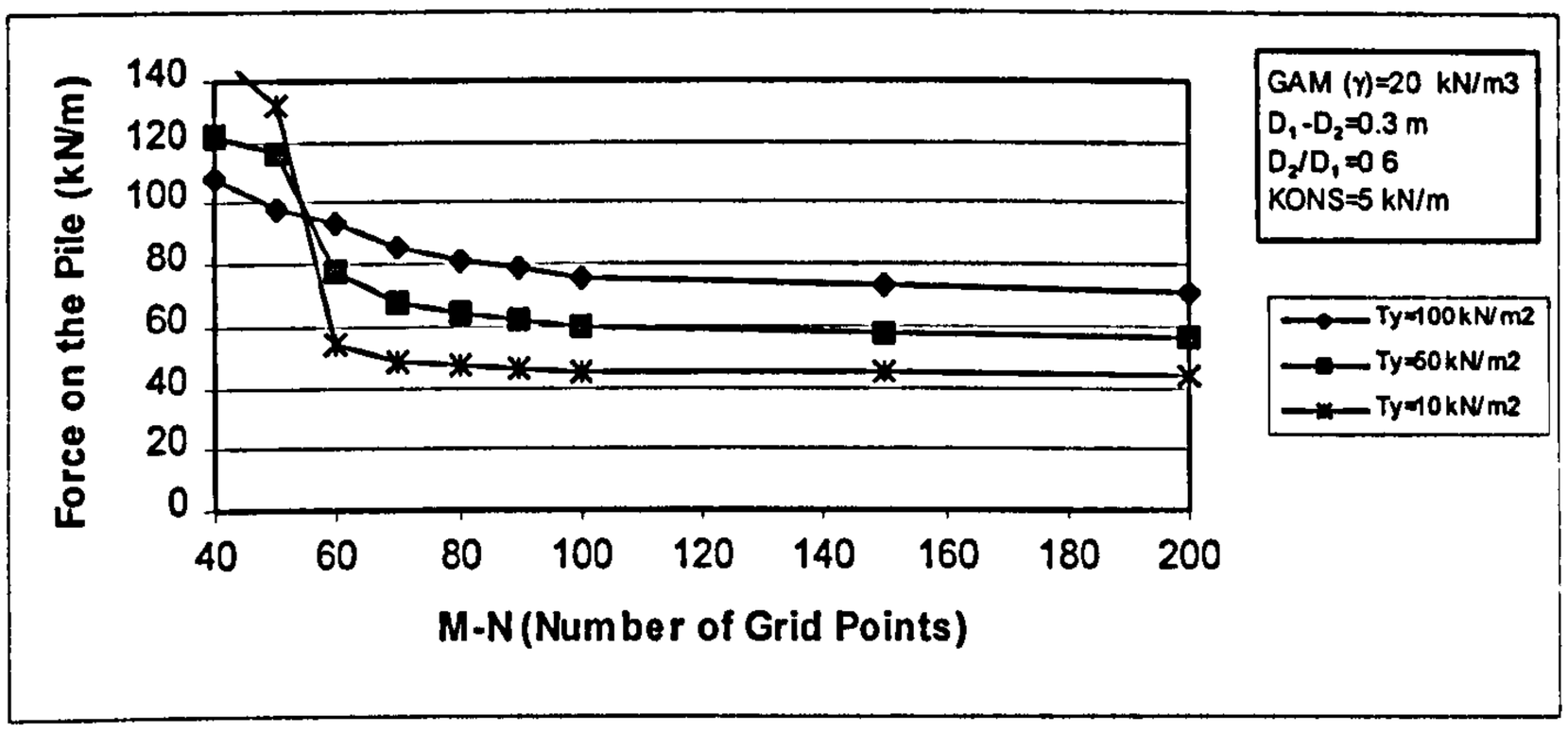

Figure 6.21 Convergence criterion.

The theoretical force variation calculated from the theory of visco-plastic flow past a row of piles, are shown in Figs. 6.22-27. It is seen that when the diameter of the pile is constant, the lateral force on the pile per unit length increases as the ratio D_2/D_1 decreases, as is expected.

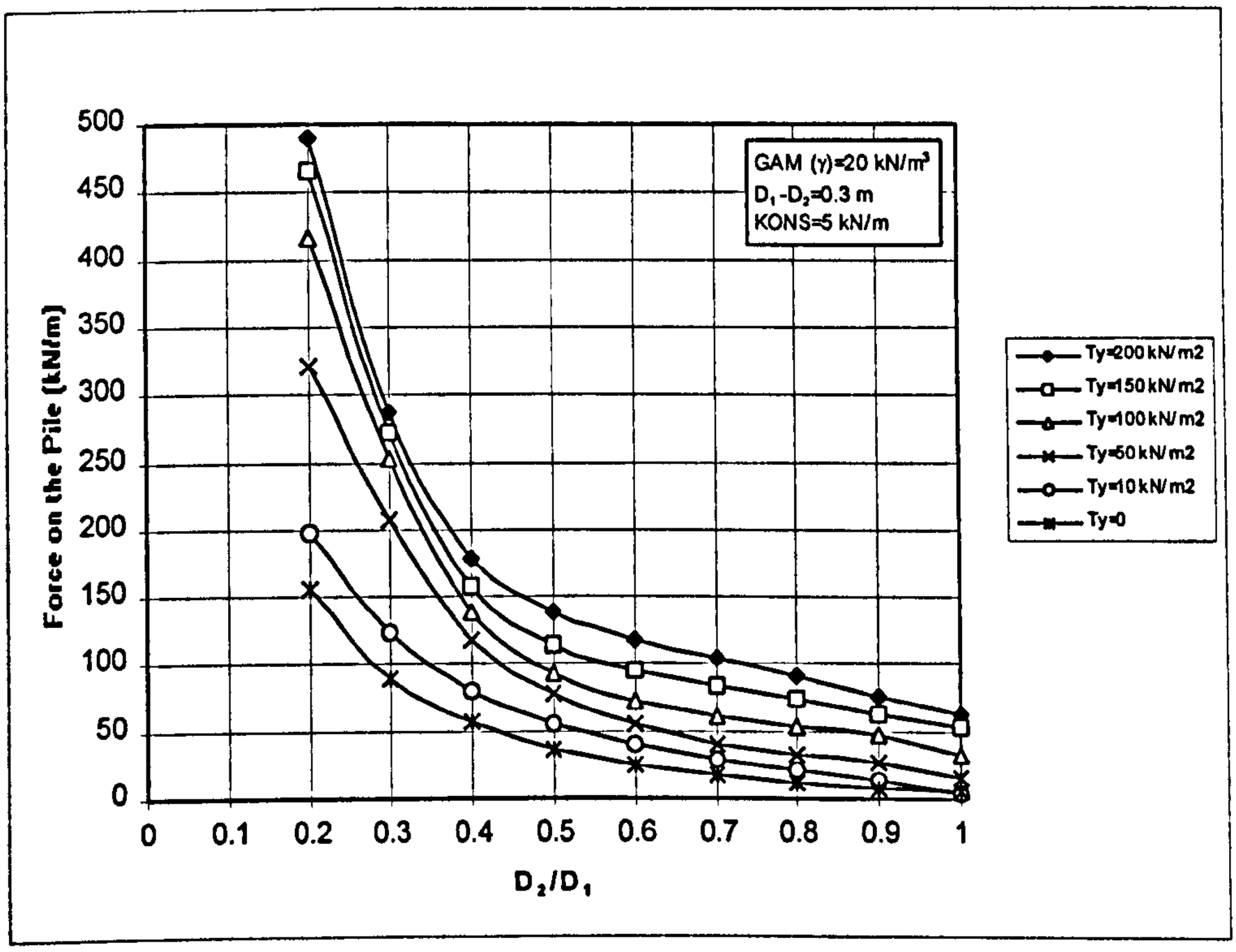

Figure 6.22 The effect of yield stress τ_y (Ty) on the force/m of the pile.

As can be seen from Fig. 6.22, the lateral force (F) variations display non-linear increases with yield stress τ_y (= c) values. This tendency is correct because when the yield stress τ_y is larger, the soils around piles are harder to pass through a row of piles.

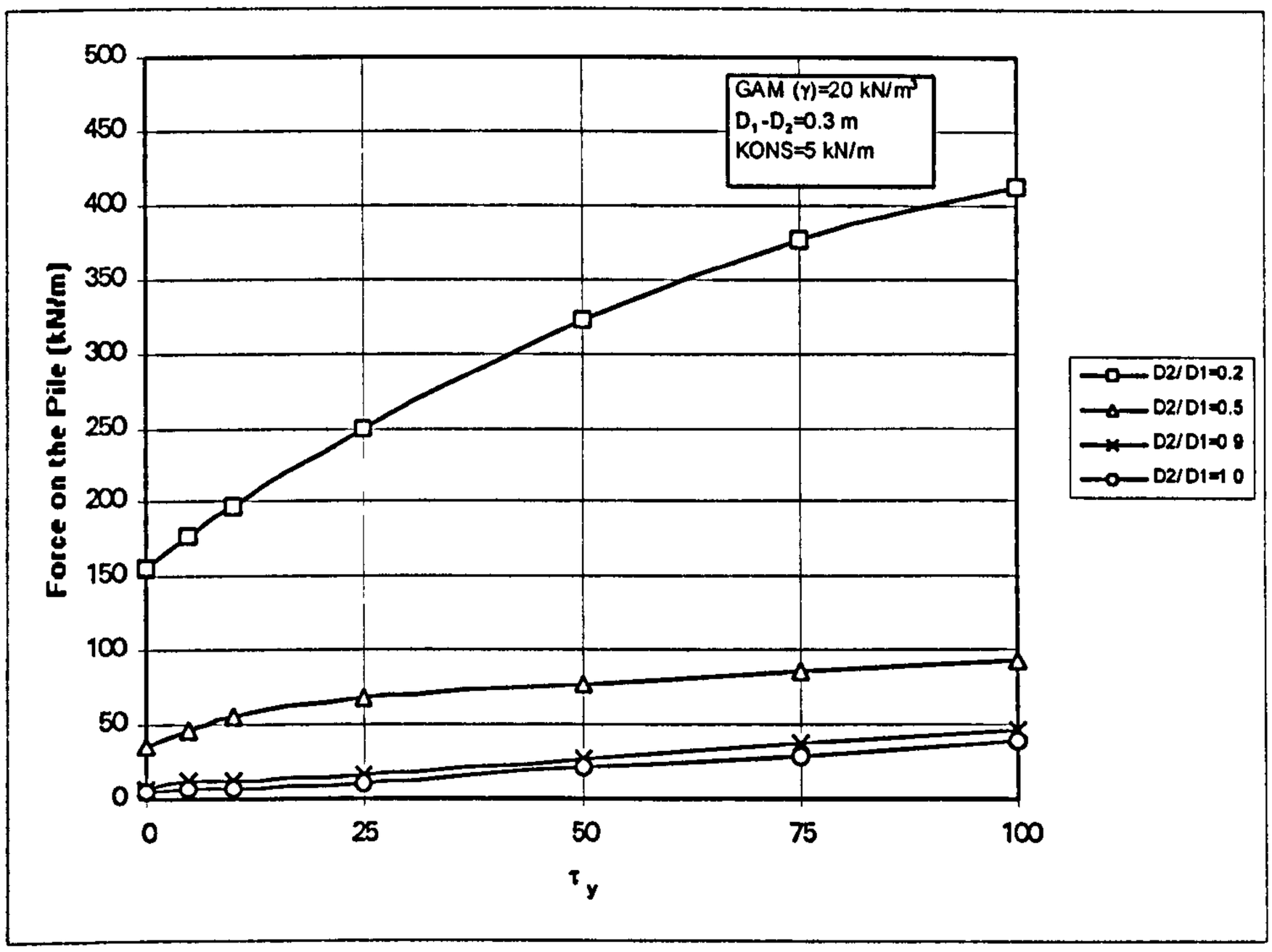

Figure 6.23 The parametric study of (D_2/D_1) on the force/m and τ_y plots.

The trends in variation of force/m and D_2/D_1 are identical but clearly variations are expected with numerical changes in τ_y (= c), KONS = ($V\eta_p$) and physical dimensions i.e. D_2 , D_1 and hence (D_2-D_1).

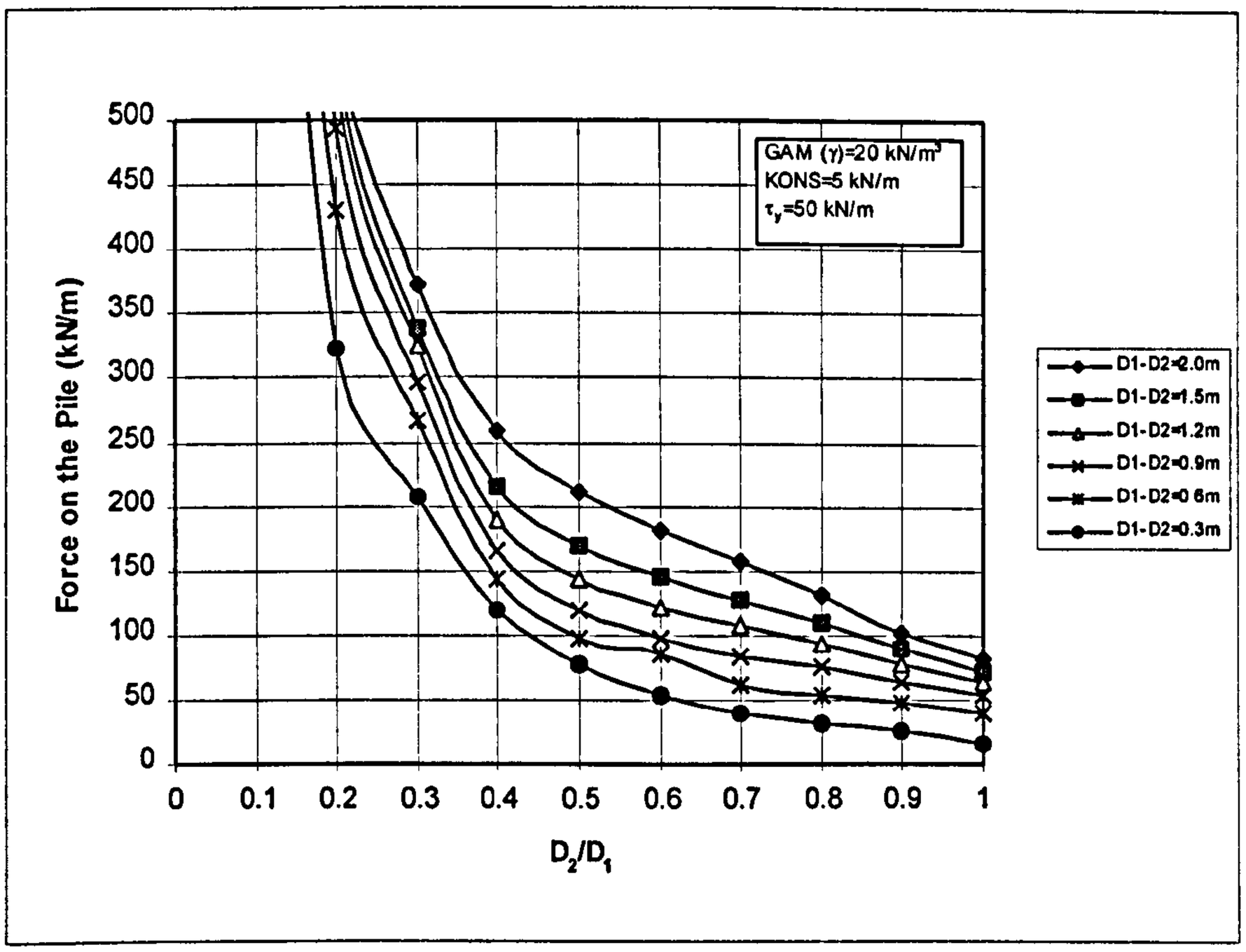

Figure 6.24 The effect of pile diameter (D_1-D_2) on the theory of visco-plastic flow.

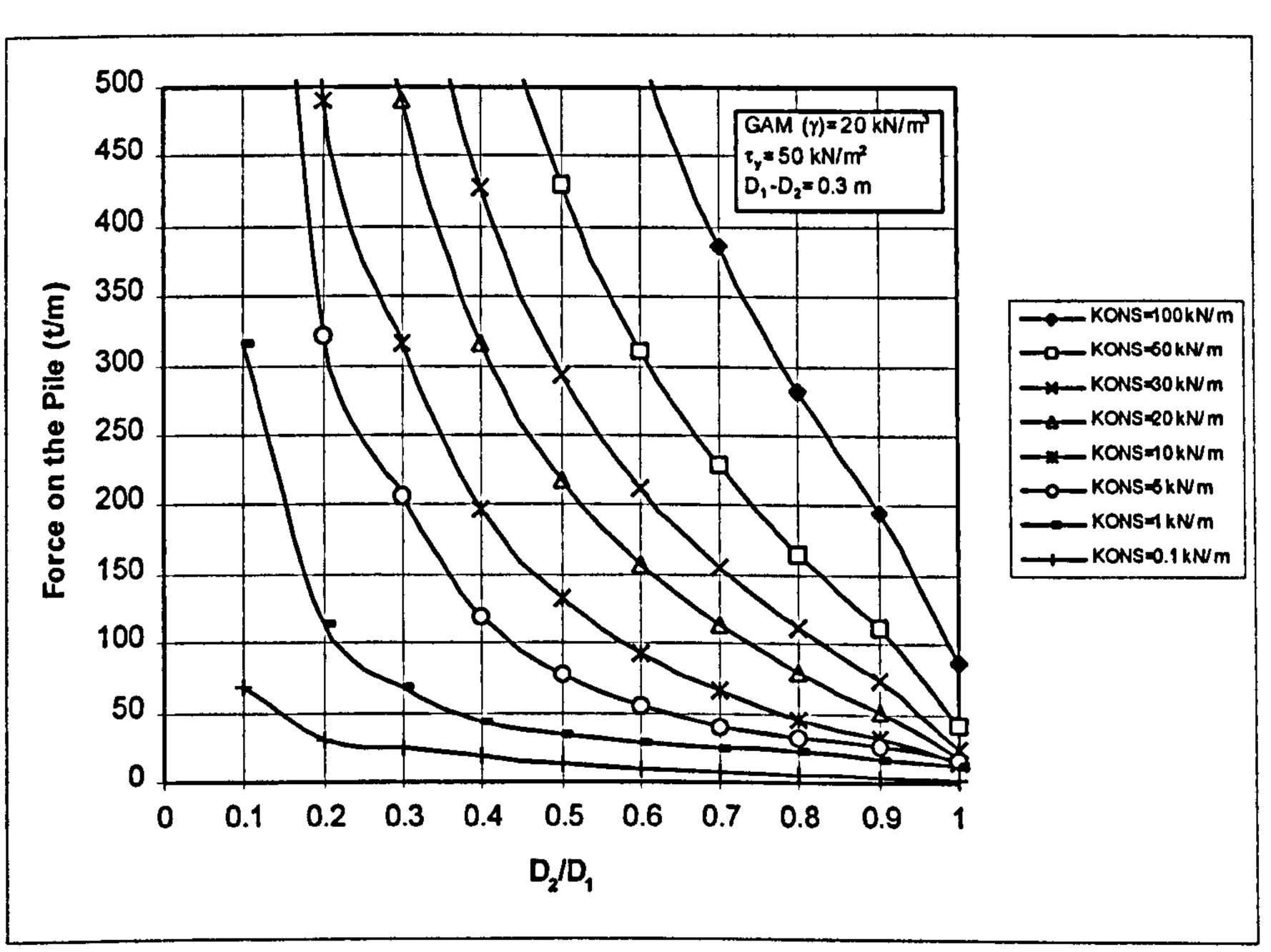

Figure 6.25 The effect of product of flow velocity and plastic viscosity (KONS) on the theory visco-plastic flow.

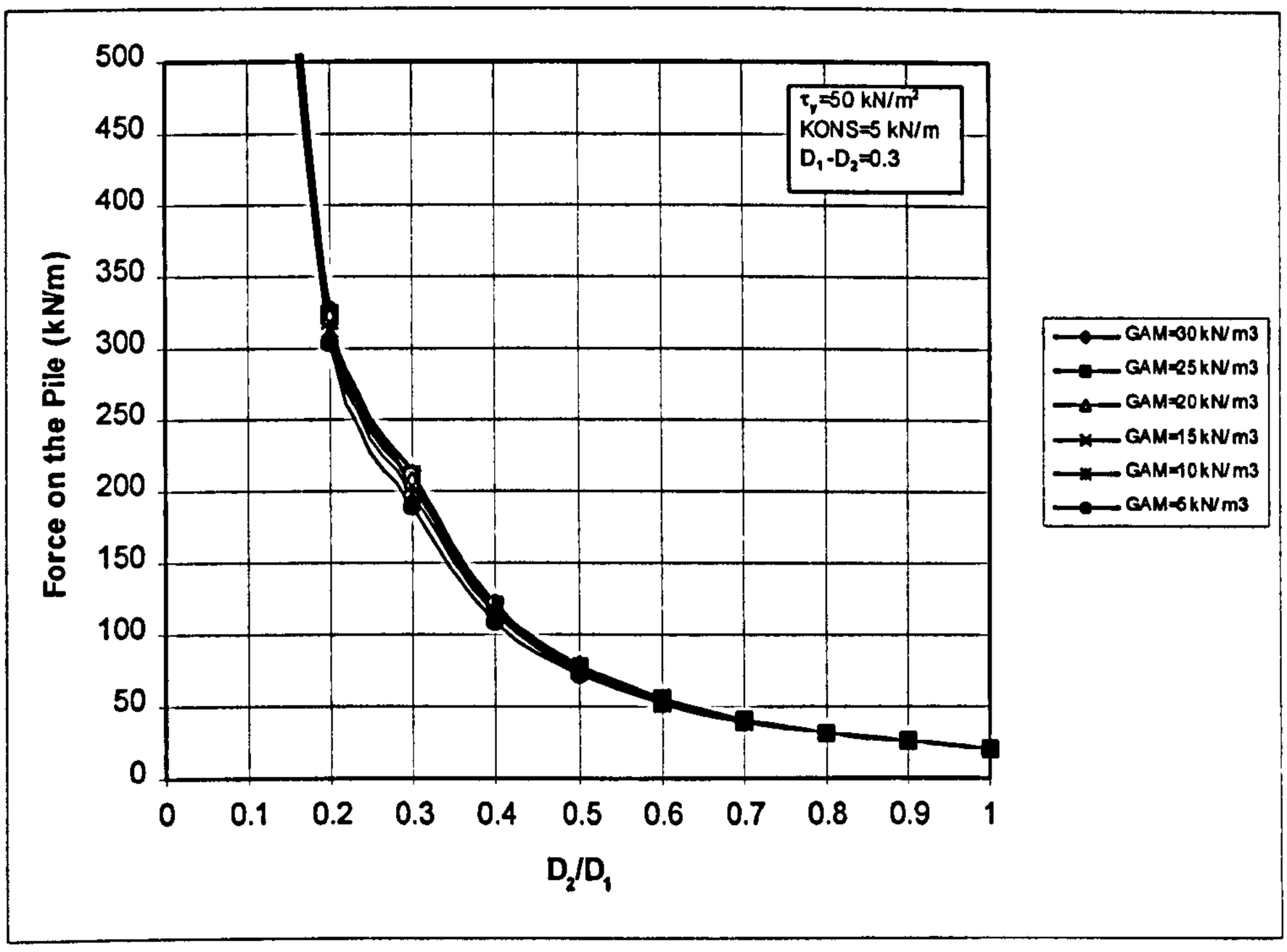

Figure 6.26 The effect of unit weight of soil γ (GAM) on the theory of visco-plastic flow.

The effect of unit weight of soil (γ) on the calculation of force on the pile is shown in Fig. 6.26. As can be seen, the lateral force is hardly influenced by the unit weight of soil which is hence an insignificant factor.

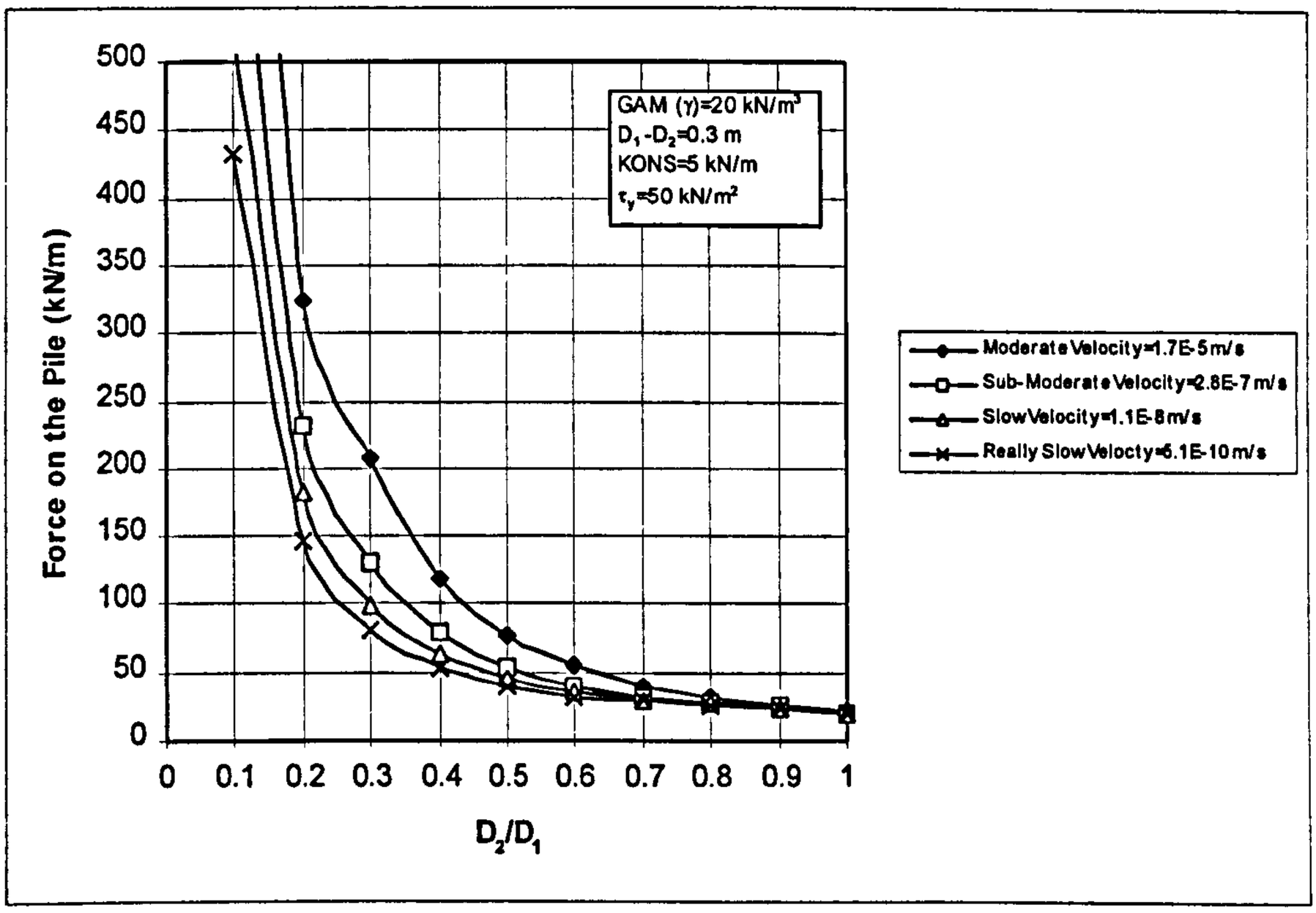

Figure 6.27 The effect of flow velocity in visco-plastic flow formulation.

To show the effect of velocity (V), Fig. 6.27, contains a range of speed values taken from Table 6.2. It is seen that when the clear distance between two piles (D_2) is sufficiently large then the effect of velocity is less prominent.

6.7 Conclusions

This chapter is dedicated to estimating the lateral forces due to a viscous flow field on cylindrical (stabilising) piles. The work presented here is carried out based on analysis only. The results obtained will be used in Chapter 9 for slope stabilisation along with other methods.

Conclusions on the present work may be summarised as;

- The calibration process is carried out to determine the appropriate ξ_0 (effective distance on the vicinity of pile) value for each Reynolds number (Re) to match the true Oseen value (a classical activity in viscous flow problem solving).
- A single pile solution is also obtained using a visco-plastic flow model.
- The theoretical solution of the lateral force is obtained by considering the interval between piles in a row and the theory of visco-plastic flow. This has involved extensive use of symmetry properties inherent in the flow geometry.
- The analysis focuses on determining the variation force/m on a pile due to the influence of a number of key parameters.
- The lateral force on the pile per unit length increases as D_2/D_1 decreases when the diameter of pile is constant.
- In the theory of visco-plastic flow, the lateral force/m increases as τ_y, (D_1-D_2), KONS and velocity of flow increases.
- The influence of soil density on force/m is seen to be small.

CHAPTER 7: METHODS OF ESTIMATING LATERAL LOADS ON PILES, USED TO STABILISE SLOPES

7.1 Introduction

Despite the extensive use of piles installed within the slope as landslide countermeasures, the interaction mechanism between the piles and the surrounding soil has not been well established. The only reported measurement available to the author is due to the Ito and Matsui method (Anagtopoulos et al., 1991). Since site measurement procedures are known to be costly, it was decided to consider theoretical predictive methods to establish bounded solutions in order to examine a range of stability factors. All mention of piles from now onwards will be in the context of slope stabilisation.

Three different methods of lateral force estimations have been identified. The relative merits and demerits of each method will be outlined in this Chapter. Some of these methods were coded to provide predictive numerical values for the lateral forces on piles installed for stabilising slopes. Although historically there are different methods for lateral force estimations, only the developments due to Ito and Matsui (1975, 1978) and De Beer and Carpentier (1977) are presented. The underlying reason for not including the work of other researchers is the constraints in research time. The chosen methods will be compared with the proposed visco-plastic flow given in Chapter 6.

In order to design the piles, the lateral forces need to be estimated as accurately as possible. For the laterally loaded pile these forces are a function of the displacement of the sliding mass and hence provide an interactive situation between the soil and the pile.

Generally, the lateral forces may vary from zero in the case of no movement of the soil mass, to a large value in the case of large landslide displacements (Hassiotis et al. 1997).

An accurate estimation of the lateral force is an important key point for the stability analysis, because the lateral force influences both pile and slope stabilities. Therefore, overestimation of the lateral forces on the pile will naturally lead to conservative pile design and unconservative slope stability design and vice versa. This is because estimated lateral loads are used as extra resisting force(s) on slope stability calculations due to the pile reaction. More details will be given in Chapter 9 for the above mentioned procedure.

7.2 Methods assuming plastic deformation of soils

7.2.1 Ito and Matsui method

Ito and Matsui (1975, 1977, 1978), Ito et al. (1979, 1981, 1982) and Matsui et al. (1982, 1984) have developed an analysis to show that piles placed in plastically

deforming ground, such as landslide mass movement, can prevent further plastic deformations.

The theory proposed by the above authors, called the theory of plastic deformation, estimates the lateral force between the two extremes of zero and large landslide mass movement. It is assumed that no reduction in shear resistance along the sliding surface has taken place as a result of strain-softening caused by the movement in a potential landslide. For this reason it is assumed that the state of plastic equilibrium occurs only in the soil just around the piles, satisfying the Mohr-Coulomb yield criterion. Therefore, the lateral force acting on the pile may be estimated neglecting the change of equilibrium condition of the whole slope. In order to analyse the lateral force by the theory of plastic deformation the following assumptions have been made:

- When the soil layer deforms, two sliding surfaces, AEB and $A'E'B'$, are prominent in which the lines EB and $E'B'$ make an angle $\left[(\pi/4)+(\phi/2)\right]$ with the x-axis, see Fig.7.1.
- The soil layer becomes plastic only in the area *AEBB'E'A'* where the Mohr-Coulomb yield criterion is applied.
- The active earth pressure acts on line *AA'* in the direction of the x-axis.
- The soil layer is in plane-strain condition with respect to depth.
- The piles are rigid.

When the stress distribution in the soil *AEBB'E'A'* is considered, the frictional forces on surfaces AEB and *A'E'B'* are neglected.

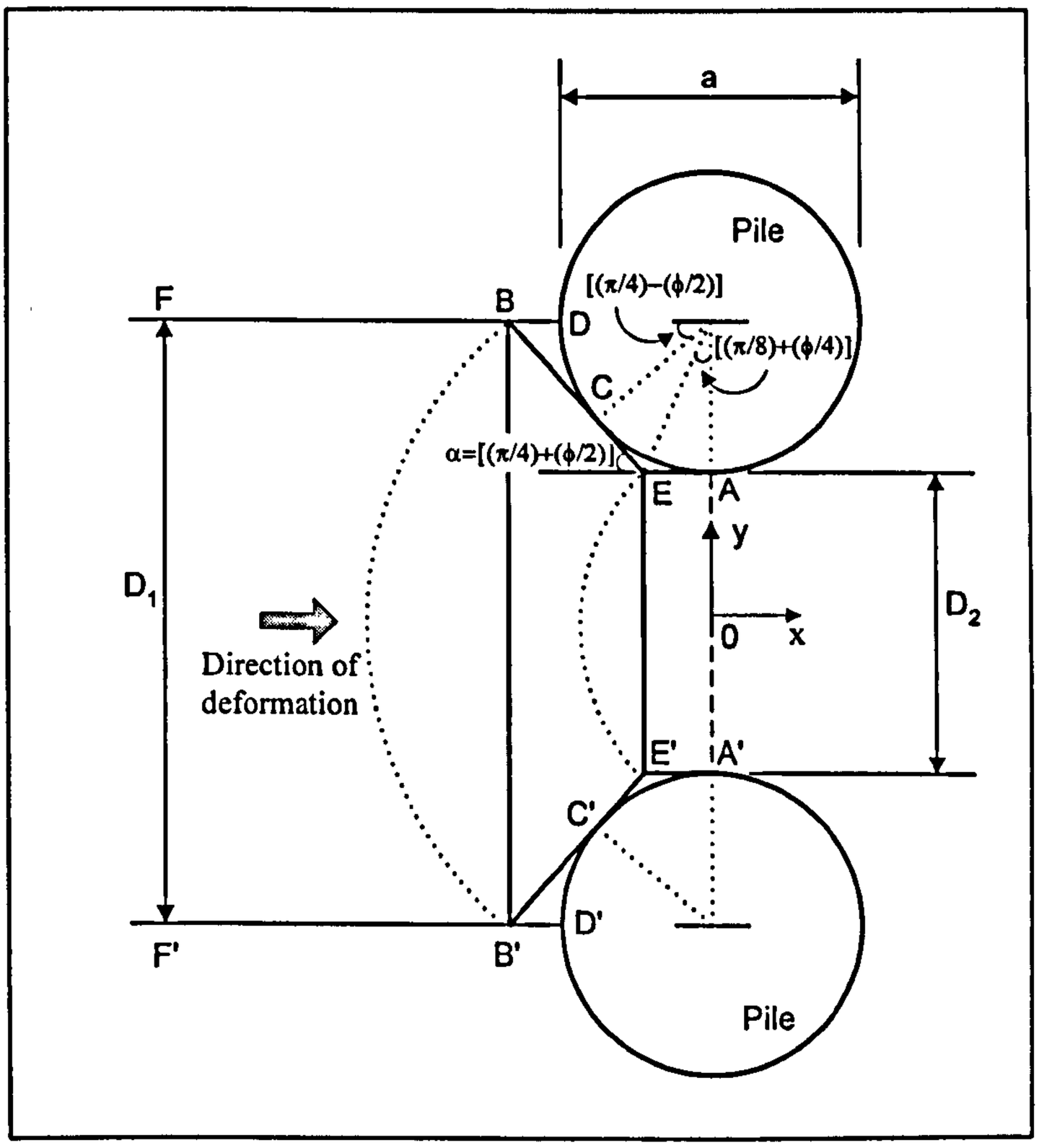

Figure 7.1 Plan view of a row of piles and plastic state of soil just around piles (Ito and Matsui, 1975).

Therefore, a theoretical equation for the lateral force p per unit length may be given as follows (Ito and Matsui, 1975);

$$p = A\tau_y\left[\frac{1}{N_\phi\tan\phi}\left\{\exp\left(\frac{D_1 - D_2}{D_2}N_\phi\tan\phi\tan\left(\frac{\pi}{8}+\frac{\phi}{4}\right)\right)-2N_\phi^{1/2}\tan\phi-1\right\}+\frac{2\tan\phi+2N_\phi^{1/2}+N_\phi^{-1/2}}{N_\phi^{1/2}\tan\phi+N_\phi-1}\right]-\tau_y\left[D_1\frac{2\tan\phi+2N_\phi^{1/2}+N_\phi^{-1/2}}{N_\phi^{1/2}\tan\phi+N_\phi-1}-2D_2N_\phi^{-1/2}\right] \quad 7.1$$

$$+\frac{\gamma z}{N_\phi}\left[D_1\left(\frac{D_1}{D_2}\right)^{\left(N_\phi^{1/2}\tan\phi+N_\phi-1\right)}\exp\left(\frac{D_1-D_2}{D_2}N_\phi\tan\phi\tan\left(\frac{\pi}{8}+\frac{\phi}{4}\right)\right)-D_2\right]$$

where $N_\phi = \tan^2\left[(\pi/4)+(\phi/2)\right]$ and $A = D_1\left(\frac{D_1}{D_2}\right)^{\left(N_\phi^{1/2}\tan\phi+N_\phi-1\right)}$.

Hence, the total corresponding lateral force induced per unit length of the pile, due to the plastically deforming soil layer will be obtained by the integration of Eqn. [7.1] along the soil depth layer (or until a critical slip surface).

In the case of a purely frictional soil (putting the cohesion $c = 0$ in Eqn. [7.1]) the lateral force, p, per unit length may be obtained by integrating Eqn. [7.2] along the depth, z;

$$p=\frac{\gamma z}{N_\phi}\left[D_1\left(\frac{D_1}{D_2}\right)^{\left(N_\phi^{1/2}\tan\phi+N_\phi-1\right)}\exp\left(\frac{D_1-D_2}{D_2}N_\phi\tan\phi\tan\left(\frac{\pi}{8}+\frac{\phi}{4}\right)\right)-D_2\right]. \qquad 7.2$$

In the case of a cohesive soil, the angle of friction ϕ may be neglected i.e. $\phi = 0$. Therefore, the lateral force p per unit length may be obtained as the function of depth as follows;

$$p=\tau_y\left[D_1\left(3\log\frac{D_1}{D_2}+\frac{D_1-D_2}{D_2}\tan\frac{\pi}{8}\right)-2\left(D_1-D_2\right)\right]+\gamma z\left(D_1-D_2\right). \qquad 7.3$$

As can be seen from the above equations, the theory of plastic deformation may be applicable to any soil type.

7.2.2 De Beer and Carpentier method

The theory of plastic deformation was first proposed by Ito and Matsui (1975) and later discussed by De Beer and Carpentier (1977). The latter authors developed comparable equations by modifying the Ito and Matsui's method and gave the following equations as another way of obtaining the lateral force p per unit length induced on the piles;

$$p = \frac{\gamma z}{N_\phi}\left(1+\frac{\sin\phi}{2}N_\phi\right)\left[D_1\left(\frac{D_1}{D_2}\right)^{F_1(\phi)} e^{\frac{D_1-D_2}{D_2}F_2(\phi)} - D_2\right] + \tau_y \cot g\phi$$
$$\left[D_1\frac{(D_1/D_2)^{F_1(\phi)}}{N_\phi}\left(1+\frac{\sin\phi}{2}N_\phi\right)e^{\frac{D_1-D_2}{D_2}F_2(\phi)} - D_1 - D_2\frac{1+\frac{\sin\phi}{2}N_\phi}{N_\phi} + D_2\right] \qquad 7.4$$

where

$$F_1(\phi) = \frac{N_\phi}{\tan\left(\frac{\pi}{4}+\frac{\phi}{2}\right)}(1-\sin\phi)\tan\phi + N_\phi(1-\sin\phi) - 1 \text{ and}$$

$$F_2(\phi) = \frac{1-\sin^2\phi}{1+\sin^2\phi}\tan\phi\tan\left(\frac{\pi}{8}+\frac{\phi}{4}\right).$$

As indicated in section 7.2.1 the lateral force, p, acting on the piles is obtained by integrating Eqn. [7.4] along the depth of the soil layer.

For the case of cohesionless soil $c(\tau_y) = 0$ in Eqn. [7.4], hence by integrating along the depth the lateral force per unit length may be obtained;

$$p = \frac{\gamma z}{N_\phi}\left(1+\frac{\sin\phi}{2}N_\phi\right)\times\left[D_1\left(\frac{D_1}{D_2}\right)^{F_1(\phi)} e^{\frac{D_1-D_2}{D_2}F_2(\phi)} - D_2\right]. \qquad 7.5$$

For the case of cohesive soil, putting $\phi = 0$ and by integrating along the depth of the pile, the lateral force per unit length may be obtained as;

$$p = \tau_y\left[D_1\left(2\ln\frac{D_1}{D_2} + \frac{D_1-D_2}{D_2}\tan\frac{\pi}{8}\right) - \frac{3}{2}(D_1-D_2)\right] + (D_1-D_2)\gamma z\,. \qquad 7.6$$

7.3 Plastic flow

7.3.1 Ito and Matsui method

Ito and Matsui (1975, 1978) proposed a method of estimating the lateral force on a pile in which the soil is considered as a visco-plastic solid. This was named the theory of plastic flow. In their theory the following assumptions were made:

- A visco-plastic flow occurs around the piles (see Fig. 7.2).
- The soil layer is in a steady state condition and is represented by the Bingham model together with a yield stress τ_y $(c = \tau_y)$and a plastic viscosity η_p.
- The soil layer flows uniformly in the direction of depth.
- The laterally acting force is the sum of the force due to earth pressure and the viscous force calculated by assuming a visco-plastic flow in a channel.
- Piles are rigid.

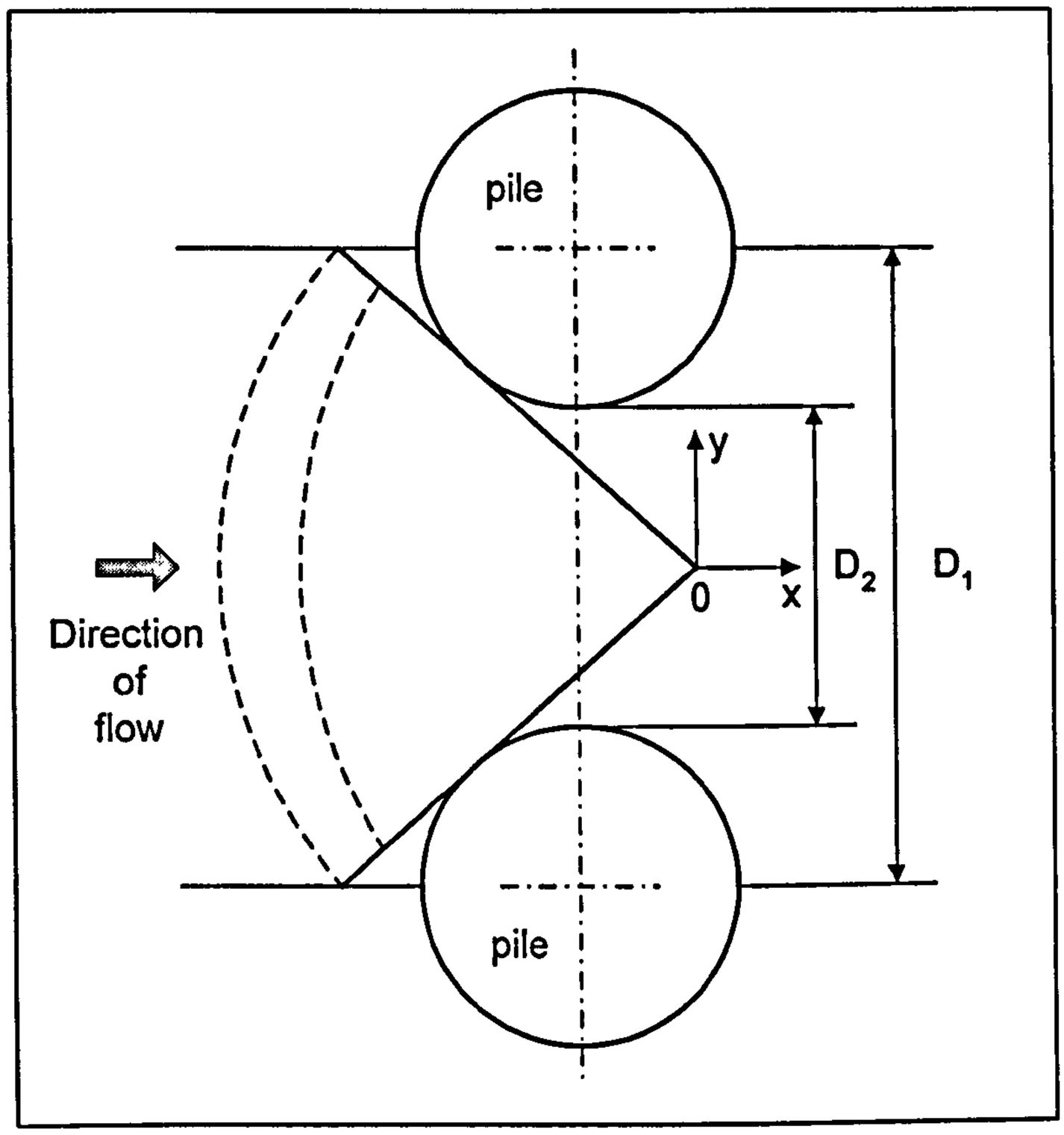

Figure 7.2 State of plastic flow (Ito and Matsui, 1975).

The lateral force, per unit length, acting on the pile due to plastic flow may be obtained by integrating along the pile depth as follows;

$$p = \sqrt{2m\tau_y}\left\{\sqrt{1+\frac{m}{2\tau_y D_2^2}} - \sqrt{1+\frac{m}{2\tau_y D_1^2}} + \log\frac{D_1\left(1+\sqrt{1+\frac{m}{2\tau_y D_1^2}}\right)}{D_2\left(1+\sqrt{1+\frac{m}{2\tau_y D_2^2}}\right)}\right\}$$

$$+(D_1-D_2)\left\{\frac{(\sqrt{2}-1)\pi^2 m}{8D_2^2} + (\sqrt{2}-1)\sqrt{\left(\frac{\pi^2 m}{8D_2^2}\right)^2 + \frac{\pi^2 m\tau_y}{4D_2^2}}\right. \qquad 7.7$$

$$\left. + \frac{m}{D_1 D_2} + \sqrt{2}\tau_y - 2\tau_y + \gamma z\right\}$$

where $m = 16\eta_p V D_1/\pi^2$.

7.3.2 De Beer and Carpentier method

De Beer and Carpentier (1977) developed an alternative set of equations for the theory of plastic flow, modifying the Ito and Matsui's method. The following equation is given as an alternative way of obtaining the lateral force per unit length by using the theory of plastic flow;

$$p = (D_1 - D_2)\left[\gamma z - \frac{3}{2}\tau_y + \frac{D_1}{D_2}\tan\frac{\pi}{8}\tau_y\right] + D_1\left(\ln\frac{D_1}{D_2}\right)(2\tau_y + 5.14\tau_y)$$

$$+\tau_y D_1 \ln\frac{1+\sqrt{1+\dfrac{2\tau_y D_2^2}{m''}}}{1+\sqrt{1+\dfrac{2\tau_y D_1^2}{m''}}} + \frac{m''}{D_2}\left[\frac{D_1 - D_2}{D_2}\left(\frac{1}{2}\frac{D_1 + D_2}{D_1} + \frac{D_1}{D_2}\tan\frac{\pi}{8}\right)\right. \qquad 7.8$$

$$\left.+\frac{D_1}{D_2}1+\sqrt{1+\frac{2\tau_y D_2^2}{m''}}\left(\frac{1}{2}\frac{D_1 + D_2}{D_1}\tan\frac{\pi}{8}\right) - \frac{1}{2}\frac{D_2}{D_1}\sqrt{1+\frac{2\tau_y D_1^2}{m''}}\right]$$

7.4 Visco-plastic flow

The proposed visco-plastic flow, past a single pile and a row of piles, has been described in Chapter 6 in detail, the assumptions for which may be summarised as follows:

- The visco-plastic flow is two-dimensional and is assumed to be uniform in the direction of depth.

- Flow past a cylinder is stationary, steady and symmetrical.
- The fluid is deemed incompressible.
- A coupled non-linear pair of partial differential equations were used to obtain a stream function ψ and vorticity ω using Finite Difference solution techniques.
- In order to analyse the flow past a single pile and a row of piles, a purely viscous fluid model has been used.
- The soil layer is represented by a Bingham plastic model approximation together with yield stress τ_y and plastic viscosity η_p.
- The force acting in a row of piles is perpendicular to the pile shaft.

The lateral force F per unit length acting on the cylindrical pile may be estimated numerically by;

$$F = \frac{2}{\mathrm{Re}} \int_0^{\pi} \left(\eta\omega - \frac{\partial}{\partial \xi}(\eta\omega) \right) \sin\theta \, d\theta \,. \qquad 7.9$$

It should be noted that as the depth of the soil layer increases, the lateral pressure on the pile increases as well. This is considered in the following manner, using passive pressure so that $p' = \gamma z$, or force per meter run of pile becomes;

$$\varpi = \gamma a z \,.$$

where p' is the earth pressure due to gravity, ϖ is the force per unit length of pile, γ is the unit weight of the soil layer, a is the pile diameter and z is the depth along the pile. This additional lateral force, shown in Fig. 7.3, is added to contribution of Eqn.

[7.9]. This present numerical studies have been based on the assumption used by Ito and Matsui (1978).

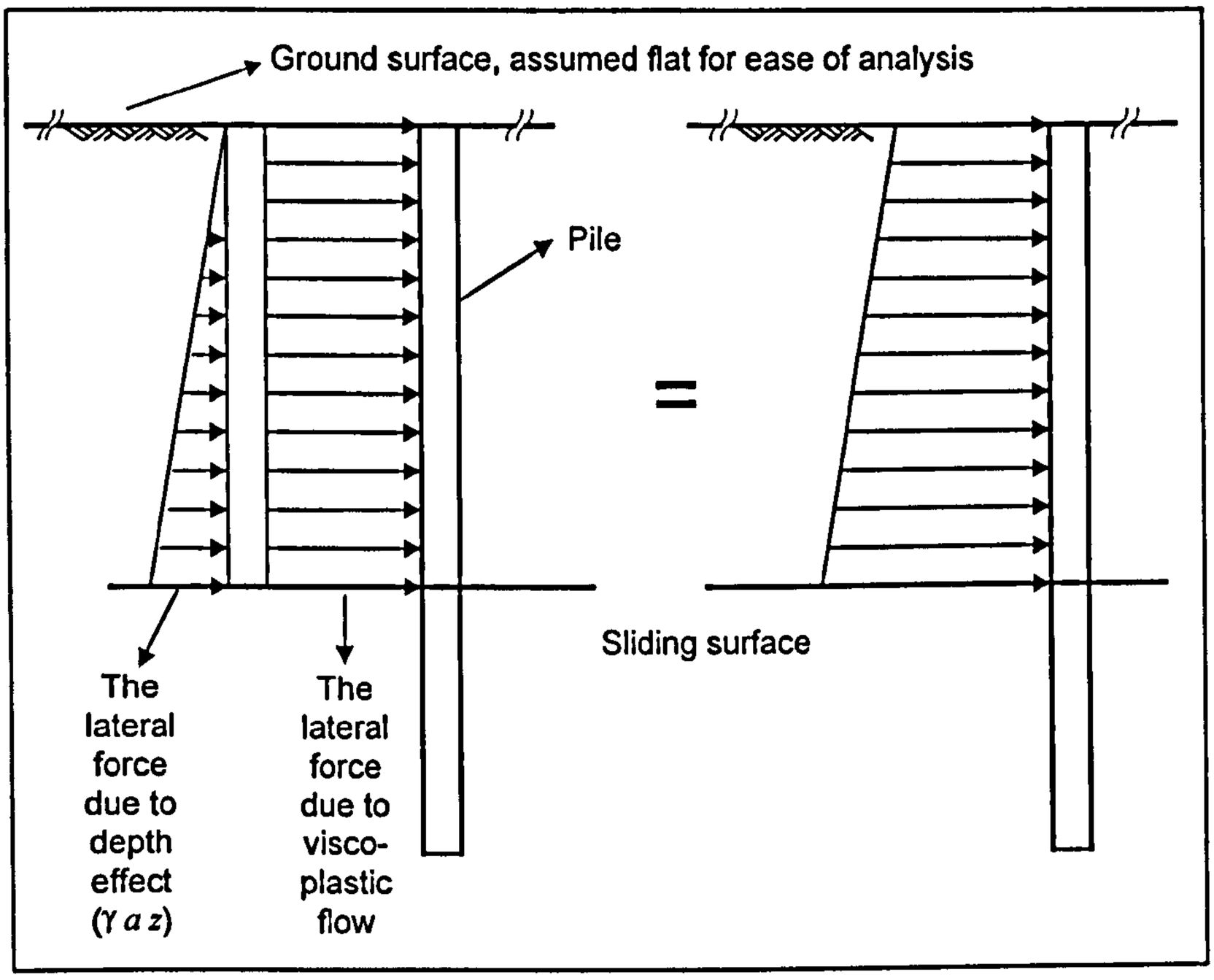

Figure 7.3 Inclusion of the depth effect on the estimation of the lateral force.

For the design case illustrated, Fig. 7.3, passive pressure in front of the pile has been neglected on the assumption that the soil will yield. In reality, the soil may develop passive resistance which will lead to an enhanced *FOS*.

7.5 Comparison of forces for bench mark results

Three different lateral force estimations are shown in Figs. 7.4(a)-(c) and the proposed visco-plastic flow is tested against available data in the aforementioned literature.

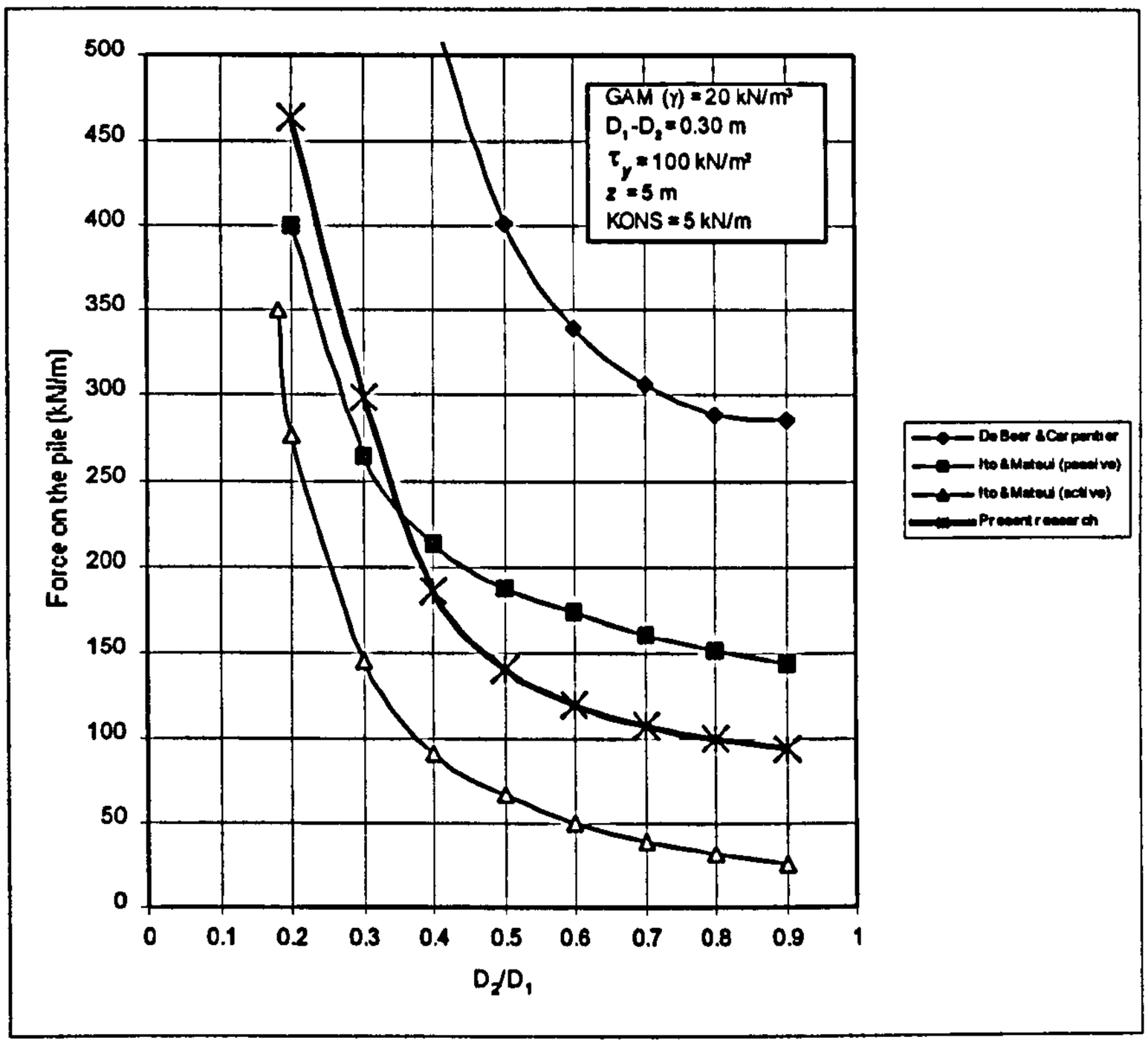
GAM (γ) = 20 kN/m³
D1-D2 = 0.30 m
τy = 100 kN/m²
z = 5 m
KONS = 5 kN/m
De Beer &Carpentier
Ito &Matsui (passive)
Ito &Matsui (active)
Present research
Force on the pile (kN/m)
D2/D1
500
450
400
350
300
250
200
150
100
50
0
0 0.1 0.2 0.3 0.4 0.5 0.6 0.7 0.8 0.9 1

(a)

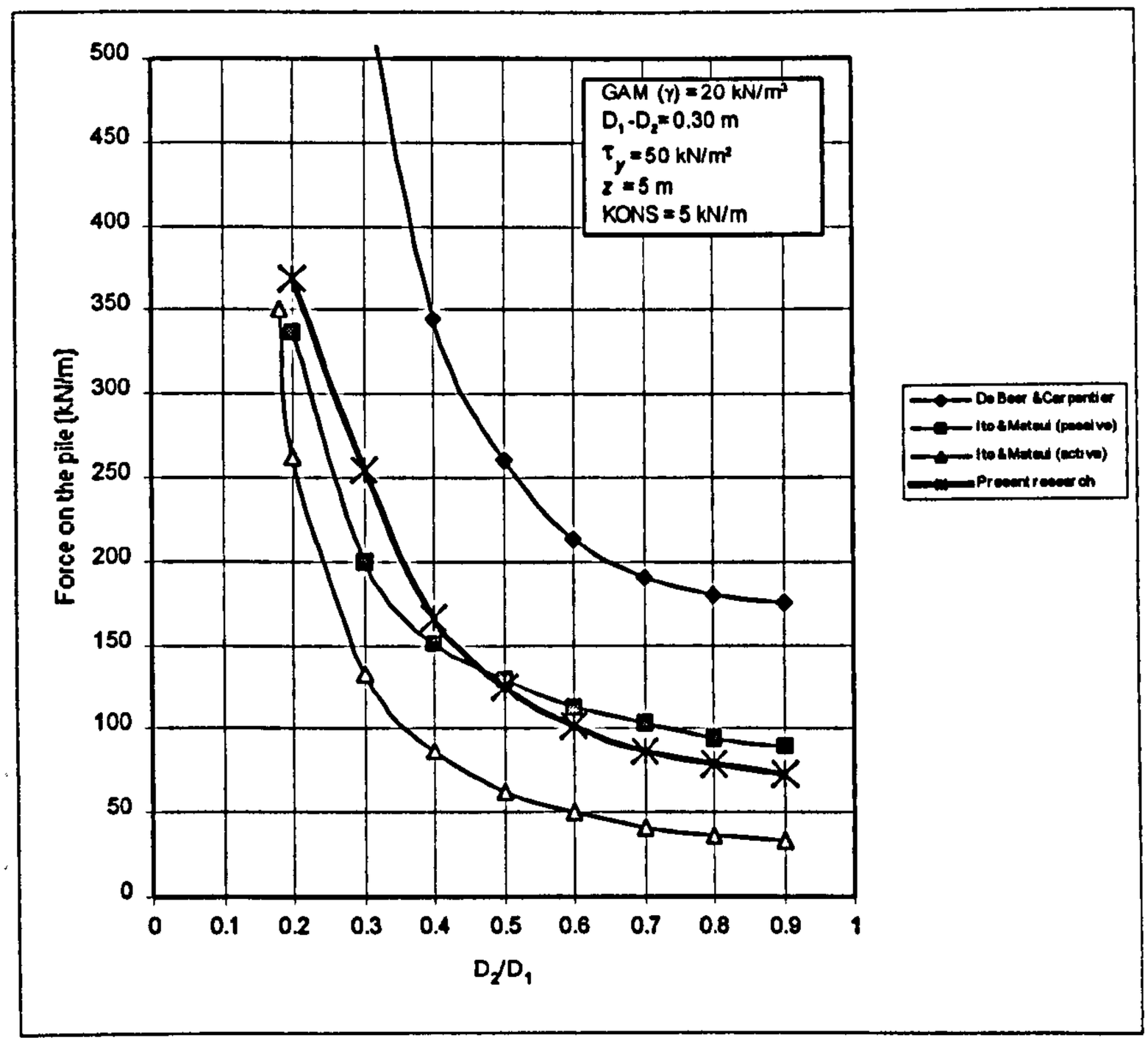
GAM (γ) = 20 kN/m³
D1-D2 = 0.30 m
τy = 50 kN/m²
z = 5 m
KONS = 5 kN/m
De Beer &Carpentier
Ito &Matsui (passive)
Ito &Matsui (active)
Present research
Force on the pile (kN/m)
D2/D1
500
450
400
350
300
250
200
150
100
50
0
0 0.1 0.2 0.3 0.4 0.5 0.6 0.7 0.8 0.9 1

(b)

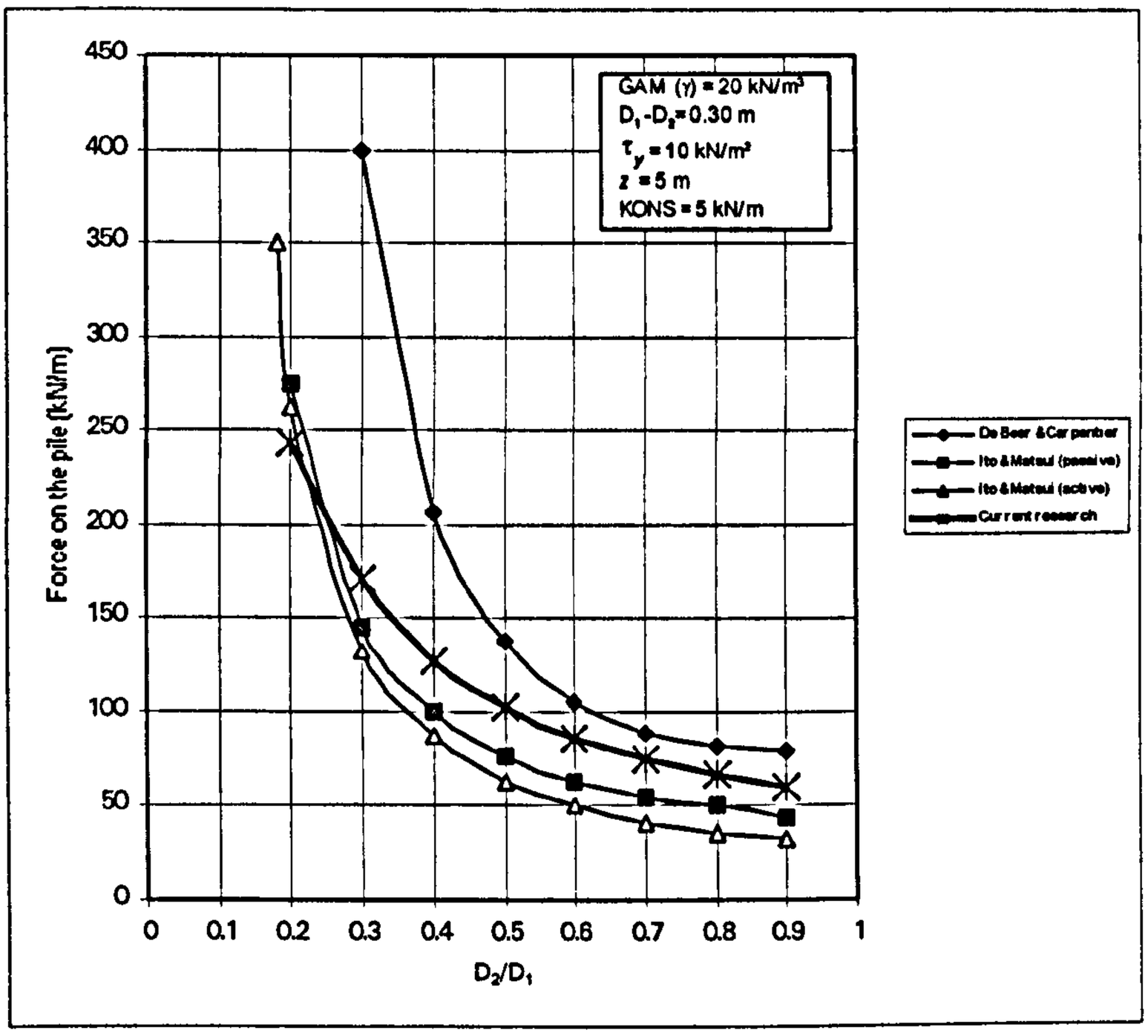

(c)

Figure 7.4 (a), (b), (c) Comparison of three different force estimations for varying values of τ_y.

Forces from the plastic deformation theory together with the visco-plastic flow will be considered in Chapter 9 to show the pile influence on the stabilisation of slopes. Figure 7.4 (a), (b) and (c) illustrates the variation of the lateral force on the pile versus the ratio D_2/D_1. It can also be seen that the proposed method displays a trend where lateral load predictions from this work lie between the data given by De Beer & Carpentier and Ito & Matsui.

It is seen that in addition to parametric variation of inter-pile distance, D_2/D_1, the mechanical properties of the flowing soil mass has also been varied from τ_y = 10 kN/m^2 to 50 and then 100. It is also noted that lateral forces converge in all three methods as shear stress τ_y tends to zero.

Figure 7.5 is given in colour form to emphasize the differences between the author's generated data and other researchers (Ito & Matsui, 1975, 1978 and De Beer & Carpentier, 1977). In this figure, τ_y is used as values of 100, 50 and 10 kN/m^2 for each researcher. The following numbers represent the relevant research work and can be found in the legend of Figure 7.5;

(1) represents De Beer and Carpentier (1977).

(2) represents Ito and Matsui in terms of passive earth pressure (1978).

(3) represents Ito and Matsui in terms of active pressure (1975).

(4) represents present research.

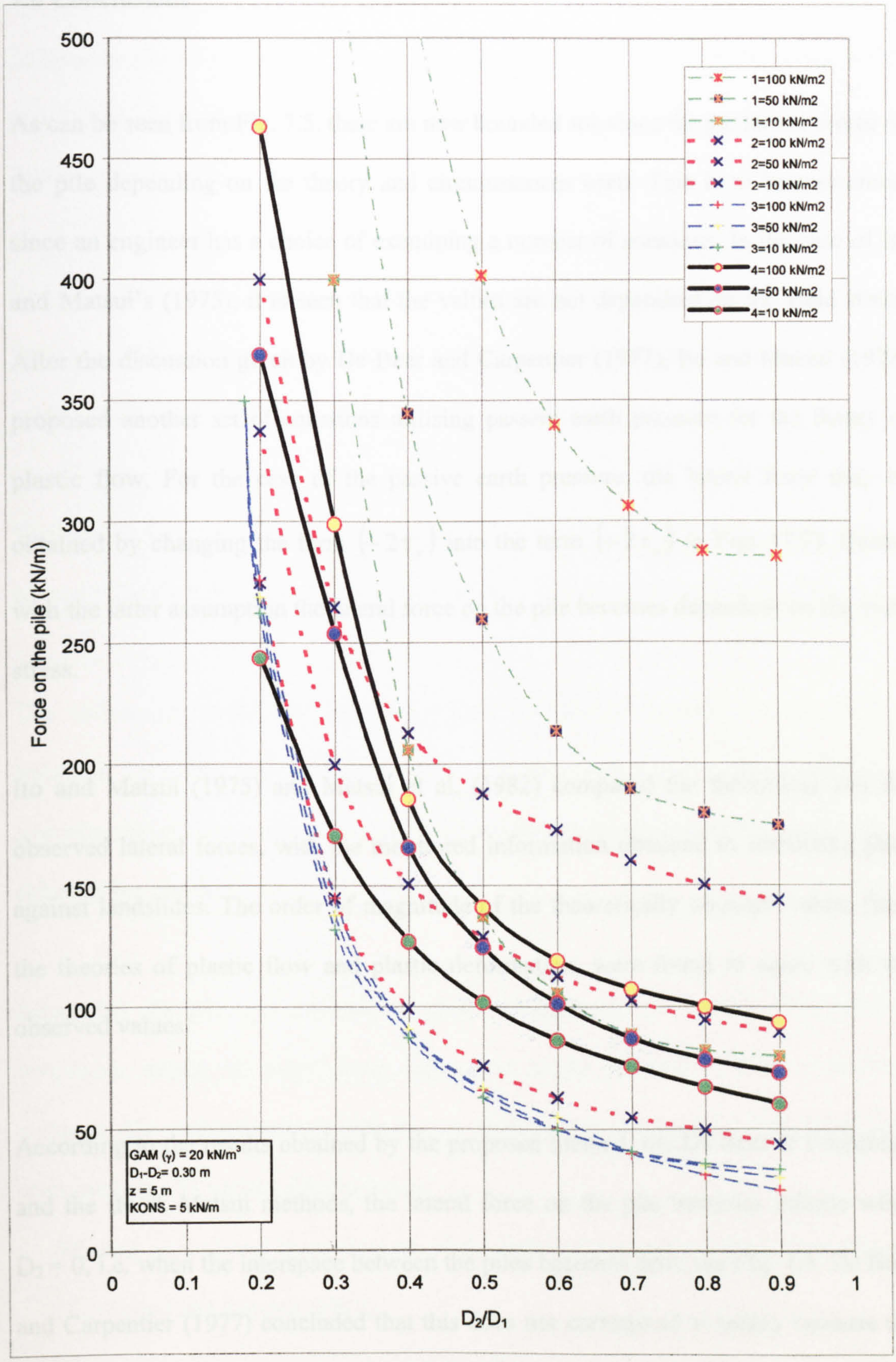

Figure 7.5 Comparison of lateral load predictions for different theories.

7.6 Conclusions

As can be seen from Fig. 7.5, there are now bounded solutions for the lateral forces on the pile depending on the theory and circumstances used. This is to be welcomed, since an engineer has a choice of examining a number of solutions. In the case of Ito and Matsui's (1975), it is seen that the values are not dependent on the yield stress. After the discussion given by De Beer and Carpentier (1977), Ito and Matsui (1978) proposed another set of equations utilising passive earth pressure for the theory of plastic flow. For the case of the passive earth pressure, the lateral force may be obtained by changing the term $\left(-2\tau_y\right)$ into the term $\left(+2\tau_y\right)$ in Eqn. [7.7]. Hence, with the latter assumption the lateral force on the pile becomes dependent on the yield stress.

Ito and Matsui (1975) and Matsui et al. (1982) compared the theoretical and the observed lateral forces, with the monitored information obtained in stabilising piles against landslides. The order of magnitude of the theoretically obtained values from the theories of plastic flow and plastic deformation, were found to agree with the observed values.

According to the results obtained by the proposed method, the De Beer & Carpentier and the Ito & Matsui methods, the lateral force on the pile becomes infinite when $D_2 = 0$, i.e. when the interspace between the piles becomes zero, see Fig. 7.5. De Beer and Carpentier (1977) concluded that this does not correspond to reality because the forces generated by the piles cannot be larger than those needed for the equilibrium of

the soil mass which is located "upstream" of the pile row (in the event of a potential landslide). For this reason they suggested that the gap (D_2) between two piles, for the case of the plastic flow, should be 2/3 a, and for plastic deformation 3/5 a, where a is the diameter of the pile used.

The modified assumption by De Beer and Carpentier (1977) gave much larger lateral forces on the pile than those obtained using either the assumptions of the proposed method or Ito and Matsui's method.

The lateral force estimated by the proposed visco-plastic flow lies between those given by De Beer & Carpentier and Ito & Matsui's plastic deformation method.

The author has noted that the results from the present research occupy an "in-between" position to the previously reported data. The general trend is overwhelmingly confirmed without the current results being the arithmetic average of either of the plastic theories.

Altogether the previous methods of plastic deformation and plastic flow provide invaluable means of lateral force assessment in the absence of other equivalent methods. The author however feels that he should point out the following points have been excluded by virtue of formulation:

- Sloping ground and shear strength of the failure plane are not taken into account (Leventhal and Mostyn, 1987).
- No provision to account for pile deformibility.

- Absence of frictional forces at the soil/cylinder (i.e. pile) interface in the lateral force calculations, particularly for the case of the plastic deformation method.
- The theory of plastic deformation has been developed in terms of a total stress analysis. No recommendations are given as how best to include soil properties for effective stress conditions.

As clearly stated by Nash (1987), "...a total or an effective stress approach could be used to analyse any slope, although since soils are predominantly frictional materials an effective stress analysis seems inherently more logical especially for the analysis of long term problems. In practice for short-term stability problems a total stress analysis is often simpler and more convenient as there is usually difficulty in predicting pore pressure changes...".

For great simplicity, a total stress analysis is generally used but for the long-term, the fully drained condition will be reached and only an effective stress analysis will be appropriate (Craig, 1997).

The merits for plastic deformation and plastic flow may be summarised as follows:

- Pile-soil interaction well established (Anagtopoulos et al., 1991).
- Lateral load estimation for a single pile, as well as for a pile in a row, is analysed.
- Site measurements agree with theoretical lateral force estimations.

CHAPTER 8: BEHAVIOUR PREDICTION OF LATERALLY LOADED PILES USED IN STABILISING SLOPES

8.1 Introduction

Piles are modelled as beams when subjected to lateral loads arising from active stabilisation of slopes. This is to cater for horizontal forces which exist due to the movement of the soil mass. It is generally accepted that for pile stabilisation, two different investigations should be undertaken, one for the pile and the other for slope stability analysis. Both are carried out individually assuming no interaction. At a later stage the forces are allowed to interact, since the whole stability of the slope which contains piles in a row (or multi-row) can never be valid unless both stabilisations of the slope and the action of the pile are simultaneously satisfied.

In this chapter pile stability is examined with emphasis on laterally loaded piles and predictions for their safety analysis. The Finite Element Method (FEM) is used to obtain displacements, shear force and bending moment.

8.2 Background theories for piles in lateral soil movement

Piles were used as a prevention of landslides over a century ago (Fukuoka, 1977). Since then many successful applications have been reported by many researchers, such as De Beer and Wallays (1972); Sommer (1977, 1979); Morgenstern (1982);

Hassiotis and Chameau (1984); Snedker (1985); Wei et al. (1991); Rollins and Rollins (1992); Kalteziotis et al. (1993); Poulos (1995); Ulusay et al. (1996), and others. Some of the methods are given below.

8.2.1 Method of Broms

Broms (1964-a, 1964-b) proposed two approaches to evaluate the ultimate capacity of a vertical pile acted upon by a horizontal load for cohesive and cohesionless soils. The behaviour at working loads has been analysed by the elastic theory assumption that a laterally loaded pile behaves as an elastic member, and that the supporting soil behaves as an ideal elastic material.

8.2.2 Method of De Beer and Wallays

De Beer and Wallays (1972) utilised a method to estimate the force and moment on a pile produced by the horizontal load under the influence of a non-uniform distribution of lateral surcharges around the pile. The method was based on Hansen's (1961) assumption, which emphasises the ultimate resistance of rigid piles against transverse forces.

8.2.3 Method of Wang and Yen

Wang and Yen (1974) developed a design method for soil arching (stress transfer through the mobilisation of shear strength) in slopes assumed to have a rigid-plastic

soil. The method utilised a row of piles, in an infinite slope, although practical problems involve various slope geometries, see Fig. 8.1.

The analysis allows the estimation of the effective pile spacing of both cohesive and cohesionless soils and this is given as a function of soil properties and slope. The size of the piles is not directly involved in this assumption, but it is tacitly assumed that the practical sizes will be sufficiently large and rigid to allow the soil arching phenomenon to develope.

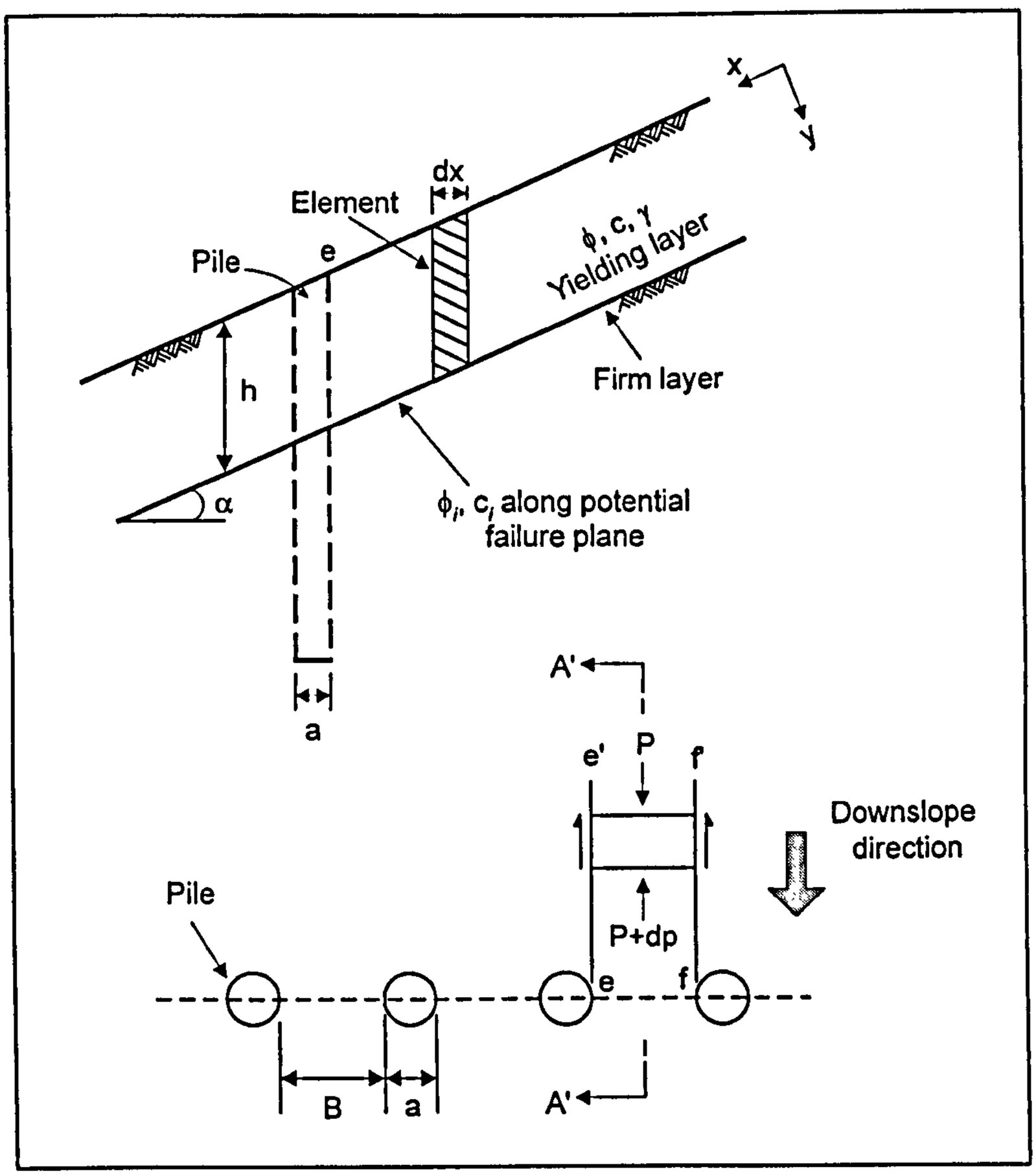

Figure 8.1 Plan view of series of piles installed in a infinite slope (Wang and Yeng, 1974).

8.2.4 Method of Ito and Matsui

Ito and Matsui (1975) developed the theory of plastic deformation, stiff soil, and plastic flow, soft soil, to calculate lateral forces on a pile (details are given in Chapter 7).

Hassiotis and Chameau (1984) and lately Hassiotis et al. (1997) have selected the plastic deformation theory of Ito and Matsui (1975) and implemented a computer program to estimate the pressures acting on a typical pile. They used the friction circle method (Taylor, 1937) for slope stability, to take into account the force exerted by the pile on the slope. They recommended that the force predicted using the plastic state assumption, be divided by the *FOS* of the slope to obtain the mobilised force.

In their work, the pile is analysed in two sections along its length to compute the bending moment, shear force and displacement point along the pile shaft. The portion above the critical slip surface is analysed using a closed-form (Eqn. 8.3) solution since the pressure that acts on this section is known. The section below the critical slip surface is analysed as a Winkler foundation using the Finite Difference (FD) numerical technique. They recommended that for a maximum *FOS*, the piles should be placed in the upper middle part of the slope.

Anagnostopoulos et al. (1991) also modified the plastic deformation theory of Ito and Matsui (1975) in order to study the influence of rigid piles in stabilising landslides.

8.2.5 Method of Fukuoka

Fukuoka (1977) applied a Winkler model for the pile-soil interaction in slopes subjected to creep. He assumed that the disturbing force that causes the soil movement is a function of the velocity of the moving soil. Therefore the velocity measurements are necessary to estimate the driving forces. The velocity distribution is not necessarily uniform in the direction of the depth of soil mass. However, for convenience, he assumed a uniform velocity distribution. He further proposed that piles provided extra resisting forces to resist the moving soil mass. For this, Fukuoka gave equations to estimate the lateral resistance of the pile against landslide using the modulus of the Subgrade Reaction method. He also gave equations for the calculation of the deflection curve, the bending moment and horizontal reactions of the pile. De Beer (1977) and Hassiotis and Chameau (1984) pointed out that it is difficult to define a coefficient of Subgrade Reaction, when the soil mass is moving.

8.2.6 Method of Viggiani

Viggiani (1981) analysed pile-soil interaction between a sliding soil mass and a pile restraining it, and penetrating into the stable underlying soil, using the limit equilibrium method. The general design approach involves the following steps.

- Evaluating the total shear force needed to increase the safety factor of the slope of the desired value.
- Evaluating the minimum shear force that each pile can receive from the sliding soil and transmit to the stable underlying soil.

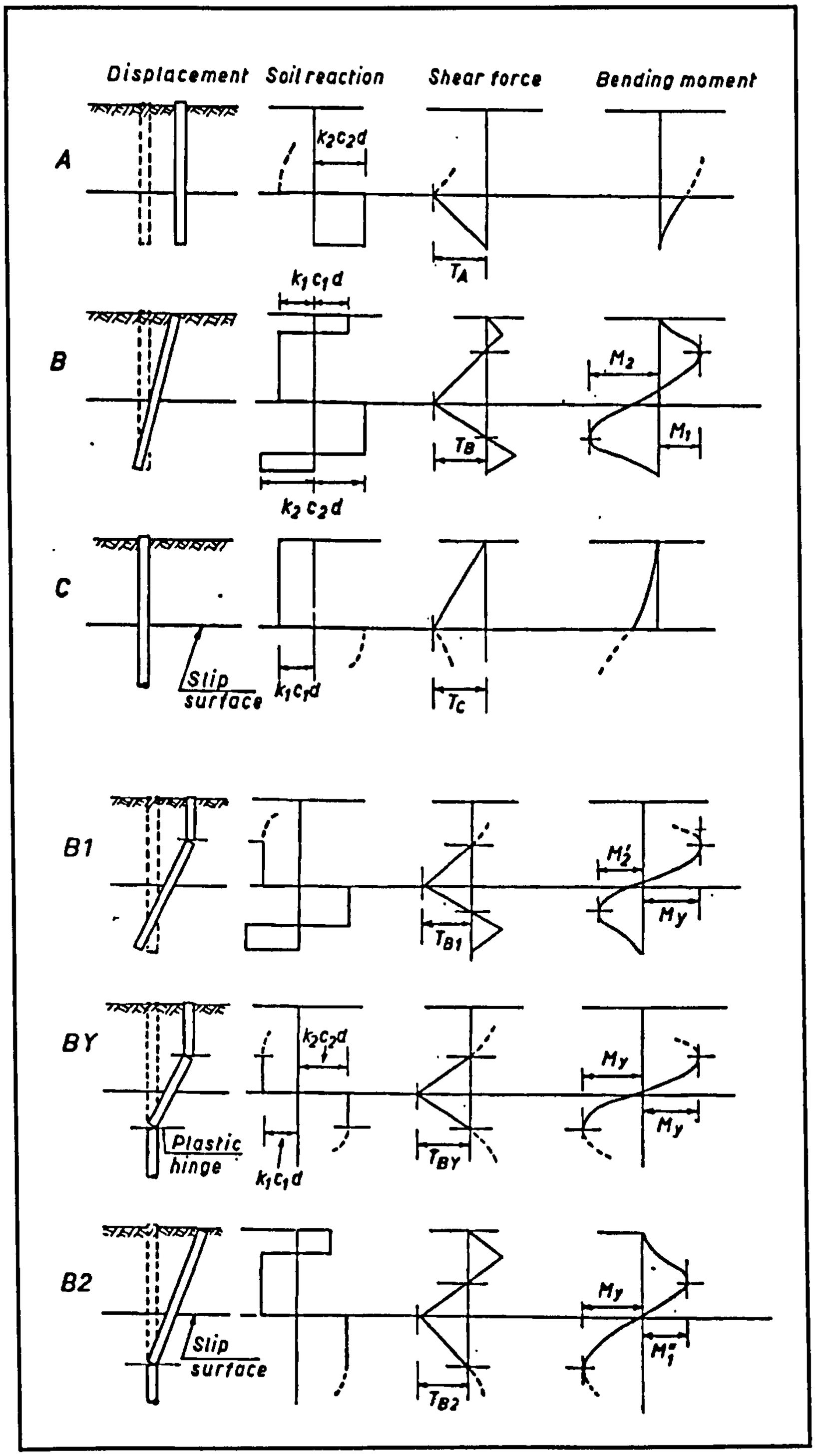

Figure 8.2 Failure modes for rigid piles (*A*, *B*, *C*) and for piles with plastic hinges (*B1*, *BY*, *B2*) (Viggiani, 1981).

- Selecting the type and number of piles and their optimum location on the slope for stability purposes.

Viggiani's approach is based on the concept developed by Broms (1964) who predicted the ultimate capacity of a vertical pile acted upon by a horizontal load. He analysed six possible failure mechanisms for a pile depending on the soil parameters and pile yield strength, Fig. 8.2. However, Viggiani's approach is only applicable in a two-layer purely cohesive soil.

8.2.7 Method of Nethero

Nethero (1982) reported that drilled cantilever pier walls had been successfully used in the Ohio River valley for prevention of slope stability problems. He assumed that a single line individual pier forms a continues structure through the principle of soil arching which allows restraint to the active forces which tend to promote movement of soil between the piers. The interval between the piers (piles) is directly related to the applied forces, soil strength, groundwater level etc. Nethero specified a safe open space of between piers of 2 to 3 times the diameter of pier used, see Fig. 8.3.

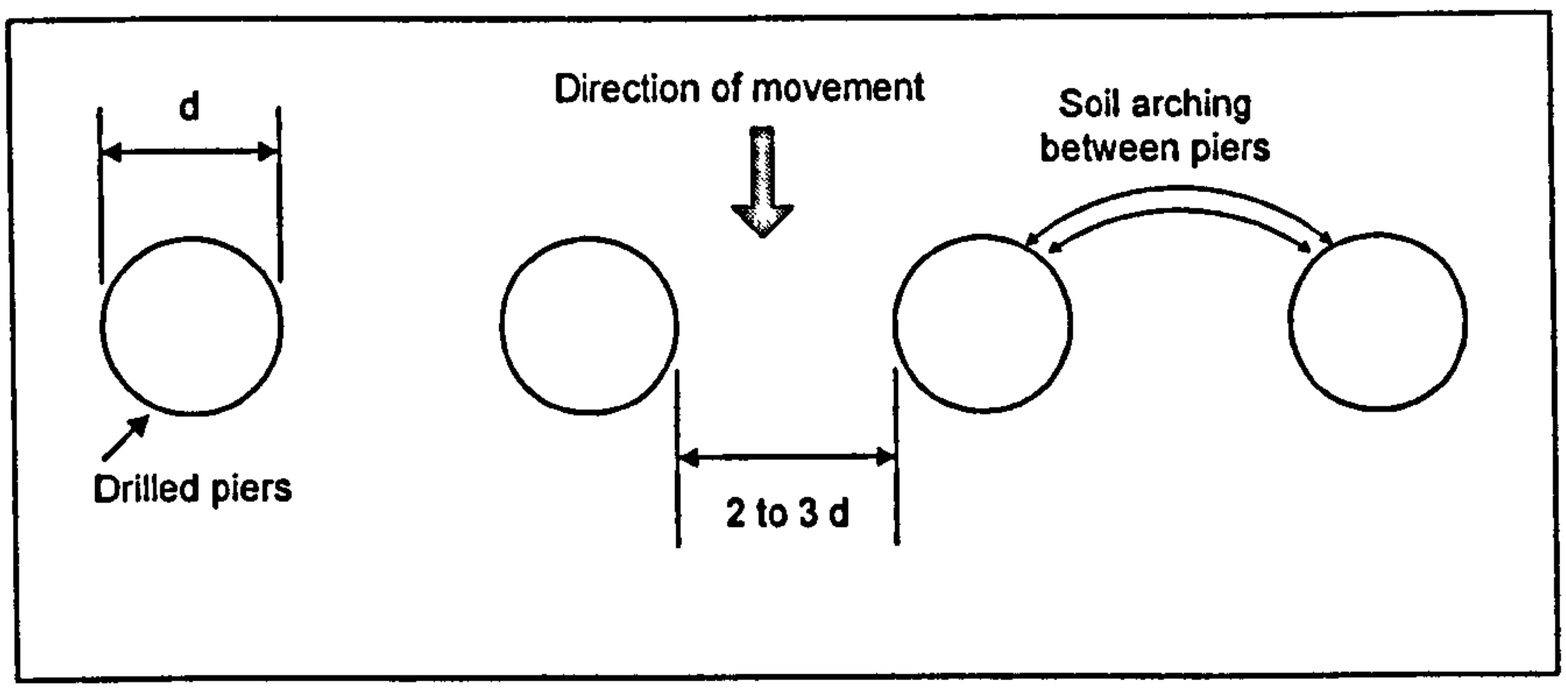

Figure 8.3 Soil arching principle (Nethero, 1982).

The following assumptions have been made by Nethero(1982):

- A series of drilled piers consisting of a group of individual piers, assumed to act as a retaining wall, are subjected to lateral loading.
- A two-dimensional stress system due to earth pressures is assumed to develop continuously along the pier wall.
- Rankine earth pressures are used where no friction is assumed to occur at the soil-wall interface.
- Passive earth pressure above the failure surface has been neglected on the downhill side of the piers. This accounts for long term creep which would cause separation of the soil from the shaft and eventual loss of resistance.
- The applied load is static.

Hassiotis and Chameau (1984) pointed out that if the pile group were to be assumed to act as a retaining wall, this would lead to a conservative design because the soil arching mechanism between the piles may not have been taken into account.

8.2.8 Method of Winter et al.

Winter et al. (1983) proposed a method to stabilise slopes by piles based on a viscosity law for cohesive soils. There were two requirements to satisfy the theory;

1. a desired reduction of the sliding velocity, and
2. a safe maximum bending moment on the pile to be satisfied by the well established geometrical parameters of pile spacing and pile diameter.

The above authors stated that the method can be best used for cohesive slopes undergoing creep.

Gudehus and Shwarz (1985) presented further case studies and a design approach for the stabilisation of creeping slopes by dowel piles. In this method, soil is assumed as a viscous fluid. The aim of the slope stabilisation is reduction of the sliding velocity as mentioned Winter et al. (1983). They pointed out that a large diameter pile is displaced mainly by tilting rather than bending. The lateral pressures on the upper and lower parts of the pile are almost linearly distributed. For large diameter piles where the displacements are small, it is considered that the ultimate lateral pressure and the ultimate bending moment are not fully mobilised. Therefore, the use of large pile diameter is uneconomical. The design of the stabilisation is carried out assuming the dowels as elastic beams with a constant coefficient of lateral Subgrade Reaction (K_s).

8.2.9 Method of Nakamura

Nakamura (1984) considered a solution of rigid dowel piles using the Subgrade Reaction method. The analysis uses a limit equilibrium method for multi-layered soils. Once the lateral force for a single pile was determined, the numbers of piles were calculated for a given width of landslide. The method involves the analysis of bending moments, shear forces, pile displacement profile and hence the soil reaction on the pile.

8.2.10 Method of Yamagami et al.

Yamagami et al. (1991) developed Nakamura's (1984) method for single and multi-rows of piles. The salient aspect of this method is that the sliding masses above and below each row of piles are allowed to have different values of the *FOS*. The Janbu simplified method was used to obtain a stabilised *FOS*. Accordingly, the *FOS* was seen to increase from 1.03 for unstabilised slope, to 1.2 when using either one row or two rows of piles. For this method (Yamagami et al. (1991)) the positions of the rows of the piles play a very important role, as can be seen by the above stabilised *FOS* (i.e. 1.2).

8.2.11 Method of Reese et al.

Reese et al. (1992) presented a method to analyse laterally loaded piles for slope stabilisation using the Subgrade Reaction method. They assumed a "passive wedge" type of failure for piles in a row or rows. The method presented by the above authors includes:

- procedures for estimating the loads due to earth pressures from a potentially sliding mass of soil,
- methods for assessing the resistance of the soil below the possible surface of sliding,
- sequences for estimating the response of the pile, both above and below the estimated sliding surface, and
- suggestions for estimating the factor of safety of a slope that is reinforced by piles.

8.2.12 Methods due to Poulos

Poulos (1973, 1976) has utilised a method for active piles based on the assumption of an elastic-plastic material. The solution is obtained by imposing compatibility of displacement between the pile and the adjacent soil. The pile displacement is estimated from the equation of flexure of a thin strip. The soil displacement is evaluated from the Mindlin equation (Mindlin, 1936) for lateral displacements due to horizontal loads within a semi-infinite mass. The Finite Difference method is used to solve the problem of a single pile, installed in an ideal elastic-plastic material.

Later Poulos and Davis (1980) and, more recently Hull et al. (1991), Lee et al. (1991, 1995) and Poulos (1995) developed Poulos's (1973, 1976) method based on elastic interaction of the moving soil and the pile, allowing for the limiting pressure that the soil may exert on the pile. As stated by Fleming et al. (1992), their method relies on an initial estimate of the horizontal soil movement. For this assumption Hull et al. (1991), Lee et al. (1991) and Poulos (1995) presented the following modes of failure:

1. "Flow mode", when the slide is shallow and the unstable soil acquires "fluid" states and flows around the pile.
2. "Short pile mode", when the slide is relatively deep and the length of pile in the stable soil is relatively shallow.
3. "Intermediate", in which the soil resistance is fully mobilised, along the pile length, in both stable and unstable soil layers.
4. "Long pile failure", the maximum bending moment in the pile reaches the yield moment of the pile before complete development of the above three modes.

Lee et al. (1991) used a parametric study in analysing the Hull et al. (1991) method. Using the Boundary Element Method (BEM), the values of shear force, bending moment and deflection were obtained. This was achieved by dividing the pile length into 60 equally spaced elements.

Poulos (1995) clearly stated that the stabilising piles must posses the following characteristics:

- Piles must be relatively stiff, so that a large stabilising force can be generated without causing failure of the piles.
- Piles must extend well below the critical failure surface so that the failure surface is not merely shifted downwards below the pile tips with a *FOS* still less than the target value.
- Piles should be placed in the vicinity of the centre of the critical slip surface to avoid merely relocating the failure surface behind, or in front of, the piles.

In this same manner, Poulos (1995), using the above mentioned criteria, analysed a piled-slope using the Bishop simplified slip circle analysis. He increased the *FOS* from 1.15 to 1.50 using a row of piles.

Rowe and Poulos (1979) presented an application of the FEM for slope stabilisation. They employed a two-dimensional FEM analysis for soil-structure interaction. The method involves the effects of failure within the soil and flow past the piles. For the problem considered, the following conclusions have been drawn:

- The effect of piles upon shape stability increases gradually with increasing pile stiffness and it may be necessary to use very stiff piles to obtain any significant improvement in slope performance.
- The effectiveness of piling is enhanced by provision of restraint at the head.
- The beneficial influence of piling is also enhanced in cases where the soil stiffness and strength increases with depth.

Chen and Poulos (1993, 1994) presented a FEM analysis for the study of rigid set of piles in soil undergoing lateral movement. The soil has been assumed to be a purely cohesive, undrained clay, the behaviour of which is described by an elastic-plastic model. The solution involved modelling the pile shaft at two different segments:

1. The pile section in the upper unstable soil layer was modelled to be subject to the lateral soil movement and is thus treated as a "passive" pile;
2. The pile section in the lower stable soil layer was subjected to lateral loading transmitted from the upper pile portion and was hence regarded as an "active" pile.

It is known that the soil has limited ability to take tension so that separation between the pile and the soil may occur. Chen and Poulos assumed that the soil had zero tensile strength and was allowed to separate rather than transmit tensile stress.

The method proposed by Chen and Poulos (1993, 1994) may be applicable for a single pile and piles in a row (or two rows). Chen and Poulos (1994) concluded that for piles in a row subjected to lateral soil movement, the ultimate soil pressure

increases slightly with decreasing clear distance between piles. This is provided that the clear distance is less than about four times the pile width (or diameter). Piles in a row develop a higher soil pressure than piles in two parallel rows.

More recently Poulos and Chen (1997) presented a theoretical procedure to analyse the lateral response of vertically installed piles subjected to lateral soil movement. Such soil movements were estimated by using the FEM and the lateral pile response was computed via a simplified BEM. The latter was idealised as an elastic beam and the soil as an elastic continuum. They concluded that accurate assessments of lateral soil movement, soil Young's modulus and limiting pile-soil contact pressure (which is related to the group effect) are vital parameters for prediction of the lateral pile response.

Sommer (1977, 1979) stabilised a creeping clay slope with movement rate of 1cm/month using a row of 3m diameter thick reinforced concrete piers (piles). Sommer stated that a sliding slope could be stabilised, increasing its safety factor by only a few percent.

Hsiung and Chen (1997) presented a simplified method for the analysis and design of long piles under lateral load in uniform clays. The method is based on the concept of the coefficient of Subgrade Reaction (*SR*) with consideration of the soil properties being extended to include elasto-plastic behaviour. Using the FEM, bending moments and deflections were found under the lateral load.

Briaud (1997) presented a method to solve a laterally loaded pile by assuming that the pile is an elastic member and the soil is represented by a series of non-linear horizontal springs. Assuming soil behaviour to be modelled by the Winkler theory, pile bending moment, shear force and deflection profiles were obtained for an infinitely long, and for a rigid short pile.

Goh et al. (1997) presented an FEM to analyse the response of single piles to lateral soil movements. The flexural bending of the pile is modelled by beam elements and the pile-soil interaction is modelled by hyperbolic soil springs which are represented by a mathematical function.

Ashour et al. (1998) presented a strain wedge method based upon dividing the soil profile and the loaded pile into sublayers and segments of constant thickness. Each layer of soil is considered to behave as a uniform soil and have individually defined properties. They stated that the "beam on elastic foundation theory" provides an efficient solution for the problem of a laterally loaded pile. The accuracy of such a solution depends on the characterisation of the interaction between the pile and the surrounding soil. They indicated that modulus of *SR* which depends on pile properties (width, shape, bending stiffness, and pile head conditions) as well as soil properties, provides a reasonable set of calculation parameters for a wide range of laterally loaded piles.

8.3 Subgrade Reaction approach

The Subgrade Reaction (*SR*) approach, which is attributable to Winkler in 1867 (Hassiotis and Chameau, 1984), characterises the soil as a series of springs along the length of the pile. As shown in Fig. 8.4, the pile is regarded as being supported laterally by a series of independently acting mechanical springs (Broms, 1972). The spring stiffness, K_s, which gives the load per unit length of pile induced for unit lateral deflection of the pile, is generally called the coefficient of Subgrade Reaction (Fleming et al., 1992).

It should be noted that the concept of a coefficient of *SR* does not take into account the continuity of the soil mass (Broms, 1972). This well-known approach to soil structure interaction certainly does not represent the true soil behaviour since the displacements at a point are influenced by stresses and forces at other points within the soil (Jamiolkowski and Garassino, 1977, Hassiotis and Chameau, 1984).

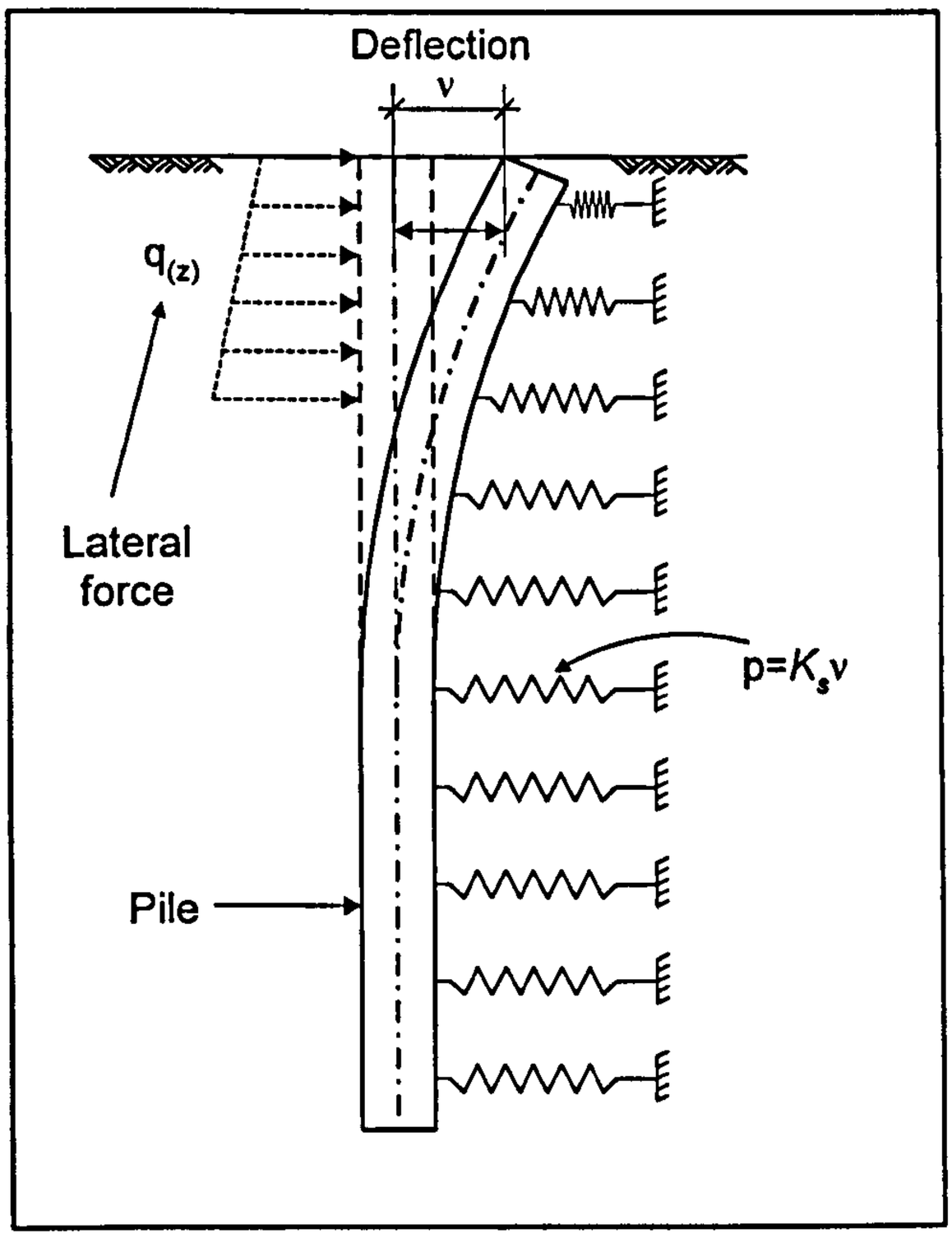

Figure 8.4 Subgrade Reaction model of soil around pile.

Despite the above limitations, Jamiolkowski and Garassino (1977) indicate that, the *SR* method is likely to remain a widely used design approach owing to:

- Analytical simplicity.
- Large world-wide experience gained in *SR* method applications, supported by many well-documented case records.
- Ability to carry out relatively simple and efficient calculations, by taking into account factors such as variations of soil stiffness with depth and layering of the soil profile.

8.3.1 Coefficient of Subgrade Reaction for soils

In this research, the theory of Subgrade Reaction approach is used to model the pile-soil interaction below the critical failure surface, see Fig. 8.5. Evaluation of the coefficient of the *SR*, K_s, is essential to estimate the pile displacements, bending moments and shear forces. It is the preferred approach owing to its ease of use and to the substantial savings in computer computation time (Bowles, 1996).

The theories of Subgrade Reaction are based on the simplifying assumptions (Terzaghi, 1955):

- The coefficient of Subgrade Reaction at every point is independent of the contact pressure.
- It has a constant value at every point along the contact face.

Both of these assumptions are approximations of the real conditions (Terzaghi, 1955, Hassiotis and Chameau, 1984).

The coefficient of Subgrade Reaction may be determined empirically by one of the following methods for laterally loaded piles (Jamiolkowski and Garassino, 1977):

- Full scale lateral loading test.
- In situ tests such as plate loading test, pressure-meter and flat dilato-meter tests.
- Empirical correlation with other soil properties.

According to Hassiotis and Chameau (1984) and Smith and Pole (1980), the above three methods to estimate the modulus of *SR* may provide satisfactory results since the pile deflections, bending moments and shear forces will not be very sensitive to small changes in soil modulus.

Terzaghi (1955) discussed the use of plate loading tests. In his paper, Terzaghi assumed that the coefficient of horizontal reaction for a vertically placed pile in sand is a function of the depth below the surface, *z*, the width of pile, *b*, the effective unit weight of the sand, γ', and the relative density of the sand. At any depth *z* below the surface, the modulus of elasticity of sand, E_s, is given by;

$$E_s = \gamma' z A, \qquad 8.1$$

wherein A is a coefficient which depends only on the density of the sand, Table 8.1. The values suggested by Terzaghi have been converted into S.I. (Systeme International d'Units) units and rounded off, see Tables 8.1 and 8.2. Terzaghi also gave the following relationship between K_s and E_s;

$$K_s = \frac{E_s}{1.35b}. \qquad 8.2$$

Substitution of Eqn. [8.1] into the Eqn. [8.2] results in;

$$K_s = \frac{\gamma' z A}{1.35 b}. \qquad 8.3$$

For a pile embedded in stiff clay, Terzaghi recommended a value of K_s which is independent of depth;

$$K_s = \frac{K_{s1}}{1.5 b}. \qquad 8.4$$

Relative density of sand	Loose	Medium	Dense
Range of values of A	35320-106000	106000-353170	353170-706340
Adopted values of A	70635	211900	530000

Table 8.1 Values of coefficient A to calculate K_s (kN/m^3) for a pile embedded in moist or submerged sand (Terzaghi, 1955).

Consistency of soil	Stiff clay	Very stiff clay	Hard clay
Values of q_u (kN/m^2)*	107-215	215-430	>430
Range for K_{s1} (square plates)	17660-35320	35320-70635	>70635
Proposed values (square plates)	26500	53000	106000

Table 8.2 Values of K_{s1} (kN/m^3) for a square plate (0.305m x 0.305m) resting on precompressed clay (Terzaghi, 1955) [Where q_u is unconfined compressive strength of the clay].

To estimate K_s values, one may also use Table 8.3, where q_a is the allowable bearing capacity.

Soil	K_s (kN/m^3)
Loose sand	4800-16 000
Medium dense sand	9600-80 000
Dense sand	64 000-128 000
Clayey medium dense sand	32 000-80 000
Silty medium dense sand	24 000-48 000
Clayey soil:	
qa ≤ 200 kPa	12 000-24 000
200 < qa ≤ 800 kPa	24 000-48 000
qa > 800 kPa	>48 000

Table 8.3 Range of coefficient of Subgrade Reaction (Bowles, 1996).

8.3.2 Governing equations

A pile supported along its whole length by an elastic medium, and subjected to any type of horizontal loading system, deflects and orientates constantly, in response to the contact distributed forces within the confining medium. It is assumed that the intensity p of these forces is proportional to the lateral deflection ν of the pile (or beam), see Fig. 8.4;

$$p = K\nu \qquad 8.5$$

For a pile of width b, the elastic constant K is related to the coefficient of Subgrade Reaction K_s as given by;

$$K = b\,K_s. \tag{8.6}$$

In order to design a pile to resist lateral soil movement, the following variations along the pile axis are needed; (a) deflection, ν, (b) bending moment, BM and, (c) shear force, SF. In many problems, the well-known closed form solution of the beam equation is used. The basic differential equation governing the pile displacements, ν, is obtained by satisfying the equilibrium of an infinitesimal element and is given;

$$K_s\nu + EI\frac{d^4\nu}{dz^4} = q(z), \tag{8.7}$$

where EI is the pile (or beam) flexural rigidity and $q(z)$ is the lateral load variation with depth, z.

8.4 Pile stability analysis

For the pile stability analysis, an appropriate analytical method may be applied, considering that piles are subjected to the lateral loads, $q(z)$, through the soil portion above the critical slip surface, see Fig. 8.5. The laterally distributed force acting on a pile may also be obtained by using either the theory of visco-plastic flow (details in Chapter 6), or the theory of plastic deformation (given in Chapter 7).

Equation [8.7] which is developed into two parts, considering the pile segments above and below the critical slip surface, is re-written to be represented in differential operator form;

$$\left(K_s + EI \frac{d^4}{dz^4} \right) \nu = q(z) \qquad 8.8$$

where $K_s = 0$, and $q(z) \neq 0$, for $0 \leq z \leq H$, and

$K_s \neq 0$ and $q(z) = 0$ when $H < z < H + L$ (see Fig. 8.5).

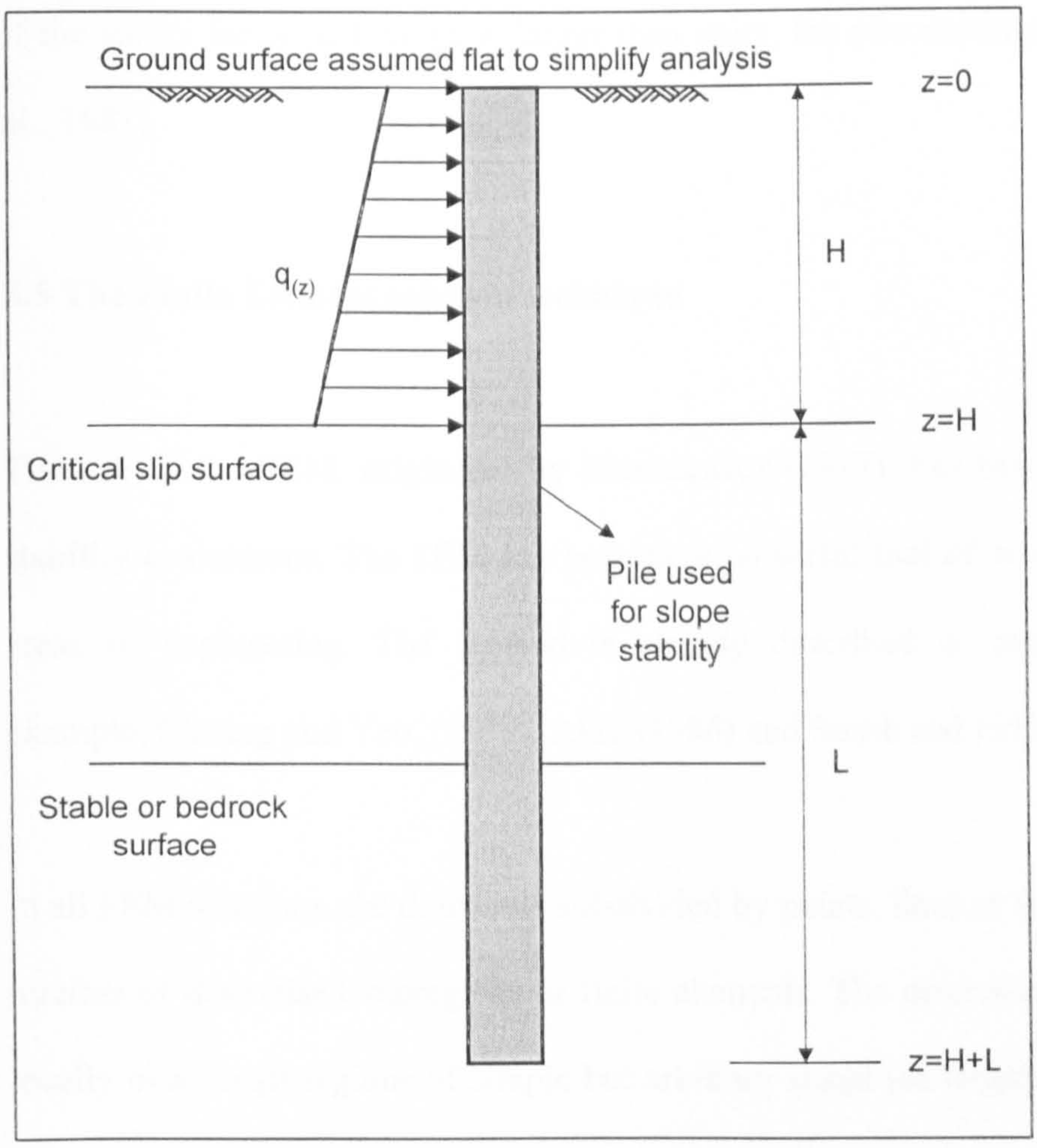

Figure 8.5 Stabilising pile embedded in bedrock (Hassiotis et al., 1997).

The distribution of deflection, shear force and bending moment, (the calculation details are given in section 8.5), may be evaluated using the above equation. The *FOS* (for pile) due to bending moments is considerably smaller than the corresponding *FOS* for shearing forces for piles (Ito et al., 1979). Therefore, the *FOS* $(F_s)_{pile}$ for the pile stability, may be obtained by comparing the allowable bending stress $(\sigma_{allow.})$ with the corresponding maximum induced value $(\sigma_{max.})$. This is represented by;

$$(F_s)_{pile} = \frac{\sigma_{allow.}}{\sigma_{max.}}. \qquad 8.9$$

If the safety factor in Eqn. [8.9] larger than unity, the pile stability is assured (Ito et al., 1981).

8.5 The Finite Element solution technique

The use of the FEM, originated by Zienkiewicz (1977), has been extended to pile stability evaluations. The FEM has become a powerful tool of analysis in almost all areas of engineering. The method is already described in many textbooks, for example, Cheung and Yeo, (1979), Akin (1986) and Smith and Griffiths (1988).

In all FEM solutions, the domain is subdivided by points, lines or surfaces into a finite number of discretised subregions or finite elements. The discretisation is carried out locally over small regions of simple but arbitrary shape (or length). This results in a matrix representation, relating the actions at specified points located at the extremities

of the elements (the nodes) to the response (displacements) at these same points (Smith and Griffiths, 1988).

8.5.1 Beam element

Consider a beam member on an elastic foundation, shown in Fig. 8.6; a continuous elastic support has been placed beneath the basic beam member. The end nodes are subjected to shear forces and moments which result in displacements and rotations, see Fig. 8.6. Therefore, each node has two degrees of freedom (dof).

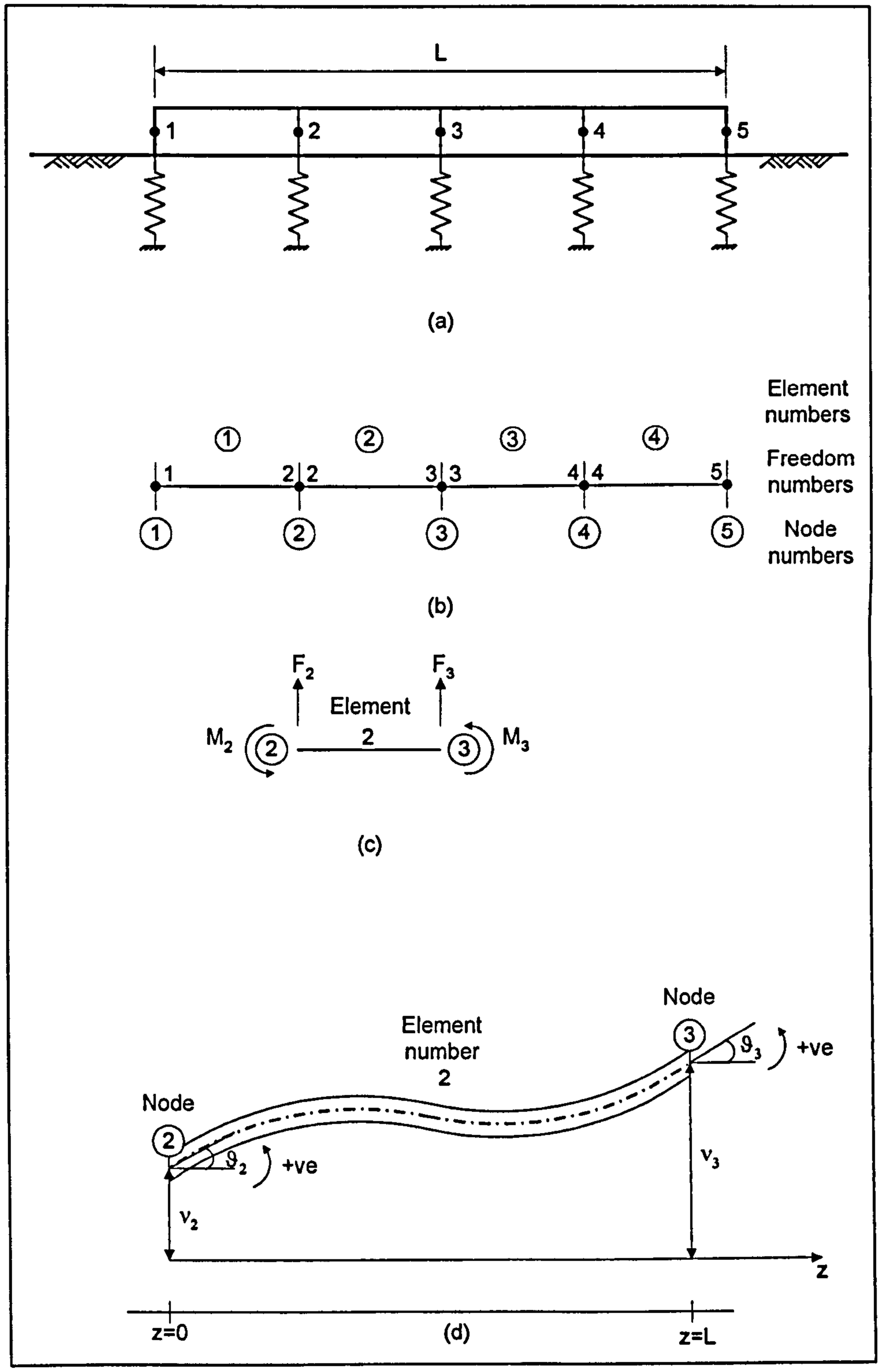

Figure 8.6 Developing the element: (a) Actual structure and the discritised model of Finite Elements; (b) Node, freedom and element numbers; (c) Number of actions at each node and sign conventions for each element; (d) Boundary conditions for a single element.

8.5.2 Conventional formulation

The following is a standard method deployed for beam element formulation, which gives a maximum cubic variation for the lateral displacement response, represented by;

$$\nu(z) = A_0 + A_1 z + A_2 z^2 + A_3 z^3 . \qquad 8.10$$

$$\vartheta(z) = 0 + A_1 1 + 2A_2 z + 3A_3 z^2 . \qquad 8.11$$

$$BM(z) = EI(0 + 0 + 2A_2 + 6A_3 z). \qquad 8.12$$

$$SF(z) = EI(0 + 0 + 0 + 6A_3). \qquad 8.13$$

where ν is deflection, ϑ the rotation, BM is the bending moment, SF is the shear force and A_0, A_1, A_2 and A_3 are the presently unknown beam response constants. These relationships are extended to derive the following stiffness matrix for an elastic uniform element in the z, y plane.

$$\begin{Bmatrix} \nu_1 \\ \vartheta_1 \\ \nu_2 \\ \vartheta_2 \end{Bmatrix} = \begin{bmatrix} 1 & 0 & 0 & 0 \\ 0 & 1 & 0 & 0 \\ 1 & L & L^2 & L^3 \\ 0 & 1 & 2L & 3L^2 \end{bmatrix} \begin{Bmatrix} A_0 \\ A_1 \\ A_2 \\ A_3 \end{Bmatrix}, \qquad 8.14$$

where rows 1 and 3 are evaluated at $z = 0$ and the rest at $z = L$.

The stiffness matrix of a beam member is then written as;

$$[K] = EI \begin{bmatrix} 12/L^3 & 6/L^2 & -12/L^3 & 6/L^2 \\ 6/L^2 & 4/L & -6/L^2 & 2/L \\ -12/L^3 & -6/L^2 & 12/L^3 & -6/L^2 \\ 6/L^2 & 2/L & -6/L^2 & 4/L \end{bmatrix} \begin{Bmatrix} \nu_1 \\ \vartheta_1 \\ \nu_2 \\ \vartheta_2 \end{Bmatrix} \qquad 8.15$$

where rows and columns of the stiffnes matrix [*K*] refer to the dof appearing sequentially (i.e. $\nu_1, \vartheta_1, \nu_2$ and ϑ_2).

8.5.3 Boundary conditions

At the pile head, $z = 0$ shown in Fig. 8.5, the boundary conditions are dependent on the type of restraint used. One of the following four boundary conditions should be modelled to restrain the pile head driven into the slope:

- Free head; at the pile head, deflection and rotation are not zero (i.e., $\nu, \vartheta \neq 0$).
- Unrotated head; at the pile head, deflection is not zero but rotation is zero (i.e., $\nu \neq 0\ ,\ \vartheta = 0$).
- Hinged head; at the pile head, deflection is zero but rotation is not zero (i.e., $\nu = 0\ ,\ \vartheta \neq 0$).
- Fixed head; at the pile head, deflection and rotation are set to zero (i.e., $\nu, \vartheta = 0$).

8.5.4 Generation of bending moment, shear force, displacement and rotation variations

This is a complex activity where a sign convention has to be observed rigidly. The variation of displacements and rotations are not difficult to estimate since they could be interpolated from Eqns. [8.10] and [8.11].

Calculations of bending moments and shear forces are however non-standard since the use of constitutional relationship can only provide a linear and constant response respectively.

The present work may be regarded as innovative, since it side-steps the linear and constant responses above, providing genuine curvilinear variations both for bending moments and shear forces (Delpak, 1998).

8.5.5 The Subgrade Reaction matrix

A similar formulation is used to derive the matrix relating to the *SR* of the soil in contact with an elastic uniform element. Derivation of the matrix is in a standard form by extending the mass matrix formulation to the *SR*, and is due to Smith and Griffiths (1988). The mass matrix may be written in a modified form as;

$$[SR]=\frac{K_s L^2}{420}\begin{bmatrix} 156/L & 22 & 54/L & -13 \\ 22 & 4/L & 13 & -3L \\ 54/L & 13 & 156/L & -22 \\ -13 & -3L & -22 & 4L \end{bmatrix}\begin{Bmatrix} \nu_1 \\ \vartheta_1 \\ \nu_2 \\ \vartheta_2 \end{Bmatrix}, \qquad 8.16$$

where [*SR*] is Subgrade Reaction matrix, and K_s is the coefficient of *SR*.

According to Bowles (1996), the FEM is the most efficient means for solving a beam on elastic foundation type problem based on Eqn. [8.3] or Eqn. [8.4] but requires a computer. The FEM is more versatile than the Finite Difference Method (FDM), since for the former, one may write an equation modelled for a typical element and use it for each element within the beam (or pile). For the FDM all of the elements must be of the same length and cross section. Different equations are required for the end nodes as opposed to the intermediate nodes.

Using the beam element requires two degrees of freedom per node, but the matrix is always symmetrical and can be banded for economy of solution. Another advantage of the FEM over the FDM is that the former has both node translation and rotation, whereas the FDM only possesses the translational degrees of freedom.

8.6 Conclusions

The numerical example indicating the versatility of the FEM formulation, applied to piles, cannot be divorced from studying the pile performance in actual case studies. These studies are carried out in Chapter 9 where it is believed that relative merits of formulation will be demonstrated.

CHAPTER 9: PILE STABILISATION OF SLOPES, SUSCEPTIBLE TO FAILURE RISK

9.1 Introduction

Failures of mass movements often result in extensive property damage and loss of human life. It is recognised that ensuring the stability of both natural and man-made slopes continues to be a fundamental issue in geotechnical engineering. There is no universally accepted method for the prevention or correction of landslides. Each slide is unique and should be considered on the basis of unique inherent characteristics.

Stabilisation of a slope may depend on a number of factors e.g. (a) its geometry, (b) surface and groundwater conditions, (c) strength of materials, and (d) the reason for stabilisation (Leventhal and Mostyn, 1987). A number of techniques have been developed to stabilise slopes considering the above mentioned conditions. These techniques are:

1. Control of ground water conditions,
2. Alteration of slope geometry,
3. Retaining walls,
4. The use of geotextiles to reinforce the soil (slope),
5. Soil nailing,
6. Piling,
7. Vegetational control of shallow sliding,

8. Lightweight fills,

9. Lime/Cement/Bituminous stabilisation,

10. Thermal or electrochemical stabilisation.

Slope stabilisation methods generally reduce disturbing forces and/or increase resisting forces. Before the most appropriate method can be selected, the actual or potential causes of slope instability should be determined. Frequently, there are multiple contributing factors that cause or could cause a landslide or slope instability. Some type of slope stabilisation methods are given below (Abramson et al., 1996):

1. Unloading
    a) Excavation
        - Removal of the head of a slope
        - Removing all unstable or potentially unstable materials
        - Flattening of slopes
        - Benching of slopes
    b) Lightweight Fill
2. Buttressing
    a) Soil and rock fill
    b) Counterberms
    c) Shear keys
    d) Mechanically stabilised embankments
    e) Pneusol (tiresoil)
3. Drainage
    a) Surface drainage

b) Subsurface drainage

- Subsurface drainage blankets
- Trenches
- Cut-off drains
- Horizontal drains
- Relief wells
- Drainage tunnels or galleries

4. Reinforcement

a) Soil nailing

b) Stone columns

c) Reticulated micropiles

d) Geosynthetically reinforced slopes

5. Retaining walls

a) Gravity and cantilever retaining walls

b) Driven piles

c) Drilled shaft walls

d) Tieback walls

6. Vegetation

7. Surface slope protection

a) Shotcrete

b) Chunam plaster

c) Masonry

d) Rip-rap

8. Soil hardening

a) Compacted soil-cement fill

b) Electro-osmosis

c) Thermal treatment

d) Grouting

e) Lime injection

f) Preconsolidation

9.2 Design methods for slope stabilisation by piles

The above methods may be used as possible countermeasures to prevent landslides. Included amongst these are piling and soil nailing methods [Ito and Matsui (1977), Poulos (1995) and Soil Nailing Recommendations (1991)].

During the past two decades soil nailing and piling have become two of the more important innovative techniques for slope stabilisation (Poulos, 1995). The interaction behaviour between pile and soil is a complicated phenomenon due to its three-dimensional nature and can be influenced by many factors, such as the characteristics of deformation and the strength parameters of both pile and soil. In addition, movement of the failure mass (landslide) involves a complicated mechanism. It is recognised that pile design for slope stabilisation is too simplified for the complicated event. Nevertheless, there is no precise design method for the stabilising piles so as to utilise effectively the pile effect in slope stabilisation. In fact, many slopes failed or continuously moved even after the installation of stabilising piles (Ito et al., 1982).

The present work does not dwell on merits or demerits of piling or soil nailing. The candidate and the supervision team have devised a method by which calculations are facilitated and the influence of stabilisation agencies brought into account. These are discussed as follows:

9.2.1 Short pile stabilisation solution to the slope instability problem

A short pile model is analysed here in terms of a critical slip surface which goes under the inserted pile intended for instability remediation. When a failure surface is relatively deep and the length of the pile in the stable soil is comparatively shallow, this type of failure is expected to occur. The implementation procedure of this failure is explained below.

9.2.1.1 Computer codification

Among the limit equilibrium methods, it is the simplified form of the Bishop's method, which gives an acceptable factor of safety and is also relatively simple to use. For these reasons it was selected as the most suitable preliminary method of analysis. Hence, a program was written by the candidate specifically to enable a stabilisation technique to be applied to the analysis of a slope. The codification of this method was undertaken based on recommendations from Poulos and Davis (1980) and Poulos (1995). It also serves as a preliminary step before computer coding for long piles.

Mechanical stabilisation instruments such as piles and nails are grouped together and given a generalised term "constraints" which may act as boundary conditions to the failure geometry.

The values of the constraints are given using the *x-y* co-ordinate system. Any number of constraints can be input into the slope geometry but for simplicity only one constraint is considered in this example, see Fig. 9.1.

Problem 1, in Chapter 4, was re-examined by using the above solution suggested by Poulos and Davis (1980) and Poulos (1995). This utilises one piles with different locations and directions, see Fig. 9.3. The values of *FOS* using Bishop simplified method are given in Table 9.1. The *FOS* can be increased by controlling the free slope surface and imposing the constraints at any point on the slope geometry, Fig 9.2. In reality, this does not correspond to an actual stabilised *FOS*, since the pile should be designed to be long enough to prevent failure.

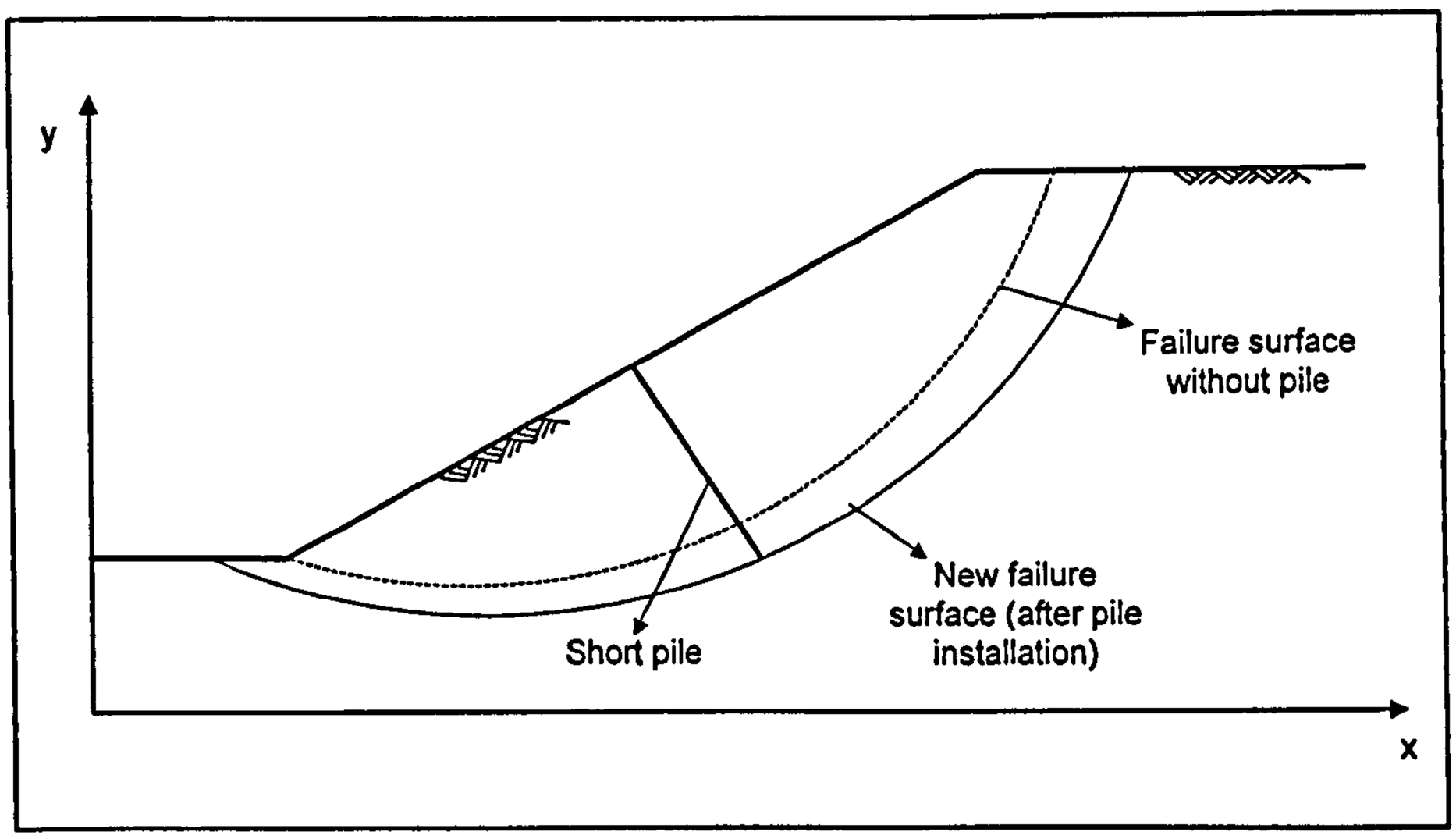

Figure 9.1 A slope with constraint and possible slip surface.

Unstabilised	F.O.S.: 1.039

(i)

Stabilised *FOS* using 1 Pile	(a)	(b)	(c)	(d)	(e)
	1.093	1.126	1.138	1.165	1.248

(ii) - [see Fig. 9.2 (a)-(e)]

Table 9.1 The influence of stabilisation interpreted as "Slope Engineering" (using the Bishop simplified method).

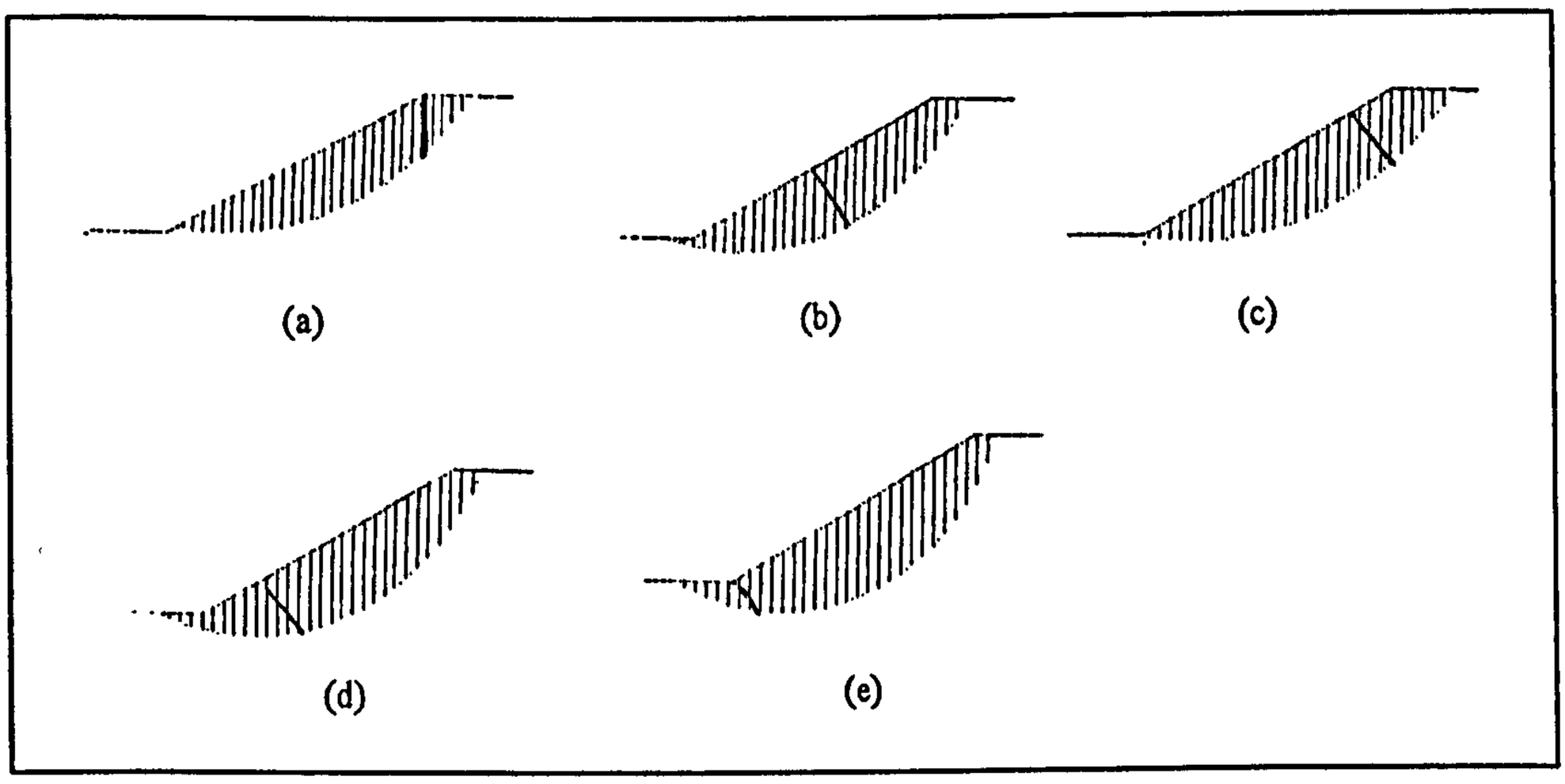

Figure 9.2 Using short piles to stabilise a slope.

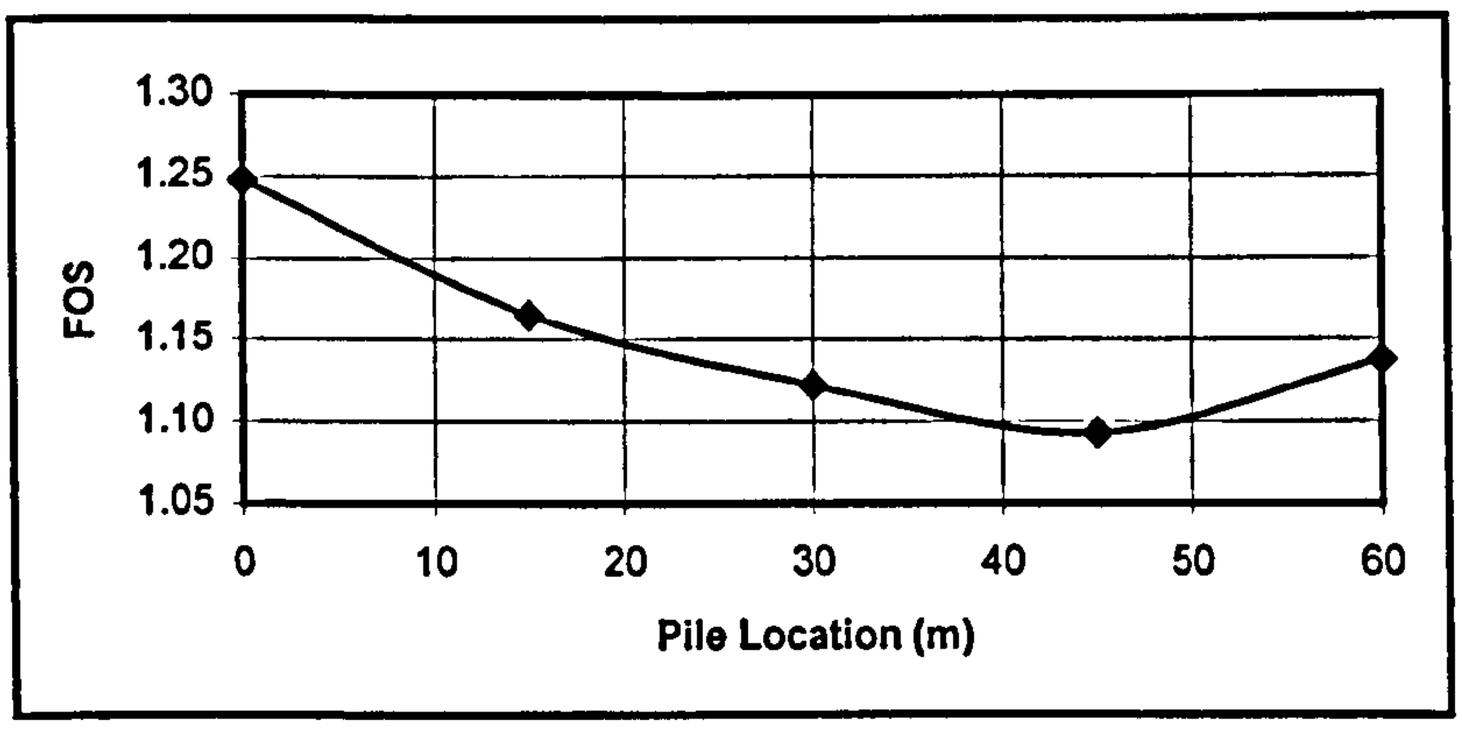

Figure 9.3 Pile locations and corresponding *FOS* values.

9.2.2 Long pile stabilisation application to the slope instability problem

For the slope stability problem containing piles in a row, two separate analyses have been carried out in terms of slope and pile stability.

The slope instability can be analysed by dividing resisting moments/forces (either together or separately, since it depends on method of analysis used, see Table 4.1) and disturbing moments/forces acting on the soil mass DBCAD, shown in Fig. 9.4. Due to pile installation, the extra resisting force provided by piles at the plane AB is added to resisting moments/forces within the parameters of normal slope stability calculations.

Pile stability may be analysed using forces acting on a single pile at the plane AB, see Fig. 9.4. This force is used as an extra resisting force for the slope stability but reactively it is also used as a design force to calculate pile integrity and stability.

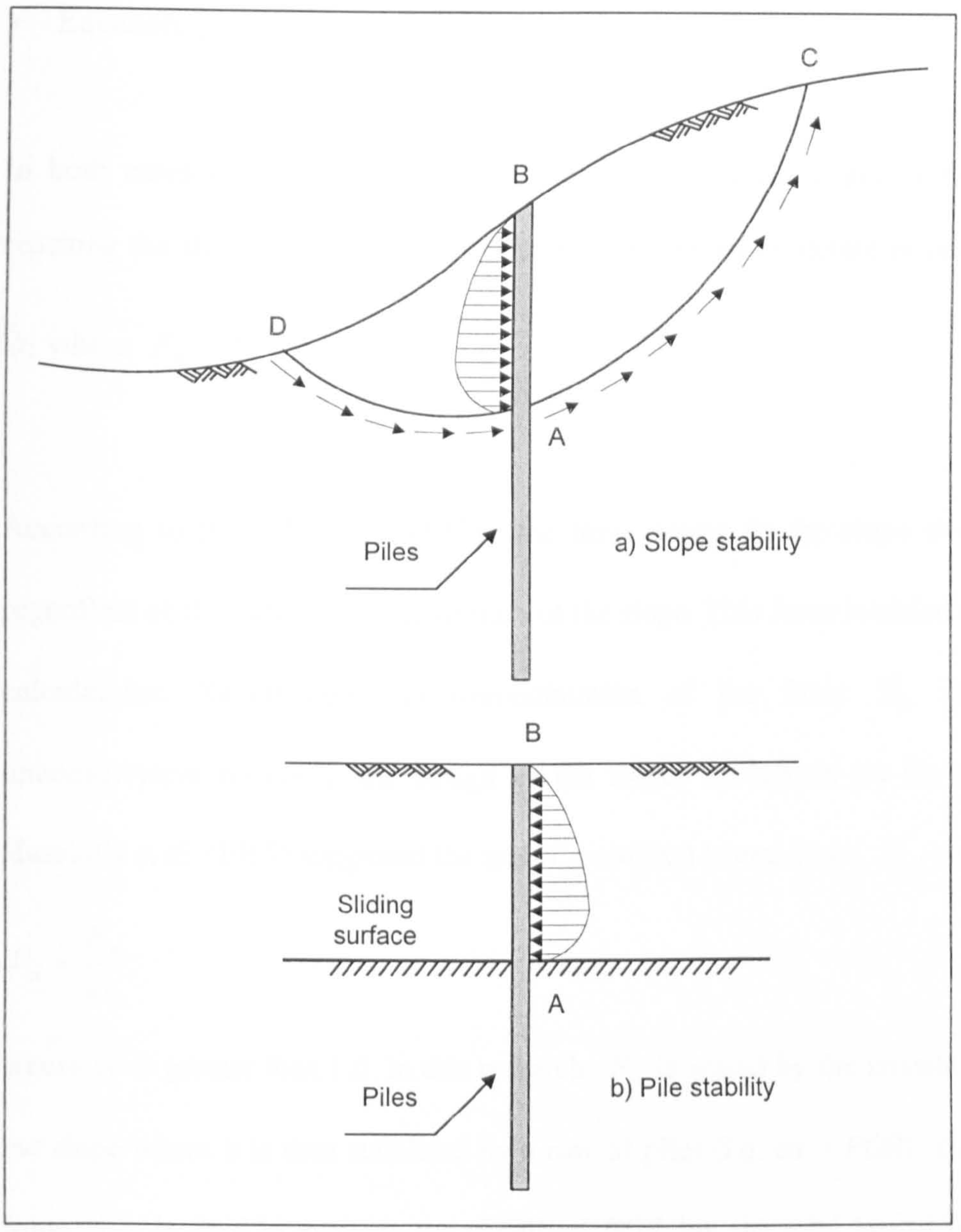

Figure 9.4 Slope stability analysis containing piles in a row (Ito and Matsui, 1977).

When a row of piles is installed into the slope, the *FOS* changes due to the additional resisting force, F_p, provided by the piles. To evaluate this force per unit width of the failure mass, the following options are used;

- Equation [7.1], dealing with the plastic deformation, or

- Equation. [7.9], in terms of visco-plastic flow.

In both cases the total force may be integrated along the depth of the pile (until reaching the slip surface). Then, the result, p, is divided by centre to centre distance, D_1 where $F_p = \frac{p}{D_1}$.

According to Ito and Matsui (1975), the force acting on the slope is equal to F_p regardless of the state of the equilibrium of the slope. This force is added into the *FOS* calculations. Nevertheless, an overestimation of the force F_p may lead to unconservative results in the design of the slope. To remain on the safe margin, Hassiotis et al. (1997) suggested the use of mobilised lateral force, F_m, so that,

$$F_m = \frac{F_p}{co},$$

where *co* is greater than 1.0. In this research, F_p is scaled by the unstabilised *FOS* of the slope where it is then stabilised by a row of piles (i.e. *co* = *FOS*). This mobilised force, F_m, is used to evaluate the stabilised *FOS*, but the total lateral force per unit length, p, is still used to design the piles.

Two distinct methods of lateral load estimations above were used to evaluate lateral loads on the piles in a row. With the piles in place and with the restraining forces of the piles against the sliding soil mass (Figs. 9.5 and 9.6), a second analysis was performed to find the new stabilised *FOS* against sliding without changing the failure surface. The stablised *FOS* values are give in Tables 9.3 and 9.5. Case studies were

examined by two different mass divisions namely method of slices (MOS) and Gauss quadrature (GQ).

The parameters are used as follows;

- *ns* (number of slices): 30 (only applicable for present research),
- *ng* (number of Gauss points): 9 (only applicable for the present research).

9.3 Case studies

9.3.1 Problem 1

This particular problem has been examined by Reese et al. (1992) shown in Fig. 9.5. The slope exists along the bank of a river where sudden drawdown is possible. According to the above authors, slides had been observed along the river at numerous places and it was found necessary to stabilise the slope to allow a bridge to be constructed. Using the Spencer's method, they analysed the sudden drawdown case taking the undrained analysis and the *FOS* was given to be 1.060. They stated that the value is in reasonable agreement with observations.

Reese et al. (1992) used drilled shafts which were 0.915 m in diameter and penetrated below the sliding surface. The tops of the drilled shafts were restrained with anchors in stable soil.

The example slope, shown in Fig. 9.5, was reanalysed by the candidate and available comparisons were made in Tables 9.2 and 9.3 in terms of unstabilised and stabilised *FOS* values. Three different pile locations were examined to find out the most suitable place(s) to obtain higher stabilised *FOS* values.

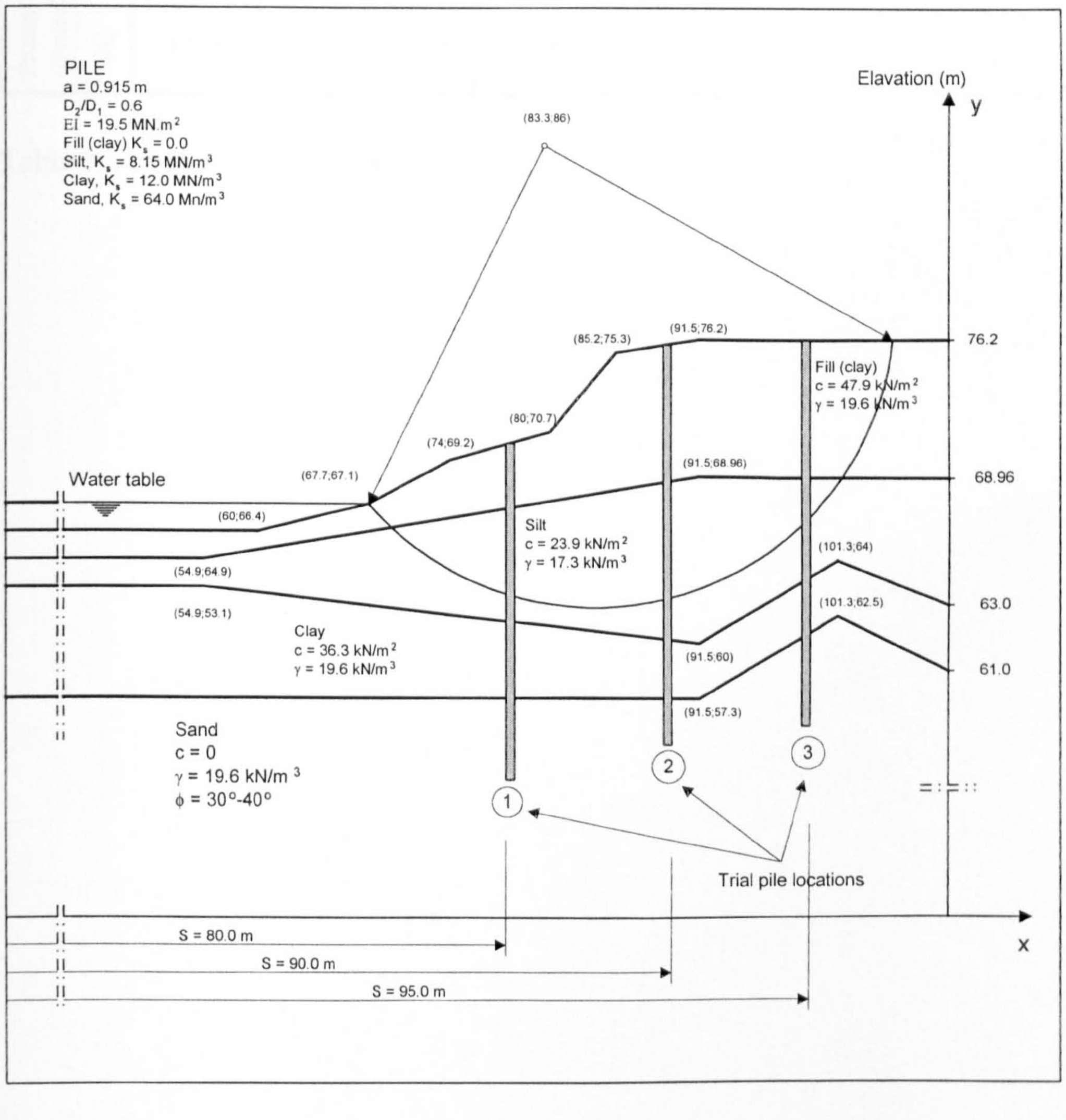

Figure 9.5 Stabilised failure surface by a row of piles (Reese et al., 1992).

Programs		Methods of analysis for *FOS* calculations (UNSTABILISED)							
		Fellenius	Bishop simple.	Janbu simple.	Janbu General.	Morg. & Price	Spencer	Sarma (K_c=0)	Fredlund & Krahn (GLE)
Reese et al.		-	-	-	-	-	1.060	-	-
SLOPE program		1.073	1.073	1.095	1.073	*	1.073	*	*
Present research	MOS	1.101	1.101	1.112	1.122	1.126	1.110	1.099	1.110
	GQ	1.085	1.085	1.110	1.120	-	1.110	1.100	1.110

Table 9.2 Unstabilised *FOS* values for problem 1.

Table 9.3 Stabilised *FOS* values by using two different lateral load estimations.

Lateral load estimations	Methods of mass division	Pile locations	Methods of analysis for (*FOS*) calculations (STABILISED)							
			Fellenius	Bishop simpli.	Janbu simpli	Janbu general.	Morg. & Price	Spencer	Sarma	Fredlund & Krahn (GLE)
Plastic deformation	Method of slices	1	1.397	1.397	1.348	1.428	1.409	1.401	1.403	1.401
		2	1.680	1.680	1.601	1.682	1.671	1.680	1.665	1.680
		3	1.571	1.571	1.510	1.582	1.585	1.575	1.569	1.575
	Gauss quadrature	1	1.385	1.385	1.351	1.421	-	1.398	1.408	1.398
		2	1.682	1.682	1.605	1.685	-	1.680	1.669	1.680
		3	1.575	1.575	1.521	1.584	-	1.580	1.577	1.580
Visco-plastic flow	Method of slices	1	1.401	1.405	1.354	1.434	1.441	1.409	1.432	1.409
		2	1.560	1.560	1.521	1.573	1.561	1.560	1.558	1.560
		3	1.450	1.450	1.405	1.469	1.465	1.453	1.451	1.453
	Gauss quadrature	1	1.410	1.410	1.351	1.429	-	1.412	1.438	1.412
		2	1.558	1.558	1.525	1.568	-	1.563	1.545	1.563
		3	1.453	1.453	1.401	1.472	-	1.455	1.442	1.455
Reese et al.			-	-	-	-	-	1.820	-	-

As can be seen in the previous tables, significant improvements were obtained by using a row of piles. Pile location 2 gives higher *FOS* due to the deep failure surface for both categories of mass divisions. It is thought that the *FOS* differences between Reese et al. (1992) and the present research are due to different lateral load estimations and failure surface assumptions which were impossible to make accurately without all the required data. In addition to that, Reese et al. (1992) used two rows of piles to stabilise the slope but the present research used only one row of piles.

9.3.2 Problem 2

This simple slope, reported by Hassiotis et al. (1997), has a height of 13.7 m, a slope angle of 30°, and is made of homogeneous material with a friction angle $\phi = 10°$, cohesion $c = 23.94$ kN/m^2, and unit weight $\gamma = 19.63$ kN/m^3, see Fig. 9.6. Since a *FOS* of 1.080 is inadequate, it is recommended that the slope be reinforced with a row of piles (Hassiotis et al., 1997).

Tables 9.3 and 9.4 include the unstabilised and stabilised *FOS* values respectively which are given in terms of the different programs available.

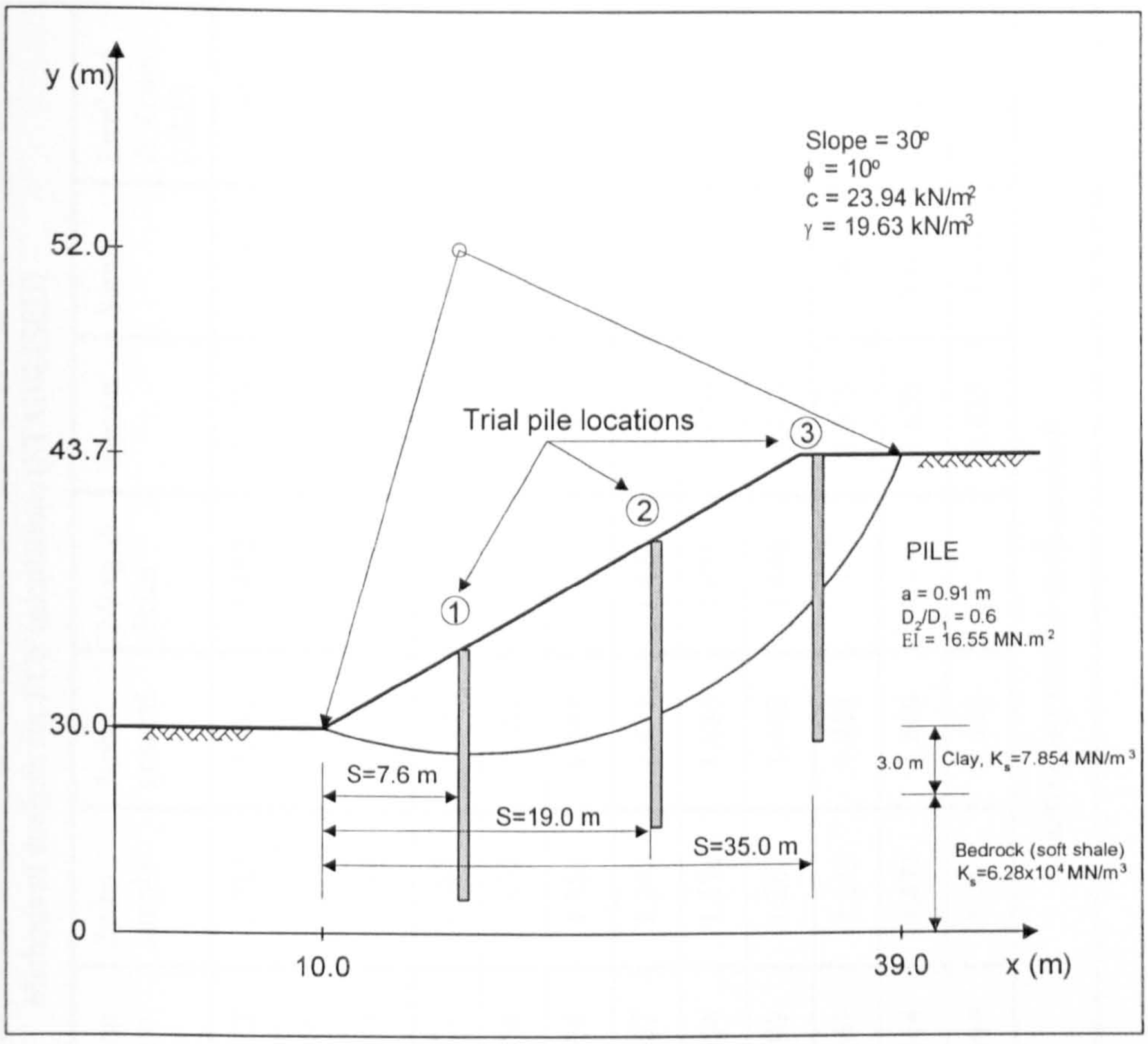

Figure 9.6 Critical failure surface and pile row locations (Hassiotis et al., 1997).

Programs		Methods of analysis for *FOS* calculations (UNSTABILISED)							
		Fellenius	Bishop simple.	Janbu simple.	Janbu general.	Morg. & Price	Spencer	Sarma (K_c=0)	Fredlund & Krahn (GLE)
SLOPE program		1.063	1.119	1.1074	1.111	*	1.111	*	*
Present research	MOS	1.070	1.116	1.049	1.115	1.109	1.116	1.115	1.116
	GQ	1.075	1.117	1.065	1.112	-	1.117	1.112	1.117
Hassiotis et al.		1.082 (using friction circle method)							

Table 9.4 Unstabilised *FOS* values for problem 2.

Table 9.5 Stabilised *FOS* values by using two different lateral load estimations.

Lateral load estimations	Methods of mass division	Pile locations	Methods of analysis for *FOS* calculations (STABILISED)							
			Fellenius	Bishop simple.	Janbu simple	Janbu general.	Morg. & Price	Spencer	Sarma	Fredlund & Krahn (GLE)
Plastic deformation	Method of slices	1	1.357	1.422	1.285	1.463	1.452	1.450	1.445	1.450
		2	1.669	1.750	1.652	1.761	1.763	1.760	1.761	1.760
		3	1.445	1.514	1.356	1.547	1.535	1.529	1.524	1.529
	Gauss quadrature	1	1.357	1.422	1.285	1.463	-	1.450	1.445	1.450
		2	1.669	1.750	1.652	1.761	-	1.760	1.761	1.760
		3	1.445	1.514	1.356	1.547	-	1.529	1.524	1.529
Visco-plastic flow	Method of slices	1	1.307	1.367	1.242	1.413	1.421	1.415	1.403	1.415
		2	1.589	1.664	1.471	1.686	1.671	1.670	1.668	1.670
		3	1.335	1.399	1.267	1.442	1.446	1.425	1.437	1.425
	Gauss quadrature	1	1.307	1.367	1.242	1.413	-	1.415	1.403	1.415
		2	1.589	1.664	1.471	1.686	-	1.670	1.668	1.670
		3	1.335	1.399	1.267	1.442	-	1.425	1.437	1.425
Hassiotis et al.			1.820 (using friction circle method)							

For problem 2, significant improvement of *FOS* values were also obtained. The difference between Hassiotis et al. (1997) and present research in terms of stabilised *FOS* values is due to a slightly different approach. For the case of Hassiotis et al. (1997) the failure surface is changed due to the additional resisting force provided by the piles. For the case of the present research, once the most critical surface was obtained, extra resisting force provided by the piles was added into the *FOS* calculations and a second analysis was performed to obtain a stabilised *FOS* value without changing the failure surface.

As can be seen from the above tables, the present research gives a lower value for the *FOS* in terms of stabilised *FOS* than Hassiotis et al. (1997). The author has confidence in the improved but somewhat smaller *FOS* value, since it was determined through exhaustive analysis.

9.4 Design of laterally loaded piles

To design piles to resist lateral loads, the forms of deflection, bending moment and shear force along the pile axis are required. It is considered that the governing equation for the pile deflection can be split into two separate forms;

1 pile segments above the failure surface and

2 pile segments below the failure surface.

A Finite Element Method (FEM) is used to analyse the pile. The section, which is below the critical failure surface, is analysed as a beam on an elastic foundation.

Equation [8.8] is rewritten here for convenience again in differential operator notation;

$$\left(K_s + EI\frac{d^4}{dz^4}\right)\nu = q(z) \qquad 9.1$$

where $K_s = 0$, and $q(z) \neq 0$, for $0 \leq z \leq H$, and

$K_s \neq 0$ and $q(z) = 0$ when $H < z < H + L$ (see Fig. 8.5).

The following figures are based on the Hassiotis at al. (1997) case study in terms of deflections Fig. 9.7, bending moments Fig. 9.8 and shear forces Fig. 9.9 but were analysed using the author's FEM. Results were obtained using 20 elements and four different boundary conditions (i.e. free head, unrotated head, hinged head and fixed head).

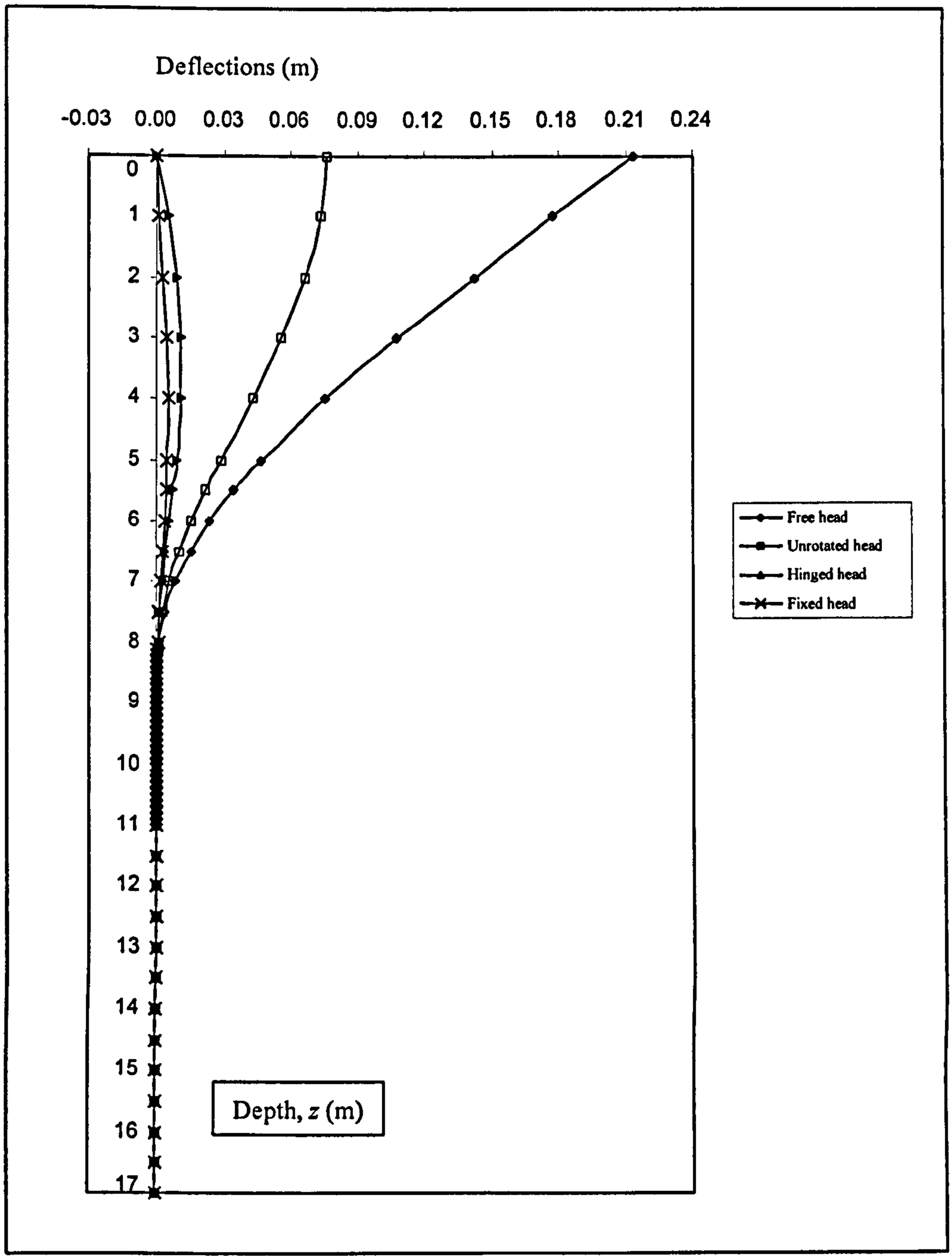

Figure 9.7 Deflection along pile with four different boundary conditions (m).

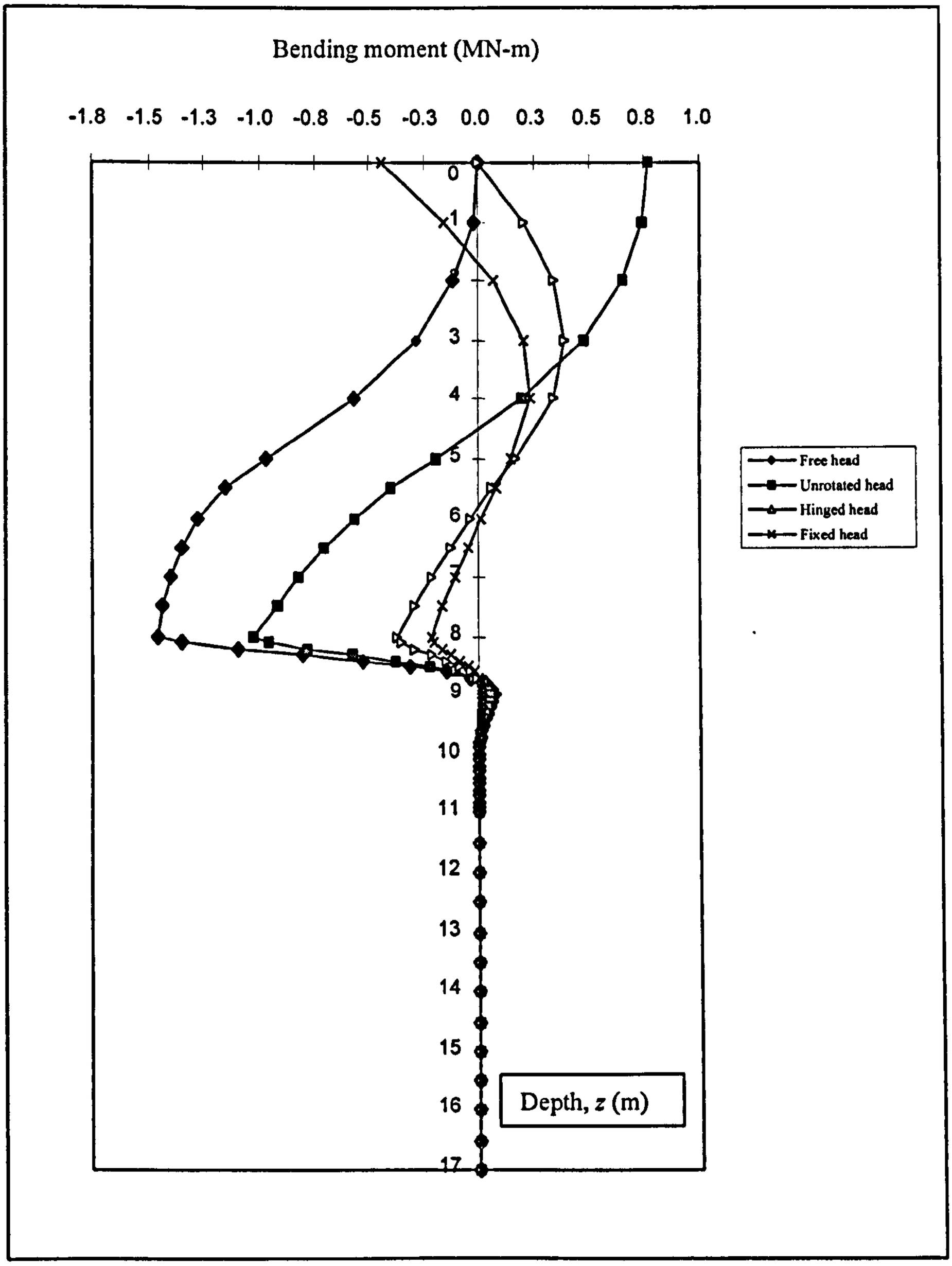

Figure 9.8 Bending moment along pile with four different boundary conditions.

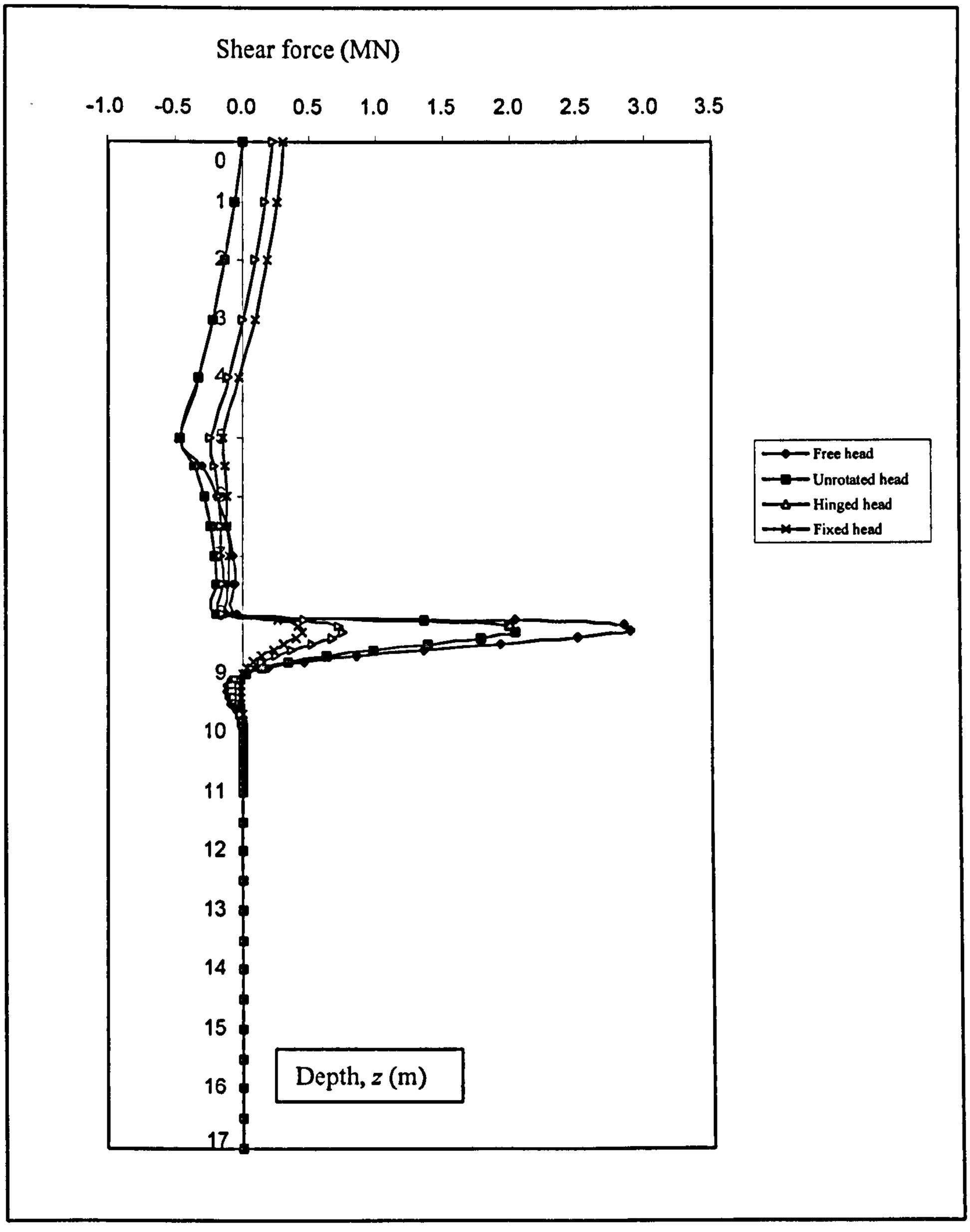

Figure 9.9 Shear force along pile with four different boundary conditions.

Pile stability was obtained by comparing bending stress ($\sigma_{allow.}$) with the maximum induced one. This is given in Eqn. [8.9]. The results in Table 9.6 are based on case studies by Reese et al. (1992) and Hassiotis et al. (1997) but using the Eqn. [8.9] as proposed by Ito et al. (1979).

Fixity conditions	Safety factor of pile stability in terms of Bending stress	
	Reese et al.	Hassiotis et al.
Free head	0.590	0.670
Unrotated head	0.655	0.740
Hinged head	1.620	1.670
Fixid head	1.470	1.520

Table 9.6 Safety factor of pile stabilities.

As can be seen in Table 9.6, a small deflection at the pile top gives a larger safety factor on the pile stability. It is suggested that the pile head should be restrained to utilise more effectively the beneficial pile stabilising influences.

9.5 Slope stabilisation and pile design

Slope stabilisation with piles requires two different stability analyses. These are slope and pile stabilities. Parameters that influence the slope stability and pile design are

analysed. The following procedures are recommended for an efficient design of the slope/pile combination:

- The degree of mobilisation of force F_m should be chosen. In this research $F_m = \frac{F_p}{FOS}$ is used to represent the reaction provided by the piles and applied to evaluate a stabilised *FOS*. This assumption will provide a conservative assessment of the stability of the reinforced slope (Hassiotis et al., 1997).
- The horizontal distance, S, between the toe of the slope and the piles in a row, may be determined by site circumstances.
- The *FOS* of the reinforced slope may be obtained as a function of the pile diameter, a, the centre to centre distance between the piles, D_l, and the location of the pile row.
- A required *FOS* should be pre-selected.
- In the earliest design stage, a pile diameter and centre to centre distance should be chosen based on experience. Then, these values are varied to obtain the desired *FOS* value.
- The magnitude of the force per unit length acting on the pile section above the failure surface, may be obtained either by the plastic deformation or proposed visco-plastic flow theories.
- The displacement, bending moment and shear force diagram along the length of the pile may be obtained assuming the pile to be a beam of infinite length embedded in an elastic foundation.
- Four different boundary conditions (i.e. free, unrotated, hinged and fixed head) are programmed to estimate the displacement, bending moment and shear force

profiles. The hinged and fixed head conditions give the least bending moment in the pile. Therefore, a restrained pile head is recommended. Furthermore, according to Ito and Matsui (1975), the lateral load acting on the pile due to plastically deforming ground may best be estimated by the theory of plastic deformation under the case of a restrained pile top (confirmed by data from site instrumentation).

- The stability of the pile may be obtained by dividing the allowable bending stress level with the maximum induced value.
- An optimum design may be obtained by studying the changes in the pile diameter, the centre to centre distance between two piles and the location of a pile row.
- The minimum length of the pile is determined at the point where bending moment and shear force become almost zero at the final analysis.

9.6 Conclusions

Slope stabilisation due to the presence of a row of piles has been investigated and the following observations are made:

i. Two distinct lateral load estimations; the theory of plastic deformation and proposed visco-plastic flow, are implemented in a series of computer codes to estimate the pressure on the piles in a row.

ii. Eight different methods of analysis were carried out to calculate *FOS* values of a slope reinforced by a row of piles.

iii. Relationships have been observed between stabilised *FOS* and the location of the pile row.

iv. A FEM computer program has been developed to evaluate the displacement, bending moment and shear force along the pile. The pile is analysed in two sections considering above and below the failure surface.

v. The pile top should be restrained (hinged or fixed) to minimise the displacement, bending moment and shear force.

vi. When bending moment and shear force have insignificant values, the minimum length of the pile is determined.

vii. The deeper the slip surface is, the higher are the stabilised *FOS* values that are calculated.

viii. When the frictional angle is zero, eight different methods of analyses give similar *FOS* values for both unstabilised and stabilised slopes.

ix. The values of stabilised *FOS* from the present research seem to be slightly lower than the reported values.

x. Stabilisation due to short piles has been examined for purposes of completeness of analysis. However, the present practical applications seem not to be significant. The analysis could provide design hints for soil nailing where the nails are rigid and short. Any penetration angle (to horizontal axis) could be specified within the present work.

The following observations are made in respect of the beam elements used as stabilising piles:

a) Innovative use is made of the conventional beam element subjected to lateral loads and Subgrade Reaction within pile stability analysis.

b) Variations of deflections, bending moments and shear forces were obtained using 20 elements. Lee et al. (1991) analysed the pile stability by the Boundary Element method using 60 equal elements.

c) The present solution does not require an iterative sequence.

CHAPTER 10: CONCLUSIONS AND RECOMMENDATIONS

10.1 Conclusions and recommendations

This research has been focused to produce a comprehensive survey of classical and modern stability determination methods under a single (but broad) analytical system. The computer program is capable of calculating the factors of safety of natural slopes as well as assessing various solutions to enhance slope stability.

The first phase of this research involved a thorough investigation of the differences between the various procedures of failure analysis, in terms of the respective mechanics of slope stability evaluation and the calculated factors of safety.

Eight distinct limit equilibrium procedures of slope stability analysis have been studied in detail. Some of these procedures (Fellenius, Bishop simplified and Janbu simplified methods) satisfy only two conditions of equilibrium (overall moment and vertical force and, for the latter, vertical and horizontal force), whereas others (Janbu generalised, Morgenstern and Price, Spencer, Sarma and GLE methods) satisfy all three conditions of equilibrium (i.e. vertical and horizontal force and, overall

moment). They all involve some simplifying assumptions to make the problem statically determinant.

It was found that the Fellenius and the Janbu simplified methods give conservative *FOS* values. The Bishop simplified method provides accurate results compared to other rigorous methods. However, there are slight differences between rigorous solutions of *FOS* values due to the variations in the assumptions involved and the corresponding calculation techniques used.

It is the author's considered judgement that the satisfaction of equilibrium conditions does not in itself provide a sufficient basis for selecting the best procedure for analysis. Therefore, it is recommended that the solution capability of different analytical methods should be compared with the corresponding factors of safety values, in order that a thorough failure risk assessment is achieved. This is regarded as particularly important for practical applications in an engineering design environment.

All eight methods of analysis involve a numerical search to determine the critical slip surface which gives the lowest *FOS*. Such a search is a long procedure and becomes time intensive for all the above methods. In addition, problems of nonconvergence are known to occur, especially for rigorous methods. To avoid these problems, the present research has used the fact that Bishop's simplified method gives accurate values for the most critical *FOS* and the corresponding slip surface. This critical slip surface is then applied to the other more rigorous methods of analysis to reduce the calculation

time. This is deployed as a means of inexpensive but accurate problem analysis which would be an important consideration in technical and commercial environments in the engineering community.

It is found that all systematic calculations require iterative procedures except for the Fellenius method. It is further noted that in most cases the Bishop and Janbu simplified methods need only five iterations for convergence, regardless of the starting value. If the Fellenius method is used for estimating the *FOS* initially, only two or three iterations are required to obtain a converged solution for either the Bishop or Janbu simplified methods. To obtain the Janbu generalised converged *FOS*'s, only one or two iterations are required once the Janbu simplified value has been established. The Sarma and Morgenstern and Price methods usually involve seven to ten iterations regardless of the starting value. The Spencer and GLE methods were found to require a series of trial-and-error sequences to produce the correct θ value, which then yielded the *FOS* (F_i), which in turn satisfied static conditions for both moment and force equilibrium requirements.

In this investigation, the method of slices has been programmed which may be the most widely used method for slope stability calculations. Since it is approximate, an adequate number of slices need to be used to obtain the optimum *FOS* value. There are reports that a high number of slices should be used to reduce the error. 32 slices are often recommended. These statements have been contrasted with the practice in the SLOPE program which is coded to take a maximum of 25 slices. The accuracy of

the *FOS* has been verified to increase with the number of slices used. The present study concludes that a minimum of 30 slices should be used for most analyses. The slopes tested in this work are based on published case studies. Some large differences between the reported *FOS*, derived during this research, and the case study results are thought to be due to differences in inputted data as a result of imprecise information.

The innovative use of Gauss quadrature, as a replacement for the method of slices, has been shown to be successful in the calculation of *FOS* values. Nine Gauss points were seen to give sufficient accuracy for the *FOS* evaluations. The author has established that fewer than five Gauss points should not be used. The use of Gaussian integration has been seen to reduce the computer calculation time significantly. The candidate has also examined a number of case studies to report on the usefulness and universal applicability of Gauss quadrature for slope stability determination through *FOS* calculations. There is no upper limit for the use of Gauss integration points for *FOS* calculations. The author has used up to 24 Gauss points, although nine points were likely to be sufficient for satisfactory convergence. This is in a calculation where from 25-30 up to 250 slices were needed for reasonable accuracy using the method of slices.

The second phase of this study has involved lateral load estimations on a row of piles used to stabilise a slope. The method of calculation of the lateral forces acting on a row of piles, due to visco-plastic flow, is given in Chapter 6. The work presented here

is carried out in theory only. The results obtained were used in Chapter 9 to stabilise slopes.

The following points are reported as a successful outcome, by using the proposed visco-plastic theory:

a) A calibration process has been given to determine the appropriate ξ_0 value for each Reynolds number (Re) to match the true Oseen value (ξ_0 is the effective distance in the vicinity of the pile).

b) A single pile solution has also been obtained using the visco-plastic flow model.

c) The theoretical solution of the lateral force has been determined by considering the interval between piles in a row and the theory of visco-plastic flow.

d) It has been found that the lateral force on the pile per unit length increases as the D_2/D_1 decreases when the diameter of pile is constant (D_1 is the pile centre to centre distance and D_2 is the clear distance between two adjacent piles).

e) In the theory of visco-plastic flow, the lateral force on the pile has been observed to increase as τ_y, (D_1-D_2), KONS and velocity of flow increases [$\tau_y = c$ (cohesion) and KONS is product of flow velocity and plastic viscosity (i.e., $V\eta_p$)].

f) When the D_2/D_1 ratio is small, the current research model and Ito and Matsui (1978) results are in agreement. The latter results were obtained using passive earth pressure theory and are similar to the author's when D_2/D_1 is small.

g) In the light of general agreement with other researchers, the candidate has confidence in using the lateral force estimation from the proposed method on a

row of piles. The candidate has also noted that the results from the present research occupy an "in-between" position to the previously reported data. The general trend is overwhelmingly confirmed without the current results being arithmetic averages of either of the earlier plastic theories

h) The lateral force, estimated by the present visco-plastic flow, lies between those given by De Beer & Carpentier and Ito & Matsui's plastic deformation method.

In Chapter 7, there are bounded solutions for the lateral forces on the pile depending on the theory and circumstances used. This is to be welcomed, since the engineer has a choice of examining a number of solutions. In the case of Ito and Matsui's (1975), it is seen that the values are not dependent on the yield stress. After the discussion given by De Beer and Carpentier (1977), Ito and Matsui (1978) proposed another set of equations utilising passive earth pressure for the theory of plastic flow. For the case of the passive earth pressure, the lateral force may be obtained by changing the term $\left(-2\tau_y\right)$ into the term $\left(+2\tau_y\right)$ in Eqn. [7.7]. Hence, with the latter assumption the lateral force on the pile becomes dependent on the yield stress.

The modified assumption by De Beer and Carpentier (1977) leads to much larger lateral forces on the pile than those obtained using either the assumptions of the currently proposed method or Ito and Matsui's method.

Altogether the previous methods of plastic deformation and plastic flow together with the author's visco-plastic formulation provide a comprehensive and practical means of lateral force assessment in the absence of other equivalent methods.

As an alternative, short piles, which are more rigid than those so far considered, can also be used. Slope stabilisation can be improved with an increased *FOS*, at an optimum value, by considering short pile installation. The technique is based on the slip surface geometry passing below the pile which is installed into the slope. The analysis is achieved by using the Bishop simplified method. However, the method has limitations corresponding to the true failure geometry and hence a realistic *FOS*.

The specialised geometry of short pile stabilisation has involved formulating a fresh grid geometry to facilitate the *FOS* calculation process. In this case, the centre of the slip circles are located by constructing normals to the slope surface. Once a few values of the *FOS* are calculated, a grid is established and a search to find the minimum factor of safety can commence. This has been verified to reduce the number of calculations required in any trial-and-error algorithm, since unnecessary search effort is reduced.

Slope stabilisation due to the presence of a row of piles has been investigated and implemented. A summary of the progress is listed below:

i. Two distinct lateral load estimations, i.e. the theory of plastic deformation and proposed visco-plastic flow, have been used in a computer program to estimate the lateral load on the piles in a row.

ii. Eight different methods of analyses to re-calculate *FOS* values of a slope reinforced by a row of piles has been developed using the method of slices. For Gauss quadrature calculations, the Morgenstern and Price method has not been included.

iii. Relationship has been observed between the stabilised *FOS* and the location of the pile row.

iv. A FEM computer program has been developed to evaluate the deflection, bending moment and shear force along a pile. The pile has been analysed in two sections considering above and below the failure surface.

v. It is found that the pile top restraining (hinged or fixed) specification is not only realistic but also minimises the overall pile displacement, bending moment and shear force.

vi. When bending moment and shear force converge to a near zero value, the minimum length of the pile can be determined.

vii. The program enables the use of two optimisation processes; (a) to locate the pile in the most strategic position and (b) to determine the minimum FOS of a failure slip surface with much improved stability.

viii. When the frictional angle is zero, all the above methods of analysis provide similar *FOS* values for the critical and stabilised conditions.

ix. The difference between the stabilised *FOS* values from the present research and the values cited in literature is marginal.

x. The more stable situation corresponds to the position on the slope where the maximum embedded depth of pile has been utilised.

SLIDE, the program developed during this research, is also capable of producing a scaled drawing of the slope together with slices, grid lines, water table, constraints, exclusion zones and slip surface(s).

10.2 Future work

The current work could be extended by research into one or more of the following areas:

- Provision for a more "user friendly" and an interactive program.
- The facility of having multi-rows of piles for slope stabilisation.
- The ability to consider a three dimensional assessment of variations in *FOS*, in comparison to the two-dimensional (present) formulation.
- The consideration of a facility for "mixed mode" stabilisation e.g. using a combination of mechanical means such as piles, soil nailing and anchoring, etc.

REFERENCES

Abramson, L. W.; Lee, T. S.; Sharma, S., and Boyce, G. M. (1996). *Slope Stability and Stabilisation Method*, John Wiley & Sons, ISBN 0 471 10622 4.

Akin, J. E. (1986). *Finite Element Analysis for Undergraduates*, Academic Press, London.

Anagnostopoulos, C.; Hada, M., and Fukuoka, M. (1991). "Piles as Landslides Countermeasures-Model Study," Landslides, *Edited by* Bell, A.A. Balkema, Rotterdam, ISBN 90 5410 032X.

Arai, K., and Tagyo, K. (1985). "Determination of Noncircular Slip Surface Giving the Minimum Factor of Safety in Slope Stability Analysis," *Soils and Foundations*, Vol. 25, No. 1, pp. 43-51.

Ashour, M.; Norris, G., and Pilling, P. (1998). "Lateral Loading of a Pile in Layered Soil Using the Strain Wedge Model," *Journal of Geotechnical and Geoenvironmental Engineering*, ASCE, Vol. 124, No. 4, pp. 303-315.

Baker, G. (1980). "Determination of the Critical Slip Surface in Slope Stability Computations," *International Journal for Numerical and Analytical Methods in Geomechanics*, Vol. 4, pp. 333-359.

Baker, G., and Garber, M. (1977). "Variational Approach to Slope Stability," Proceedings of the Ninth International Conference on Soil Mechanics and Foundation Engineering, Tokyo, Vol. 2, pp. 9-12.

Baker, G., and Garber, M. (1978). "Theoretical Analysis of the Stability of Slopes," *Geotechnique*, Vol. 28, No. 4, pp. 395-411.

Barnes, G. E. (1995). *Soil Mechanics Principles and Practice*, Macmillan.

Batchelor, G. K. (1974). *An Introduction to Fluid Dynamics*, Cambridge University Press.

Bishop, A. W. (1955). "The use of the Slip Circle in the Stability Analysis of Earth Dams," *Geotechnique*, Vol. 5, No. 1, pp. 7-17.

Bishop, A. W., and Morgenstern, N. R. (1960). "Stability Coefficients for Earth Slopes," *Geotechnique*, Vol. 10, No. 4, pp. 129-147.

Boutrop, E., and Lovell, C. W., (1980). "Searching Techniques in Slope Stability Analysis," *Engineering Geology*, Vol. 16, pp. 51-61.

Bowles, J. E. (1996). *Foundation Analysis and Design*, Fifth Edition (International), McGraw-Hill, ISBN 0-07-114052-2

Briaud, J. L. (1997). "SALLOP: Simple Approach for Lateral Loads on Piles," *Journal of Geotechnical and Geoenvironmental Engineering*, ASCE, Vol. 123, No. 10, pp. 958-964.

Bromhead, E. N. (1992). *The Stability of Slopes*, Second Edition, Blackie Academic & Professional.

Broms, B. B. (1964-a). "Lateral Resistance of Piles in Cohesive Soils," *Journal of the Soil Mechanics and Foundation Division*, ASCE, Vol. 90, No. SM3, pp. 27-63.

Broms, B. B. (1964-b). "Lateral Resistance of Piles in Cohesionless Soils," *Journal of the Soil Mechanics and Foundation Division*, ASCE, Vol. 90, No. SM3, pp. 123-156.

Broms, B. B. (1972). "Stability of Flexible Structures (Piles and Piles Group)," Proceedings of the Fifth European Conference on Soil Mechanics and Foundation Engineering, Vol. 2, pp. 239-269.

Brunsden, D. (1987). "Mudslides," *Slope Instability*, *Edited by* Denys Brunsden and David B. Prior, John Wiley & Sons, pp. 363-418.

Burden, R. L., and Faires, J. D. (1989). *Numerical Analysis*, Fourth Edition, PWS-KENT, ISBN 0 53491 585 X.

Celestino, T. B., and Duncan, J. M. (1981). "Simplified Search for Noncircular Slip Surfaces," Proceedings of the Tenth International Conference on Soil Mechanics and Foundation Engineering, Stockholm, Vol. 3, pp. 391-394.

Castillo, E., and Revilla, J. (1977). "The Calculus of Variations and the Stability of Slopes," Proceedings of the Ninth International Conference on Soil Mechanics and Foundation Engineering, Tokyo, Vol. 2, pp. 25-30.

Chandra, D., and Jiang, C. (1993). "Application of Spencer's Method for Slope Stability," Proceedings of the Fifth International Conference Computing in Civil and Building Engineering, (V-ICCCBE), pp. 1411-1420.

Chen, L., and Poulos, H. G. (1993). "Analysis of Pile-Soil Interaction Under Lateral Loading Using Infinite and Finite Elements," *Computers and Geotechnics*, Vol. 15, pp 189-220.

Chen, L., and Poulos, H. G. (1994). "A method of Pile-Soil Interaction Analysis for Piles Subjected to Lateral Soil Movement," Proceedings of the Eighth International Conference on Computer Methods and Advances in Geomechanics, A.A Balkema, Rotterdam, pp 2311-2316.

Chen, L., and Poulos, H. G. (1997). "Pile Subjected to Lateral Soil Movements," *Journal of Geotechnical and Geoenvironmental Engineering*, ASCE, Vol. 123, No. 9, pp. 802-811.

Cheney, W., and Kincaid, D. (1985). *Numerical Mathematics and Computing*, Second Edition, Brooks/Cole.

Cheung, Y. K., and Yeo, M. F. (1979). *A Practical Introduction to Finite Element Analysis*, Pitman, London.

Chowdhury, S. (1992). "Generalized Slope Stability Analysis," MSc. Thesis, University of Delaware, Newark, Del.

Chugh, A. K. (1982). "Slope Stability Analysis for Earthquakes," *International Journal for Numerical and Analytical Methods in Geomechanics*, Vol. 6, No. 3, pp. 307-322.

Clayton, C. R. I.; Milititsky, J., and Woods, R. I. (1993). *Earth-Retaining Structures*, Second Edition, Blackie Academic & Professional.

Cleary, P. W., and Campbell, C. S., (1993). 'Self-Lubrication for Long Runout Landslides: Examination by Computer Simulation', *Journal of Geophysical Research*, Vol. 98, No. B12, pp. 21,911-21,924.

Craig, D., (1981). 'Mudslide Plug Flow Within Channels', *Engineering Geology*, Vol. 17, No. 4, pp. 273-281.

Craig, R. F. (1997). *Soil Mechanics*, Sixth Edition, Chapman & Hall.

Crochet, M. J.; Davies, A. R., and Walters, K. (1984). *Numerical Simulation of Non-Newtonian Flow*, Elsevier.

De Beer, E. E., and Wallays, M. (1972). "Forces Induced in Piles by Unsymmetrical Surcharges on the Soil Around the Piles," Proceedings of the Fifth European Conference on Soil Mechanics and Foundation Engineering, Vol. 1, pp. 325-332, Madrid.

De Beer, E., and Carpentier, R. (1977). "Discussions: Methods to Estimate Lateral Force Acting on Stabilizing Piles," *Soils and Foundations*, Vol. 17, No. 1, pp. 68-82.

Delpak, R. (1996). Private communication, internal report, University of Glamorgan.

Delpak, R. (1998). Private communication, internal report, University of Glamorgan.

DeNatale, J. S. (1991). "Rapid Identification of Critical Slip Surfaces: Structure," *Journal of Geotechnical Engineering*, ASCE, Vol. 117, No. 10, pp. 1568-1589.

Department of Transport, Scottish Office, Welsh Office, Department of the Environment for Northern Ireland (1994). *Design Methods for the Reinforcement of Highway Slopes by Reinforced Soil and Soil Nailing Technique*, Vol. 4, Part 4, HA 68/94.

Duncan, J. M., and Wright, S. G. (1980). "The Accuracy of Equilibrium Methods of Slope Stability Analysis," Proceedings of International Symposium on Landslides, New Delhi, Vol. 1, pp. 247-254.

Esposito, A. (1998). *Fluid Mechanics with Applications*, Prentice-Hall, ISBN 0-13-042680-6.

Fellenius, W. (1936). "Calculation of the Stability of Earth Dams," Proceedings of the Second Congress on Large Dams, Washington, Vol. 4, pp. 445-459.

Fleming, W. G. K.; Weltman, A. J.; Randolph, M. F., and Elson, W. K. (1992). *Piling Engineering*, Second Edition, Blackie (Glasgow and London).

Fredlund, D. G. (1984). "Analytical Methods for Slope Stability Analysis," Proceedings of the Fourth International Symposium on Landslides, Vol. 1, pp. 229-250.

Fredlund, D. G., and Krahn, J. (1977). "Comparison of Slope Stability Methods of Analysis," *Canadian Geotechnical Journal*, Vol. 14, No. 3, pp. 429-439.

Fredlund, D. G., and Rahardjo, H. (1993). *Soil Mechanics for Unsaturated Soils*, John Wiley & Sons, ISBN 0 471 85008 X.

Fredlund, D. G.; Krahn, J., and Pufahl, D. E. (1981). "The Relationship Between Limit Equilibrium Slope Stability Methods," Proceedings of the Tenth International Conference on Soil Mechanics and Foundation Engineering, Stockholm, Vol. 3, pp. 409-416.

Fredlund, D. G.; Zhang, Z. M., and Lam, L. (1992). "Effect of the Axis of Moment Equilibrium in Slope Stability Analysis," *Canadian Geotechnical Journal*, Vol. 29, pp. 456-465.

Fukuoka, M. (1977). "The Effects of Horizontal Loads on Piles Due to Landslides," Proceedings of the Ninth International Conference on Soil Mechanics and Foundation Engineering, Speciality Session 10, pp. 27-42, Tokyo.

Goh, A. T. C.; Teh, C I., and Wong, K. S. (1997). "Analysis of Piles Subjected to Embankment Induced Lateral Soil Movements," *Journal of Geotechnical and Geoenvironmental Engineering*, ASCE, Vol. 123, No. 9, pp. 792-801.

Graham, J. (1984). "Methods of Stability Analysis," Slope Instability, *Edited by* D. Brunsden and D. B. Prior, pp. 171-215.

Greco, V. R. (1996). "Efficient Monte Carlo Technique for Locating Critical Slip Surfaces," *Journal of the Geotechnical Engineering*, ASCE, Vol. 122, No. 7, pp. 517-525.

Gudehus, G., and Schwarz, W. (1985). "Stabilization of Creeping Slopes by Dowels," Proceedings of the Ninth International Conference on Soil Mechanics and Foundation Engineering, Vol. 3, pp. 1697-1700, San Francisco.

Hamill, L. (1995). *Understanding Hydraulics*, Macmillan, ISBN 0 333 59910 1.

Hansen, J. B. (1961). "The Ultimate Resistance of Rigid Piles Against Transversal Forces," *The Danish Geotechnical Institute, Copenhagen*, Bulletin No. 12, pp. 1-9.

Hassiotis, S., and Chameau, J. L. (1984). "Stabilisation of Slopes Using Piles," *Rep. No. FHWA/IN/JHRP-84/8*, Purdue University, West Lafayette.

Hassiotis, S.; Chameau, J. L., and Gunaratne, M. (1997). "Design Method for Stabilisation of Slopes With Piles," *Journal of Geotechnical and Geoenvironmental Engineering*, ASCE, Vol. 123, No. 4, pp. 314-323.

Hsiung, Y. M., and Chen, Y. L. (1997). "Simplified Method for Analysing Laterally Loaded Single Piles in Clays," *Journal of Geotechnical and Geoenvironmental Engineering*, ASCE, Vol. 123, No. 11, pp. 1018-1029.

Hull, T. S.; Lee, C. Y., and Poulos, H. G. (1991). "Mechanics of Pile Reinforcement for Unstable Slopes," Research Report No. R636, School of Civil and Mining Engineering, University of Sydney, Australia.

Hutter, K., and Rajagopal, K.R., (1994). 'On Flows of Granular Materials', *Continuum Mechanics and Thermodynamics*, Vol. 6, pp. 81-139.

Ito, T., and Matsui, T. (1975). "Methods to Estimate Lateral Force Acting on Stabilizing Piles," *Soils and Foundations*, Vol. 15, No. 4, pp. 43-59.

Ito, T., and Matsui, T. (1977). "The Effects of Piles in a Row on the Slope Stability," Proceedings of the Ninth International Conference on Soil Mechanics and Foundation Engineering, Specialty Session 10, pp. 81-86, Tokyo.

Ito, T., and Matsui, T. (1978). "Discussions: Methods to Estimate Lateral Force Acting on Stabilizing Piles," *Soils and Foundations*, Vol. 18, No. 2, pp. 41-44.

Ito, T., and Matsui, T. (1978). "Discussions: Methods to Estimate Lateral Force Acting on Stabilising Piles," *Soils and Foundations*, Vol. 18, No. 2, pp. 41-44.

Ito, T.; Matsui, T., and Hong, W. Y. (1979). "Design Method for the Stability Analysis of the Slope with Landing Pier," *Soils and Foundations*, Vol. 19, No. 4, pp. 43-57.

Ito, T.; Matsui, T., and Hong, W. Y. (1981). "Design Method for Stabilising Piles Against Landslides-One Row of Piles," *Soils and Foundations*, Vol. 21, No. 1, pp. 21-37.

Ito, T.; Matsui, T., and Hong, W. Y. (1982). "Extended Design Method for Multi-Row Stabilizing Piles Against Landslide," *Soils and Foundations*, Vol. 22, No. 1, pp. 1-13.

Jamiolkowski, M., and Garassino, A. (1977). "Soil Modulus for Laterally Loaded Piles," Proceedings of the Ninth International Conference on Soil Mechanics and Foundation Engineering, Specialty Session 10, pp. 43-58, Tokyo.

Janbu, N. (1954). "Application of Composite Slip Surfaces for Stability Analysis," Proceedings of the European Conference on Stability of Earth Slope, Vol. 3, pp. 43-49, Stockholm.

Janbu, N. (1957). "Earth Pressures and Bearing Capacity Calculations by Generalised Procedure of Slices," Proceedings of the Fourth International Conference on Soil Mechanics and Foundation Engineering, Vol. 2, pp. 207-212, London.

Janbu, N. (1973). "Slope Stability Computations," *Embankment-Dam Engineering*, Casagrande Volume, *Edited by* R. C. Hirschfield and S. J. Poulos, John Wiley and Sons, New York, pp. 47-86.

Johnson , A. M., and Rodine, J. R. (1987). "Debris Flow," Slope Instability, *Edited by* Denys Brunsden and David B. Prior, John Wiley & Sons, pp. 257-361.

Kalteziotis, N.; Zervogiannis, H.; Frank, R.; Seve, G., and Berche, J. C. (1993). "Experimental Study of Landslide Stabilisation by Large Diameter Piles," Geotechnical Engineering of Hard Soils-Soft Rocks, *Edited by* Anagnostopoulos et al, A.A. Balkema, Rotterdam, ISBN 90 5410 3442.

Kumsar, H. (1993). "Computerised Mine Slope Stability Assessment by Using Inter-slice Force Transmission Theory," University of Nottingham, Ph.D. Dissertation.

Lambe, T. W., and Whitman, R. V. (1979). *Soil Mechanics, SI Version*, John Wiley & Sons.

Lee, C. Y.; Hull, T. S., and Poulos, H. G. (1995). "Simplified Pile-Slope Stability Analysis," *Computers and Geotechnics*, Vol. 17, pp. 1-16.

Lee, C. Y.; Poulos, H. G., and Hull, T. S. (1991). "Effect of Seafloor Instability on Offshore Pile Foundations," *Canadian Geotechnical Journal*, Vol. 28, No. 5, pp. 729-737.

Leshchinsky, D. (1990). "Slope Stability Analysis: Generalized Approach," *Journal of Geotechnical Engineering*, ASCE, Vol. 116, No. 5, pp. 851-867.

Leshchinsky, D., and Huang, C-C. (1992). "Generalized Slope Stability Analysis: Interpretation, Modification and Comparison," *Journal of Geotechnical Engineering*, ASCE, Vol. 118, No. 10, pp. 1559-1576.

Leventhal, A. R., and Mostyn, G. R. (1987). "Slope Stabilisation Techniques and Their Application," Soil Slope Instability and Stabilisation, *Edited by* B. F. Walker and R. Fell, A. A. Balkema, pp. 183-230.

Li, K. S., and White, W. (1987). "Rapid Evaluation of the Critical Slip Surface in Slope Stability Problems," *International Journal for Numerical and Analytical Methods in Geomechanics*, Vol. 11, pp. 449-473.

Lowe, J. III., and Karafiath, L. (1960). "Stability of Earth Dams Upon Drawdown," Proceedings of the First Pan-American Conference on Soil Mechanics and Foundation Engineering, Mexico City, Vol. 2, pp. 537-552.

Maksimovic, M. (1979). "Limit Equilibrium for Nonlinear Failure Envelope and Arbitrary Slip Surface," Proceedings of the Third International Conference on Numerical Methods in Geomechanics, Aachen, pp. 769-777.

Matsui, T.; Hong, W. Y., and Ito, T. (1982). "Earth Pressure on Piles in a Row Due to Lateral Soil Movements," Soil and Foundations, Vol. 22, No. 2, pp. 71-81.

Matsui, T.; Hong, W. Y., and Ito, T. (1984). "Closure Discussion: Earth Pressure on Piles in a Row Due to Lateral Soil Movements," *Soil and Foundations*, Vol. 24, No. 2, pp. 131-132.

Mindlin, R. D. (1936). "Force at a point in the Interior of a Semi-Infinite Solid," *Physics*, Vol. 7, pp. 195-202.

Morgenstern, N. R. (1982). "The Analysis of Wall Supports to Stabilise Slopes," Application of Walls to Landslide Control Problem, *Edited by* R. B. Reeves, American Society of Civil Engineers, pp. 19-29, Las Vegas.

Morgenstern, N. R., and Price, V. E. (1965). "The Analysis of the Stability of General Slip Surfaces," *Geotechnique*, Vol. 15, No. 1, pp. 79-93.

Morgenstern, N. R., and Price, V. E. (1967). "A Numerical Method for Solving the Equations of Stability of General Slip Surface," *Computer Journal*, Vol. 9, pp. 388-393.

Morton, K. W., and Mayers, D. F. (1994). *Numerical Solution of Partial Differential Equations: An Introduction*, Cambridge University Press, ISBN 0 521 41855 0.

Mostyn, R. M., and Small, J. C. (1987). "Methods of Stability Analysis," Soil Slope Instability and Stabilisation, *Edited by* B. F. Walker and R. Fell, A.A. Balkema, pp. 71-120.

Munson, B. R.; Young, D. F. and Okiishi, T. H., (1994). *Fundamentals of Fluid Mechanics*, Second Edition, John Wiley & Sons.

Nakamura, H. (1984). "Design of Rigid Dowel Piles for Landslide Control," Proceedings of the Fourth International Symposium on Landslides, Vol. 2, pp. 149-154, Toronto.

Nash, D. (1987). "A Comparative Review of Limit Equilibrium Methods of Stability Analysis," Slope Stability, *Edited by* M. G. Anderson and K. S. Richards, pp. 11-75.

Nethero, M. F. (1982). "Slide Control by Drilled Pier Walls," Application of Walls to Landslide Control Problem, *Edited by* R. B. Reeves, American Society of Civil Engineers, pp. 61-76, Las Vegas.

Nguyen, V. U. (1985). "Determination of Critical Slope Failure Surface," *Journal of Geotechnical Engineering*, ASCE, Vol. 111, No. 2, pp. 238-250.

Poulos, H. G. (1973). "Analysis of Piles in Soil Undergoing Lateral Movement," *Journal of the Soil Mechanics and Foundation Division*, ASCE, Vol. 99, No. SM5, pp. 391-406.

Poulos, H. G. (1976). "Behaviour of Laterally Loaded Piles Near a Cut or Slope," *Australian Geomechanics Journal*, Vol. G6, No. 1, pp. 6-12.

Poulos, H. G. (1995). "Design of Reinforcing Piles to Increase Slope Stability," *Canadian Geotechnical Journal*, Vol. 32, pp. 808-818.

Poulos, H. G., and Chen, L. (1997). "Pile Response Due to Excavation-Induced Lateral Soil Movement," *Journal of Geotechnical and Geoenvironmental Engineering*, ASCE, Vol. 123, No. 2, pp. 94-99.

Poulos, H. G., and Davis, E. H. (1980). *Pile Foundation Analysis and Design*, John Wiley and Sons, New York.

Reese, L. C.; Wang, S. T., and Fouse, J. L. (1992). "Use of Drilled Shafts in Stabilising a Slope," Stability and Performance of Slopes and Embankments-II, *Edited by* R. B. Seed and R. W. Boulanger, Geotechnical Special Publication No. 31, ASCE, Vol. 2, pp. 1318-1332, Berkeley.

Rollins, K. M., and Rollins, R. L. (1992). "Landslide Stabilisation Using Drilled Shaft Walls," Ground Movements and Structures, *Edited by* J. D. Geddes, Vol. 4, pp. 755-770.

Rowe, R. K., and Poulos, H. G. (1979). "A Method for Predicting the Effect of Piles on Slope Behaviour," Proceedings of the Third International Conference on Numerical Methods in Geomechanics, Vol. 3, pp. 1073-1085, Aechen.

Sarma, S. K. (1973). "Stability Analysis of Embankments of Slopes," *Geotechnique*, Vol. 23, No. 3, pp. 423-433.

Sarma, S. K. (1979). "Stability Analysis of Embankments of Slopes," *Journal of the Geotechnical Engineering Division*, ASCE, Vol. 105, No. GT12, pp. 1511-1524.

Sarma, S. K., and Bhave, M. V. (1974). "Critical Acceleration Versus Static Factor of Safety in Stability Analysis of Earth Dams and Embankments," *Geotechnique*, Vol. 24, No. 4, pp. 661-665.

Seed, H. B., and Sultan, H. A. (1967). "Stability Analysis for a Sloping Core Embankment," *Journal of the Soil Mechanics and Foundation Division*, Vol. 93, No. SM4, pp. 69-83.

Siegel, R. A.; Kowacs, W. D., and Lovell, C. W. (1981). "Random Surface Generation in Stability Analysis," *Journal of the Geotechnical Engineering Division*, ASCE, Vol. 107, No. GT7, pp. 996-1002.

Skempton, A. W., and Hutchinson, J. (1969). "Stability of Natural and Embankment Foundation," Proceedings of the Seventh International Conference on Soil Mechanics and Foundation Engineering, State of-the-art Report, pp. 291-340, Mexico.

Smith, G. N., and Pole, E. L. (1980). *Elements of Foundation Design*, Granada, London.

SLOPE, *Slope Stability and Reinforced Soil Analysis Program* by D. L. Borin, Distributed by Geosolve 1993.

Smith, I. M., and Griffiths, D. V. (1988). *Programming the Finite Element Method*, Second Edition, John Wiley & Sons, Chichester.

Snedker, E. A. (1985). "The Stabilisation of a Landslipped Area to Incorporate a Highway by Use of a System of Bored Piles," Proceedings of the Symposium on Failures in Earthworks, pp. 436-438, Thomas Telford, London.

Soil Nailing Recommendations (1991). "For Designing, Calculating, Constructing, and Inspecting Earth Support Systems Using Soil Nailing," French National Research Project Clouterre, U.S. Department of Transportation Federal Highway Administration, Publication No. FHWA-SA-93-026 (English Translation July 1993).

Sommer, H. (1977). "Creeping Slope in a Stiff Clay," Proceedings of the Ninth International Conference on Soil Mechanics and Foundation Engineering, Speciality Session 10, pp. 113-118, Tokyo.

Sommer, H. (1979). "Stabilisation of a Creeping Slopes in Clay with Stiff Elements," Proceedings of the Seventh European Conference on Soil Mechanics and Foundation Engineering, Design Parameters in Geotechnical Engineering, Vol. 3, pp. 269-274.

Spencer, E. (1967). " A Method of Analysis of the Stability of Embankments Assuming Parallel Inter-Slice Forces," *Geotechnique*, Vol. 17, No. 1, pp. 11-26.

Spencer, E. (1973). " Thrust Line Criterion in Embankment Stability Analysis," *Geotechnique*, Vol. 23, No. 1, pp. 85-100.

Sridevi, B., and Deep, K. (1991). "Application of Global Optimisation Technique to Slope Stability Analysis," Landslides, *Edited by* Bell, pp. 573-578, A.A Balkema, Rotterdam, ISBN 90 5410 032X.

Takahashi, T. (1991). *Debris Flow*, A.A. Balkema, Rotterdam, ISBN 90 5410 104 0.

Taylor, A. J., and Wilson, S. D. R. (1997). "Conduit Flow of an Yield-Stress Fluid", *Journal of Rheology*, Vol. 41, No. 1, pp. 93-101.

Taylor, D. W. (1937). "Stability of Earth Slopes," *Journal of the Boston Society of Civil Engineers*, Vol. 24, No. 3, pp. 197-246.

Terzaghi, K. (1955). "Evaluation of Coefficient of Subgrade Reaction," *Geotechnique*, Vol. 5, pp. 297-326.

Ting, J. M. (1983). "Geometric concerns in Slope Stability Analysis," *Journal of Geotechnical Engineering*, Vol. 109, No. 11, pp. 1487-1491.

Townsend, P. (1980). "A Numerical Simulation of Newtonian and Visco-Elastic Flow Past Stationary and Rotating Cylinder", *Journal of Non-Newtonian Fluid Mechanics*, Vol. 6, pp. 219-243.

Townsend, P. (1984). "On the Numerical Simulation of Two-Dimensional Time-Dependent Flows of Oldroyd Fluids Part 1: Basic Method and Preliminary Results", *Journal of Non-Newtonian Fluid Mechanics*, Vol. 14, pp. 265-278.

Ulusay, R.; Caglan, D., and Arikan, F., and Yoleri, M. F. (1996). "Characteristics of Biplanar Wedge Spoil Pile Instabilities and Methods to Improve Stability," *Canadian Geotechnical Journal*, Vol. 33, pp. 58-79.

Viggiani, C. (1981). "Ultimate Lateral Load on Piles Used to Stabilize Landslides," Proceedings of the Tenth International Conference on Soil Mechanics and Foundation Engineering, Vol. 3, pp. 555-560, Stockholm.

Walker, B. F.; Blong, R. J., and MacGregor, J. P. (1987). "Landslide Classification, Geomorphology, and Site Investigations," Soil Slope Instability and Stabilisation, *Edited by* B. F. Walker and R. Fell, A. A. Balkema, pp. 1-52.

Wang, W. L., and Yen, B. C. (1974). "Soil Arching in Slopes," *Journal of the Soil Mechanics and Foundation Division*, ASCE, Vol. 100, No. GT1, pp. 61-78.

Wei, J.; Heng, Y. S.; Liang, F. J., and Chong, M. K. (1991). "Slope Stabilisation Using Embankments Piles and Buttress Drains," Landslides, *Edited by* Bell, pp. 847-851, A.A Balkema, Rotterdam, ISBN 90 5410 032X.

Whipple K. X., (1997). 'Open Channel Flow of Bingham Fluids: Applications in Debris-Flow Research', *The Journal of Geology*, vol. 105, pp. 243-262.

Whitman, R. M., and Bailey, W. A. (1967). "Use of Computers for Slope Stability Analysis," *Journal of the Soil Mechanics and Foundation Division*, ASCE, Vol. 93, No. SM4, pp. 475-498.

Whorlow, R. W., (1980). *Rheological Techniques*, Ellis Horwood, ISBN 0-85312-078-1

Williams, R. W. (1998). Private communication, internal report, University of Glamorgan.

Winter, H.; Schwarz, W., and Gudehus, G. (1983). "Stabilisation of clay slopes by piles", Proceedings of the Eighth European Conference on Soil Mechanics and Foundation Engineering, Vol. 2, pp. 545-550.

Wright, S. G. (1969). "A Study of Slope Stability and the Undreaned Shear Strength of Clay Shales," Ph.D. Thesis, University of California, Berkeley, Calif.

Wright, S. G. (1992). "The Role of Benchmark Problems in Slope Stability Computations," Stability and Performance of Slopes and Embankments-II, *Edited by*

R.B. Seed and R.W. Boulanger, Geotechnical Special Publication No. 31, ASCE, Vol. 2, pp. 1067-1069.

Xiaobi, D., and Lansheng, W. (1991). "Some Kinematic Features of Landslide," Landslides, *Edited by* Bell, A.A. Balkema, Rotterdam, ISBN 90 5410 032X.

Yamagami, T.; Suzuki, H., and Yamakawa, O. (1991). "A Simplified Estimation of the Stabilising Effects of Piles in a Landslide Slope Applying the Janbu Method," Landslides, *Edited by* Bell, pp. 613-618, A.A Balkema, Rotterdam, ISBN 90 5410 032X.

Zienkiewicz, O. C. (1977). *The Finite Element Method*, Third Edition, McGraw-Hill, London.

APPENDIX A

A. Equations in the Janbu simplified method

The factor of safety is defined in terms of the mobilised shear strength of the soil for internal force equilibrium within each slice; we have;

$$S_i = \frac{1}{F}\left(c'l + N'_i \tan\phi'\right) = \frac{t_i l_i}{F} \quad . \qquad \text{A.1}$$

Resolving perpendicular to the slip surface provides;

$$N'_i = W_i \cos\alpha_i \quad . \qquad \text{A.2}$$

Resolving parallel to the slip surface gives;

$$S_i = W_i \sin\alpha_i \quad . \qquad \text{A.3}$$

Total horizontal force equilibrium of the entire slip mass is;

$$\sum S_i \cos\alpha_i = \sum N'_i \sin\alpha_i \quad ,$$

$$S_i \cos\alpha - N'_i \sin\alpha = 0 \quad ,$$

$$S_i = \frac{t_i l_i}{F} = W_i \cos\alpha \quad . \qquad \text{A.4}$$

Defining $l_i = b_i \sec\alpha_i$ and $W_i = b_i h_i \gamma$,

$$F = \frac{\sum t_i l_i \cos\alpha_i}{\sum W_i \sin\alpha_i \cos\alpha_i}$$

$$F = \frac{\sum t_i b_i \sec\alpha_i \cos\alpha_i}{\sum W_i \sin\alpha_i \cos\alpha_i} = \frac{\sum t_i b_i}{\sum (W_i \sin\alpha_i \cos\alpha_i)\dfrac{\cos\alpha}{\cos\alpha}}$$

$$F = \frac{\sum t_i b_i}{\sum W_i \tan\alpha_i \cos^2\alpha_i} = \frac{\sum t_i b_i \sec^2\alpha_i}{\sum W_i \tan\alpha_i} \quad . \qquad \text{A.5}$$

Defining p_i as $p_i = \dfrac{W_i}{b_i}$, and putting into Eqn. [A.2], yields;

$$N'_i = p_i b_i \cos\alpha_i \quad . \qquad \text{A.6}$$

Putting Eqn. [A.6] into Eqn. [A.1], we can obtain;

$$S_i = \frac{1}{F}\left[\frac{c' b_i}{\cos\alpha_i} + \left(p_i b_i \cos\alpha_i - \frac{u b_i}{\cos\alpha_i}\right)\tan\phi'\right] \quad ,$$

$$F = \frac{b_i}{S_i \cos\alpha_i}\left[c' + \left(p_i \cos\alpha_i - u\right)\tan\alpha_i\right] \quad . \qquad \text{A.7}$$

Substituting Eqn. [A.3] into Eqn. [A.7] gives;

$$F = \frac{\left[c' + \left(p_i \cos^2\alpha_i - u\right)\tan\phi'\right]}{p_i \sin\alpha_i \cos\alpha_i} \quad .$$

Using $\cos^2\alpha = 1 - \sin^2\alpha$,

$$F = \frac{\left[c' + \left(p_i\left(1 - \sin^2\alpha_i\right) - u\right)\tan\phi'\right]}{p_i \sin\alpha_i \cos\alpha_i} \quad ,$$

$$F = \frac{\left[c' + \left(p_i - u\right)\tan\phi'\right]}{p_i \sin\alpha_i \cos\alpha_i} - \frac{p_i \sin^2\alpha_i \tan\phi'}{p_i \sin\alpha_i \cos\alpha_i} \quad ,$$

$$F = \frac{\left[c' + \left(p_i - u\right)\tan\phi'\right]}{p_i \sin\alpha_i \cos\alpha_i} - \tan\alpha_i \tan\phi' \quad . \qquad \text{A.8}$$

From Eqns. [A.1] and [A.3], we have following;

$$\frac{t_i l_i}{F} = p_i b_i \sin\alpha_i \quad ,$$

$$F = \frac{t_i \dfrac{b_i}{\cos\alpha_i}}{p_i b_i \sin\alpha_i} = \frac{t_i}{p_i \sin\alpha_i \cos\alpha_i} \quad ,$$

$$p_i \sin\alpha_i \cos\alpha_i = \frac{t_i}{F} \quad . \qquad \text{A.9}$$

Putting Eqn. [A.9] into Eqn [A.8] we obtain;

$$F = \frac{[c'+(p_i - u)\tan\phi']}{\frac{t_i}{F}} - \tan\alpha_i \tan\phi' \quad ,$$

$$\frac{F}{F} = \frac{[c'+(p_i - u)\tan\phi']}{\frac{t_i F}{F}} - \frac{\tan\alpha_i \tan\phi'}{F} \quad ,$$

$$t_i = \frac{[c'+(p_i - u)\tan\phi']}{\frac{1+\tan\alpha_i \tan\phi'}{F}} \quad . \qquad \text{A.10}$$

Substituting Eqn. [A.10] into Eqn. [A.5], we have finally;

$$F = \frac{[c'+(p_i - u)\tan\phi']b\frac{\sec^2\alpha_i}{\frac{1+\tan\alpha_i \tan\phi'}{F}}}{W_i \tan\alpha_i} \quad ,$$

$$F = \frac{\sum [c'+(p_i - u)\tan\phi']b\frac{\sec^2\alpha_i}{\left(\frac{1+\tan\alpha_i \tan\phi'}{F}\right)}}{\sum W_i \tan\alpha_i} \quad . \qquad \text{A.11}$$

We can rewrite Eqn. [A.12] in the conventional way, as;

$$F = \frac{\sum [c'b_i + (W_i - u_i b_i)\tan\phi']\frac{\sec^2\alpha_i}{1+(\tan\phi'\tan\alpha_i / F)}}{\sum W_i \tan\alpha_i} \quad . \qquad \text{A.12}$$

APPENDIX B

B. Equations in the Morgenstern and Price method

This method, originally formulated by the authors, has been renewed and reformulated by Bromhead (1992). The coefficients of moments are mostly taken from Bromhead (1992).

The method has a salient feature in that there is no allowance for rotation of the slice. This condition is satisfied if the sum of the moments about the centre of the base of the slice is equal to zero. Figure 3.4 indicates that by taking moments about the midpoint of the base of the slice the following results;

$$E'\left[(y-y_t')-\left(-\frac{dy}{2}\right)\right]+P_w\left[(y-h)-\left(-\frac{dy}{2}\right)\right]-(E'+dE')\left[y+dy-y'_t-dy'_t+\left(-\frac{dy}{2}\right)\right]$$

$$-X\frac{dx}{2}-(X+dX)\frac{dx}{2}-(P_w+dP_w)\left[(y+dy)-(h+dh)-\frac{dy}{2}\right]-dP_h.g=0\ . \qquad \text{B.1}$$

After simplification and proceeding to the limit as $dx \rightarrow 0$, it can be shown readily that;

$$X = \frac{d}{dx}(E'.y'_t) - y\frac{dE'}{dx} + \frac{d}{dx}(P_w.h) - y\frac{dP_w}{dx} \quad . \qquad \text{B.2}$$

From Fig. 3.4, for equilibrium in the *N* direction (perpendicular to the slip surface), we have;

$$dN' + dP_b = dW\cos\alpha - dX\cos\alpha - dE'\sin\alpha - dP_w\sin\alpha \quad . \qquad \text{B.3}$$

Using Fig. 3.4, for equilibrium in the *S* direction (parallel to the slip surface), the following result may be obtained;

$$dS = dE'\cos\alpha + dP_w\cos\alpha - dX\sin\alpha + dW\sin\alpha \quad . \qquad \text{B.4}$$

The Mohr-Coulomb failure criterion in terms of effective stresses may be expressed as;

$$dS = \frac{1}{F}\left[c'\,dx\sec\alpha + (dN')\tan\phi'\right] \quad . \qquad \text{B.5}$$

Equation [B.5] constitutes a definition of the factor of safety in terms of shear strength.

Eliminating *dS* from Eqns. [B.4] and [B.5] we obtain the following;

$$\frac{1}{F}\left[c'\,dx\sec\alpha+(dN')\tan\phi'\right]=dE'\cos\alpha+dP_w\cos\alpha-dX\sin\alpha+dW\sin\alpha\ .\qquad \text{B.6}$$

Also by eliminating dN' from Eqns. [B.3]and [B.6] and also dividing by $dx\cos\alpha$, we have;

$$\frac{c'}{F}\sec^2\alpha+\frac{\tan\phi'}{F}\left[\frac{dW}{dx}-\frac{dX}{dx}-\frac{dE'}{dx}\tan\alpha-\frac{dP_w}{dx}\tan\alpha-\frac{dP_b}{dx}\sec\alpha\right]$$

$$=\frac{dE'}{dx}+\frac{dP_w}{dx}-\frac{dX}{dx}+\frac{dW}{dx}\tan\alpha\ .\qquad \text{B.7}$$

In the specified co-ordinate system, $\tan\alpha=-\frac{dy}{dx}$, and Eqn. [B.7] becomes;

$$\frac{c'}{F}\left[1+\left(\frac{dy}{dx}\right)^2\right]+\frac{\tan\phi'}{F}\left\{\frac{dW}{dx}-\frac{dX}{dx}+\frac{dE'}{dx}.\frac{dy}{dx}+\frac{dP_w}{dx}.\frac{dy}{dx}-r_u\frac{dW}{dx}\left[1+\left(\frac{dy}{dx}\right)^2\right]\right\}$$

$$=\frac{dE'}{dx}+\frac{dP_w}{dx}+\frac{dX}{dx}.\frac{dy}{dx}-\frac{dW}{dx}.\frac{dy}{dx}\ ,\qquad \text{B.8}$$

where

$dP_b=r_u.dW\sec\alpha$,

and r_u is the pore pressure coefficient defined by Bishop and Morgenstern (1960) as,

$$r_u=\frac{u}{h\gamma}\ .$$

Therefore, the governing differential equation becomes using Eqn. [B.2];

$$\frac{dE'}{dx}\left[1-\frac{\tan\phi'}{f}\frac{dy}{dx}\right]+\frac{dX}{dx}\left[\frac{\tan\phi'}{F}+\frac{dy}{dx}\right]=\frac{c'}{F}\left[1+\left(\frac{dy}{dx}\right)^2\right]+\frac{dP_w}{dx}\left[\frac{\tan\phi'}{F}\frac{dy}{dx}-1\right]$$

$$+\frac{dW}{dx}\left\{\frac{\tan\phi'}{F}+\frac{dy}{dx}-r_u\left[1+\left(\frac{dy}{dx}\right)^2\right]\frac{\tan\phi'}{F}\right\} \quad . \qquad \text{B.9}$$

For a specific geometry and slip surface, the internal forces are assumed to vary according to Morgenstern and Price (1965) as;

$$X = f(x)\lambda E \ . \qquad \text{B.10}$$

To investigate the stability of a soil mass with arbitrary slope and properties, the potential sliding body is to be divided into a number of small slices which are vertical lines with horizontal co-ordinates $x_0, x_1, \ldots x_n$. Within each of these slices the portion of the slip surface is assumed linear, as well as the interface between different soil types and pore pressure zones. The function f defined by equation [B.10] is taken to depend linearly on x, see Fig. 3.5. Then within each slice, it follows that;

$$y = Ax + B \quad \text{(slip surface)}, \qquad \text{B.11}$$

$$\frac{dW}{dx} = px + q \quad \text{(weight of slice)}, \qquad \text{B.12}$$

$$f = kx + m \quad \text{(change of internal forces)}. \qquad \text{B.13}$$

Equations [B.11] and [B.12] take into account a section with any arbitrary slip surface to be approximated in the analysis. Equation [B.13] assumes that the ratio of the

internal forces changes linearly over a segment of the sliding mass. This assumption is not unduly restrictive because k and m can be chosen to vary from segment to segment and any continuous distribution of internal forces may be approximated in this way.

To simplify the equations it has been found convenient to define $f(x)\lambda$, by using the total horizontal stress E instead of the effective stress E' (Morgenstern and Price, 1965), so that;

$$E = E' + P_w \quad . \tag{B.14}$$

We can obtain the point of application y_t of the total stress from;

$$Ey_t = E'y'_t + P_w h \quad . \tag{B.15}$$

Using Eqns.[B.13] to [B.13], Eqn. [B.2] becomes;

$$X = \frac{d}{dx}(Ey_t) - y\frac{dE}{dx} \quad , \tag{B.16}$$

which results in Eqn. [B.10] becoming;

$$(Kx + L)\frac{dE}{dx} + KE = Nx + P \quad . \tag{B.17}$$

where

$$K = \lambda k\left(\frac{\tan\phi'}{F} + A\right) , \tag{B.17a}$$

$$L = \lambda m\left(\frac{\tan\phi'}{F} + A\right) + 1 - A\frac{\tan\phi'}{F} \quad , \qquad \text{B.17b}$$

$$N = p\left[\frac{\tan\phi'}{F} + A - r_u\left(1 + A^2\right)\frac{\tan\phi'}{F}\right] \text{, and} \qquad \text{B.17c}$$

$$P = \frac{c'}{F}\left(1 + A^2\right) + q\left[\frac{\tan\phi'}{F} + A - r_u\left(1 + A^2\right)\frac{\tan\phi'}{F}\right] . \qquad \text{B.17d}$$

On integrating Eqn. [B.17] we evaluate E with the start and end value

E=0 and M=0 , at x=x_O and x=x_n to give;

$$E = \frac{1}{L + Kx}\left[EL + \frac{Nx^2}{2} + Px\right] . \qquad \text{B.18}$$

It is now possible to integrate Eqn. [B.16], to obtain;

$$M = E\left(y_t - y\right) = \int_{x_0}^{x}\left(X - E\frac{dy}{dx}\right)dx \ . \qquad \text{B.19}$$

For any values of λ and F , $E_n, \frac{\partial E_n}{\partial F}, \frac{\partial E_n}{\partial \lambda}, M_n, \frac{\partial M_n}{\partial F}$ and $\frac{\partial M_n}{\partial \lambda}$ can be evaluated numerically.

When calculations reach the last slice, the force and moment should both equal zero. To assert zero values the Newton-Raphson iteration method is normally used (Morgenstern and Price, 1967).

Derivations of expressions for δE from E and δM from M in terms of partial derivatives, for this method are given as;

$$\delta E_n = \frac{\partial E_n}{\partial \lambda}\delta\lambda + \frac{\partial E_n}{\partial F}\delta F \ , \qquad \text{B.20}$$

$$\delta M_n = \frac{\partial M_n}{\partial \lambda}\delta\lambda + \frac{\partial M_n}{\partial F}\delta F \ . \qquad \text{B.21}$$

Dividing the above by $\frac{\partial E_n}{\partial \lambda}$ and $\frac{\partial M_n}{\partial \lambda}$ respectively, we obtain;

$$\frac{\delta E_n}{\partial E_n/\partial \lambda} = \delta\lambda + \left(\frac{\partial E_n}{\partial F}\Big/\frac{\partial E_n}{\partial \lambda}\right)\delta F \ , \qquad \text{B.22}$$

$$\frac{\delta M_n}{\partial M_n/\partial \lambda} = \delta\lambda + \left(\frac{\partial M_n}{\partial F}\Big/\frac{\partial M_n}{\partial \lambda}\right)\delta F \ . \qquad \text{B.23}$$

Eliminating $\delta\lambda$;

$$\frac{\delta E_n}{\partial E_n/\partial \lambda} - \left(\frac{\partial E_n}{\partial F}\Big/\frac{\partial E_n}{\partial \lambda}\right)\delta F = \frac{\delta M_n}{\partial M_n/\partial \lambda} - \left(\frac{\partial M_n}{\partial F}\Big/\frac{\partial M_n}{\partial \lambda}\right)\delta F$$

$$\frac{\delta E_n}{\partial E_n/\partial \lambda} - \frac{\delta M_n}{\partial M_n/\partial \lambda} = \left[\frac{\partial E_n}{\partial F}\Big/\frac{\partial E_n}{\partial \lambda} - \frac{\partial M_n}{\partial F}\Big/\frac{\partial M_n}{\partial \lambda}\right]\delta F \ . \qquad \text{B.24}$$

Multiply throughout by $\frac{\partial M_n}{\partial \lambda}\ \frac{\partial E_n}{\partial \lambda}$ so that;

$$\frac{\partial M_n}{\partial \lambda}\delta E_n - \frac{\partial E_n}{\partial \lambda}\delta M_n = \left[\frac{\partial E_n}{\partial F}\frac{\partial M_n}{\partial \lambda} - \frac{\partial M_n}{\partial F}\frac{\partial E_n}{\partial \lambda}\right]\delta F \ ,$$

$$\delta F = \frac{\delta E_n \dfrac{\partial M_n}{\partial \lambda} - \delta M_n \dfrac{\partial E_n}{\partial F}}{\dfrac{\partial E_n}{\partial \lambda}\dfrac{\partial M_n}{\partial F} - \dfrac{\partial E_n}{\partial F}\dfrac{\partial M_n}{\partial \lambda}} \ , \qquad \text{B.25}$$

similarly,

$$\delta \lambda = \frac{\delta E_n \dfrac{\partial M_n}{\partial F} + \delta M_n \dfrac{\partial E_n}{\partial F}}{\dfrac{\partial E_n}{\partial \lambda}\dfrac{\partial M_n}{\partial F} - \dfrac{\partial E_n}{\partial F}\dfrac{\partial M_n}{\partial \lambda}} \ . \qquad \text{B.26}$$

If in *i*-th slice the x is measured from x_{i-1} to x_i then the solution of Eqn. [B.17] is;

$$E = \frac{1}{L_i + K_i x}\left(L_i E_{i-1} + P_i x + \frac{1}{2}N_i x^2\right). \qquad \text{B.27}$$

Putting $b_i = x_i - x_{i-1}$

$$E_i = \frac{1}{L_i + K_i b_i}\left(L_i E_{i-1} + P_i b_i + \frac{1}{2}N_i b_i^{\,2}\right). \qquad \text{B.28}$$

Derivatives of E, with respect to F and λ , can be obtained by differentiating Eqn.[B.28].

On differentiating Eqn. [B.28] with respect to F;

$$\frac{\partial E_i}{\partial F} = \frac{1}{(L_i + K_i b_i)}\left\{\left(-\frac{\partial L_i}{\partial F} - b_i \frac{\partial K_i}{\partial F}\right)E_i + L_i \frac{\partial E_{i-1}}{\partial F}\right.$$

$$\left. + E_{i-1}\frac{\partial L_i}{\partial F} + b_i \frac{\partial P_i}{\partial F} + \frac{1}{2} b_i{}^2 \frac{\partial N_i}{\partial F}\right\}, \qquad \text{B.29}$$

and after differentiating with respect to λ;

$$\frac{\partial E_i}{\partial \lambda} = \frac{1}{(L_i + K_i b_i)}\left\{\left(-\frac{\partial L_i}{\partial \lambda} - b_i \frac{\partial K_i}{\partial \lambda}\right)E_i + L_i \frac{\partial E_{i-1}}{\partial \lambda} + E_{i-1}\frac{\partial L_i}{\partial \lambda}\right\}. \qquad \text{B.30}$$

The derivatives of K, L, N and P may be obtained from Eqns.[B.17a], [b], [c] and [d] with respect to λ and F follows;

$$\frac{\partial K}{\partial F} = \lambda k\left(-\frac{\tan\phi'}{F}\right), \qquad \text{B.31a}$$

$$\frac{\partial K}{\partial \lambda} = k\left(\frac{\tan\phi'}{F} + A\right), \qquad \text{B.31b}$$

$$\frac{\partial L}{\partial F} = \lambda m\left(-\frac{\tan\phi'}{F^2}\right) + A\frac{\tan\phi'}{F^2}, \qquad \text{B.31c}$$

$$\frac{\partial L}{\partial \lambda} = m\left(\frac{\tan\phi'}{F} + A\right), \qquad \text{B.31d}$$

$$\frac{\partial N}{\partial F} = p\left(-\frac{\tan\phi'}{F^2} + r_u\left(1 + A^2\right)\frac{\tan\phi'}{F^2}\right), \qquad \text{B.31e}$$

$$\frac{\partial P}{\partial F} = -\frac{c'}{F^2}\left(1 + A^2\right) + q\left(-\frac{\tan\phi'}{F^2} + r_u\left(1 + A^2\right)\frac{\tan\phi'}{F^2}\right). \qquad \text{B.31f}$$

Also initially at x_0, we have;

$$E_0 = \frac{\partial E_0}{\partial F} = \frac{\partial E_0}{\partial \lambda} = 0$$

From Eqns. [B.11] and [B.19];

$$M_i = M_{i-1} + \int_{x-1}^{x_i} (X - A_i E)\,dx \ . \qquad \text{B.32}$$

It is possible to substitute from Eqns.[B.10], [B.13] and [B.20] to obtain;

$$X = \frac{\lambda(k_i x + m_i)}{L_i + K_i x}\left(L_i E_{i-1} + P_i x + \tfrac{1}{2} N_i x^2\right), \qquad \text{B.33}$$

hence;

$$M_i = M_{i-1} + \int_0^{b_i} \frac{\{\lambda(k_i x + m_i) - A_i\}}{L_i + K_i x}\left(L_i E_{i-1} + P_i x + \tfrac{1}{2} N_i x^2\right)dx. \qquad \text{B.34}$$

Differentiating Eqn. [B.34] with respect to F and λ, the moment differential coefficients become;

$$\frac{\partial M_i}{\partial F} = \frac{\partial M_{i-1}}{\partial F} + \int_0^{b_i} \frac{\{\lambda\,(k_i x + m_i) - A_i\}}{L_i + K_i x}$$

$$\left\{L_i \frac{\partial E_{i-1}}{\partial F} + E_{i-1} \frac{\partial L_i}{\partial F} + \frac{\partial P_i}{\partial F} x + \tfrac{1}{2} \frac{\partial N_i}{\partial F} x^2 \right\} dx$$

$$- \int_0^{b_i} \frac{\{\lambda(k_i x + m_i) - A_i\}}{(L_i + K_i x)^2} \left(L_i E_{i-1} + P_i x + \tfrac{1}{2} N_i x^2\right)$$

$$\left(\frac{\partial L_i}{\partial F} + \frac{\partial K_i}{\partial F} x\right) dx \ , \qquad \text{B.35}$$

and

$$\frac{\partial M_i}{\partial \lambda} = \frac{\partial M_{i-1}}{\partial \lambda} + \int_0^{b_i} \frac{(k_i x + m_i)}{L_i + K_i x} \left(L_i E_{i-1} + P_i x + \tfrac{1}{2} N_i x^2\right) dx$$

$$+ \int_0^{b_i} \frac{\{\lambda(k_i x + m_i) - A_i\}}{L_i + K_i x} \left(L_i \frac{\partial E_{i-1}}{\partial \lambda} + E_{i-1} \frac{\partial L_i}{\partial \lambda} \right) dx$$

$$- \int_0^{b_i} \frac{\{\lambda(k_i x + m_i) - A_i\}}{(L_i + K_i x)^2} \left(L_i E_{i-1} + P_i x + \tfrac{1}{2} N_i x^2\right) \left(\frac{\partial L_i}{\partial \lambda} + \frac{\partial K_i}{\partial \lambda} x \right) dx \ . \qquad \text{B.36}$$

It is possible to change the scale of x in above integrals so that the range of integration is from 0 to 1, and by letting;

$$H_i = \frac{K_i b_i}{L_i} \ , \qquad \text{B.37}$$

then Eqns. [B.34], [B.35] and [B.36] appear as;

$$M_i = M_{i-1} + \int_0^1 \frac{1}{1 + H_i x} \left\{ \sum_{j=0}^{3} T_i x^j \right\} dx \ , \qquad \text{B.38}$$

$$\frac{\partial M_i}{\partial F} = \frac{\partial M_{i-1}}{\partial F} + \int_0^1 \frac{1}{(1+H_i x)^2}\left\{\sum_{j=0}^{4} U_j x^j\right\} dx \ , \qquad \text{B.39}$$

$$\frac{\partial M_i}{\partial \lambda} = \frac{\partial M_{i-1}}{\partial \lambda} + \int_0^1 \frac{1}{(1+H_i x)^2}\left\{\sum_{j=0}^{4} V_j x^j\right\} dx \ . \qquad \text{B.40}$$

where the coefficients $T_0 ... T_3$, $U_0 ... U_4$ and $V_0 ... V_4$ are given as follows;

$$T_0 = b_i \left(\lambda m_i - A_i\right) E_i \ , \qquad \text{B.41a}$$

$$T_1 = \frac{b^2}{L_i}\left\{\left(\lambda m_i - A_i\right) P_i + k_i E_i L_i\right\} \ , \qquad \text{B.41b}$$

$$T_2 = \frac{b_i^3}{L_i}\left\{\tfrac{1}{2}\left(\lambda m_i - A_i\right) N_i + \lambda k_i P_i\right\} \ , \qquad \text{B.41c}$$

$$T_3 = \frac{b_i^4}{L_i}\tfrac{1}{2}\left(\lambda k_i N_i\right) \ . \qquad \text{B.41d}$$

$$_0 = b_i\left(\lambda m_i - A_i\right)\frac{\partial E_i}{\partial F} \ , \qquad \text{B.42a}$$

$$U_1 = \frac{b_i^2}{L_i^2}\left\{\left(\lambda m_i - A_i\right)\left[K_i\left(\frac{\partial E_i}{\partial F}L_i + E_i\frac{\partial L_i}{\partial F}\right) + L_i\frac{\partial P_i}{\partial F} - E_i L_i\frac{\partial K_i}{\partial F} - P_i\frac{\partial L_i}{\partial F}\right]\right.$$

$$\left. + \lambda m_i L_i^2\frac{\partial E_i}{\partial F}\right\} \ , \qquad \text{B.42b}$$

$$U_2 = \frac{b_i^3}{L_i^2}\left\{\lambda k_i\left[K_i\left(\frac{\partial E_i}{\partial F}L_i + E_i\frac{\partial L_i}{\partial F}\right) + L_i\frac{\partial P_i}{\partial F} - E_i L_i\frac{\partial K_i}{\partial F} - P_i\frac{\partial L_i}{\partial F}\right]\right\}$$

$$-\frac{b_i^3}{L_i}\left\{\left(\lambda m_i - A_i\right)\left[\tfrac{1}{2}L_i\frac{\partial N_i}{\partial F} + K_i\frac{\partial P_i}{\partial F} - P_i\frac{\partial K_i}{\partial F} - \tfrac{1}{2}N_i\frac{\partial L_i}{\partial F}\right]\right\} \ , \qquad \text{B.42c}$$

$$U_3 = \frac{b_i^4}{L_i^2}\left\{\lambda m_i\left[\tfrac{1}{2}L_i\frac{\partial N_i}{\partial F} + K_i\frac{\partial P_i}{\partial F} - P_i\frac{\partial K_i}{\partial F} - \tfrac{1}{2}N_i\frac{\partial L_i}{\partial F}\right]\right.$$

$$\left(\lambda m_i - A_i\right)\left[\tfrac{1}{2} K_i \frac{\partial N_i}{\partial F} - N_i \frac{\partial K_i}{\partial F}\right]\Bigg\} \quad , \qquad \text{B.42d}$$

$$U_4 = \tfrac{1}{2}\frac{b_i^5}{L_i^2}\left\{\lambda k_i\left(K_i \frac{\partial N_i}{\partial F} - N_i \frac{\partial K_i}{\partial F}\right)\right\} \quad . \qquad \text{B.42e}$$

$$V_0 = \frac{b_i}{L_i^2}\left\{m_i E_{i-1} L_i^2 \left(\lambda m_i - A_i\right) L_i^2 \frac{\partial E_{i-1}}{\partial \lambda}\right\} \quad , \qquad \text{B.43a}$$

$$V_1 = \frac{b_i^2}{L_i^2}\left\{k_i L_i^2 E_{i-1} + m_i\left(L_i P_i + E_{i-1} L_i K_i\right) + \lambda k_i L_i^2 \frac{\partial E_{i-1}}{\partial \lambda}\right\}$$

$$+\frac{b_i^2}{L_i^2}\left\{\left(\lambda m_i - A_i\right)\left(K_i L_i \frac{\partial E_{i-1}}{\partial \lambda} + K_i E_{i-1} \frac{\partial L_i}{\partial \lambda} - E_{i-1} \frac{\partial K_i}{\partial \lambda} L_i - P_i \frac{\partial L_i}{\partial \lambda}\right)\right\} , \qquad \text{B.43b}$$

$$V_2 = \frac{b_i^3}{L_i^2}\left\{m_i\left(\tfrac{1}{2} L_i N_i + K_i P_i\right) + \lambda k_i\left(K_i L_i \frac{\partial E_{i-1}}{\partial \lambda} + K_i E_{i-1} \frac{\partial L_i}{\partial \lambda} - E_{i-1} \frac{\partial K_i}{\partial \lambda} L_i - P_i \frac{\partial L_i}{\partial \lambda}\right)\right\}$$

$$+\frac{b_i^3}{L_i^2}\left\{k_i\left(L_i P_i + E_{i-1} L_i K_i\right) - \left(\lambda m_i - A_i\right)\left(P_i \frac{\partial K_i}{\partial \lambda} + \tfrac{1}{2} N_i \frac{\partial L_i}{\partial \lambda}\right)\right\} \quad , \qquad \text{B.43c}$$

$$_3 = \frac{b_i^4}{L_i^2}\left\{\tfrac{1}{2} m_i K_i N_i + k_i\left(\tfrac{1}{2} L_i N_i + K_i P_i\right)\right\}$$

$$-\lambda k_i\left\{\left(P_i \frac{\partial K_i}{\partial \lambda} - \tfrac{1}{2} N_i \frac{\partial L_i}{\partial \lambda}\right) - \tfrac{1}{2}\left(\lambda m_i - A_i\right) N_i \frac{\partial K_i}{\partial \lambda}\right\} \quad , \qquad \text{B.43d}$$

$$V_4 = \frac{b_i^5}{L_i^2} k_i N_i \tfrac{1}{2}\left(K_{i-1} - \lambda \frac{\partial K_i}{\partial \lambda}\right) \quad . \qquad \text{B.43e}$$

When $H_i < -0.4$ and $H_i > 0.5$, and we may evaluate M_n (moment) and its derivatives accurately, as follows;

$$B_J = \int_0^1 \frac{x^J}{\left(1 + H_i x\right)} dx \quad , \qquad \text{B.44a}$$

then,

$$B_0 = \frac{1}{H_i}\log_e(1+H_i) \ , \qquad \text{B.44b}$$

$$B_{j+1} = \frac{1}{H_i}\left(\frac{1}{j+1} - B_j\right) \ , \quad j = 0, 1, ..,4 \qquad \text{B.44c}$$

The summation in Eqns. [B.42a, b, c, d] and [B.44a, b, c] is as below;

$$\sum_{j=0}^{3} B_j T_j \ . \qquad \text{B.45}$$

Since,

$$C_j = \int_0^1 \frac{x^j}{(1+ H_i x)^2} dx \ , \qquad \text{B.46a}$$

then,

$$C_0 = \frac{1}{1+ H_i} \ , \qquad \text{B.46b}$$

$$C_{j+1} = \frac{1}{H_i}(B_j - C_j) \ . \qquad \text{B.46c}$$

The summation is Eqns. [B.46b, c] and [B.42a, b, c, d, e] to provide;

$$\sum_{j=0}^{4} C_j U_j \text{ (or } V_j) \ . \qquad \text{B.47}$$

If $-0.4 < H_i < 0.5$ then, a five-point Gauss numerical integration is used to evaluate moments and derivatives accurately. Then;

$$M_i = M_{i-1} + \sum_{n=1}^{5} W_n \frac{1}{(1+H_i x_n)} \left(\sum_{j=0}^{3} T_j x_n^j \right) dx \ , \qquad \text{B.48}$$

$$\frac{\partial M_i}{\partial F} = \frac{\partial M_{i-1}}{\partial F} + \sum_{n=1}^{5} W_n \frac{1}{(1+H_i x_n)^2} \left(\sum_{j=0}^{4} U_j x_n^j \right) dx \ , \qquad \text{B.49}$$

$$\frac{\partial M_i}{\partial \lambda} = \frac{\partial M_{i-1}}{\partial \lambda} + \sum_{n=1}^{5} W_n \frac{1}{(1+H_i x_n)^2} \left(\sum_{j=0}^{4} V_j x_n^j \right) dx \ . \qquad \text{B.50}$$

Here x_n are the abscissa and W_n weights associated with this integration rule.

The calculation of the moment integrals in the above, is a complex procedure. Hence, by using approximate integration formulae for narrow slices, based on the trapezium rule, considerable savings in computer time can be obtained. From Eqns. [B.10], [B.13] and [B.32], one may obtain;

$$M_i = M_{i-1} + \tfrac{1}{2} b_i \left\{ \left(\lambda_i (k_i b_i + m_i) - A_i \right) E_i + \left(\lambda_i m_i - A_i \right) E_{i-1} \right\}, \qquad \text{B.51}$$

$$\frac{\partial M_i}{\partial F} = \frac{\partial M_{i-1}}{\partial F} + \tfrac{1}{2} b_i \left\{ \left(\lambda_i (k_i b_i + m_i) - A_i \right) \frac{\partial E_i}{\partial F} + \left(\lambda_i m_i - A_i \right) \frac{\partial E_{i-1}}{\partial F} \right\} \ , \qquad \text{B.52}$$

$$\frac{\partial M_i}{\partial \lambda} = \frac{\partial M_{i-1}}{\partial \lambda} + \tfrac{1}{2} b_i \left\{ \left(\lambda_i (k_i b_i + m_i) - A_i \right) \frac{\partial E_i}{\partial \lambda} + (k_i b_i + m_i) E_i \right\}$$

$$\tfrac{1}{2} b_i \left\{ + \left(\lambda m_i - A_i \right) \frac{\partial E_{i-1}}{\partial \lambda} + m_i E_{i-1} \right\} \ . \qquad \text{B.53}$$

These approximate formulae are used repeatedly until the F and λ converge suitably.

The procedure is then to switch to exact integration formulae to refine these values.